Modeling of PVA Degradation in a Continuous Photochemical Reactor using Experimental Step Testing and Process Identification

By

Mustafa Mohamed Shahwan

B.Sc. of Engineering, Ryerson University, Toronto, 2011.

A thesis

presented to Ryerson University

in partial fulfillment of the requirements for the degree of

Master of Applied Science (MASc)

in the program of Chemical Engineering

Toronto, Ontario, Canada, 2018
© Mustafa Shahwan, 2018

AUTHOR'S DECLARATION FOR ELECTRONIC SUBMISSION OF A THESIS

I hereby declare that I am the sole author of this thesis. This is a true copy of the thesis, including any required final revisions, as accepted by my examiners.

I authorize Ryerson University to lend this thesis to other institutions or individuals for the purpose of scholarly research.

I further authorize Ryerson University to reproduce this thesis by photocopying or by other means, in total or in part, at the request of other institutions or individuals for the purpose of scholarly research.

I understand that the thesis may be made electronically available to the public.

Author's Signature,

Mustafa Shahwan.

ABSTRACT

Modeling of PVA degradation in a continuous photochemical reactor using experimental step testing and process identification

Mustafa Mohamed Shahwan

Master of Applied Science, 2018

Chemical Engineering

Ryerson University.

In AOP processes, the flow of oxidant must be controlled to minimize the oxidant residuals in a post biological treatment and to maximize the total organic carbon (TOC) removal and degradation. Designing a controller to regulate the hydrogen peroxide (H_2O_2) begins with a dynamic model determination of a chemical process. Therefore, a step testing technique is employed to construct a dynamic model of the UV/H_2O_2 degradation of polyvinyl alcohol (PVA) process based on pH and TOC responses to H_2O_2 step change. The experimental design consists of three different initial PVA concentrations, of 60.0, 280.0, and 500.0 mg PVA/L. Eight experimental tests were conducted for different hydrogen peroxide mass flowrates ranging from 0.336 to 125 mg H_2O_2/min. For every test, a transfer function was experimentally determined to describe the dynamics of the UV/H_2O_2 photochemical reactor for the degradation of PVA. System identification toolbox in Matlab software was used to determine first order plus time delay (FOPTD), second order plus time delay (SOPTD) and ARX polynomial models. The transfer functions and ARX models are a good model representation of the pH response data of a specific step change of H_2O_2 concentration. For example, the standard deviation of the process gain of test # 1 and its replicate was calculated to be 1.18 and standard deviation of the time constant was calculated to be 1.27. The pH response of the first test was fitted with a FOPTD model with a data fitting score of 88.8%. Test # 2 pH response data was fitted with a SOPTD transfer function with data fitting score of 83.6%. Tests # 6 and 7's pH response was fitted with a FOPTD model with a data fitting score of 94.3 and 87.7 % respectively. The different transfer functions obtained for the low, average, and high PVA concentrations indicate the nonlinearity aspect of polymer systems. All quality models are quite reliable estimations of the pH and TOC response data, since they were developed from experimental tests and parameter estimation techniques based on nonlinear regression approach.

ACKNOWLEDGMENTS

DEDICATION

This thesis is dedicated to:

My mother, Eman Al-Sief

My father, Mohamed Mustafa Shahwan

My wife, Alaa Ghadban

TABLE OF CONTENTS

LIST OF TABLES

LIST OF FIGURES

NOMENCLATURE

A   Absorbance of light

A_{254} UV light absorbance at wave length 254 nm

B   UV light path length in the photochemical reactor, cm

C   Concentration, mg/L, g/L

c Speed of light, $3.0 \times 10^8 m/s$

C_f TOC concentartion in the efflluent, mg Carbon/L

C_i TOC concentartion in the inffluent, mg Carbon/L

c_i Concentration of the light absorbing chemical species

$C_{H_2O_2}$ Hydrogen peroxide concentration, mg/L

C_{PVA} PVA solution concentration, mg/L

E   The energy absorbed from UV light absorption by chemical species, in Joule

f_i Fraction of radiation absorbed by chemcial species i in the polymer solution

h Planck's constant, 6.63×10^{-34} J.s

I   Number of chemical species

I_a Absorbed UV light intensity , W/m^2

I_o Incident UV light intensity, W/m^2

I_λ Specific monochromic UV light intensity, W/m^2

mV   Millivolts

$\overline{M}n$ Number Avergae Molecular weights of the PVA g/mol

$\overline{M}w$ Weight Avergae Molecular wight of the PVA

n Number of Variables

P_1 Vinyl alcohol Monomer

P_n Dead PVA polymer of chain length, n

$P_n^\bullet$ Live PVA radical with a chain length, n

P_s Dead PVA polymer of chain length , s

$P_s^\bullet$ Live PVA radical with a chain length , s

Q_{PVA} PVA solution feed fow rate in mL/min

$Q_{H_2O_2}$ H_2O_2 solution feed flow rate in mL/min

$R_{uv,i}$ Local volumetric rate of photon absorption

R   Geometric series coefficient

s Laplace transform variable in the form of complex number

t Time , sec

τ Time constant corresponding to 63.25% of the final output response

τ_1 First time constant, in a first order transfer function or higher

τ_2 Second time constant in a second order transfer function or higher

τ_3 Third time constant in a 3 pole transfer function denominator

τ_w Underdamped transfer fuction time constant product of, τ_1 and τ_2

τ_z Zero of the transfer function$(1 + \tau_z s)$ in the Nominator

u(t)   Process Input variable, H_2O_2 mass flow rate into the reactor

V   Reactor volum in L, or cm^3

$V_{PVA\ stock}$ Volume of PVA stock solution

V_{eff} Photochemical reactor effective volume

x_{PVA} Mass fraction of PVA in the total solution mixture g PVA/g total solution

$x_{H_{2O}}$ Mass fraction of H_2Oin total solution gH_2O/g total solution

$x_{H_2O_2}$ Mass fraction of H_2O_2 in total solution gH_2O_2/g total solution

y TOC removal %

z The z − domain of a discrete time data set

Greek Letters

η Degradation effeciency , %

λ UV light wave length in nm

ε Molar Absorptivity, L/mol. cm

ζ	Underdamped transfer function coefficent
v	UV light frequency
ϕ_i	Ratio of the amount of UV photons absorbed to the number of chemical species
θ	Residence time in the photochemical reactor, corresponding to the time delay
θ_{ef}	Residance time of the effleuent from the exit of the reactor to the effluent exit
θ_{in}	Residance time of PVA solution from the intake Tank to the reactor

Acronyms

ANN	Artificial neural network
AOP	Advanced Oxidation process
ARX	MatLab polynomial model in the form $A(z)y(t) = B(z)u(t) + e(t)$, (Auto $-$ Regressive with eXogenous input)
GPC	Gel Permeation Chromatography
FOPTD	First order plus time delay model
LVREA	Local volumetric rate of energy absorption, W/m^2
LVRPA	Local volumetric rate of photon absorption , W/m^2
PVA	Poly Vinyl Alcohol
SOPTD	Second order plus time delay model
TF	Transfer Function
TOC	Total Organic Carbon
TOPTD	Third order plus time delay model
US	Ultrasound
UV	Ultraviolet

CHAPTER 1
INTRODUCTION

Treatment of water resources to get clean water is considerably important and essential for life of human beings and all other living species. The wastewater produced from the manufacturing of chemical compounds must be well treated to eliminate any harmful impact in the ecosystem environment. Conventional biological techniques using microbes and bacteria to degrade toxic chemicals from wastewater systems, are not sufficient to degrade some organic materials. Many of these complex compounds are resistant to conventional wastewater treatment and biological degradation. Scientists and engineers understand the need for advanced oxidation processes (AOPs) to complement and improve conventional biological wastewater treatment processes (Ardekani, 2015). In fact, advanced oxidation processes have been proven to degrade complex toxic chemicals more efficiently. AOPs include Fenton process, UV/ H_2O_2, ozonation process, and ultrasound coupled with ultraviolet light with the presence of hydrogen peroxide, or combination of each (Lutterbeck et al., 2015). In advanced oxidation processes active hydroxyl radicals are produced to degrade complex organic compounds by attacking the long molecular chains (Tabrizi and Mehrvar, 2004; Mohajerani et al., 2010). In particular, UV light coupled with a powerful oxidant such as hydrogen peroxide, turned out to be a promising technique that is widely adopted by researchers and engineers in many studies (Mehrvar et al., 2015; Ardekani, 2015; Daneshvar et al., 2007; Felis et al., 2011). The AOP technique includes two stages of reactions, the first is the production of active hydroxyl radicals ($HO^\bullet$), that are produced from the photolysis of hydrogen peroxide (H_2O_2), and the second stage is the attack of long chains organic compounds by the active free hydroxyl radicals in the treated wastewater.

Further, several water-soluble polymers such as polyvinyl alcohol (PVA), polyacrylic acid (PAA), and polyacrylamide (PAM) are not degradable by biological treatments (Ghafoori et al., 2014). Also, many pharmaceutical compounds are not easily degradable by means of conventional biological treatments. Previous studies undertaken by Ghafoori (2013) and Hamad (2015) have focused on experimental and theoretical investigations of polymer degradation in UV/H_2O_2 photochemical reactor using photochemical kinetic approach. They developed dynamic models for process dynamic simulation, but these models may not be used for process control design.

In this thesis, an identification procedure is undertaken as a primary step before addressing the design of control systems that would regulate the flow of hydrogen peroxide into a UV/H_2O_2 tubular reactor. Another reason that motivated the step testing on the photochemical reactor was the fact that hydrogen peroxide has a scavenging effect if exceeded its optimum concentration. This study addresses the identification of a photoreactor degrading PVA in the presence of H_2O_2 by step testing. The photochemical reactor was set to operate in a continuous mode.

The step testing technique is to manipulate an input variable of the process and measure its output response. The input chosen in this research project was the concentration of hydrogen peroxide, and the measured responses were the pH and TOC of the effluent. The input variable alteration was introduced to the process at a defined time, when a first steady state has been reached. By monitoring the pH measurements for the treated PVA polymeric solution at known intervals, a first steady state was observed. The first steady state was achieved when the pH values has reached a first plateau. At a known time, a predetermined step change of the input concentration of H_2O_2 was introduced into the system. The pH and TOC response were measured for the step change input variation, and a transfer function that relates the change in the input to the measured response was determined. This procedure was repeated for different PVA concentrations.

This thesis discusses the experimental procedure to develop a series of transfer functions by system identification techniques.

Chapter Two is a literature review on advanced oxidation processes with different applications. Advanced oxidation processes are reviewed including UV/H_2O_2, photo-Fenton process, ozonation process, and other combination of advanced oxidation process. The objectives of this study are also stated.

Chapter Three discusses the process description of PVA degradation using 254 nm ultraviolet photochemical reactor with the presence of hydrogen peroxide. The photolysis of hydrogen peroxide and the possible polyvinyl alcohol reactions with hydroxyl and hydroperoxyl radicals are also discussed in this chapter. The experimental procedure is also described and explained as well as the required materials and instruments.

Chapter Four presents the process identification technique theory based on Laplace transform representation. For discrete time domain, the z-transform is used to convert differential equations into the discrete time domain, and then into z-domain. Chapter Five describes the transfer functions

determination using graphical method. Transfer functions stemming from pH and TOC output responses corresponding to a predetermined step change were calculated. The graphical transfer functions were verified using System Identification tool box in Matlab. The second part of the chapter presents the polynomial transfer functions in the z-domain. The transfer functions in the z-domain were extracted using System Identification toolbox. Auto-Regressive with eXogenous input (ARX), polynomial models were also extracted in Chapter Five for certain experimental conditions.

Concluding remarks of the research results are discussed in Chapter Six as well as the suggested future work.

CHAPTER 2
LITERATURE REVIEW

Open literature shows that many studies have been conducted to evaluate the photoreaction of many pollutants such as pharmaceutical products, detergents, polymers and disinfecting processes in wastewater streams. Conventional biological techniques using microbes and bacteria to degrade toxic chemicals from wastewater systems are not sufficient to degrade new complex materials (Harimurti et al., 2014). However, advanced oxidation processes (AOP) are efficient techniques to treat wastewater effluents.

For instance, Fernanbo et al. (2009) studied the degradation of pharmaceutical compounds atenolol and primidone using UV/H_2O_2 process. Also, the mechanisms of the degradation of poly (ethylene glycol) were determined by the UV/H_2O_2 oxidation process (Santos et al., 2009). The mechanisms were determined by studying the photooxidation of small model molecules, such as di, tri, tetra and ethylene glycol. Mowla et al. (2014) studied the degradation of pharmaceutical compounds using $UV/US/H_2O_2$ technique. The study concluded that $UV/US/H_2O_2$ method resulted in the highest TOC removal.

In hydrocarbon industries, Harimurti et al. (2014) investigated a UV/H_2O_2 process to degrade alkanolamine in effluents of a refinery of sweetening processes. Alkanolamine is used in the formulation of cosmetic and pharmaceutical products, and also are used as solvents. During the scheduling maintenance of adsorption and desorption columns, effluent with high concentrations of alkanolamine are generated from sweeting process at refineries. Harimurti et al. (2014) reported that this particular effluent cannot be treated in a biological process. Therefore, AOP processes are promising techniques in the treatment of toxic organic compounds. However, most methods used in the pre-treatment of refinery effluents are Fenton reagents, UV/Ozone and UV/H_2O_2. As a result of no sludge production, the high efficiency in the production of hydroxyl radicals for the brakeage of organic compounds, and the treatment of refinery wastewater with high concentration of methyldiethanolamine (MDEA), UV/H_2O_2 process was chosen (Harimurti et al., 2014). Also, the degradation of bisphenol A was performed using UV only and UV/H_2O_2 (Felis et al., 2011).

The degradation efficiency of UV/H$_2$O$_2$ treating hospital laundry wastewater was investigated. After physiochemical, coagulation, flocculation, and anthracite filtration, it was proven that UV/H$_2$O$_2$, decreased the concentration of chemical oxygen demand (COD) and totally removed it (Zotesso et al., 2016).

Behnajady et al. (2005, 2015) did a lot of work on Malachite green (MG), which is commonly used as a dye in clothing industry, a wound disinfectant, antibacterial and antifungal substance. Behnajady et al. (2015) investigated the decolorization and degradation of Malachite Green (MG) using US/UV/H$_2$O$_2$. The results concluded that the kinetics of US/UV/H$_2$O$_2$ where similar to that of UV/H$_2$O$_2$ process for the degradation of MG. These findings where directly related to the role of hydroxyl radicals in the reaction. In this study, the ultra sonic waves where also used for the dissociation of H$_2$O$_2$ to produce hydroxyl radicals. The use of mercury UV light in the deactivation of chlorine resistance microorganisms proved to be efficient without the production of unwanted by-products (Jenny et al., 2014).

A UV/H$_2$O$_2$ process was used as a secondary stage in a post rotating bioreactor process in order to remove chemical oxygen demand (COD) and biological oxygen demand (BOD) from industrial wastewater (Ardekani, 2015). As a result of the high cost of UV/H$_2$O$_2$ treatment, advanced oxidation processes are commonly used with traditional biotreatments. The main purpose of the study was to evaluate the efficiency of UV/H$_2$O$_2$ process followed by a moving bed bioreactor (MBBR). For three hydraulic retention times of 4, 8, 12 h, the effluent of the treated industrial wastewaters was then introduced to a MBBR. For this particular study, optimum conditions were determined to be 7.0 pH, H$_2$O$_2$ concentration of 1000 g/L, and a reaction time of 90 min. This condition resulted in a COD removal of 74.68% and a BOD removal of 66.15% where initially the samples had 4,400 mg COD, and 1,950 mg BOD. The combined UV/H$_2$O$_2$ process followed by a moving biological bed reactor may lead to an environmentally friendly wastewater effluent (Ardekani, 2015).

MTBEs (methyl tert-butyl ether) and aromatic hydrocarbons were degraded using UV/H$_2$O$_2$ (Vaferi et al., 2014). The aromatics and MTBEs were found in synthetic wastewaters. The aim of this study was to experimentally as well as theoretically investigate the UV/H$_2$O$_2$ treatment of aromatics as well as MTBE (methyl tert-butyl ether) in industrial wastewaters. An artificial neural

network (ANN) was developed to model the pollutant degradation extent as a function of initial concentrations of H_2O_2 contaminants, pH, solution temperature, reaction time and UV intensity.

Water-soluble polymers such as polyphthalamide (PPA), polyvinyl alcohol (PVA), and polyacrylamide (PAM), and other polymers listed in Table 2.1. are frequently utilized in several commodity and industrial applications such as textile industry, oil field products, detergent-based industry and cosmetics (Aarthi et al., 2007). The degradation of the polyethylene glycol by UV/H_2O_2 gave rise to smaller carboxylic acids such as formic, glycolic and oxalic acids (Santos et al., 2009).

Table 2.1 illustrates some common water-soluble polymers that may be found in municipal and industrial wastewater effluents.

Table 2.1. Applications of some Water-Soluble Polymers

Soluble Polymers in water	Applications
Polyvinyl alcohol (PVA)	Detergent, dissolvable laundry packages, paper and textile coatings.
Polyacrylamide (PAM)	Flocculants, adhesive, lubricant, paint and pigment dispersant.
Polyacrylic acid (PAA)	Detergent, thickener, super absorbent.
Polyaspartic acid (PASP)	Detergent, paint, fertilizer, cosmetics, biomedical (drug delivery, artificial skin, dialysis membranes).
Polyethylene glycol (PEG)	Tissue engineering, drug delivery, cosmetic.
Polyethylene oxide (PEO)	Tissue engineering, drug delivery, cosmetic.
Polycarboxylates (PAA-PMA)	Pharmaceutical compound (vaccine).
Galactomannan (Guar)	Food additives, Rheology modifier.
Polyethyleneimines (PEI)	Detergent, lubricant, binder.
Polyvinylpyrrolidone (PVP)	Pharmaceutical compound (disinfectant), emulsifier, adhesive.

Polyethylene oxide was degraded using a UV/H_2O_2 photoreactor (Ghafoori et al., 2012). The study included the kinetics of the degradation based on experimental data obtained from a recirculating batch photoreactor. Hamad et al. (2016) studied the photochemical degradation of polyvinyl alcohol (PVA), in a tubular photochemical reactor in the presence of H_2O_2. The H_2O_2 feeding strategy in a photochemical UV/H_2O_2 was investigated to optimize the process and maximize TOC removal from the polymeric wastewaters. A thorough experimental design was conducted to understand the optimum parametric conditions for a batch, fed-batch, and a continuous UV/H_2O_2 photochemical degradation of PVA. The methodology of conducting the experiments was illustrated with thorough explanations of TOC measurement techniques of the treated polymeric solution effluent. The technique to measure the H_2O_2 residuals in the effluent and GPC analysis of aqueous PVA solution samples are explained in detail by Hamad (2015). The GPC analysis allowed to assess the degree of PVA degradation, the weight average molecular weight of the degraded PVA and the polydispersity index of the degraded PVA. The importance of UV exposure time in a semi batch reactor with the presence of H_2O_2, and its effect on the pH was presented. The optimum concentration and feed strategy of H_2O_2 were also determined (Hamad, 2015).

Ghafoori (2013) and Hamad (2015) have done very interesting and original studies on modeling polymer degradation in UV/H_2O_2 photochemical reactor using photochemical kinetic approach. These dynamic models are very useful for process dynamics simulation, but not quite straightforward for process control design and applications.

Alternatively, process identification is another important approach to describe the dynamics of industrial processes form input and output measured signals of a process such as the identification of a bioreactor (Pramod and Chidambaram, 2000), pulp and paper process identification (Allison and Ogawa, 2003).

Fedele (2009) proposed a method of process identification to estimate a first order plus time delay (FOPTD) transfer function from step testing. The method required no iteration to estimate the parameters of FOPTD model. In the current study, the time constant is calculated at 63.2 % of the total response of the output of a definite step change. A similar identification work was done on an unstable bioreactor using an optimization technique to determine the parameters of FOPTD transfer functions to describe the dynamics of the process (Pramod and Chidambaram, 2000). Initial guess of the three parameters of the transfer function was assumed and a corresponding PID

controller was designed for the bioreactor. Modeling a bioreactor using identification technique is quite delicate due to high non-linearity and complexity of the biochemical reactions (Ramaswamy et al., 2005). Another example of a complex process which can be modelled by experimental or statistical methods is the pulp and paper plant. In this study, two manipulated inputs and one controlled output were adopted (Allison and Ogawa, 2003). Due to the complexity of pulp and paper reactors, a kinetic study would not be practical on such a reactor. On the other hand, mass, and energy balances would not converge to an accurate model as the internal dynamics of such a reactor would be non-deterministic. Hence the author of this study used an identification method to model the reactor with experimental data. Due to the complex nature of such a process, the study proposed an identification method to determine four parameters of a second order transfer function plus time delay SOPTD model (Ramakrishnan and Chidambaram, 2003). To avoid tedious mass, energy and momentum balances, plus the dynamics of the process, the study used an identification technique to determine the parameters of a SOPTD transfer function that describes the process. The SOPTD transfer functions that were extracted from experimental data were suitable for designing a proper controller. The four parameters of the process were extracted from experimental data using asymmetrical relay testing.

In this study, an identification method was used to determine the three parameters of FOPTD transfer function for low, medium and high concentrations of PVA at different step changes. This identification technique was employed to thoroughly understand the UV/H_2O_2 photodegradation of PVA.

This thesis consists of developing a dynamic model of UV/H_2O_2 photochemical reactor that degrades a PVA solution. The dynamic modeling of the photochemical reactor was achieved by applying step testing technique on the process. The step testing technique consists of altering a key input variable and measuring the process response. In this study, the input variable was the concentration of hydrogen peroxide, and the measured response was the pH and the TOC of the effluent. The theory as well as the steps of identification would be thoroughly illustrated in chapters 3 and 4.

An important concept of a past study on PVA degradation was the optimum mass ratio between hydrogen peroxide and polyvinyl alcohol (Hamad, 2015). This concept holds true for all initial concentrations of PVA. Depending on which region of the optimum value of hydrogen peroxide

the step change was applied, the increase of hydrogen peroxide flow into the reactor either increases the TOC removal if on the left side of the optimum peak or decreases the TOC removal if on the right side of the optimum peak. Figure 2.1 illustrates the concept of hydrogen peroxide optimum value:
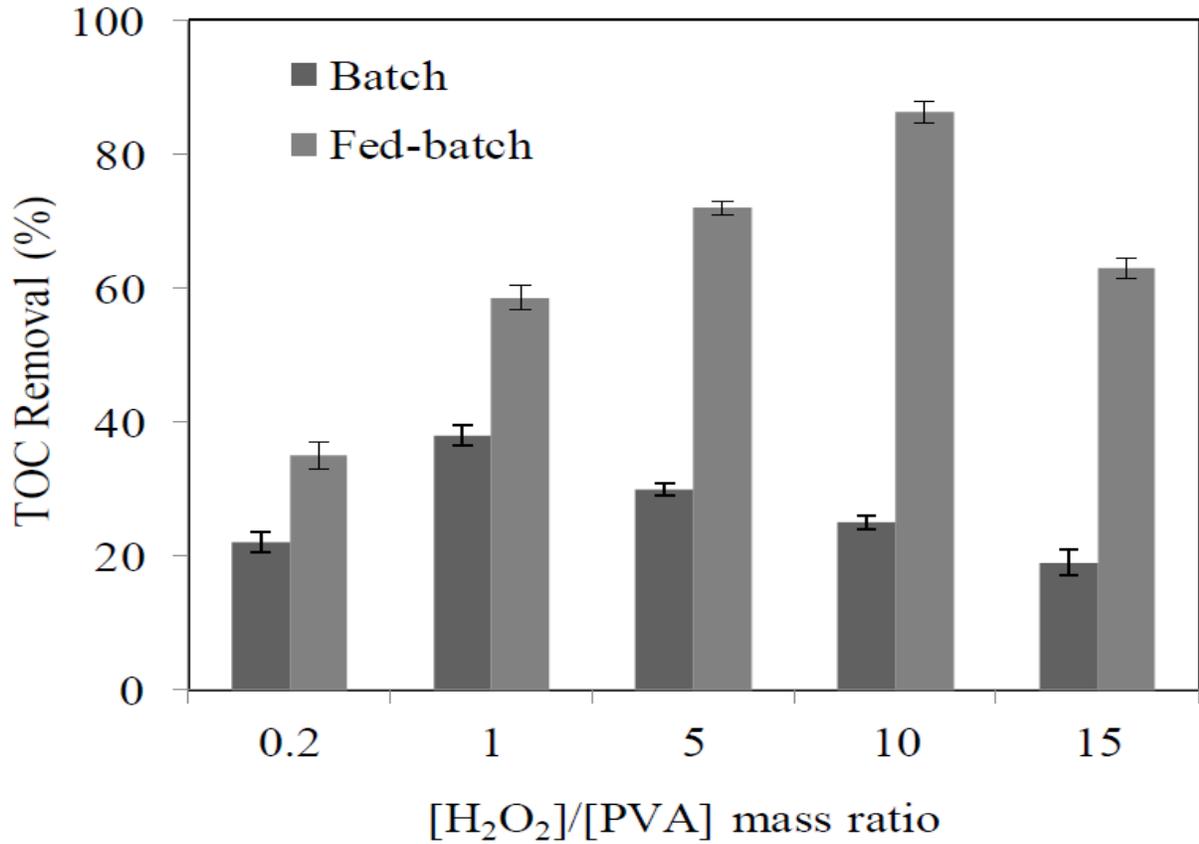
Figure 2.1. TOC removal for batch and fed-batch reactors for different $[H_2O_2]/[PVA]$ mass ratios (Hamad, 2015).

2.1. Objectives

The objective of this study is to dynamically model the degradation of PVA solution in a photochemical reactor with the presence of hydrogen peroxide H_2O_2. It also aims at extracting FOPTD transfer functions for pH and TOC responses using graphical techniques. Also, this study aims at determining FOPTD and SOPTD transfer functions using system identification toolbox. Finally, it aims at determining polynomial ARX models for pH response of predetermined step change of hydrogen peroxide concentration.

The approach to achieve the objectives of this thesis is to conduct a set of experimental tests on the UV/H_2O_2 continuous tubular photoreactor in order to develop input-output dynamic models for the degradation of PVA. System identification is a black-box method to determine transfer functions that can relate the measured input variables to the output variables. The study is to demonstrate how to cope with the process non-linearity and develop a reliable model using the identification technique. The system identification of the process includes choosing experimental conditions that includes different initial PVA concentrations.

The transfer functions can be used in future studies to design a controller to regulate the flow of hydrogen peroxide into the photochemical reactor. A proper controller would enhance the PVA photodegradation and overcome the limitations of the UV/H_2O_2 process when operated in a continuous mode.

CHAPTER 3
PROCESS DESCRIPTION AND EXPERIMENTAL PROCEDURE

3.1. Principle of PVA degradation

This thesis studies the degradation process of polyvinyl alcohol in a photochemical reactor using UV/H_2O_2 process. PVA properties are presented in Table 3.1.

Table 3.1. Physical and chemical properties of polyvinyl alcohol.

Property	Values
Molecular weight	100,000 g/mole
Molecular formula	$(C_2H_4O)_n$
Boiling point	$228°C$
Melting point	$150 - 190°C$
Density at 25 ℃	1.19-1.31 g/ml
Viscosity at 25 ℃	$0.9\ mPa.s$

Few studies have demonstrated that hydrogen peroxide can degrade PVA in presence of UV light. The UV light brakes down hydrogen peroxide molecules into hydroxyl radicals, which attack the polyvinyl alcohol chains in the reaction mixture. Thus, a scission reaction is initiated. As the scission reaction progresses, a lower molecular PVA chains is produced. Some of the new polymeric molecules are dead polymers and others are live PVA radicles. The general degradation of PVA is schematically illustrated in Reactions (3.1) and (3.2) (Hamad et al., 2018):

$$PVA\ long\ polymer\ Chain \xrightarrow{OH^\bullet} oligomers, trimers, dimers \xrightarrow{OH^\bullet}$$

$$caroxylic\ acids \xrightarrow{OH^\bullet} carbon\ dioxide + Water \tag{3.1}$$
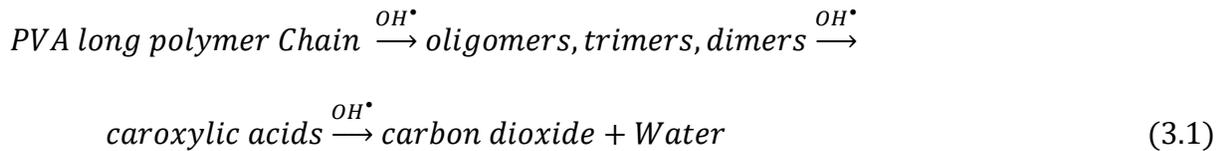
The previous equation is the overall representation of the reaction mechanism of the degradation of PVA in a UV/H_2O_2 tubular photochemical reactor.

$$[C_2H_4O]_n + H_2O_2 \xrightarrow{UV\ light} Intermediates \rightarrow CO_2 + H_2O \tag{3.2}$$
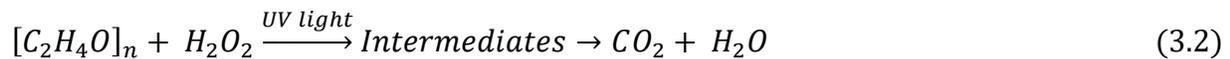
As the scission reaction is driven to completion, a final mineralization reaction produces formic and, acetic acid and finally carbon dioxide and water. The final mineralization step is summarized by (Peng and Kong, 2007):

$$C_2H_4O + 5\,H_2O_2 \xrightarrow{UV\ light} Intermediates \rightarrow 2CO_2 + 7\,H_2O \tag{3.3}$$
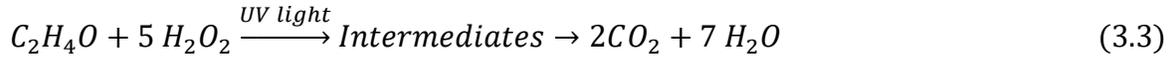
The degradation of PVA in UV/H_2O_2 photochemical reactor is summarized in three main steps:

1- The photolysis of hydrogen peroxide into hydroxyl and hydroperoxyl radicals.
2- The degradation of the long PVA chains.
3- Mineralization of the intermediates into CO_2 and H_2O.

3.2. PVA Degradation Steps

A. Hydrogen Peroxide Photolysis

The UV light causes the breakage of the hydrogen peroxide bond into the formation of hydroxyl radicals that are very active oxidant. In the scope of degrading PVA, the aim of the research project is to produce efficient amount of hydroxyl radicals that can drive the PVA degradation reaction to completion. The ultimate phase of the process to totally mineralize any PVA traces in the process to environment friendly components i.e. water and a non-toxic gas i.e. carbon dioxide. The scavenging effect of reacting hydroxyl radicles with hydrogen peroxide must be reduced. The reaction that occurs in the photochemical reactor is the scission reaction of the high molecular weight PVA chains. The scission reactions occur in the UV-tubular photochemical reactor at the presence of hydrogen peroxide. The hydrogen peroxide oxidizer decomposes into two hydroxyl radicals as shown in the following reaction:

$$H_2O_2 \xrightarrow{h\nu} 2HO^{\bullet} \tag{3.4}$$

The hydroxyl radical may further react with hydrogen peroxide molecule to form the hydroperoxyl radical and water as follow (Buxton et al., 1988):

$$HO^{\bullet} + H_2O_2 \rightarrow HO_2^{\bullet} + H_2O \tag{3.5}$$

The photolysis of hydrogen peroxide triggers several intermediates of recombination reactions as shown in the mechanism below (Ghafoori, 2013):

$$HO^\bullet + HO^\bullet \rightarrow H_2O_2 \tag{3.6}$$

$$HO_2^\bullet + HO_2^\bullet \rightarrow H_2O_2 + O_2 \tag{3.7}$$

$$HO_2^\bullet + HO^\bullet \rightarrow H_2O + O_2 \tag{3.8}$$

$$H_2O_2 + HO_2^\bullet \rightarrow HO^\bullet + H_2O + O_2 \tag{3.9}$$
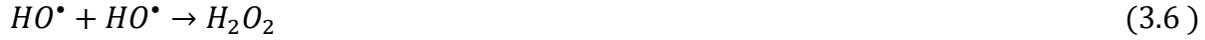
Two hydroperoxyl radicals may react to give one hydroperoxyl radical with a hydrogen ion as well as an oxygen radical with a negative charge as follows (Bielski and Cabelli, 1991):

$$HO_2^\bullet \rightarrow O_2^{\bullet-} + H^+ \tag{3.10}$$

B. PVA Degradation

The PVA degradation occurs by means of PVA backbone scission reaction. The hydroxyl radical $(HO^\bullet)$ as well as hydroperoxyl radicals $(HO_2^\bullet)$ react with the PVA polymer on a hydrogen abstraction mechanism. A polymer live radical is produced with both water and hydrogen peroxide as illustrated in Reactions (3.11) and (3.12) (Hamad, 2015):

$$P_n^{-H} + HO^\bullet \rightarrow P_n^\bullet + H_2O \tag{3.11}$$

$$P_n^{-H} + HO_2^\bullet \rightarrow P_n^\bullet + H_2O_2 \tag{3.12}$$
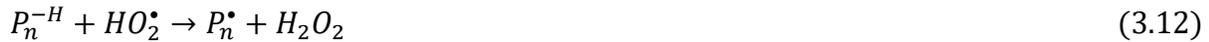
The previous reaction mechanism was proven in another study (Hamad et al., 2016). P_n is the dead PVA and $P_a^\bullet$ is the PVA active radical both molecules with an (n) chain length. The mechanism of the degradation of PVA is attributed to the hydroxyl radicals attacking the bonds of the long molecules. The reaction yields a dead and an active PVA molecule of shorter chain where both molecules sum up to the original PVA macromolecule. The degradation of the large PVA molecule with chain length (n) is presented in Reaction (3.13) (Hamad 2018):

$$P_n + HO^\bullet \rightarrow P_{n-a} + P_a^\bullet \tag{3.13}$$

A special case of Reaction (3.13) is when $a = 1$. In this case, the scission reaction is just the breakage of the last repeating PVA monomer at the end of the PVA mother chain. An end PVA chain scission is called β scission and is illustrated in equation (3.14) as follows (Hamad, 2018):

$$P_n \rightarrow P_1 + P_{n-1}^{\bullet} \tag{3.14}$$

As many vinyl alcohol monomers are produced, a mineralization reaction may occur to finally produce water and carbon dioxide.

C. Mineralization of Vinyl Alcohol Monomer

As many end chain β scission reactions occur, many vinyl alcohol monomers would be produced in the reaction mixture. Hydroxyl and hydroperoxyl radicals would still attack the single chain molecule to produce formic and acetic acid. The observations of Peng and Kong (2007), Taghizadeh et al. (2015) and Hamad (2018) illustrate the reaction mechanisms from Reactions (3.15) to Reaction (3.22) as follows:

$$P_1 + HO^{\bullet} \rightarrow HCOOH + HO_2^{\bullet} \tag{3.15}$$

$$P_1 + HO_2^{\bullet} \rightarrow CH_3COOH + HO^{\bullet} \tag{3.16}$$

The acidity of the solution mixture would drop as formic and acetic acid are formed. The following reaction mechanisms illustrate the drop in pH value as a result of the production of (H^+) ion as follows:

$$HCOOH \rightleftarrows HCOO^- + H^+ \tag{3.17}$$

$$CH_3COOH \rightleftarrows CH_3OO^- + H^+ \tag{3.18}$$

The basic hydroxyl ion is also produced in the following mechanisms:

$$P_1 + HO_2^{\bullet} + O_2^{\bullet -} \rightarrow HCOOH + OH^- \tag{3.19}$$

$$CH_3OO^- + H_2O_2 \rightarrow CO_2 + H_2O + OH^- \tag{3.20}$$

The last step of the degradation of PVA is the conversion of acetic acid to formic acid by the reaction of hydroperoxyl radical with the acetic acid as follows:

$$CH_3COOH + 2HO_2^\bullet \rightarrow 2HCOOH + H_2O_2 \qquad (3.21)$$

Lastly, the formic acid would be converted to water and carbon dioxide by the hydroxyl radicals as follows:

$$HCOOH + 2HO^\bullet \rightarrow Intermediates \longrightarrow CO_2 + 2H_2O \qquad (3.22)$$
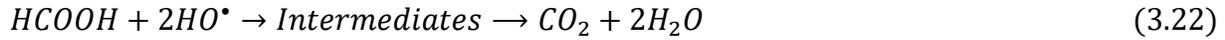
As the degradation of PVA reaches the last step and the reaction is driven to completion, the PVA would be fully mineralized to harmless carbon dioxide and water.

Taking pH as well as the total organic carbon (TOC) measurements of the effluent samples, indicates the degree of the PVA degradation reaction. Gel Permeation Chromatography (GPC) analysis is designed to measure the degree of molecular chain breakage and molecular weight distribution of the degraded polymer.

For the scope of this study, the output variables pH and TOC of the effluent samples would be measured. A transfer function that relates the output variable y(t) to the input variable, the concentration of hydrogen peroxide u(t), is then determined. The transfer functions then would be used to identify the process for different influent PVA initial concentrations and hydrogen peroxide flow rate alteration.

3.3. Photochemical Reactor Setup

The experimental setup was a continuous annular photoreactor with a low-pressure mercury UV lamp at its core. A low flow peristaltic pump of the type A 100N Flexflo delivered the polymeric solution to and through the photoreactor. The hydrogen peroxide H_2O_2 solution was delivered to the PVA solution stream just before entering the photoreactor. H_2O_2 was pumped to the photoreactor by a multichannel peristaltic pump of the type FH 100M Thermo Scientific. The PVA solution would be pumped to the reactor in a continuous mode simultaneously with the H_2O_2 flow to the inlet of the reactor.

The low-pressure UV lamp at the core of the photoreactor has a wavelength of 254 nm and is 28.5 cm long and 2.00 cm width. The UV lamp is protected in a quartz sleeve to prevent the fouling of UV light as shown in Figure 3.1.

1- Photochemical reactor.
2- PVA solution influent tank.
3- Low flow PVA solution peristaltic pump.
4- Hydrogen peroxide peristaltic pump.
5- Hydrogen peroxide acrylic Jar.
6- Treated PVA solution effluent tank.
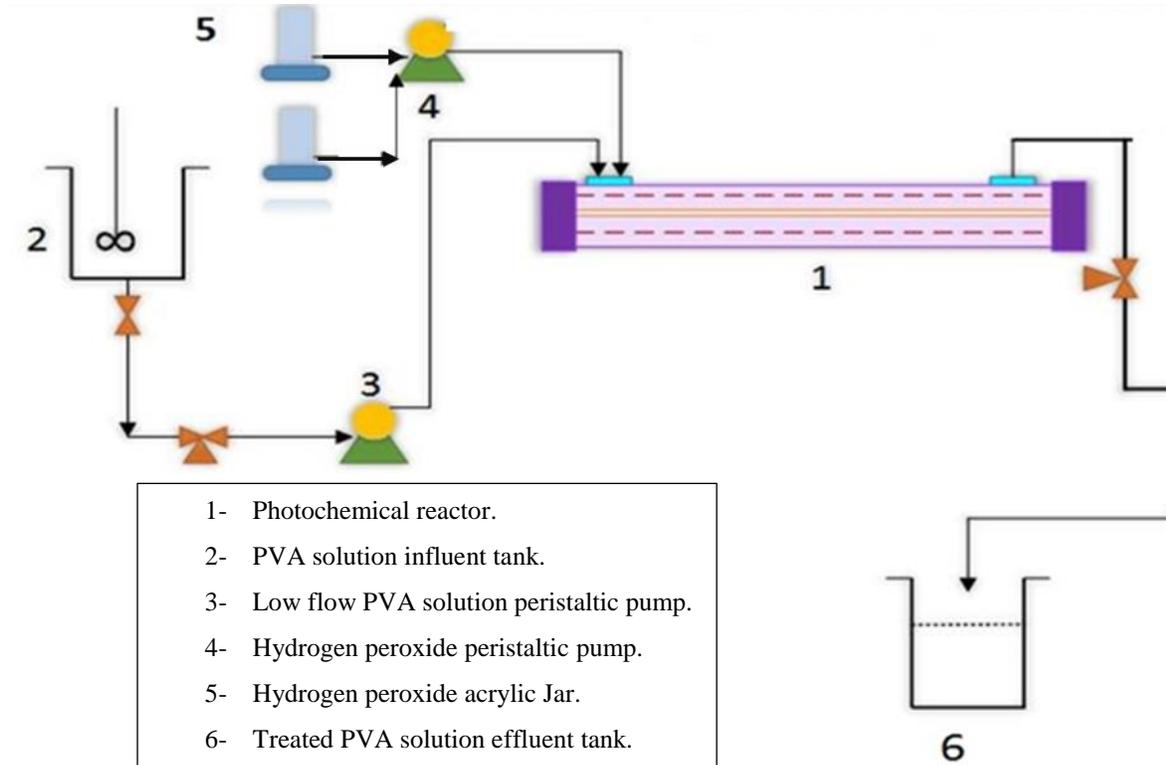
Figure 3.1. PVA photochemical degradation reactor setup

From the literature review, it was concluded that there is a lack of study on the mechanical control approach scheme to control H_2O_2 flow into the PVA degradation process. This project focuses on dynamically identifying the UV/H_2O_2 photochemical reactor setup for degrading PVA solution. A dynamic model would be experimentally accomplished by introducing an input parameter into the process and measuring an output pH response as well as a TOC of the effluent PVA solution. A transfer function would then be determined for different PVA concentrations and different hydrogen peroxide step changes.

From previous studies, it was apparent that the photodegradation process of polyvinyl alcohol is not fully understood. A study on the degradation of polyvinyl alcohol was conducted and concluded that it was not trivial to identify the photochemical reactor process (Hamad et al., 2016).

To better understand the degradation of PVA in a photochemical reactor with the presence of hydrogen peroxide a step testing identification technique was employed in this study. Furthermore, the transfer functions that would be acquired for the process would be used to design a controller to regulate the flow of hydrogen peroxide into the system. A proper flow of hydrogen peroxide into the process would lead to fully degrading the PVA, minimize the hydrogen peroxide residuals, minimize the hydrogen peroxide consumption and maximising TOC removal from the effluent stream.

3.4. Experimental Conditions

The experimental design consists of low, average and high PVA concentrations of 60.0, 280.0 and 500.0 mg PVA/L respectively. The low concentration of polyvinyl alcohol models the amounts of PVA found in municipal wastewater streams. The high concentration of PVA was chosen for academic reasons in previous studies to ease GPC measurements of the effluent PVA molecular weight distributions and polydispersity index. The 280.0 mg PVA/L, was chosen as an average of the low and the high concentration of PVA. Table 3.2, summarizes the experimental conditions for this study.

Table 3.2. Experimental conditions of the UV/H$_2$O$_2$ photochemical degradation tests.

Test #	PVA Concentration $\left(\frac{mg\,PVA}{L}\right)$	Mass Flow $\left(\frac{mg\,PVA}{min}\right)$	Total PVA solution mass flow rate $\left(\frac{g}{min}\right)$	Step change [H$_2$O$_2$]/[PVA]	Step-test	Mass Flowrates $\left(\frac{mg\,H_2O_2}{min}\right)$
1	60.0	3.0	50.00057	1.0 to 5.0		3.0 to 15.0
2	60.0	3.0	50.00057	1.0 to 0.20		3.0 to 0.6
3	280.0	14.0	50.00266	1.0 to 5.0		14.0 to 70.0
4	280.0	14.0	50.00266	1.0 to 0.20		14.0 to 2.8
5	280.0	14.0	50.00266	0.12 to 0.024		1.68 to 0.336
6	500.0	25.0	50.00475	1.0 to 5.0		25.0 to 125.0
7	500.0	25.0	50.00475	1.0 to 0.2		25.0 to 5.0
8	500.0	25.0	50.00475	0.12 to 0.024		3.0 to 0.6
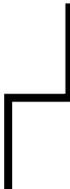
3.5 Materials

3.5.1. Polyvinyl Alcohol

A 5% polyvinyl alcohol was purchased from VWR (Mississauga Ontario), with a molecular weight of 100,000.0 g/mol. PVA solutions with certain concentrations were prepared from the stock solution.

3.5.2. Water

Distilled water from the lab was used for all experiments to prepare the hydrogen peroxide and polyvinyl alcohol solutions. Distilled water was also used to run through the photochemical reactor setup for a considerable amount of time to rinse the photochemical reactor.

3.5.3. Hydrogen Peroxide

30% hydrogen peroxide was purchased from Aldrich. The hydrogen peroxide that was used for all experiments was a 30% mass of H_2O_2/total solution mass. It was 34.04 g/mol molecular weight with a density of $1.11 g/cm^3$.

3.6. Treated PVA solution effluent samples

A step change of the inlet hydrogen peroxide solution was applied after the system has reached a first steady state. The step change was conducted by altering the hydrogen peroxide concentration, by changing the hydrogen peroxide to a new H_2O_2 concentration. The samples were collected and the pH was measured. The collected pH data of the effluent samples would indicate the response of the system at a known change in the input H_2O_2 concentration. The samples would continue to be collected until a second steady state was observed in the system. The samples would then be collected and tested for its TOC content. The second vial in the sample tray would contain the PVA influent sample. The third vial until the second last vial would contain the effluent samples collected at a 7 minutes interval of sampling periods. The last vial in the tray would contain distilled water for rinsing purposes. The pH of each sample was measured three times to determine

an average pH value with a low standard deviation. The TOC content for each sample would then be determined using the TOC analyser. The TOC analyzer would repeat the TOC analysis for each sample three times and would determine the standard deviation.

3.6.1. pH measurement of the effluent samples

The importance of the pH readings in this study is significant as the pH is the only possible on-line output measurement in the effluent solution. A new pH probe was purchased prior to starting the experiments with a Thermo Orion pH meter, (model 230 Aplus with an accuracy of 0.02) instrument. The meter had three significant figure readings and all three figures were recorded for every sample reading. The pH meter was calibrated prior to starting the pH measurements of the samples. The calibration had a high 90.0's % calibration slops. The pH measurements for all samples were recorded to two decimal places.

3.6.2. TOC measurement of the effluent sample

Teledyne Tekmar Apollo 9000 Combustion TOC analyser was used to measure the total organic carbon (TOC). The extent of the degradation of the PVA to CO_2 and water was linked to the level of total organic carbon in the effluent sample. The TOC analyser oxidises the sample by combustion to up to 780^oC to carbon dioxide and water and subtracts the inorganic carbon CO and CO_2 from organic carbon. The TOC analyzer readings are four decimal places of accuracy and all the decimal places were recorded.

3.7. Error analysis

3.7.1. pH measurement

The pH meter was calibrated every time an experiment was conducted. The pH meter was calibrated with low buffer and neutral one and the calibration resulted in high 90% slop. The slop in the pH calibration is the ratio between the actual pH meter conversion values from the difference

in electrical potential to the pH value, to the theoretical conversion value. For example, if the theoretical value is -59.18 mV/pH and the calibration slop was found to be 97 .7%, then the pH meter would convert each -57.82 mV to an equivalence of 1 pH. Three pH values were measured for each effluent sample and an average of the three measurements was considered as the sample pH value.

3.7.2. TOC measurement

The TOC analyser device measures the combustion signal and converts it to TOC value in ppm. The machine has an option of measuring the sample three times to determine an average TOC value. On every sampling tray, a distilled water blank was placed in the first and last sampling holder.

3.7.3. Homogeneity of the PVA solution

The homogeneity of the PVA solution is important in achieving accurate results. To ensure an efficient mixing of the solution, glass rod was used to stir the solution periodically. Although an effort was done to ensure that the PVA solution is highly homogenous, there was no assurance that the PVA was totally homogenous.

3.7.4. Repeatability and data reproducibility

As a result of the low standard deviations for both the pH and the TOC response data, for the experimental conditions, the experimental data are reproducible.

3.8. Experimental Procedure

Initially, distilled water was pumped through the photoreactor system to rinse out any residuals from previous experiments. In the preliminary experiments, the PVA solution was prepared from a solid PVA that was 130.0 kg/mol number average molecular weight. The solid PVA was a white crystalline material that had a long dissolving time and needed extra care to ensure that PVA crystals were totally dissolved.

The desired concentration of PVA solution was prepared with the aid of an analytical scale that was used to weigh the amount of solid PVA with a precision of four decimals. After carefully measuring the amount of solid PVA needed to prepare the desired PVA polymeric solution, the solid PVA was poured into 2 liters of distilled water. The solid PVA was added to the distilled water in a two-liter flask that was directly placed on the top of a magnetic stirrer that was mounted with a heater. By visual inspection, and sufficient stirring time, a complete dissolving of PVA solid particles was ensured. Then, the PVA solution was added to the 15 L feed tank. Distilled water was carefully added to the initial PVA solution and a stirring procedure was established using a glass rod to ensure a homogenous PVA polymeric solution. The experiments were later performed using a stock solution of 5 W/W%PVA with a number average molecular weight of 100,000 g/mol.

The hydrogen peroxide (H_2O_2) solution was then prepared by the dilution of a 30W/W% of H_2O_2 stock solution to a desired hydrogen peroxide concentration. The prepared hydrogen peroxide solution was then introduced to the system using a peristaltic pump that was connected by rubber tubing to the inlet of the photoreactor.

The low-pressure mercury UV lamp was then turned on. After a start-up check list was performed, a stopwatch was initiated simultaneously with the start up of both the PVA solution peristaltic pump and the hydrogen peroxide peristaltic pump. A volumetric flow rate of 50.0 ml/min of the initial PVA solution was delivered to and through the photochemical reactor. The flow rate of hydrogen peroxide of 4RPM the equivalent of 0.5 ml/min was established.

Samples of the effluent was collected in a glass vials of 40.0 ml volume on a 7.0 minutes sampling period interval. The samples were then subjected to a pH and TOC analysis.

A step change testing was conducted on the photochemical reactor system, where a sudden H_2O_2 concentration change was imposed on the setup and a pH response was then measured. The exact

timing of the step change was then recorded in order to correlate pH versus time plots and TOC versus time plots. The desired outcome of the mentioned plots was to establish a specific transfer function that relates the process response to a specific input change in the PVA photoreactor system corresponding to a specific nonlinear region of the process.

3.9. Test 1: 60.0 mg PVA/L, Step change from 1.0 to 5.0 [H₂O₂]/[PVA]

Initially the feed tank would be properly cleaned and rinsed with distilled water. The feed tank would then be filled with 15 L of distilled water and the peristaltic pump would be turned on to transport the distilled water through the photochemical reactor. The pump flow rate was set to 50 ml/min flow rate, and the system stayed running until the influent tank has emptied.

Two litres graduated cylinder was used to prepare the PVA solution. At first, the volume of the PVA bulk solution was calculated, then the bulk PVA solution was pipetted into the 2 L graduated cylinder. The volume of the 5% PVA bulk solution was calculated to produce a 15 L of a final PVA concentration of 60.0 mg/L.

The amount of PVA needed to prepare 15 L of 0.06 g PVA/L was 0.9 g. The following cross multiplication illustrates the required volume of PVA stock solution (X L) to prepare 15 L of 0.06 g PVA/L.

$$1L \ Bulk \ PVA \ solution \ - \rightarrow 50 \ g \ PVA$$
$$X \ L \ Bulk \ PVA \ solution \ - \rightarrow 0.9 \ g \ PVA$$

$$V_{PVA \ stock} = \frac{0.90 \ g \ PVA \times 1000 \ ml \ stock \ PVA \ solution}{50 \ g \ PVA}$$

$$V_{PVA \ stock} = 18 \ ml \ of \ stock \ PVA \ solution.$$

Where $V_{PVA \ stock}$ is the volume of the 5% PVA stock solution that is required to prepare the desired PVA solution.

Therefore, the volume of 5.0% PVA bulk solution needed to prepare 15.0 L, of 0.06 g PVA/L, is 18.0 ml.

The 18.0 ml of 5% stock solution was pipetted into the 2 L graduated cylinder, and distilled water was then added to the graduated cylinder to the 2 L mark. When the mark on the graduated cylinder was carefully verified, the 2 L cylinder content was emptied into the 15 L feed tank. After emptying the 2 L cylinder in the influent tank, the 2 L graduated cylinder would then be filled with distilled water 6 additional times and all emptied into the feed tank. Finally, a 1 L of distilled water was added to the 14 L of PVA solution. Figures A.1 and A.2, illustrate the steps to prepare a 0.06 g PVA/L solution. Figure A.2 in the appendix illustrates the addition of the 13.0 L of distilled water to the initial 2.0 L of PVA solution, to finally result in the 0.06 g PVA/L solution

As the homogeneity of the solution is essential in achieving accurate result, the prepared PVA solution was stirred continuously with a glass rod. The stirring of the PVA solution was held for at least 15.0 minutes before turning on the photochemical reactors process. The stirring of the PVA solution continued during the run in different time intervals.

For this experiment the input change would be the concentration of hydrogen peroxide H_2O_2. The initial concentration of hydrogen peroxide would be prepared as follows:

3.10. Initial H_2O_2 Concentration Calculations

PVA calculations:

$$\frac{\mathbf{0.06gPVA}}{\mathbf{L}} \times \frac{50ml}{min} \times \frac{1\ L}{1000\ ml} = \frac{\mathbf{0.003\ g\ PVA}}{\mathbf{min}}$$

Initial concentration ratio between the hydrogen peroxide and the PVA is 1.0 as follows:

$$1.0 = \frac{[H_2O_2]}{[PVA]} = \frac{X\ g\ H_2O_2/min}{0.003\ g\ PVA/min}$$

Solving the previous equation results in hydrogen peroxide mass flowrate of:

$$[H_2O_2] = \frac{0.003\ g\ H_2O_2}{min}$$

$$\frac{6.0 \; g \; H_2O_2}{L} \times \frac{0.5 \; ml}{min} \times \frac{1 \; L}{1000 \; ml} = \frac{0.003 \; g \; H_2O_2}{min}$$

To prepare 6.0 g H_2O_2 solution in a 100.0 ml volumetric flask, the following calculations are essential:

Bulk H_2O_2 solution is 30%:

$1 \; L \; of \; H_2O_2 \; bulk \; solution \; -------------------- \rightarrow 300g \; H_2O_2$

6 g H_2O_2 is needed in 1 L of distilled water

And

0.6 g H_2O_2 are needed in the 100.0 ml volumetric flask.

$1 \; L \; of H_2O_2 \; bulk \; solution \; ------------------- \rightarrow 300g \; H_2O_2$

$X \; L \; of H_2O_2 bulk \; solution \; -------------------- \rightarrow 0.6 \; g \; H_2O_2$

$Therefore, 0.002 \; L \; of \; bulk \; solutions \rightarrow \; 0.6 \; g \; of \; H_2O_2 \; into \; the \; 100 \; ml \; volumetric \; flask.$

And 2.0 ml of H_2O_2 30 % bulk H_2O_2 is added into the graduated cylinder. The H_2O_2 solution that is prepared in the graduated cylinder in 6.0 g H_2O_2/L. The 6.0 g H_2O_2/L, then emptied in acrylic 100 ml brown jar. The preparation of the hydrogen peroxide solutions was illustrated in Figure A.3.

3.14 Step change H_2O_2 concentration calculations:

1.0-5.0 [H₂O₂]/[PVA]

The 1.0 initial Ratio:

$$\frac{0.06 \; g \; PVA}{L} \times \frac{50 \; ml}{min} \times \frac{1 \; L}{1000 \; ml} = \frac{0.003 \; g \; PVA}{min}$$

In the calculation of the initial ratio of 1.0 [H_2O_2]/[PVA], it was determined that the concentration of the hydrogen peroxide must be 6.0 g/L as follows:

$$\frac{6.0 \; g \; H_2O_2}{L} \times \frac{0.5 \; ml}{min} \times \frac{1 \; L}{1000 \; ml} = \frac{0.003 \; g \; H_2O_2}{min}$$

Now to calculate a step change of 5.0 [H₂O₂]/[PVA]:

$$5.0 = \frac{[H_2O_2]}{[PVA]} = \frac{X\ g\ H_2O_2/min}{0.003\ g\ PVA/min}$$

By solving the previous equation, the change in the input hydrogen peroxide mass flow rate was determined as:

$$[H_2O_2] = \frac{0.015\ g\ H_2O_2}{min}$$

To achieve the input step change from $1.0\ to\ 5.0\ [H_2O_2]/[PVA]$, a concentration of hydrogen peroxide is calculated as follows:

The 5.0 step change Ratio:

$$\mathbf{\frac{30.0\ g\ H_2O_2}{L} \times \frac{0.5\ ml}{min} \times \frac{1\ L}{1000\ ml} = \frac{0.015\ g\ H_2O_2}{min}}$$

To achieve a mass flow rate of 0.015 g H₂O₂/min- the required step change input- a step change concentration of 30.0 g H₂O₂/L, solution would be introduced to the system at time zero. That is equivalent to 3.0 g of H₂O₂ in to 100.0 ml volumetric flask. Therefore, to prepare the 0.015 g H₂O₂ solution, 3.0 g of H₂O₂ is needed to be added into the 100.0 ml volumetric flask. The following calculation illustrates the volume of bulk H₂O₂ needed to be added to the 100.0 ml volumetric flask:

$1\ L\ of\ H_2O_2\ bulk\ solution\ - \rightarrow 300g\ H_2O_2$

$X\ L\ of\ H_2O_2\ bulk\ solution\ - \rightarrow 3.0\ g\ H_2O_2$

0.01 L of bulk 30.0% H₂O₂ solution is needed to prepare 0.015 g H₂O₂/L solution. That is 10.0 ml of bulk 30.0% solution would be pipetted into the 100.0 ml volumetric flask.

The photochemical reactor setup was started after a check list was performed. The UV lamp was turned on simultaneously with the peristaltic pump of the influent PVA solution and the peristaltic

pump of the H_2O_2 solution. The pH of the PVA influent solution was initially measured. Then, samples of the effluent PVA treated solution was then collected very 7 minutes and analysed for pH. The system was allowed to reach a first steady state. By monitoring the pH of the initial samples, a first steady state would be reached when the pH values reach a plateau. After a first plateau was reached a prepared step change of H_2O_2 concentration was introduced to the system by changing the H_2O_2 intake tube, rapidly from the initial H_2O_2 concentration to the second step change H_2O_2 concentration.

CHAPTER 4

MODELING APPROACH BY SYSTEM IDENTIFICATION TECHNIQUE

A mathematical model is a theoretical representation of a process relating process inputs, outputs and operating conditions. An example of such a mathematical model is a transfer function that represents a UV/H_2O_2 process for the degradation of PVA. The dynamics of a process can be modeled by means of two different techniques. The first principle method is the conservation principles of mass/energy and the second is a system identification technique which is basically a black-box approach.

4.1. Process Dynamics

The dynamics of a process such as a photochemical reactor can be mathematically modeled by the conservation principles of physics which is based on mass/molar, momentum and energy balances. In general, this approach leads to a set of non-linear ordinary differential equations ODEs which once linearized, they can be arranged as follows:

$$a_n y^{(n)}(t) + a_{n-1} y^{(n-1)} + \cdots + a_i y^1(t) + a_0 y(t)$$

$$= b_m u^{(m)}(t) + b_{m-1} u^{(m-1)}(t) + \cdots + b_1 u^1(t) + b_0 u(t) \tag{4.1}$$

1- Where y(t) is the process output variable and u(t) is the process input variable,

  $y^{(n)}$ is the nth derivative of y(t), and t is the time, i.e. the independent variable.

2- $a_i(i = 1\ to\ n)$ are the process parameters to be estimated from experimental data.

As an illustration a third order process is given below :

$$a_3 \frac{d^3 y(t)}{dt^3} + a_2 \frac{d^2 y(t)}{dt^2} + a_1 \frac{dy(t)}{dt} + y(t) = Ku(t) \tag{4.2}$$

For mathematical solution in process control systems, it is more suitable to use Laplace transform to represent the dynamics of the process in an algebraic form. The Laplace transform is defined in Equation (4.3).

$$F(s) = \int_0^\infty f(t)e^{-st}\,dt \tag{4.3}$$

where s is a complex number defined as $s = \sigma + j\omega$ in which σ is the real part and ω is the imaginary part. Laplace Transform is used to transform differential equations into an algebraic model. Taking the Laplace transform of the dynamic model, gives:

$$G(s) = \frac{Y(s)}{U(s)} = \frac{b_m s^m + b_{m-1} s^{m-1} + \cdots + b_1 s + b_0}{a_n s^n + a_{n-1} s^{n-1} + \cdots + a_i s + a_0} \equiv \frac{N(s)}{P(s)} \tag{4.4}$$

Where Y(s), is the Laplace transform of the process output y(t), and the U(s) is the Laplace transform of the process input u(t) and K is the steady state process gain. For realizable systems, it is required that $n \geq m$.

$$G(s) = \frac{Y(s)}{U(s)} \tag{4.5}$$

Where G(s) is the process transfer function defined as the ratio of process output over process input in s-domain; where P(s) is the characteristic polynomial of the G(s). The roots of N(s) are called the zeros of the transfer function, and the roots of the P(s) are called the poles.

4.2. Stability Concepts

A chemical process can be fast, slow, stable or unstable. Most chemical reactors are unstable. A system is stable if once it is disturbed for a brief time, it comes back to its original state. The stability is a very important characteristic in dynamic system analysis. A system is asymptotically stable if and only if all the poles have negative real parts (i.e. in the left-half of the complex plane). If any pole has a positive real part then the system is unstable (Corripio and Smith, 1997). This feature is graphically illustrated in Figure 4.1.

s-plane:
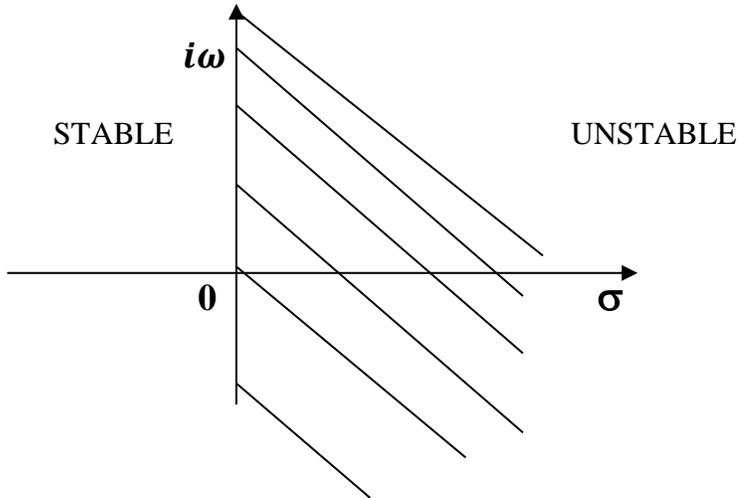
Figure 4.1. Stability diagram of dynamic systems.

Any system of higher order two or more may be reduced to a first order system with delay as follows:

$$G(S) = \frac{Ke^{-\theta s}}{1 + \tau s} \tag{4.6}$$

Where K is the gain of the process defined as:

$$K = \frac{\Delta y}{\Delta u} \tag{4.7}$$

Time constant τ is the time required for the response to reach 63.2% of the final output change, corresponding to the method of the tangent (Corripio and Smith, 1997). The time delay θ is equivalent to the theoretical residence time i.e. reactor length over the average process velocity.

4.3. System Identification

Identification modeling of a process consists of collecting input-output data to develop a dynamic model. It can be accompanied with a parameter estimation technique, such as least square method, to develop a dynamic model. In practical applications, discrete models are considered. This is

evident, since the experimental data are usually collected at a given time interval called sampling period (Stephanopoulos, 1984).

4.4. Discrete Model

Since the data in each experiment is collected at definite time interval measured in seconds, minutes or hours, the time domain is considered as discrete. For a discrete time domain, the continuous differential equations are transformed into discrete algebraic equations, hence the dynamic Equation (4.1) is written as:

$$y(k) + a_1 y(k-1) + \cdots + a_n y(k-n)$$
$$= b_0 u(k) + b_1 u(k-1) + \cdots + b_m u(k-m) \qquad (4.8)$$

Equations (4.1) and (4.8) are both linear functions as long as all $a_i (i = 1, to\ n)$ are constant over specific range of process operations.

4.5. z-Transfer Function

For experimental data collected at discrete time intervals, Equation (4.8) is not continuous, and the Laplace transform in s cannot be used. Equivalent transform function called z-transform is adopted instead (Stephanopoulos, 1984). Hence, the difference Equation (4.8) represents a linear process. Therefore, one can determine the corresponding z-transfer function, which is equivalent to Equation (4.4), and it is written as follows:

$$G(z^{-1}) = \frac{Y(z)}{U(z)} = \frac{b_0 + b_0 z^{-1} + \cdots + b_m z^{-1}}{1 + a_1 z^{-1} + \cdots + a_n z^{-n}} = \frac{B(z^{-1})}{A(z^{-1})} \qquad (4.9)$$

Where $z^{-1} = e^{-sT}$ represents the delay due to the sampling period T_s, the polynomials $A(z^{-1})$ and $B(z^{-1})$ play similar role as the polynomials P(s) and N(s), respectively. In some cases, the polynomial order of numerator and denominator are the same. If the process contains a dead time $\theta = T_s.d$, where T_s is the sampling period and d is an integer with $d = 1, 2, ...,$ then z-transfer function is given as:

$$G(z^{-1}) = \frac{B\,(z^{-1})}{A\,(z^{-1})}\, z^{-d} \tag{4.10}$$

4.6. Difference Equations

The z-transform is the equivalence to Laplace transform for discrete systems. For

$Y(z) = z(y(k))$ using the sampling delay concept,

$$z^{-1} = e^{-sT_s} \tag{4.11 a}$$

$$Z(y(k-i) = z^{-i}.Y(z) \tag{4.11.b}$$

$Where\ i = 1\ to\ n$

Then Equation (4.8) becomes:

$$y(z)(1 + a_1z^{-1} + \cdots + a_nz^{-n}) = u(z)(b_0 + b_1z^{-1} + \cdots + b_mz^{-m}) \tag{4.12}$$

4.7. Identification Procedure

A flow chart of the system identification technique begins with the desire to mathematically represent the system. A design of the experiments can be determined by maximizing the descried outcome. Then, the experiments should be performed and transfer functions relating the input to the output variables are therefore determined. The mathematical model in a form of a transfer function is then validated, if the desired parameter estimation accuracy is satisfied (Pelckmans, 2012). The flow chart shown in Figure 4.2. illustrates the steps to perform the identification procedure.
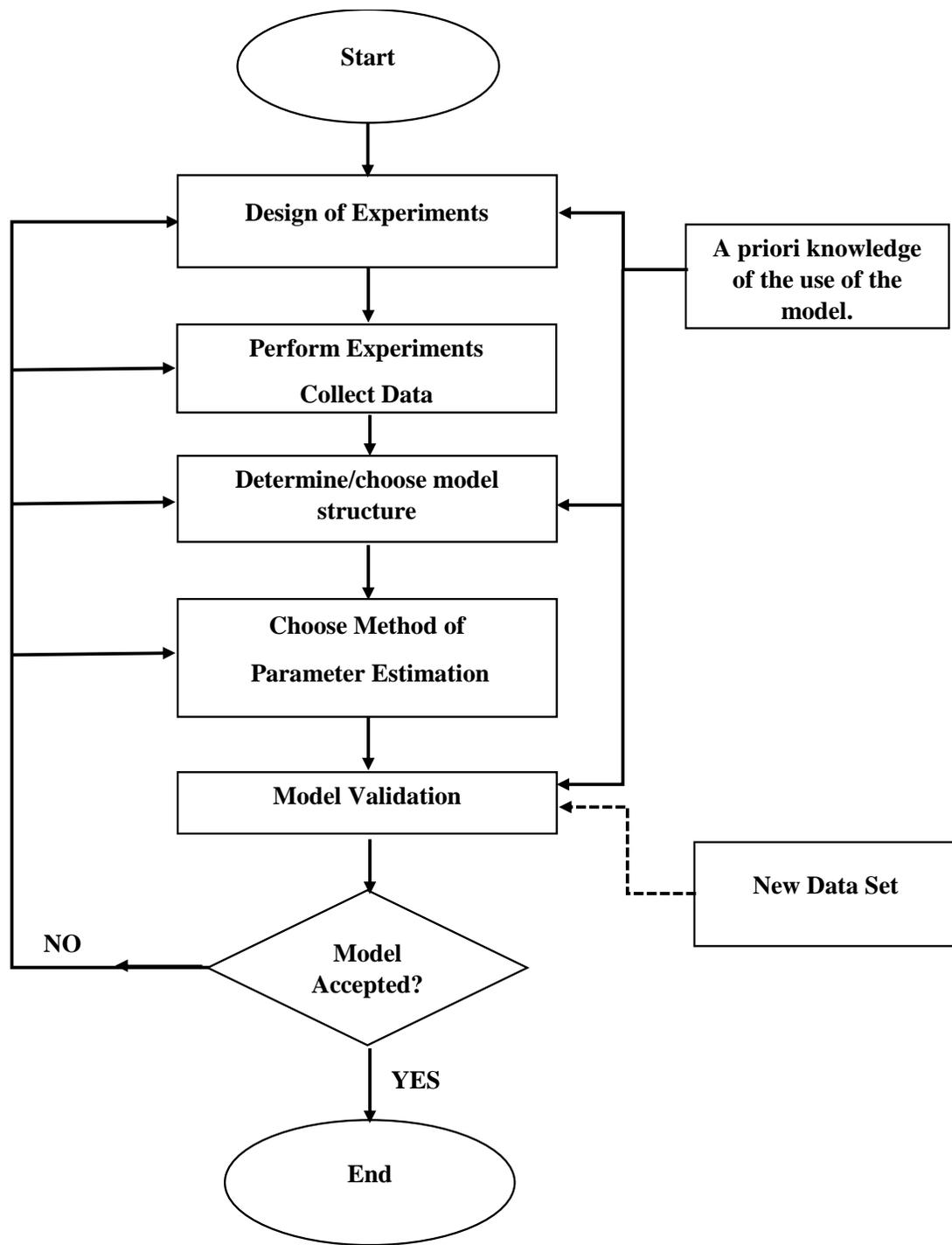
Figure 4.2. Flow chart of system identification of chemical processes (Pelckmans, 2012).

The identifying technique is to introduce a step change of the input variable that is known and at an exact instant. A step change is illustrated in Figure 4.3.

$$u(t) = \begin{cases} 0 & t < 0 \\ 1 & t \geq 0 \end{cases}$$
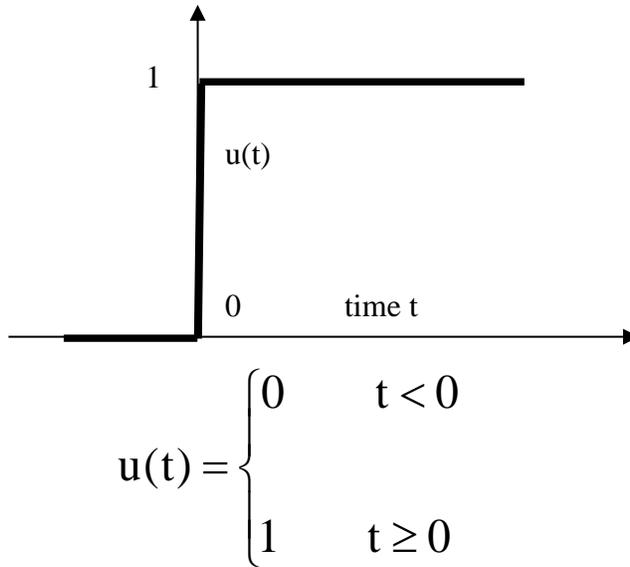
Figure 4.3. Unit step function for the identification technique.

Referring to Equation (4.3), the transfer function of a unit step is given by:

$$F(s) = L\big(u(t)\big) = \frac{1}{s} \tag{4.13}$$

And its equivalent discrete form is presented in Equation (4.14) as follows:

$$F(z) = \frac{z}{z-1} = \frac{1}{1-z^{-1}} \tag{4.14}$$

In the scope of this study, a possible output response may correspond to a first order transfer function, a first order with delay, a second order, or a third order or even higher order system with/without delay, and possibly with a lead term. i.e. $(\tau s + 1)$ in the numerator. A second order or higher can be approximated to a first order transfer function with delay. Figure 4.4 illustrates some common possible output responses.
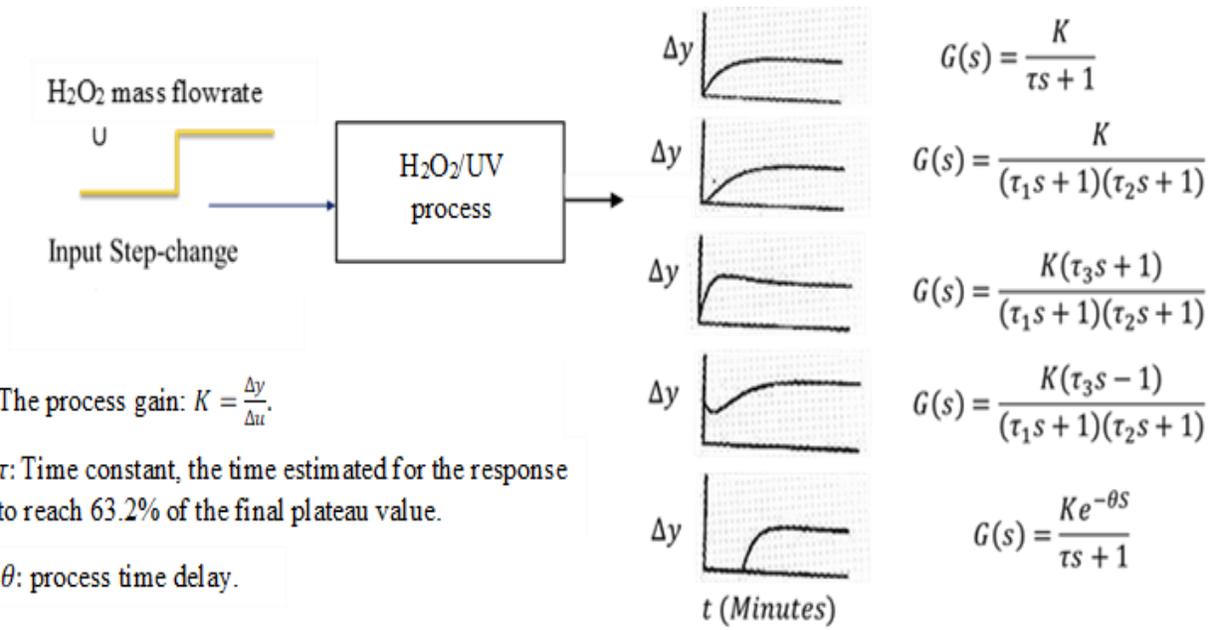
Figure 4.4. Process output response and its transfer function.

A first order response data set looks like the plot in Figure 4.5, where the response data are in general above the 45° line, y(t) stands for the process output like the pH or TOC measurements and u(t) is the process input variable which can be the concentration of hydrogen peroxide in the PVA solution influent.
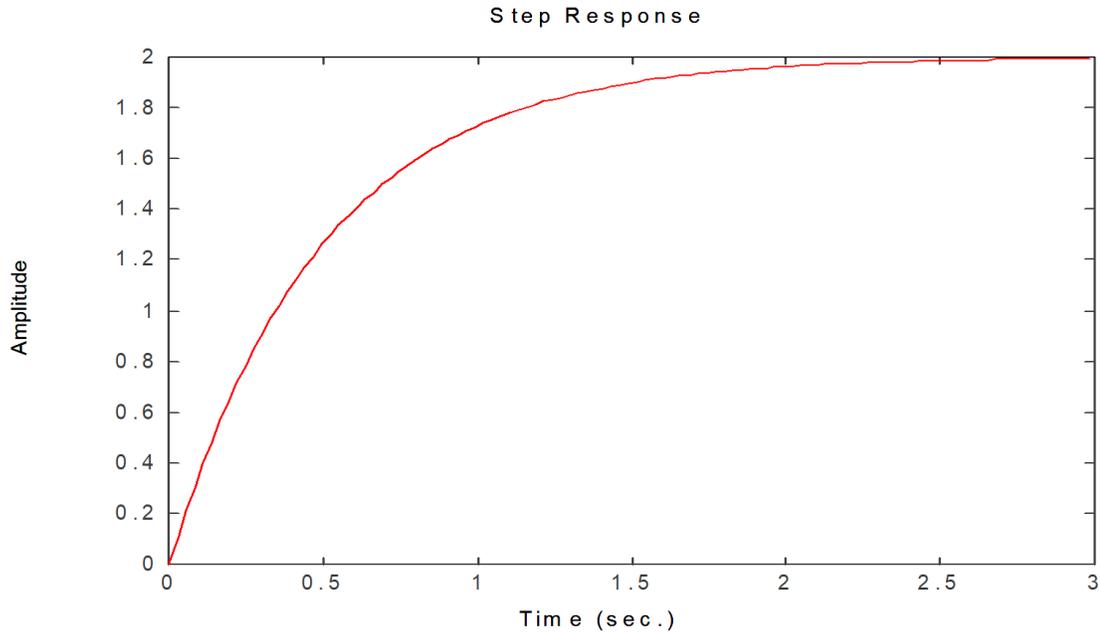
Figure 4.5. A first order transfer function.

The ratio of Y(s) to U(s) is the transfer function G(s):

$$G(s) = \frac{Y(s)}{U(s)} = K\frac{1}{1 + \tau s} \tag{4.15}$$

The transfer function G(s) is not measurable, but the input variable and the output variables are measurable. The time constant τ is defined as the time required for the process response to reach 63.2% of its final steady value. The tangent on the response curve initiating at t=0, intersects with the second plateau horizontal line. If a perpendicular line drops to the time axis, it intersects with the response curve at 63.2 % of the final second plateau value. The time that takes the response to reach 63.2% of the final second plateau value, is called the time constant (Corripio and Smith, 1997). The plot in Figure 4.6 illustrates the mathematical meaning of the time constant τ.
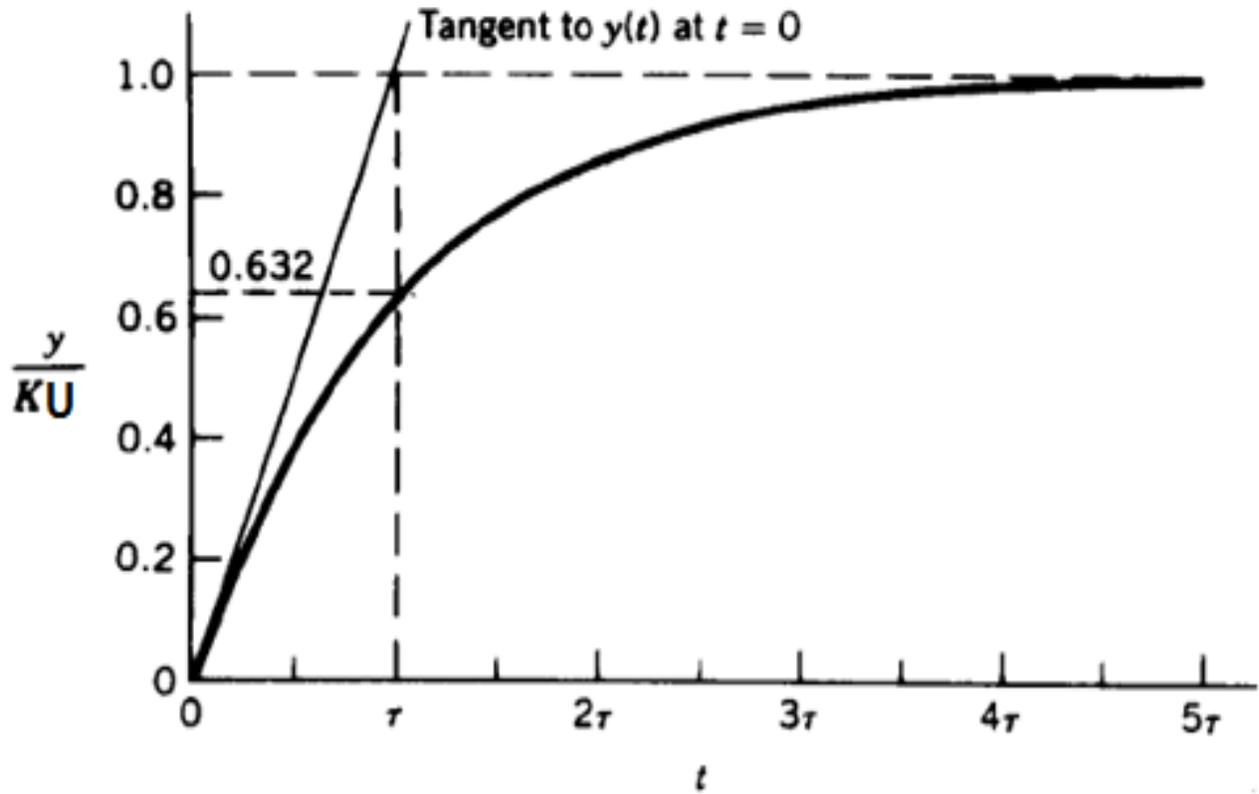
Figure 4.6. The tangent method from the end of the delay period at t=0, intersecting the second plateau line at a time constant corresponding to a 63.2 % of the total response.

An example of a first order transfer function with a delay time $\theta = 0.5 \, sec$ is presented in Figure 4.7.

$$G(s) = K \frac{e^{-\theta s}}{1 + \tau s}$$

Y(t)
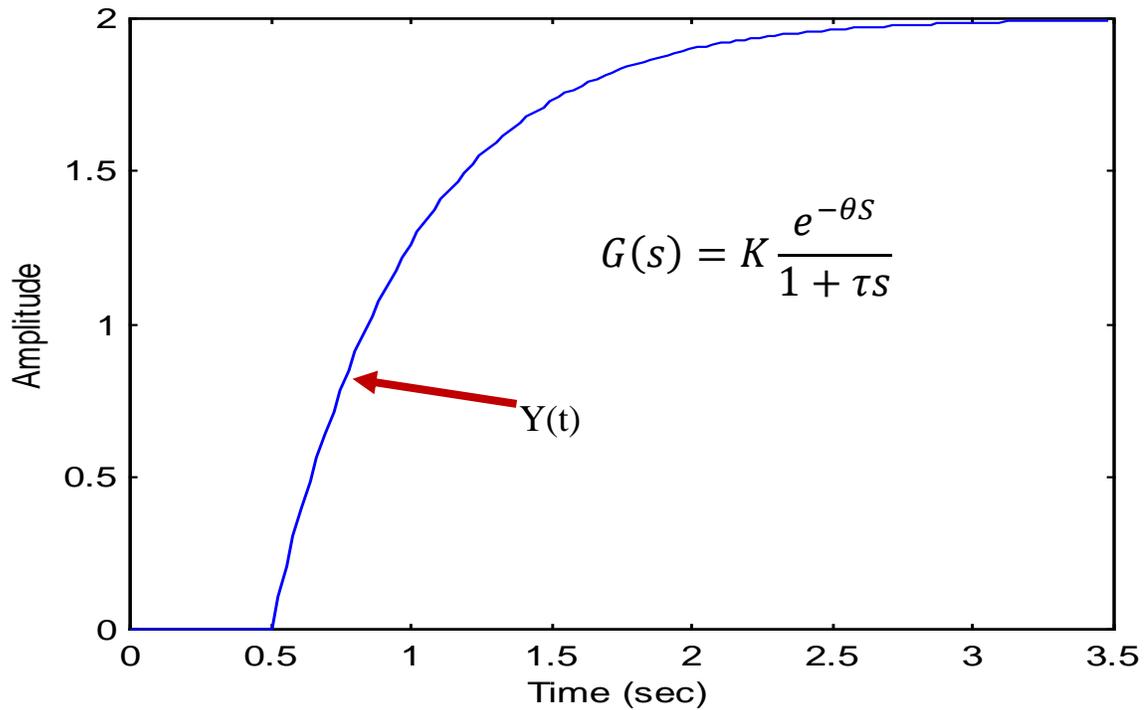
Figure 4.7. An example of first order transfer function with a delay of 0.5 sec.

A first order with delay transfer function has the following format:

$$G(s) = \frac{Y(s)}{U(s)} = K \frac{e^{-\theta s}}{1 + \tau s} \tag{4.16}$$

where θ is the time delay that the system requires to start responding to an input step change.

4.8 ARX polynomial model

ARX model stands for Auto Regressive exogenous model. It's a polynomial model for best fit data based on the optimization process of lease square error difference between measured data and predicted ones. Two sets of data are needed to apply this method. A set of data for the response of a step test, and a set of data for the input change. For an ARX model of [1 1 1], the least square equation that would be derived in respect to the evacuated parameter is as follows:

$$P = \sum_{i=1}^{n} (y_n - a_1 y_{n-1} - b_1 u_{n-1})^2 \tag{4.17}$$

Deriving Equation (4.17) with respect to the parameter a_1 yields the following:

$$\frac{\partial P}{\partial a_1} = \sum_{i=1}^{n} 2(y_n - a_1 y_{n-1} - b_1 u_{n-1})(-y_{n-1}) \tag{4.18}$$

Using all data points to evaluate Equation (4.18) and setting the derivative to zero yields an equation in the form of:

$$\frac{\partial P}{\partial a_1} = C_1 - a_1 C_2 - b_1 C_3 \tag{4.19}$$

Deriving Equation (4.17) with respect to the parameter b_1 yields the following:

$$\frac{\partial P}{\partial b_1} = \sum_{i=1}^{n} 2(y_n - a_1 y_{n-1} - b_1 u_{n-1})(-u_{n-1}) \tag{4.20}$$

Where u is the input variable and the y is the output.

Using all data points to evaluate Equation (4.20) and setting the derivative to zero yields an equation in the form of:

$$\frac{\partial P}{\partial a_1} = C_4 - a_1 C_5 - b_1 C_6 \tag{4.21}$$

Using Equations (4.19) and (4.21), parameters of ARX model with the order of [1 1 1] can be evaluated.

To evaluate the ARX model, a_1 and b_1 must satisfy Equation (4.22) by using all response data points and an evaluation of the optimum must yield close to a zero value (Stephanopoulos,1984).

$$P = \frac{1}{n}\sum_{i=1}^{n}(y_n - a_1y_{n-1} - b_1u_{n-1})^2 \cong 0 \qquad (4.22)$$

Where P is the sum of all the square of error differences divided by the number of data points used (n). The response value y_n is the response point measured at the current sampling time, whereas the response value y_{n-1}, represent the response measured previous sampling time. The corresponding input value at n-1 sampling time is u_{n-1} (Stephanopoulos, 1984).

CHAPTER 5
RESULTS AND DISCUSSION

5.1. Transfer Functions by Identification using Graphical Method

When modeling the photochemical reactor for the degradation of polyvinyl alcohol three major steps have been considered:

a. Running the photochemical reactor in continuous modes with known inlet PVA and hydrogen peroxide concentrations, the system was allowed to reach an initial steady state. The pH was monitored online, and a first steady state was reached when no variations in the pH of the solution was observed. i.e., pH remained constant while the reactor was still running.

b. In the second step, a known step change input was introduced to the system and its output response was measured. The output responses were recorded during the reaction time, until the second steady state was reached.

c. Measuring the pH and TOC output responses, and calculating a transfer function corresponding to a PVA concentration and the input variable change of hydrogen peroxide concentration.

   To properly identify the photochemical reactor, three concentration levels where chosen for the dissolved PVA:

   a- Low concentration of PVA of 60 mg PVA/L of solution;

   b- High concentration of PVA of 500 mg PVA/L of solution;

   c- Average concentration of PVA of 280 mg PVA/L of solution.

For each concentration of PVA, a step change to alter the concentration of H_2O_2 was applied. The concentration of H_2O_2 was quickly altered by changing the container of the H_2O_2 to a different known concentration. An increase or decrease of the hydrogen peroxide concentration produced a response in the pH values that were measured on line. The TOC was also measured for each sample off line.

The fourth step consisted of graphically plotting the process response and calculating the gain, the time constant τ, by determining the 63.2 % of the response and reading the corresponding time on the x-axis of the pH or TOC response plot (Corripio and Smith, 1997).

For example:

If the corresponding time constant τ was 140 minutes, and the step change of the concentration of H_2O_2 was at time 100 minutes, and the response was delayed 8 minutes, then the time constant τ was calculated as follows:

$$\tau = t_{@63.0\% \, gain} - \theta - t_{of \, step-change} \tag{5.1}$$

$$\tau = 140.0 - 100.0 - 8.0$$

$$\tau = 32.0 \, Minutes.$$

The gain is defined as the change in the output response variable divided by the change in the input variable which is the concentration of the hydrogen peroxide:

$$K = \frac{\Delta Y}{\Delta U} = \frac{value \, of \, pH \, or \, TOC \, at \, second \, steady \, state - pH \, or \, TOC \, at \, FST}{change \, in \, the \, concentration \, of \, H_2O_2} \tag{5.2}$$

The transfer function of a first order plus time delay is expressed as:

$$G(s) = \frac{Ke^{-\theta s}}{\tau s + 1} \tag{5.3}$$

The fifth step was to confirm the transfer function of the response of both the pH and TOC by Matlab software. Matlab transfer function checking was done as follows:

1- Transferring the response data from Excel to Matlab.
2- As the time of the response data begins at the time of step change, the data are modified to correspond to zero time.
3- Matlab is used to draw the transfer functions that were extracted graphically from the pH and TOC responses.
4- The transfer function parameters were modified manually in order to get a better fit of the response data.

   This method was used to extract transfer functions in the Laplace domain, to represent the response data.

For the low concentration of 60.0 mg PVA/L, a transfer function of the effluent pH response was constructed for a step change in the inlet concentration of H_2O_2 from 1.0 to 5.0 [H_2O_2]/ [PVA] and

1.0 to 0.2 [H₂O₂]/[PVA]. The fraction [H₂O₂]/[PVA] is a weight to weight ratio of hydrogen peroxide to polyvinyl alcohol polymer.

5.1.1. Transfer Function of low concentration of 60.0 mg PVA/L system

5.1.1.1. Step change from 1.0 to 5.0 [H₂O₂]/[PVA], Test # 1

Three parameters of a first order plus time delay (FOPTD) transfer function were determined. The process gain defined as the change in the output response of the pH divided by a change in the hydrogen peroxide mass flow rate into the reactor from a step change. The process gain was measured to be:

$$K = -80.0 \frac{pH.Min}{g\ H_2O_2}$$

The time constant was graphically determined by marking the 63.2 % of the total pH output response, starting from the moment the system begins to depart from the first steady state until the output response reaches a plateau. For this specific experiment, the time constant of the FOPTD was found to be 15.0 minutes. The third parameter of the FOPTD transfer function was the time delay. It was estimated from the time of the step change to the time when the output begins to depart from the first steady state. The time delay was estimated to be about 8 minutes. Although an output TOC measurement for this specific run was not performed for a low concentration of 60.0 mg PVA/L, other experiments concluded that the TOC values increased as pH values decreased when the concentration of hydrogen peroxide passed from 1.0 to 5.0 mass ratio of hydrogen peroxide to PVA. Figure 5.1 illustrates the FOPTD graphical estimation of test 1.
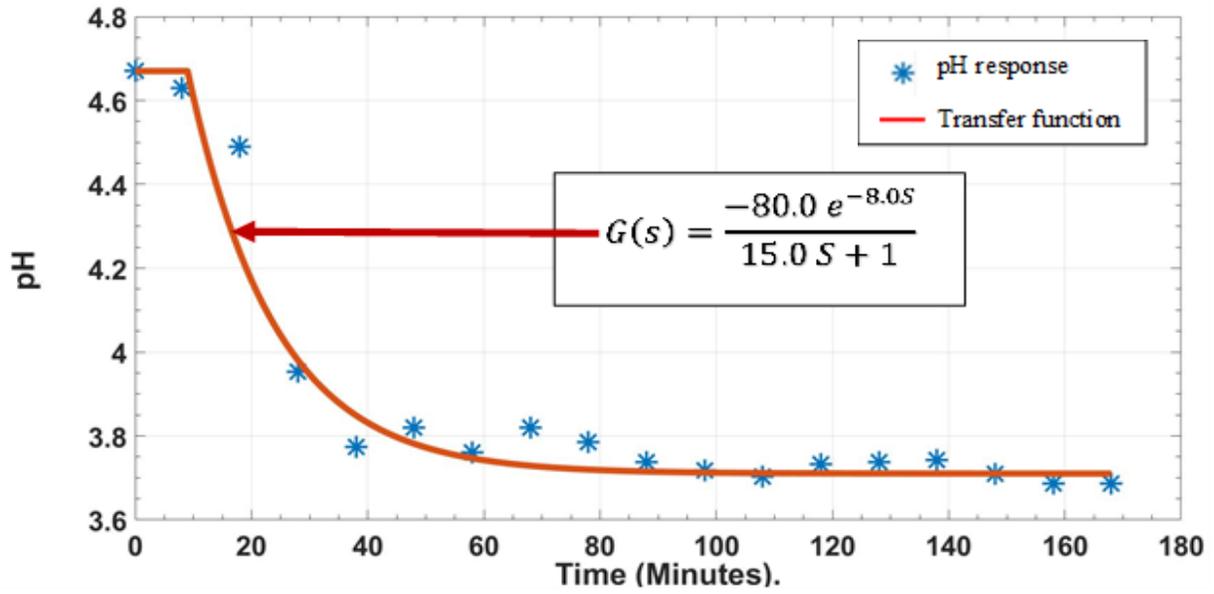
Figure 5.1. pH response versus time, for a step change from 1.0 to 5.0 [H₂O₂]/ [PVA];

[PVA]₀ = 60 mg PVA/L.

A replicate of the first test resulted in a FOPTD Transfer Function that is similar to the transfer function of test 1 first test. The process gain is:

$$K = -81.67 \frac{pH.min}{g\ H_2O_2}$$

with a time constant of 13.2 minutes, and a time delay of 8.0 minutes. Although the first point of the influent PVA solution are not identical as was anticipated, the pH response followed a very similar FOPTD transfer function.
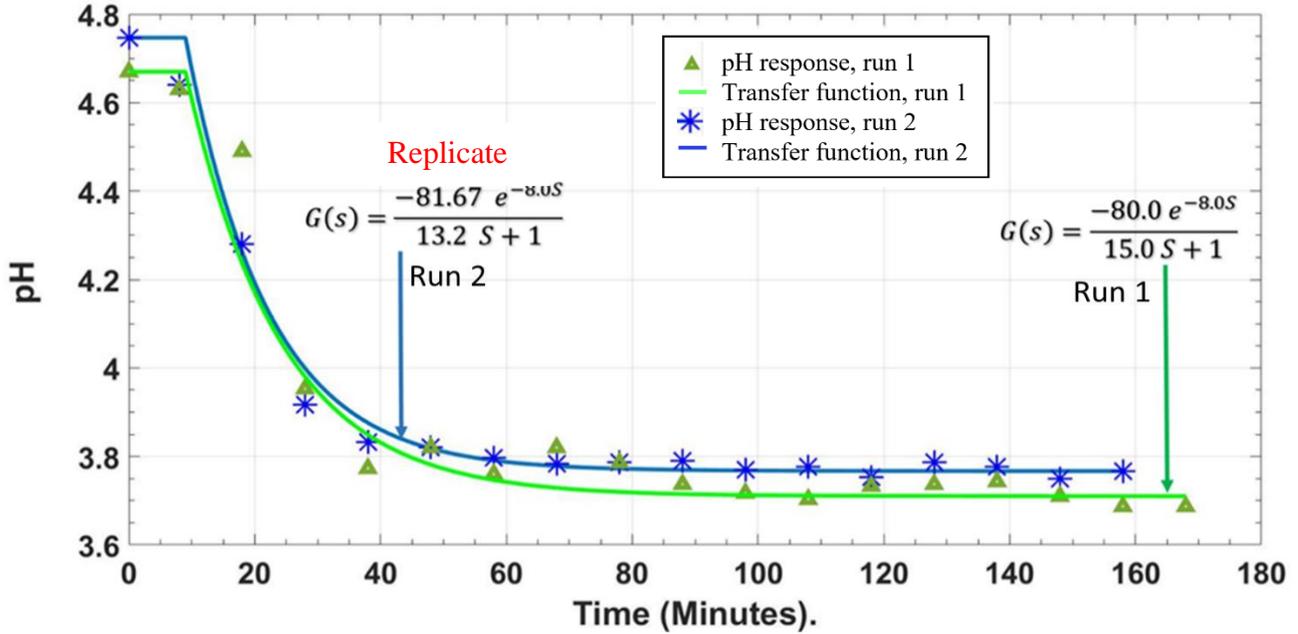
Figure 5.2. Replicate of pH response versus time, for a step change from 1.0 to 5.0 [H₂O₂]/ [PVA]; [PVA]$_0$ = 60 mg PVA/L.

5.1.1.2. Step change from 1.0 to 0.20 [H₂O₂]/[PVA], Test # 2

When combining the pH responses of 60.mg step change of 1.0 to 0.20 [H₂O₂]/ [PVA], where

$$\frac{[H_2O_2]}{[PVA]} \; is \; in \; units \; of \; \frac{g \; H_2O_2/min}{g \; PVA/min}$$

For test # 2, a step change of 1.0 to 0.20 mass ratio of hydrogen peroxide to PVA concentration the graphical technique was used to determine the three parameters of a FOPTD transfer function. The gain was determined to be:

$$K = -320.83 \frac{pH.min}{g \; H_2O_2}$$

A time constant of 22 minutes and a delay time of 8 minutes were obtained. The replicate had the same time delay as was anticipated, but with a slightly different time constant of 20.0 minutes, and a process gain:

$$K = -258.33 \frac{pH.min}{g\ H_2O_2}$$

The TOC removal increases as the hydrogen peroxide concentration is decreased.

Figure 5.3 presents the pH output response in test # 2 and its replicate with a FOPTD model representing both.
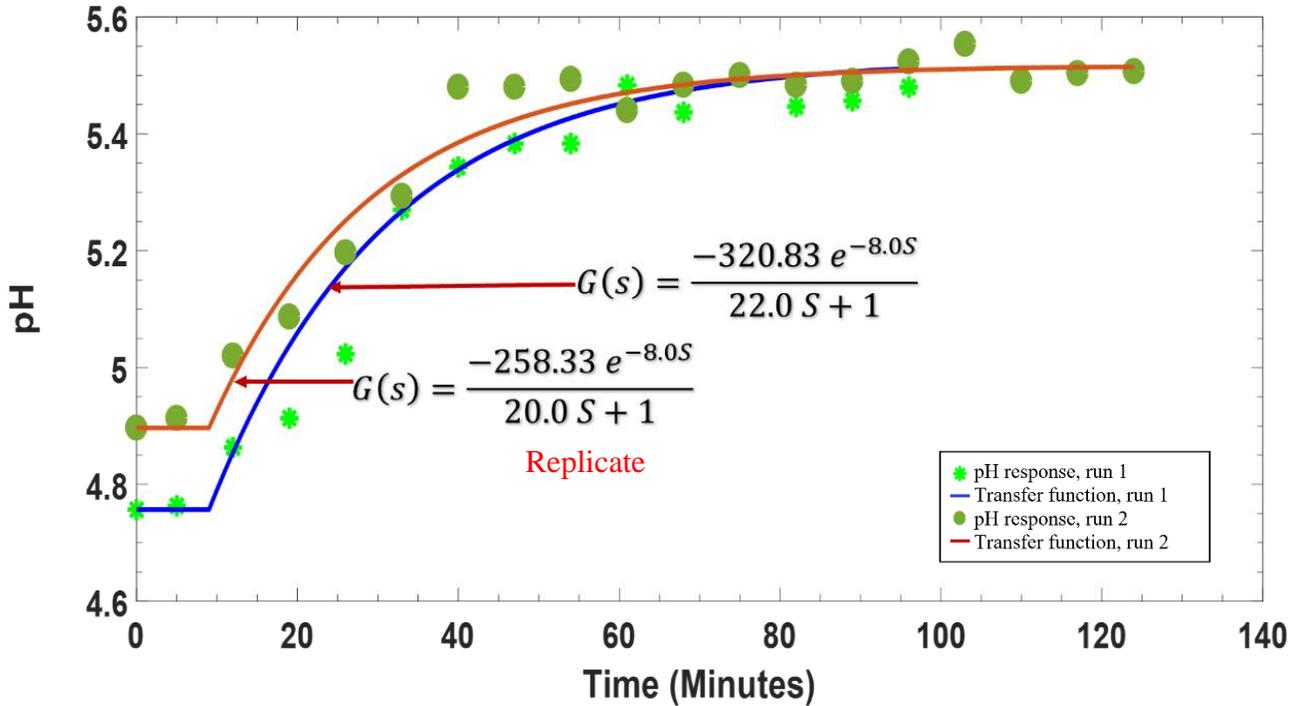
Figure 5.3. Replicate of pH response versus time for a step change from 1.0 to 0.20 [H₂O₂]/ [PVA]; [PVA]₀ = 60 mg PVA/L.

5.1.2. Transfer function of average concentration of 280.0 mg PVA/L system
5.1.2.1 Step change from 1.0 to 5.0 [H₂O₂]/[PVA], Test # 3

As hydrogen peroxide mass flow rate increases for the average concentration of 280 mg PVA/L, the pH value decreases from the first steady state value. The TOC value of the measured PVA effluent samples are anticipated to increase and as a result the TOC removal decreases. A FOPTD transfer function was determined for the average concentration of 280.0 mg PVA/L, a step change

from 1.0 to 5.0 mass ratio between hydrogen peroxide and PVA. The time constant was determined to be 12 minutes from the time the process response departs from the first steady state until it reaches the 63.2 % of the total response. The process gain for this test was determined to be:

$$K = -25.4 \frac{pH.Min}{g\ H_2O_2}$$

Lastly a delay time of 8.0 minutes was determined for this FOPTD model. Figure 5.4 illustrates the FOPTD transfer function prediction in solid line and the pH response data in star symbols.

$$G(s) = \frac{-25.357e^{-8.0S}}{12.0\ S + 1}$$
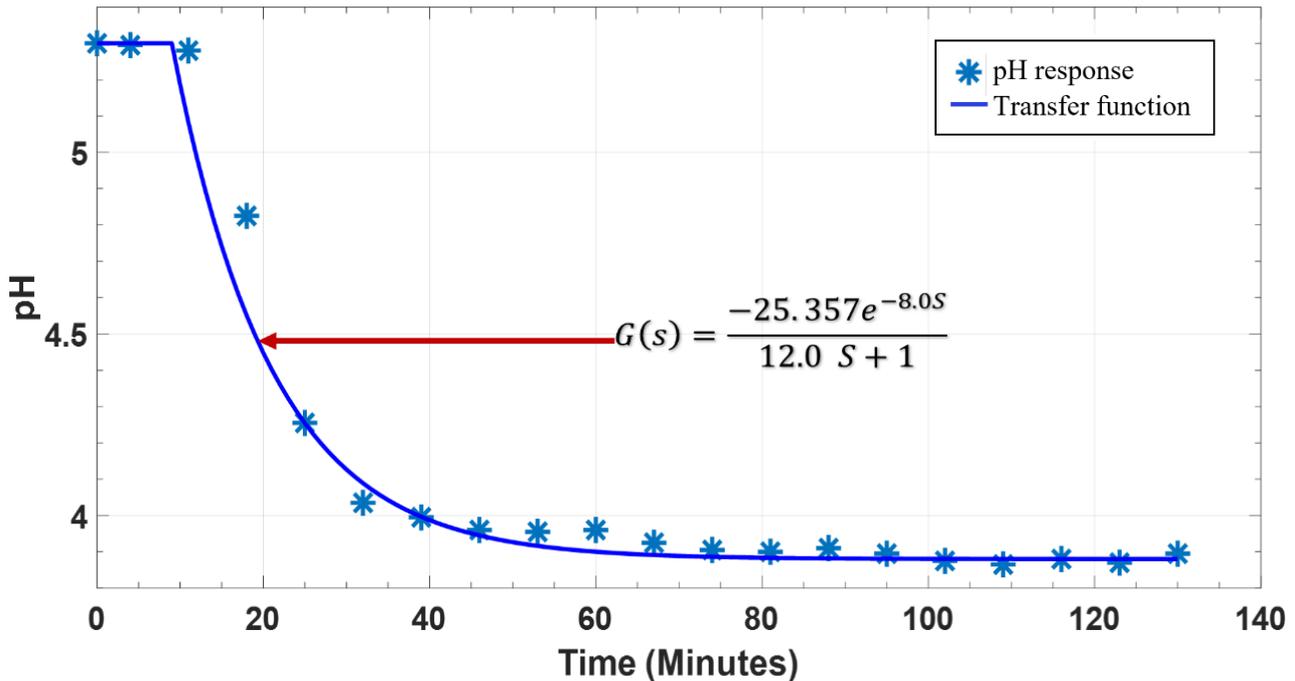
Figure 5.4. pH response versus time for a step change from 1.0 to 5.0 [H₂O₂]/[PVA];

[PVA]₀ = 280.0 mg PVA/L.

It was noticed that the TOC content in the PVA effluent samples increases above the initial steady state as the pH response data decreases from the first steady state plateau. Although the TOC response data was estimated by a FOPTD transfer function, the TOC response data appears to follow the trend of higher order transfer function. The gain was determined to be:

$$K = 3089 \frac{TOC\ (ppm).Min}{g\ H_2O_2}$$

The time constant was determined to be 27 minutes and a time delay of 8 minutes. Figure 5.5 illustrates the proposed FOPTD model for the TOC response of 280.0 mg PVA/L, step change

47

from 1.0 to 5.0 [H$_2$O$_2$]/[PVA]. TOC measurements vary significantly, and the FOPTD model cannot predict all the TOC response data properly.
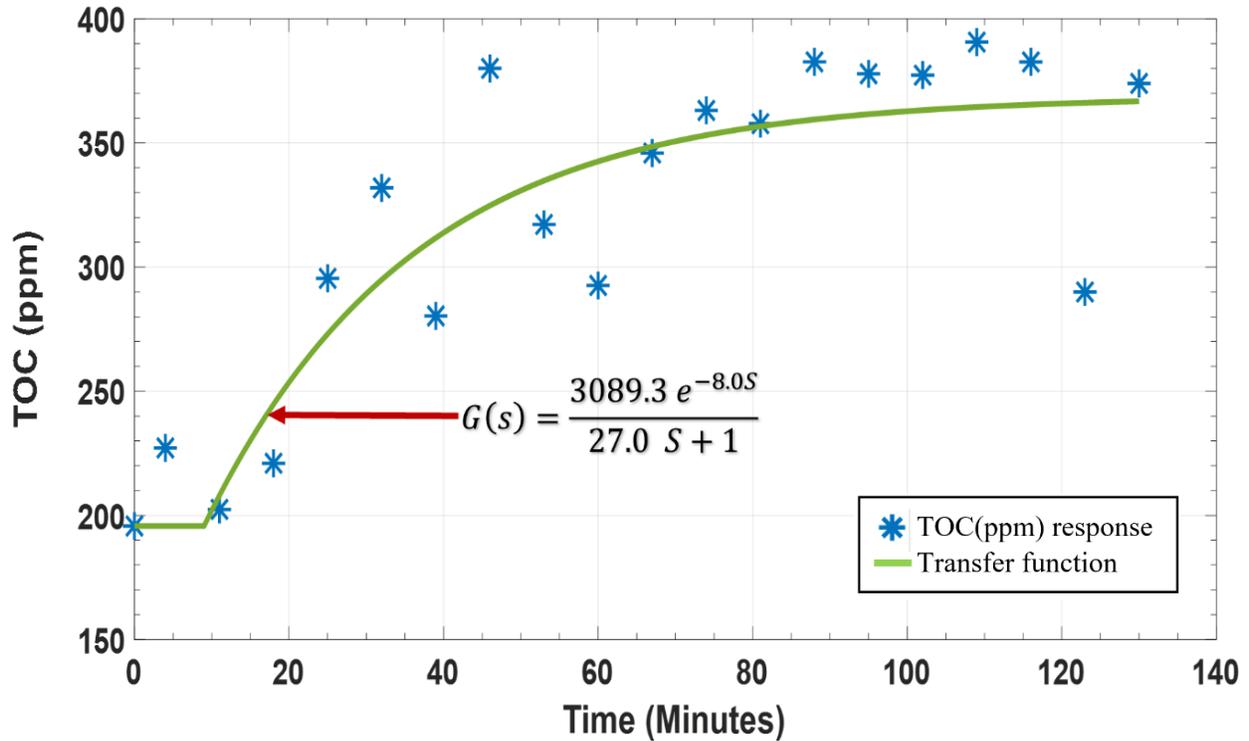
Figure 5.5. TOC (ppm) response versus time for a step change from 1.0 to 5.0 [H$_2$O$_2$]/[PVA]; [PVA]$_0$ = 280.0 mg PVA/L.

Figure 5.6 shows the inverse proportionality between the pH and TOC of the same effluent samples of test 3. As the TOC response of the average PVA concentration is over imposed on the pH response, an inversely proportional relationship between the pH values of the measured effluent samples and the TOC (ppm) values of the same samples was observed. As more TOC is produced, the solution becomes more acidic.

- pH and TOC (ppm) versus. time (min):
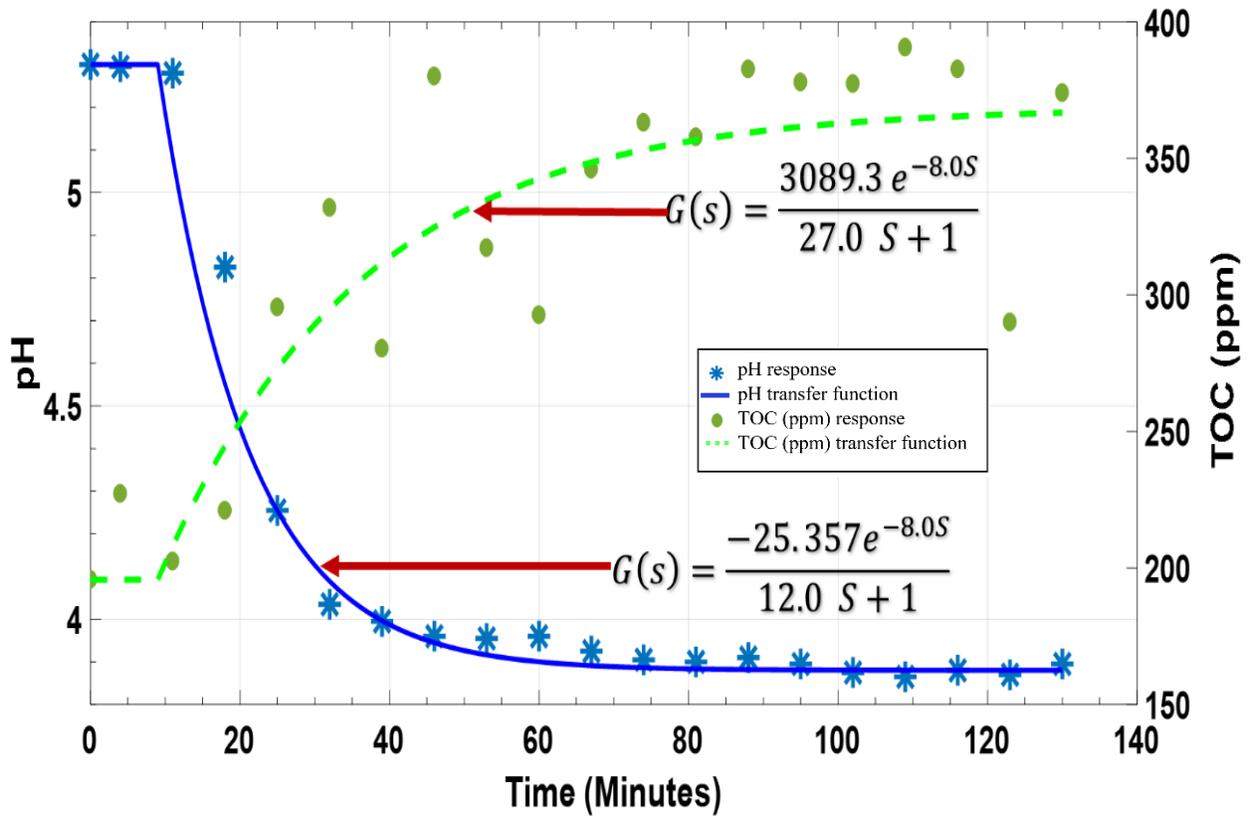
Figure 5.6. pH and TOC (ppm) response data versus time for a step change from 1.0 to 5.0 [H$_2$O$_2$]/[PVA]; [PVA]$_0$ = 280.0 mg PVA/L.

5.1.2.2. Step change from 1.0 to 0.20 [H$_2$O$_2$]/[PVA], Test # 4

The first data point of the pH must be a measurement error. The time constant and time delay both were estimated to be 49 and 8 min, respectively, and the process gain is given by:

$$K = -35.5 \, \frac{pH.\,Min}{g \, H_2O_2}$$

Figure 5.7 shows the pH experimental data and the model prediction.

■   pH vs. Time

$$G(s) = \frac{-35.54\,e^{-8.0S}}{49.0\,S + 1}$$
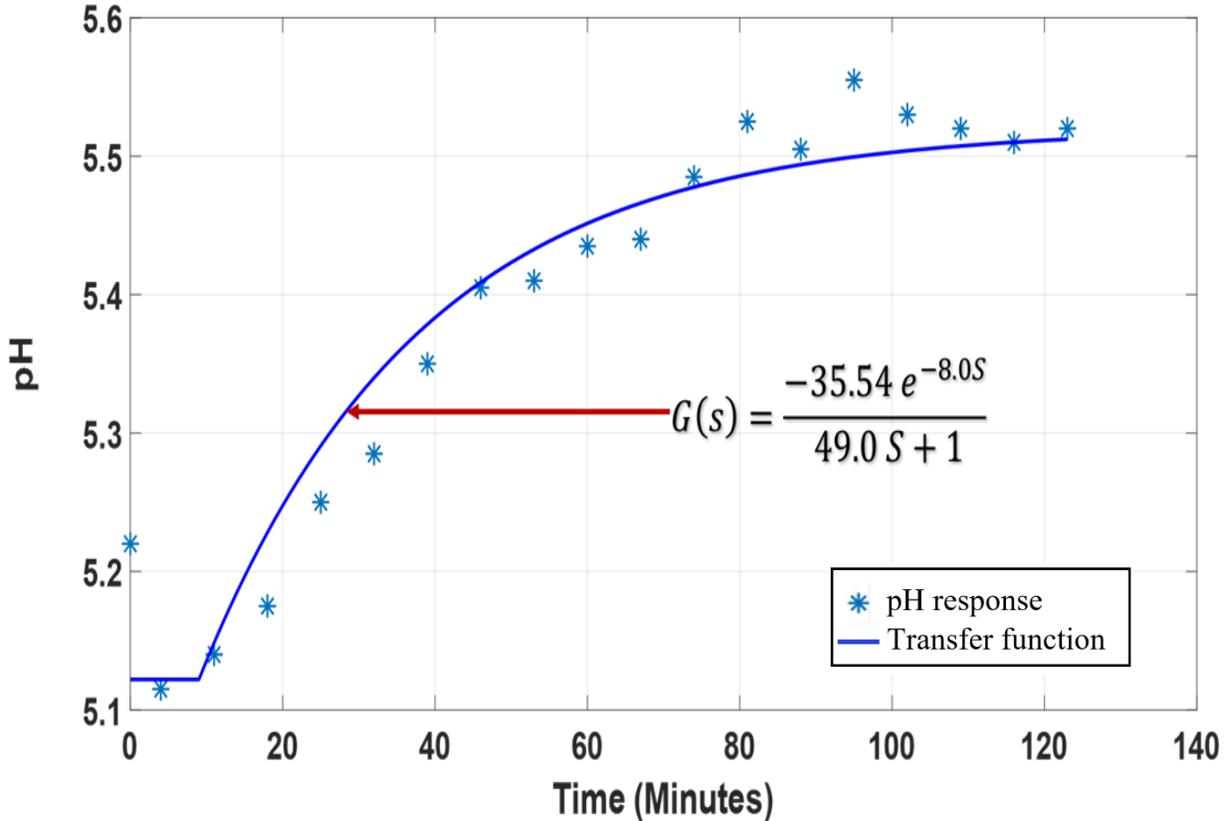
Figure 5.7. pH response data versus time for a step change from 1.0 to 0.20 $[H_2O_2]/[PVA]$; $[PVA]_0 = 280.0$ mg PVA/L.

Figure 5.8 shows TOC response to a step change in hydrogen peroxide from 1.0 to 0.20 $[H_2O_2]/[PVA]$ for an average concentration of 280 mg PVA/L. The TOC response was determined for a change in hydrogen peroxide mass flow rate. A time constant of 23 minutes and a time delay of 8 minutes were determined. An accurate TOC response of a step change from 1.0 to 0.20 would be accurately presented as a higher order and can be determined using the system identification in Matlab. In this test, the measured data of the TOC response are very noisy. It is very likely that the TOC variations are due to measurement errors. The TOC process gain is:

$$K = 5803.6\ \frac{TOC\ (ppm).\,Min}{g\ H_2O_2}$$
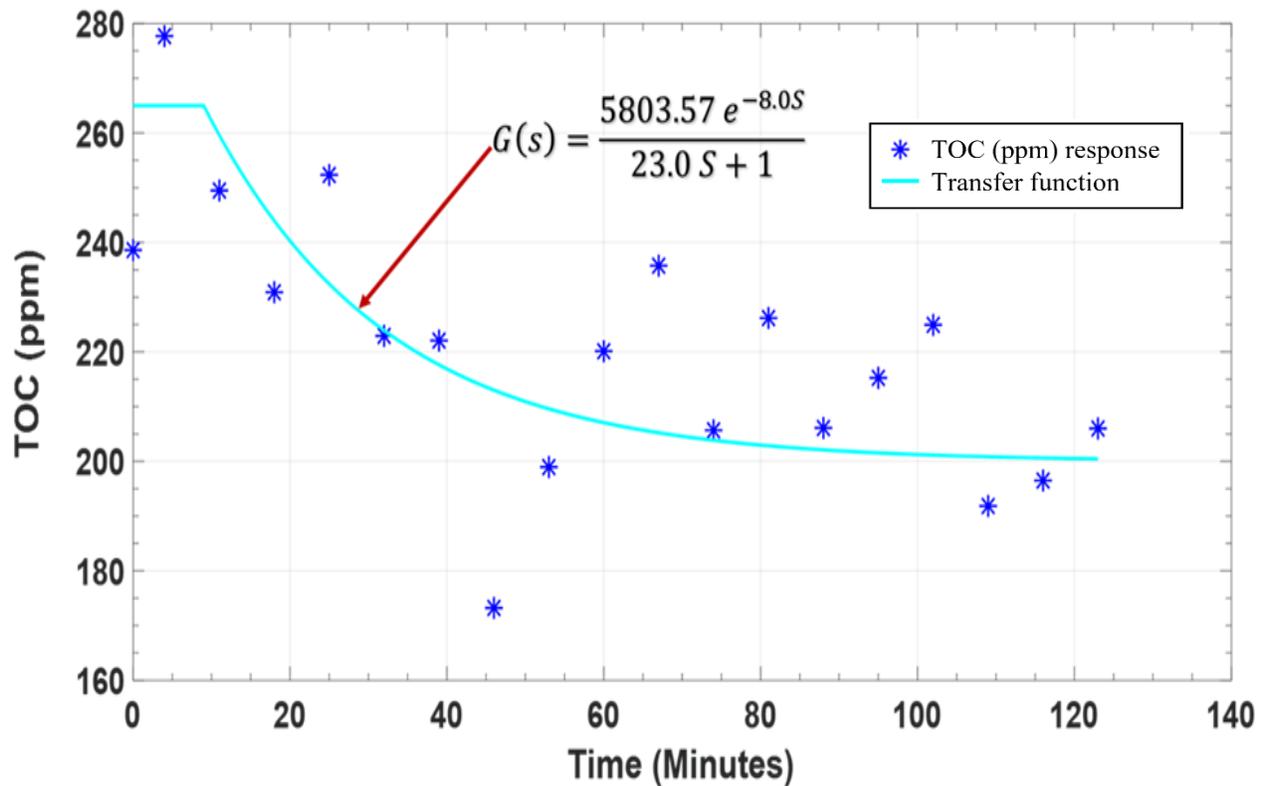
Figure 5.8. TOC (ppm) response data versus time for a step change from 1.0 to 0.20 [H$_2$O$_2$]/[PVA]; [PVA]$_0$ = 280.0 mg PVA/L.

In the average PVA concentration, the hydrogen peroxide is decreased of the step test of 1.0 to 0.20 mass ratio, the pH value increases and the TOC values decrease. This specific test caused an increase in the TOC removal. This test is a good example of ending a scavenging effect of H$_2$O$_2$ by decreasing the amount of H$_2$O$_2$ flowing into the reactor. The TOC removal has increased in the post step change reaction time. Figure 5.9 illustrates the relation of increasing TOC removal, when pH eluent values approaches neutral pH value of 7.0.
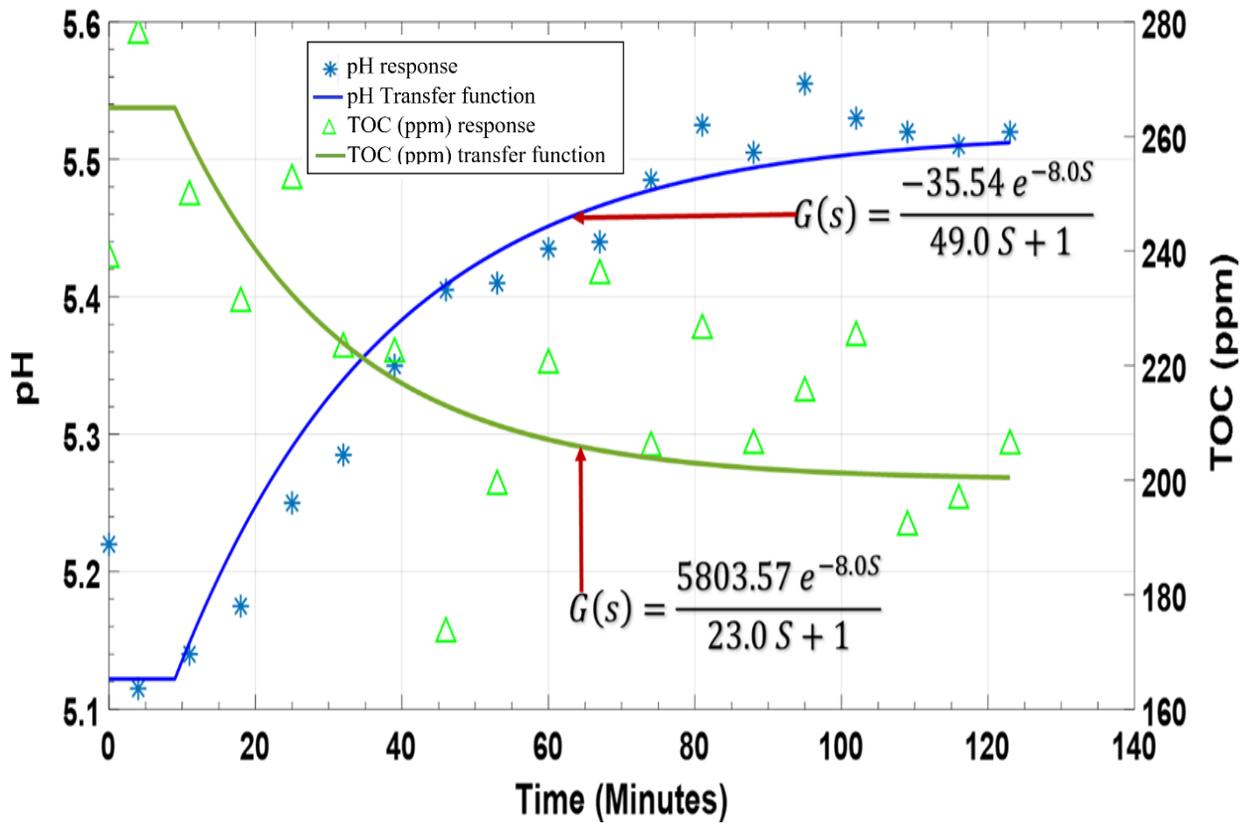
Figure 5.9. pH and TOC (ppm) response data versus time for a step change from 1.0 to 0.20 [H_2O_2]/[PVA]; [PVA]$_0$ = 280 mg PVA/L.

5.1.2.3. Step change from 0.12 to 0.024 [H₂O₂]/[PVA], Test # 5

Using a PVA concentration 280.0 mg PVA/L, Figure 5.10 shows the pH response for a step change of hydrogen peroxide mass flow rate into the reactor from 0.12 to 0.024. The transfer function below was determined using the 63.2% method:

$$G(s) = \frac{-137.65 \, e^{-8.0S}}{34.0 \, S + 1}$$

For a very low hydrogen peroxide concentration between 0.024 and 0.12 (mass ratio basis), the FOPTD is not a good fit for the pH response data. The pH response data can be better represented by an underdamped model.
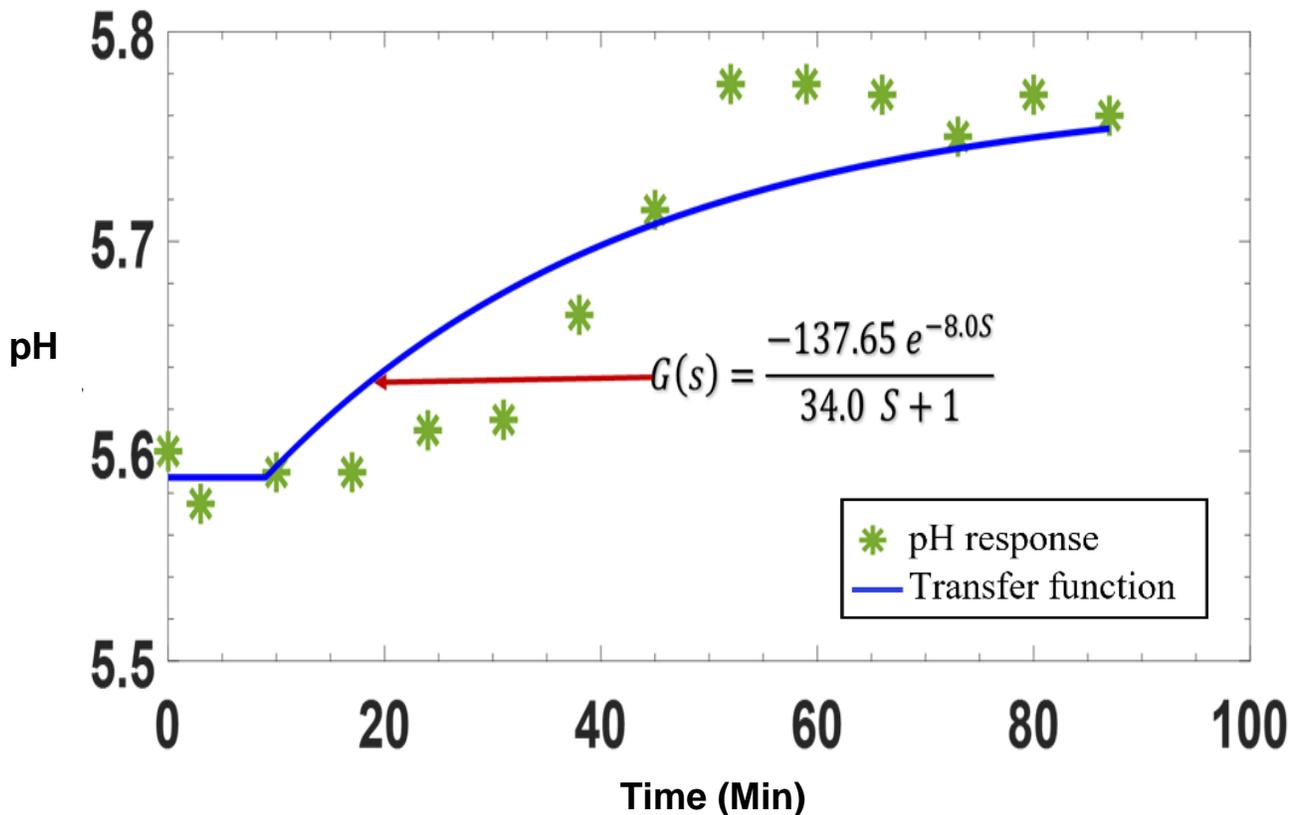
Figure 5.10. pH response data points versus time for a step change from of 0.12 to 0.024 [H₂O₂]/ [PVA]; [PVA]₀ = 280 mg PVA/L.

The Matlab graphical testing of the FOPTD transfer function over the pH response data points, the graphical transfer function was drawn under the data points. The time constant τ, was altered to

correct the transfer function until the transfer function was flowing throw the pH response data points. The final transfer function that presented the data pointes was:

$$G(s) = \frac{-137.65 \, e^{-20.0S}}{20.0 \, S + 1}$$

The FOPTD model best fitting the pH response data is illustrated in figure 5.11 in solid light green line.
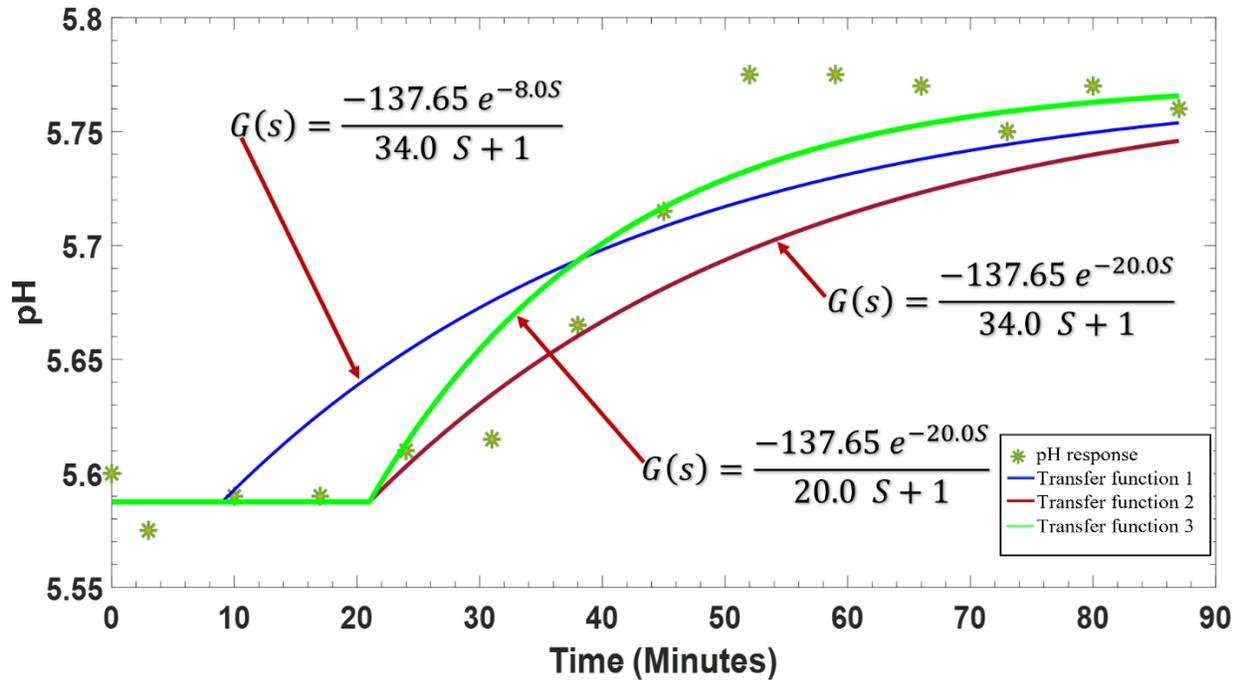
Figure 5.11. pH response data points vs time for a step change from 0.12 to 0.024 [H_2O_2]/ [PVA]; [PVA]$_0$ = 280.0 mg PVA/L.

Increasing the time delay from 8 minutes to 20 minutes to make up for the higher order property of the transfer function, resulted in a process gain of

$$K = -137.65 \frac{pH.Min}{g \, H_2O_2}$$

A time constant of 20 minutes and a delay time of 20 minutes. Figure 5.12 presents the final FOPTD representation of the pH response data of a 280.0 mg PVA/L with a step change from 0.12 to 0.024 [H_2O_2]/[PVA].

54
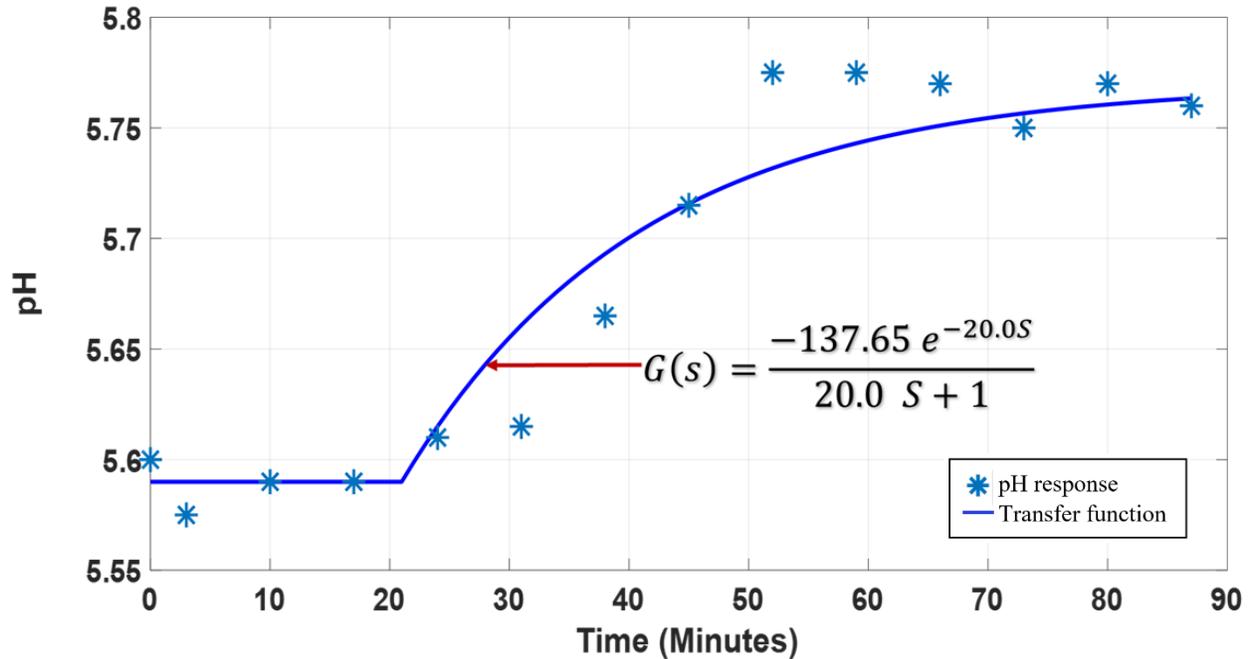
Figure 5.12. pH Response data versus time for a step change from 0.12 to 0.024 [H_2O_2]/ [PVA]; [PVA]$_0$ = 280.0 mg PVA/L.

From the average concentration of 280.0 mg PVA/L, the step change from 0.12 to 0.024 results in a higher TOC removal as the values of the effluent samples decreases and the pH response values of the PVA solution effluents increases towards the neutral pH value of 7.0.

Also, as it is apparent that as the pH response get a positive gain, the TOC (ppm), response gets a negative gain. This observation was general for all concentrations of PVA, and for all step changes that were attempted. Figure 5.13 illustrates the relation between pH response data for the 280.0 mg PVA/L with a step change from 0.12 to 0.024 [H_2O_2]/[PVA].
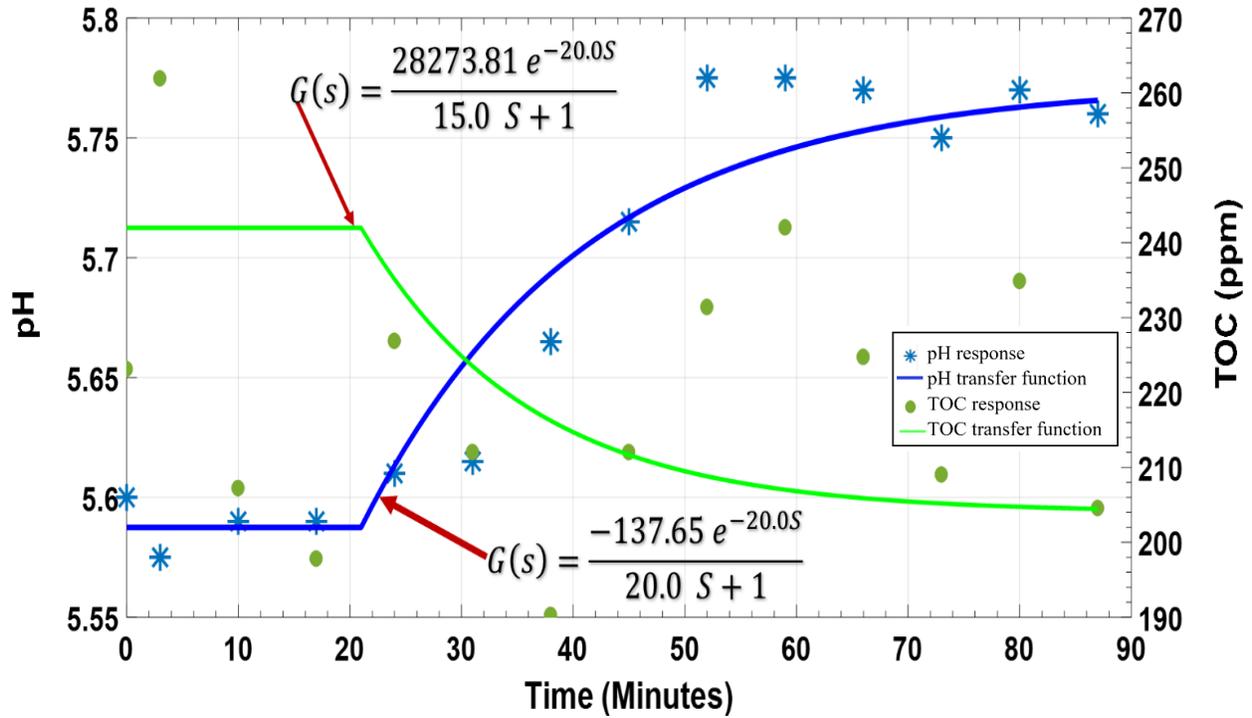
Figure 5.13. Final pH and TOC (ppm) response data versus time for a step change from 0.12 to 0.024 $[H_2O_2]/[PVA]$; $[PVA]_0 = 280.0$ mg PVA/L.

5.1.3. Transfer function of high concentration of 500.0 mg PVA/L system

5.1.3.1. Step change from 1.0 to 5.0 [H₂O₂]/[PVA], Test # 6

▪ Run 1

A FOPTD transfer function was approximated for the high concentration of PVA of 500.0 mg PVA/L with a step change from 1.0 to 5.0 [H₂O₂]/[PVA] mass ratio. The three parameters of the FOPTD transfer function was determined by a graphical method as follows:

$$K = -16.3 \frac{pH.Min}{g\ H_2O_2}$$

With a time, delay of 8 minutes and a time constant of 12 minutes. It is clear in Figure 5.14 that as the hydrogen peroxide concentration is increased, a decrease in the pH response values is observed.
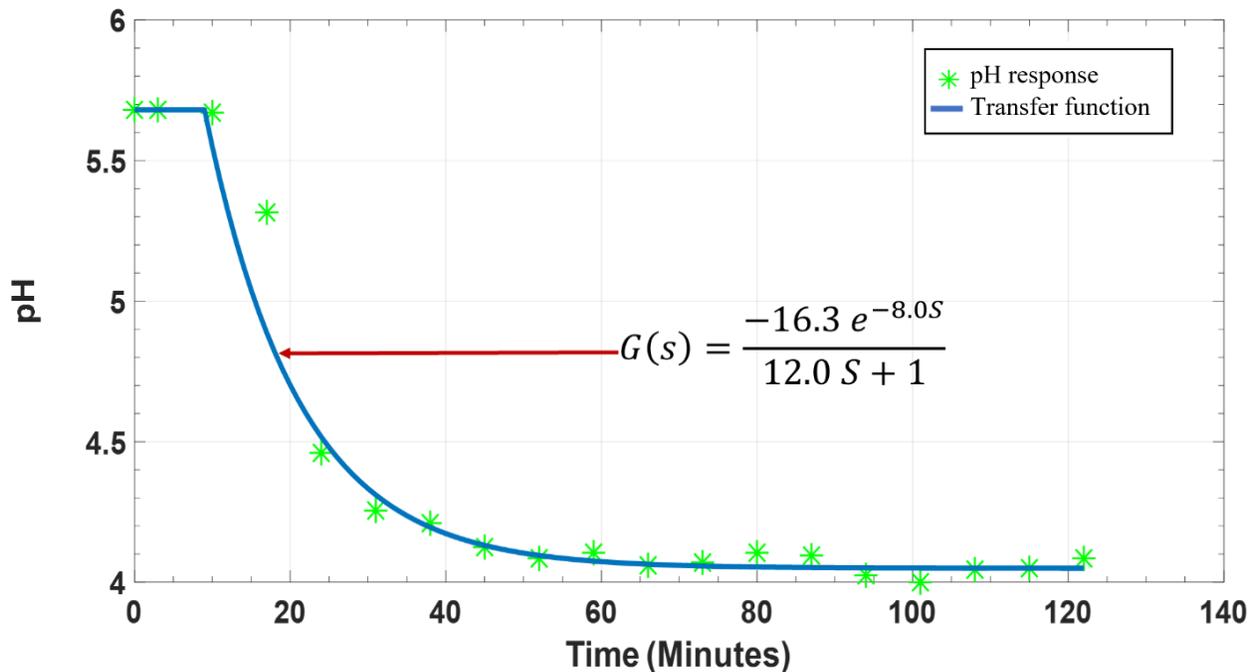
Figure 5.14. pH response data versus time for a step change from 1.0 to 5.0 [H₂O₂]/[PVA]; [PVA]₀ = 500.0 mg PVA/L.

As the pH response values decreases relative to initial steady state, the TOC values increase. The increase in TOC values results in a decrease in the TOC removal. Figure 5.15 represents the TOC response data in light blue stars and a proposed FOPTD in solid green line.

The figure contains the equation:

$$G(s) = \frac{1400.0 \, e^{-8.0S}}{19.0 \, S + 1}$$

Legend:
* TOC(ppm) response
— Transfer function
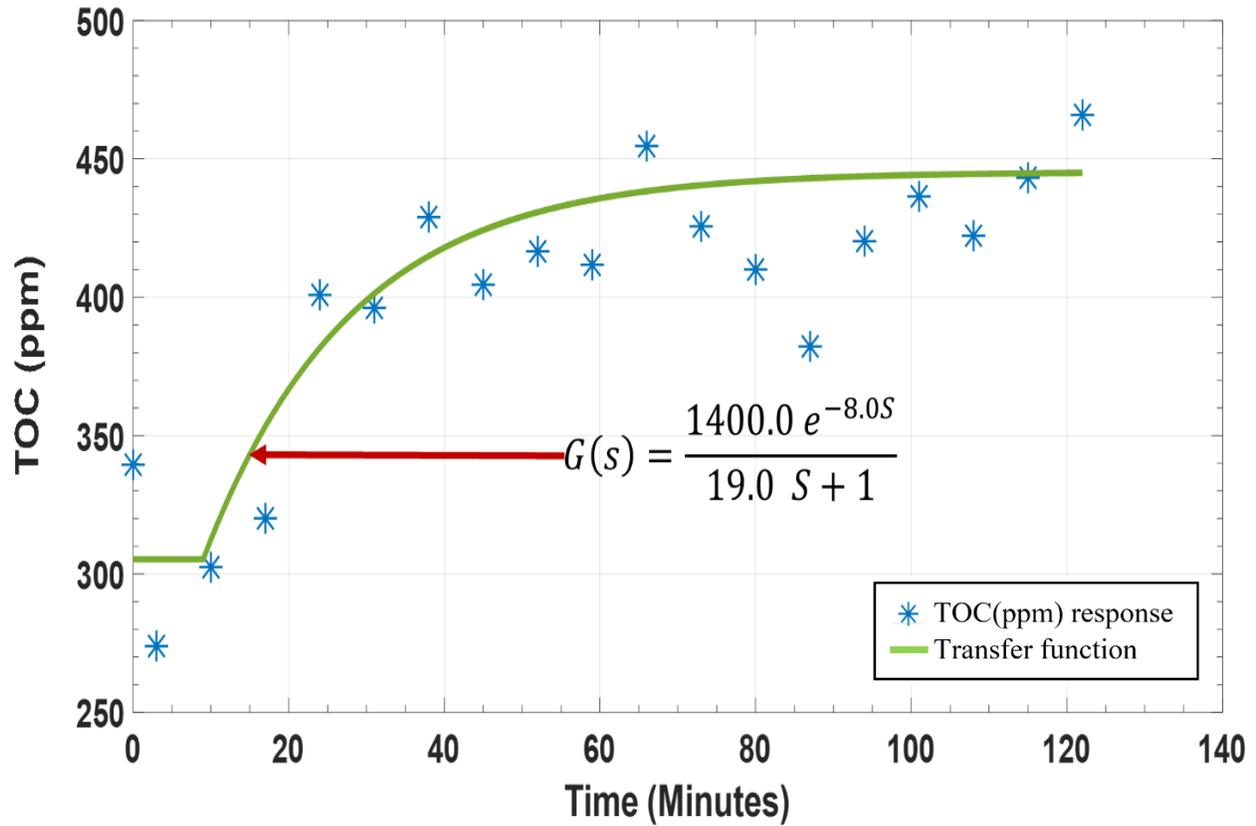
Figure 5.15. TOC (ppm) response data versus time for a step change from 1.0 to 5.0 [H$_2$O$_2$]/[PVA]; [PVA]$_0$ = 500.0 mg PVA/L.

The inverse proportionality between pH response data and its corresponding TOC response data is illustrated in figure 5.16.

The figure shows two transfer functions:

$$G(s) = \frac{1400.0\, e^{-8.0S}}{19.0\,S + 1}$$

$$G(s) = \frac{-16.3\, e^{-8.0S}}{12.0\,S + 1}$$
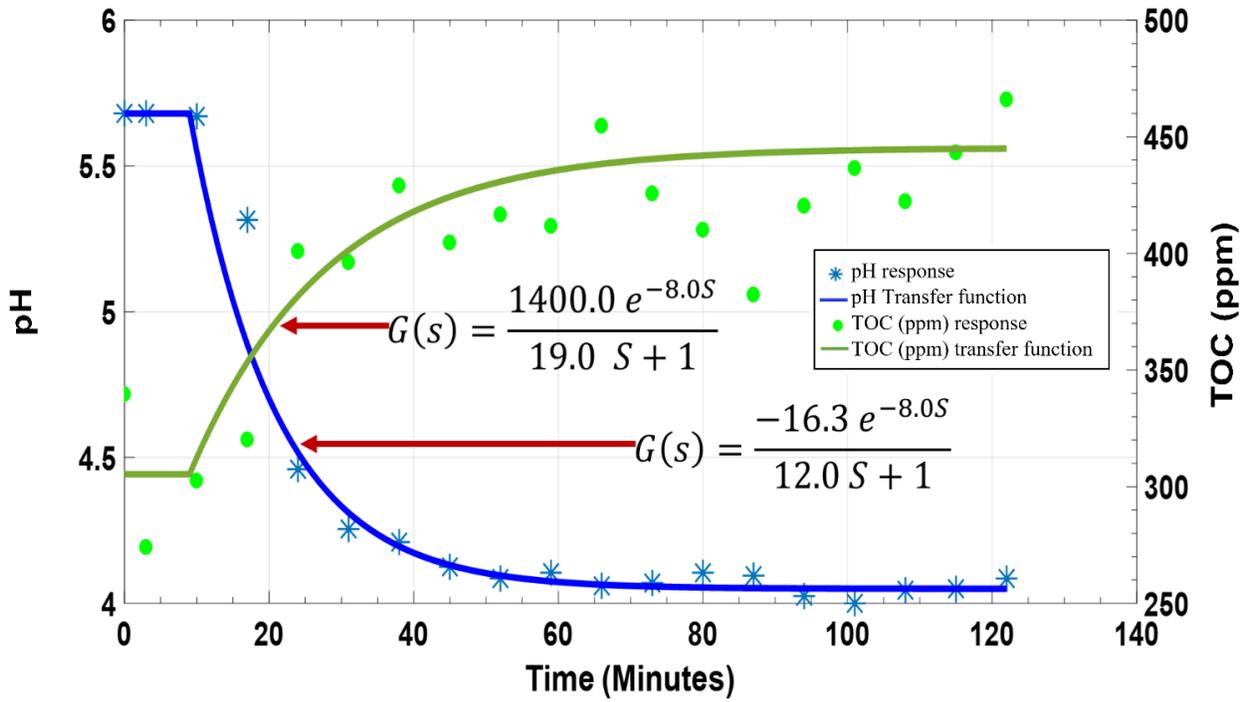
Figure 5.16. pH and TOC (ppm) response data points versus time for a step change from 1.0 to 5.0 [H₂O₂]/[PVA]; [PVA]₀ = 500 mg PVA/L.

▪ Run 2

Figures 5.17, 5.18, and 5.19 illustrate the same results as was presented in the previous figure with slight differences in the FOPTD parameters.

$$G(s) = \frac{-14.55 \; e^{-8.0S}}{10.0 \; S + 1}$$
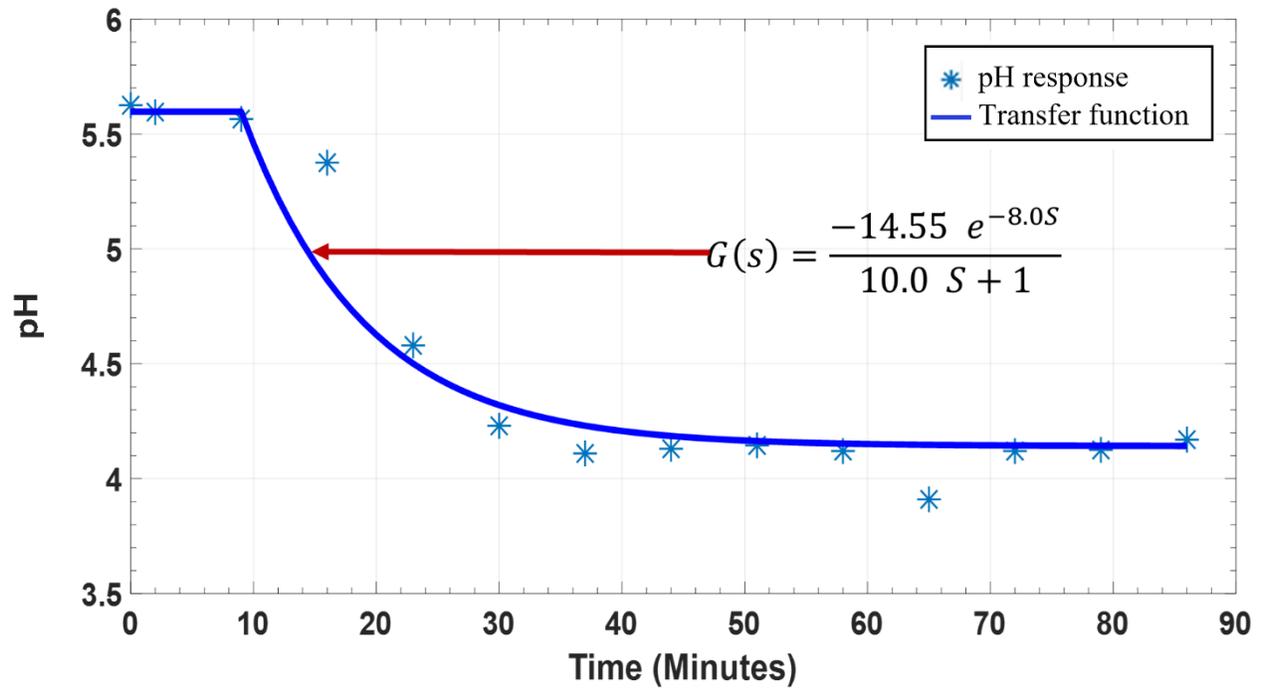
Figure 5.17. Run 2, pH response data versus time for a step change from 1.0 to 5.0 [H$_2$O$_2$]/[PVA]; [PVA]$_0$ = 500.0 mg PVA/L.
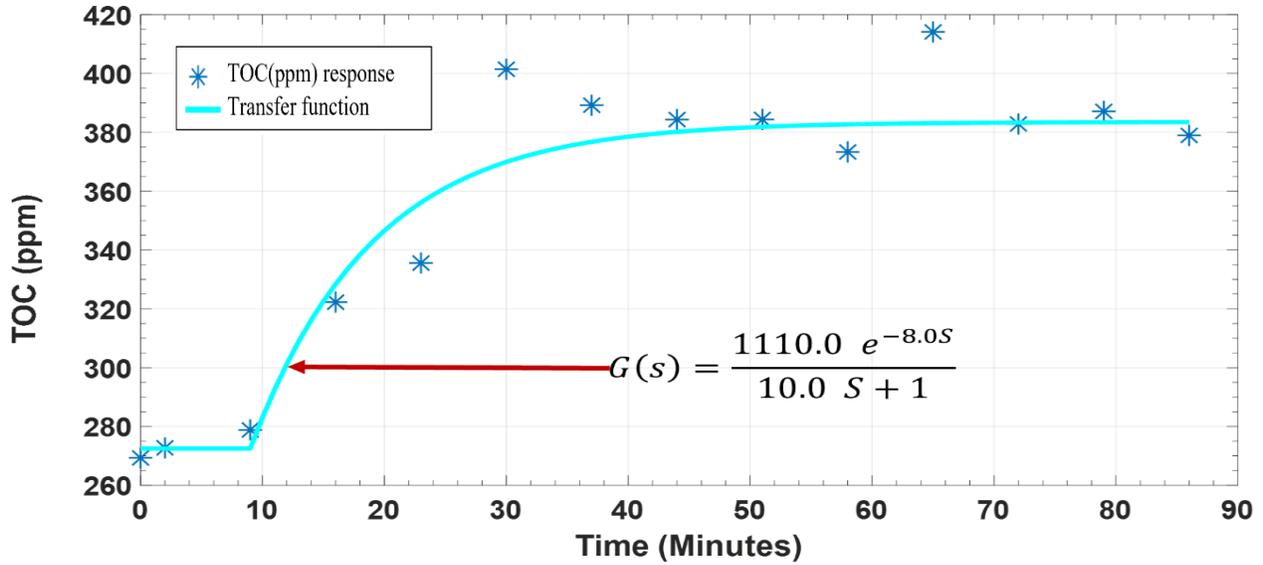
Figure 5.18. TOC (ppm) response data versus time for Run 2 with a step change from 1.0 to 5.0 [H_2O_2]/[PVA]; [PVA]$_0$ = 500 mg PVA/L.
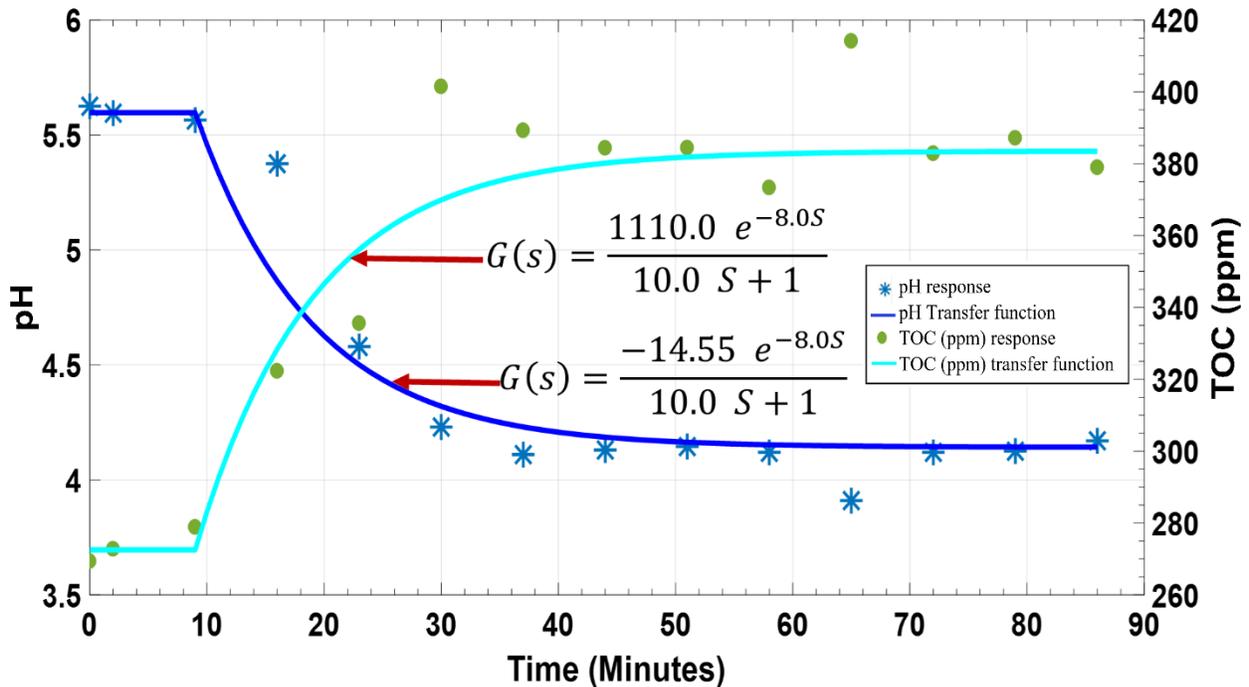
Figure 5.19. Replicate of Test #6, pH and TOC (ppm) response data versus time for a step change from 1.0 to 5.0 [H_2O_2]/[PVA]; [PVA]$_0$ = 500 mg PVA/L.

61

5.1.3.2. Step change from 1.0 to 0.20 [H₂O₂]/[PVA], Test # 7
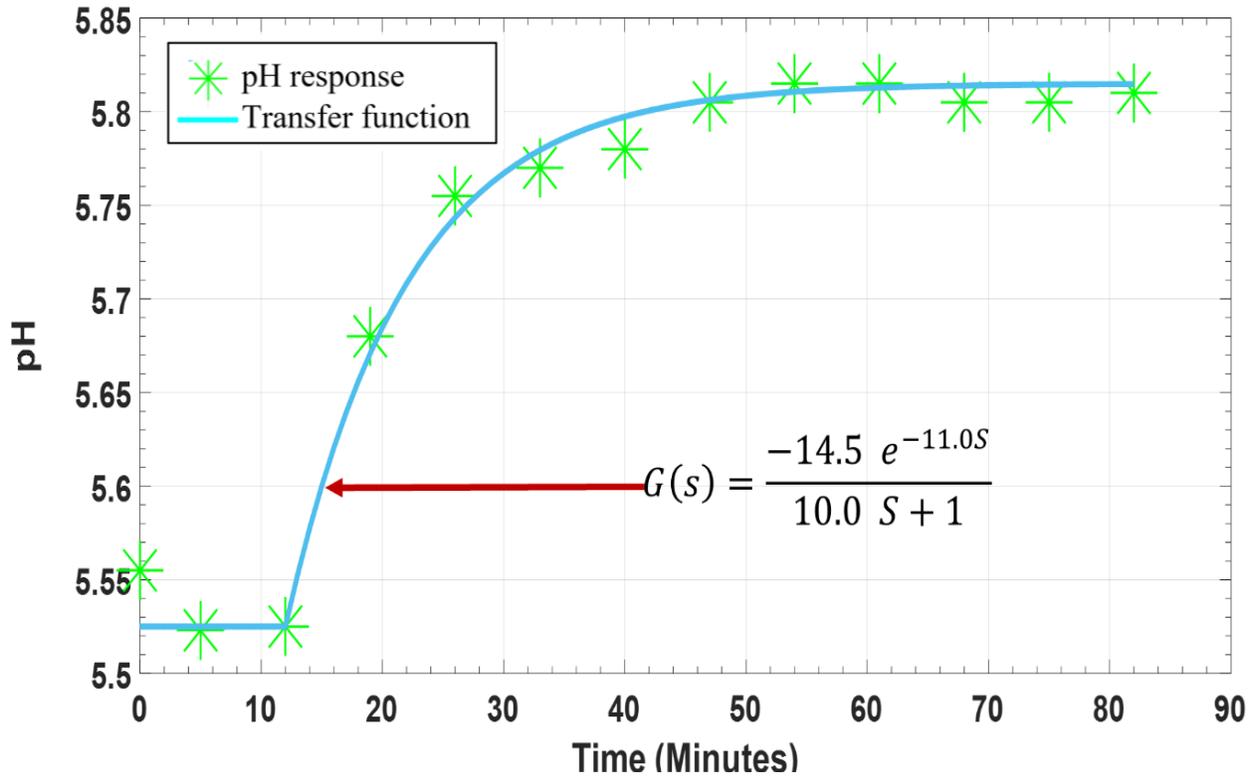
**Figure 5.20.** pH response data versus time for a step change from 1.0 to 0.20 [H₂O₂]/[PVA]; [PVA]₀ = 500.0 mg PVA/L.
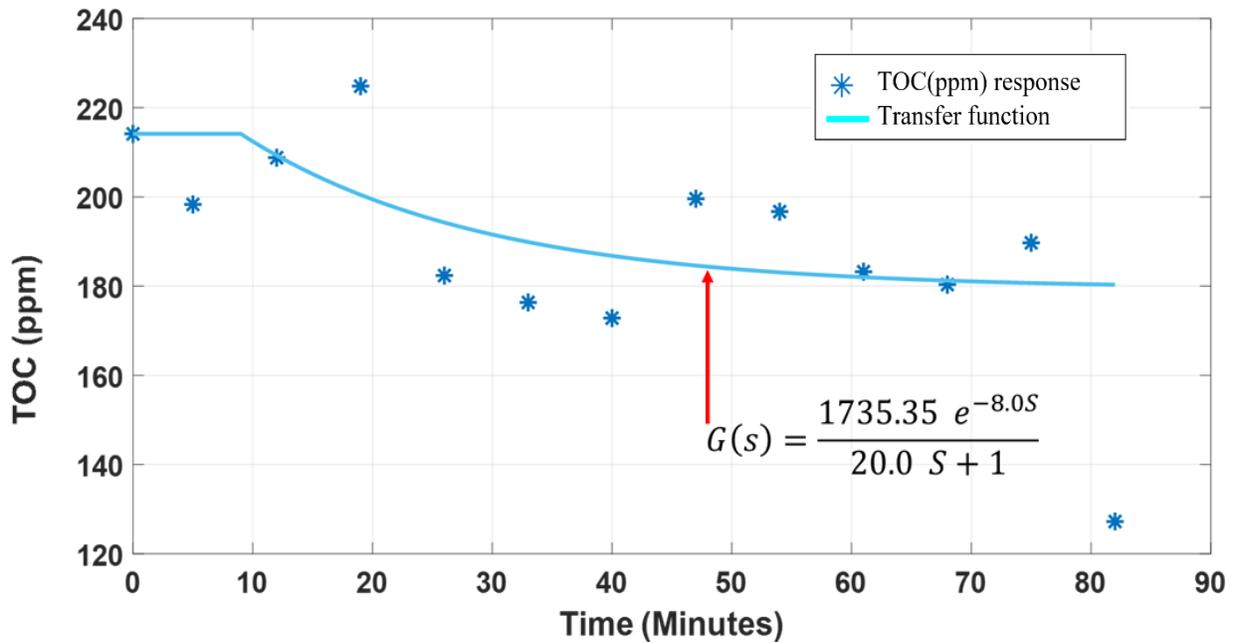
Figure 5.21. TOC (ppm) response data versus time for a step change from 1.0 to 0.20 [H₂O₂]/[PVA]; [PVA]₀ = 500.0 mg PVA/L.

A FOPTD transfer function was determined for the pH and TOC (ppm), response for the high concentration of PVA of 500.0 mg PVA/l. A step change of 1.0 to 0.20 mass ratio of hydrogen peroxide to PVA was applied. A process gain of

$$K = 14.5 \; \frac{pH.min}{g \; H_2O_2}$$

and

$$K = 1735.4 \; \frac{TOC \; (ppm).min}{g \; H_2O_2}$$

Of the pH and TOC response respectively. The time constant was 10 and 20 minutes and a time delay of 11 minutes for both FOPTD of 500.0 mg PVA/L, step change from 1.0 to 0.20 [H$_2$O$_2$]/[PVA]. Figure 5.22 illustrates the scavenging effect of H$_2$O$_2$, as the concentration decreases of hydrogen peroxide the TOC removal increases as the pH response data approaches the neutral pH value of 7.0 and the TOC values of the effluent samples decreases until it reaches the second steady state anticipated plateau.

$$G(s) = \frac{1735.35 \; e^{-11.0S}}{20.0 \; S + 1}$$

$$G(s) = \frac{14.5 \; e^{-11.0S}}{10.0 \; S + 1}$$

Legend:
* pH response
— pH Transfer function
● TOC (ppm) response
— TOC (ppm) transfer function
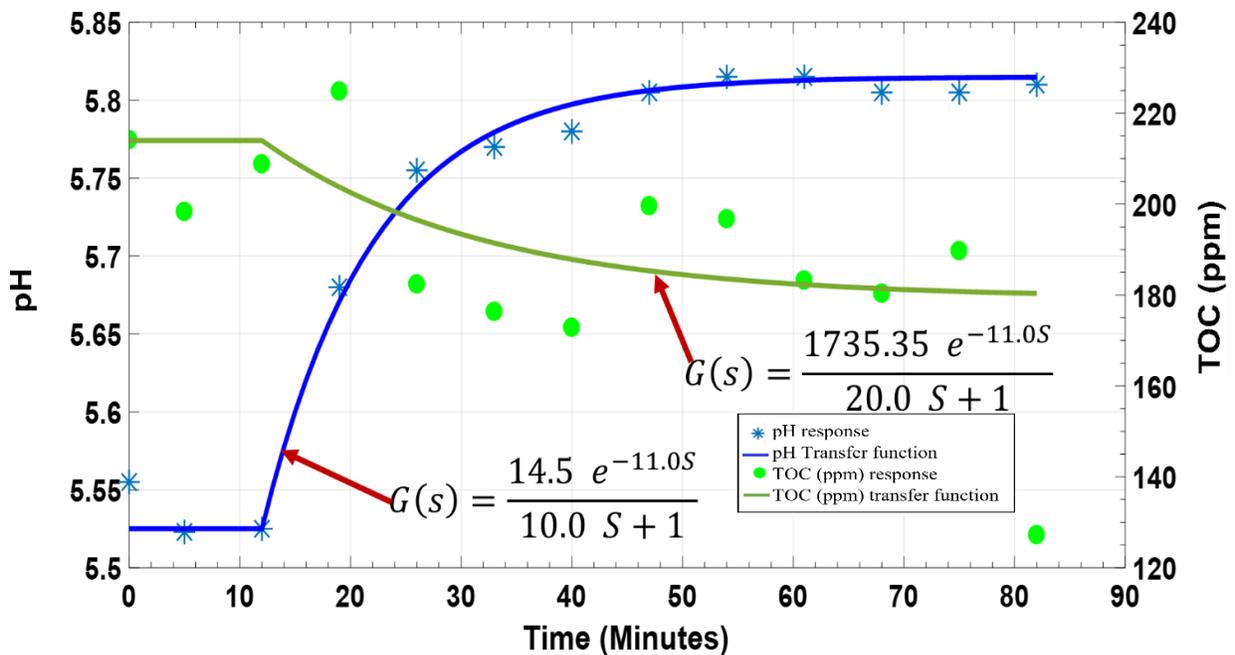
Figure 5.22. pH and TOC (ppm) response data versus time for a step change from 1.0 to 0.20 [H$_2$O$_2$]/[PVA]; [PVA]$_0$ = 500.0 mg PVA/L.

■ **Replicate 500.0 mg PVA/L, step change from 1.0 to 0.20 [H₂O₂]/[PVA]**
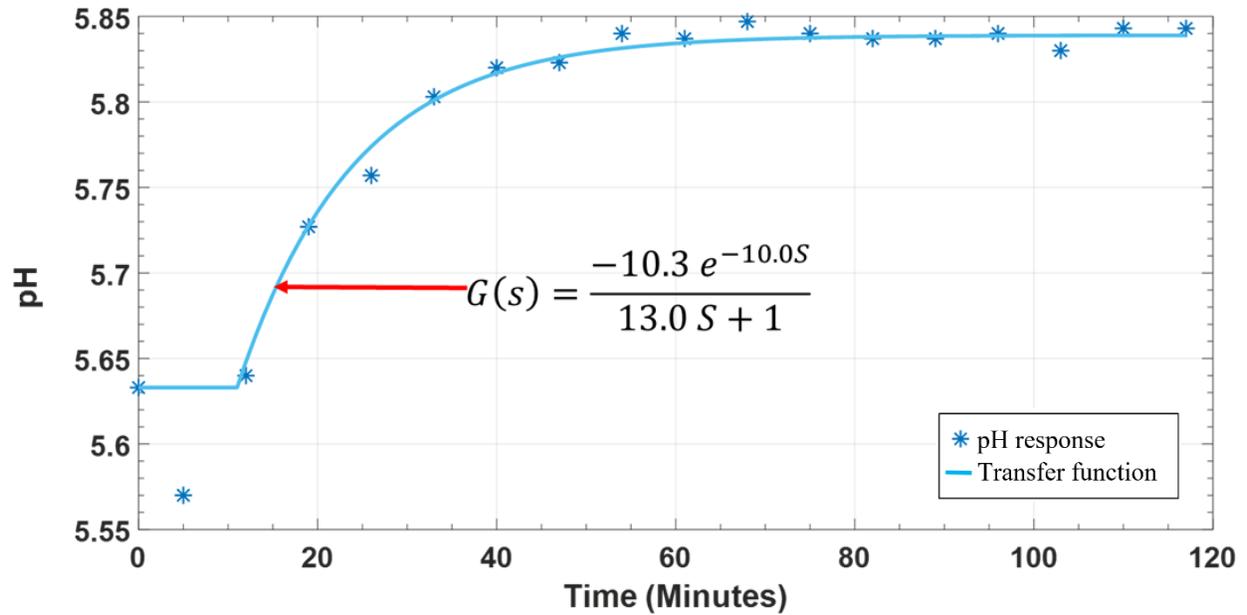
Figure 5.23. Replicate, pH response data versus time for a step change from 1.0 to 0.02 [H₂O₂]/[PVA]; [PVA]$_0$ = 500.0 mg PVA/L.

A replicate was established for a step change of 1.0 to 0.20 [H₂O₂]/[PVA], and the three parameters of the FOPTD transfer function was determined. A process gain of

$$K = 10.3 \; \frac{pH.min}{g \; H_2O_2}$$

and

$$K = 2900 \; \frac{TOC \; (ppm).min}{g \; H_2O_2}$$
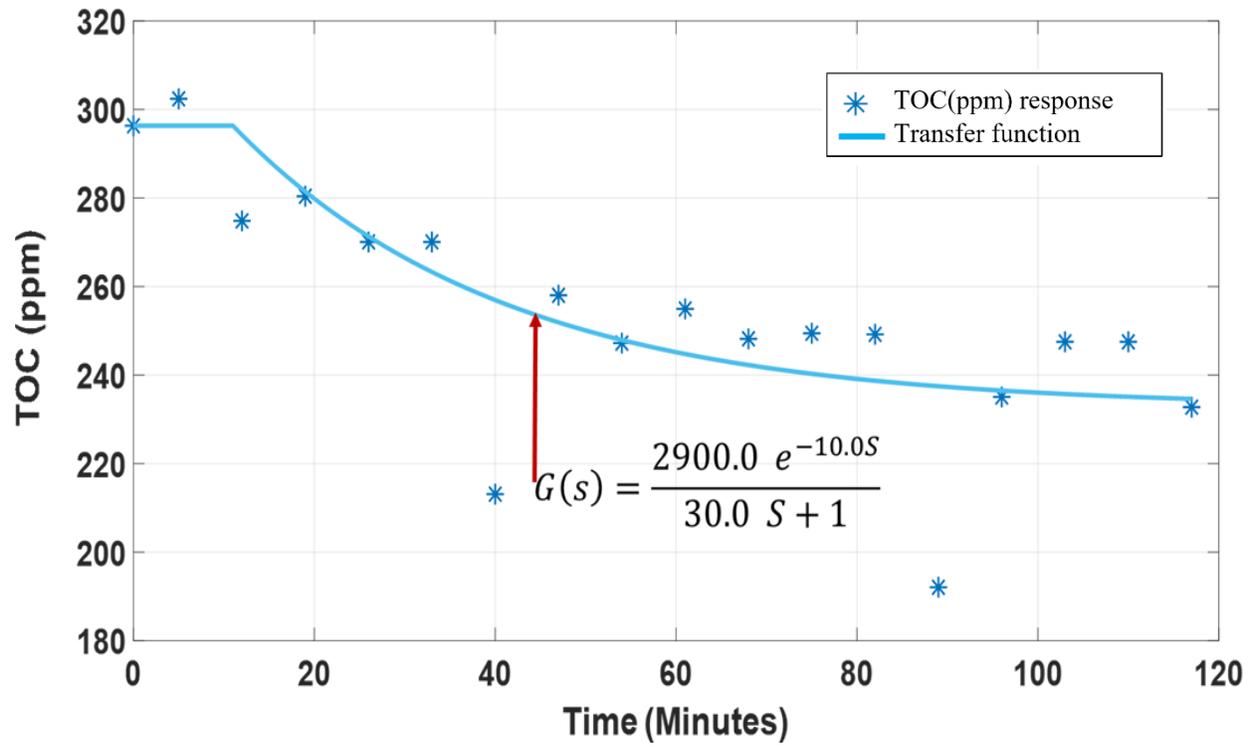
Figure 5.24. TOC (ppm) response data versus time for a step change from 1.0 to 0.20 $[H_2O_2]/[PVA]$; $[PVA]_0 = 500.0$ mg PVA/L.

Corresponding to the pH and TOC response respectively. A time delay of 10 minutes was determined for both responses and a time constant of 13 and 30 minutes respectively. Figure 5.25 illustrates the scavenging effect of H_2O_2, similar to that observed in Figure 5.22.

The figure shows the equations:

$$G(s) = \frac{-10.3\ e^{-10.0S}}{13.0\ S + 1}$$

$$G(s) = \frac{2900.0\ e^{-10.0S}}{30.0\ S + 1}$$

Legend:
* pH response
— pH Transfer function
▲ TOC (ppm) response
— TOC (ppm) transfer function
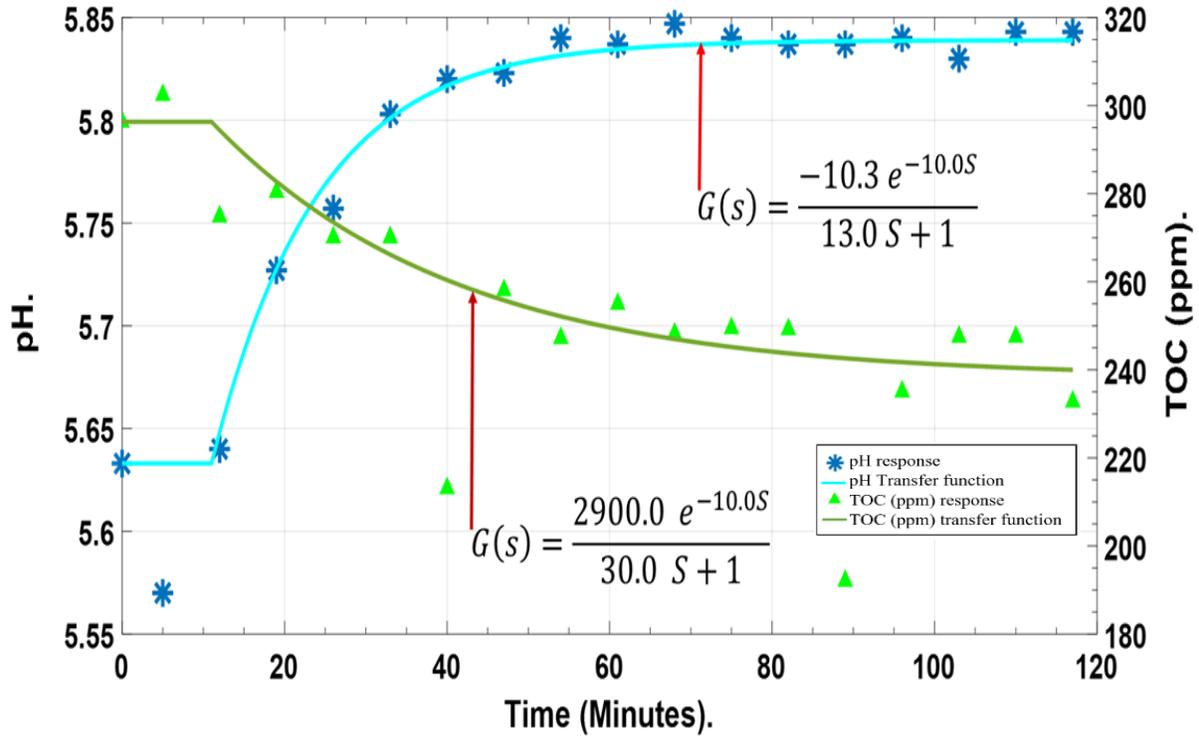
Figure 5.25. Replicate, pH and TOC (ppm) response data versus time for a step change from 1.0 to 0.20 [H_2O_2]/[PVA]; [PVA]$_0$ = 500.0 mg PVA/L.

5.1.3.3. Step change from 0.12 to 0.024 [H₂O₂]/[PVA], Test # 8

Figure 5.26 represents the pH response data for high concentration of PVA of 500.0 mg/L with a step change from 0.12 to 0.024 [H₂O₂]/[PVA]. The pH response data decreases from the initial steady state pH values. That is due to the decrease in hydrogen peroxide concentration as the hydrogen peroxide departs from the optimum concentration of hydrogen peroxide H₂O₂ for this high concentration of 500.0 mg/L with a step change from 0.12 to 0.024 [H₂O₂]/[PVA]. This phenomenon can be explained by H₂O₂ optimum value concept. As the process operates at the left

The figure shows:
$$G(s) = \frac{75.0\ e^{-8.0S}}{22.0\ S + 1}$$
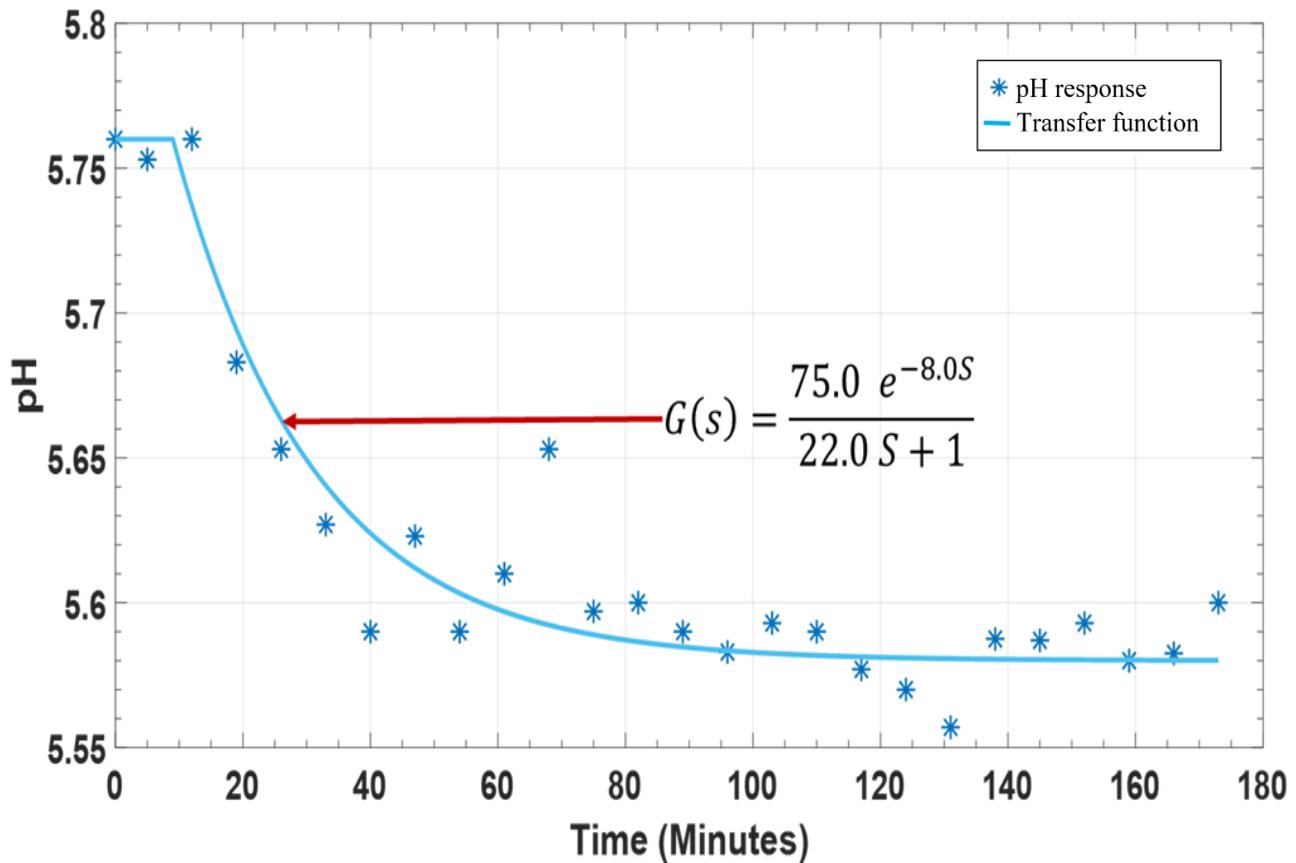
Figure 5.26. pH response data versus time for a step change from 0.12 to 0.024 [H₂O₂]/[PVA]; [PVA]₀ = 500.0 mg PVA/L.

side of the H₂O₂ optimum versus the % of TOC removal curve, it is apparent that by decreasing the flow of hydrogen peroxide, the needed value falls short of the optimum causing an increase of the intermediate acids and a drop of the pH value.

In the last test, it was evident that the hydrogen peroxide amount flowing into the photochemical reactor didn't reach its optimum. As was observed from the step change from 0.12 to 0.024 [H₂O₂]/[PVA], the pH value decreased relative to the first steady-state values. As a predictive consequence of the decrease in the pH value, the TOC removal would decrease.

- Replicate
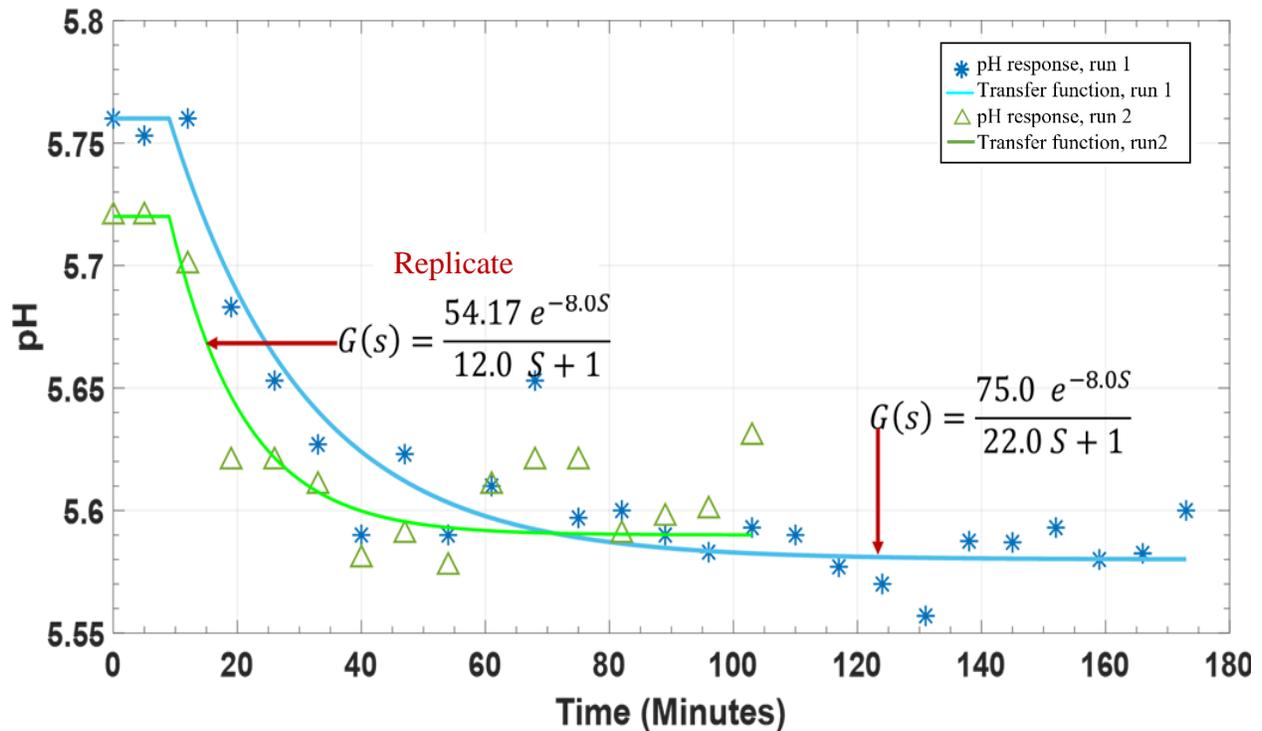
Figure 5.27. Replicate, pH response data versus time for a step change from 0.12 to 0.024 [H₂O₂]/[PVA]; [PVA]₀ = 500 mg PVA/L.

A replicate produced a similar result and three parameters for FOPTD transfer function of test 8 and its replicate was determined. The process gain of

$$K = 75 \frac{pH.MIn}{g\ H_2O_2}$$

and

$$K = 54 \frac{pH.MIn}{g\ H_2O_2}$$

For test 8 and its replicate respectively, a time delay of 8 minutes was determined for both transfer functions and a time constant of 12.0 minutes and 22.0 minutes respectively. Figure 5.27 illustrates the FOPTD model for test # 8 and its replicate in green.

Table 5.1 summarizes the FOPTD transfer function that were graphically determined for all first runs.

Table 5.1. Experimental conditions for step testing and transfer functions by graphical method.

Experimental Test	Experimental condition (Step change)	pH response Transfer Function	TOC response Transfer Function
1	60.0 mg PVA/L, 1.0-5.0 [H$_2$O$_2$]/[PVA]	$G(S) = \dfrac{-80.0e^{-8.0S}}{15.0S + 1}$	
2	60.0 mg PVA/L, 1.0-0.20 [H$_2$O$_2$]/[PVA]	$G(S) = \dfrac{-320.83\,e^{-8.0S}}{22.0\,S + 1}$	
3	280.0 mg PVA/L, 1.0-5.0 [H$_2$O$_2$]/[PVA]	$G(s) = \dfrac{-25.4\,e^{-8.0\,S}}{12.0\,S + 1}$	$G(s) = \dfrac{3{,}090.0\,e^{-8.0\,S}}{27.0\,S + 1}$
4	280.0 mg PVA/L, 1.0-0.20 [H$_2$O$_2$]/[PVA]	$G(s) = \dfrac{-36.0\,e^{-8.0\,S}}{49.0\,S + 1}$	$G(s) = \dfrac{5{,}800.0\,e^{-8.0\,S}}{23.0\,S + 1}$
5	280.0 mg PVA/L, 0.12-0.024 [H$_2$O$_2$]/[PVA]	$G(s) = \dfrac{-137.65\,e^{-20.0S}}{20.0\,S + 1}$	$G(s) = \dfrac{28{,}274.0\,e^{-20.0S}}{15.0\,S + 1}$
6	500.0 mg PVA/L, 1.0-5.0 [H$_2$O$_2$]/[PVA]	$G(s) = \dfrac{-16.3\,e^{-8.0\,S}}{12.0\,S + 1}$	$G(s) = \dfrac{1{,}400.0\,e^{-8.0\,S}}{19.0\,S + 1}$
7	500.0 mg PVA/L, 1.0-0.20 [H$_2$O$_2$]/[PVA]	$G(s) = \dfrac{-14.5\,e^{-11.0\,S}}{10.0\,S + 1}$	$G(s) = \dfrac{1{,}735.0\,e^{-11.0\,S}}{20.0\,S + 1}$
8	500.0mg PVA/L, 0.12-0.024 [H$_2$O$_2$]/[PVA]	$G(s) = \dfrac{75.0\,e^{-8.0\,S}}{22.0\,S + 1}$	

5.2. Identification Technique

5.2.1 Identification technique in Matlab to validate transfer functions from graphical methods

Transfer functions that were determined in the graphical methods, are mathematical representations of the output to an input change of the hydrogen peroxide flow into the reactor. As it is important to determine transfer functions of the response of the UV/H_2O_2 process, the identification technique in Matlab, can determine a transfer function first order, second order and higher orders with delay and without a delay term. For a certain test conditions and step change, the deviation form of output and input was entered in Matlab, As Matlab considers the deviation form of the output pH of the effluent and the deviation for of the hydrogen peroxide concentration step change. The identification tool box was used to determine the process first order and second order with delay term transfer functions. Matlab provides a percent representation to assess the accuracy of the transfer function that was determined using the system identification technique. Table 5.2 summarizes the transfer functions that were determined graphically and those first and second orders transfer functions that were determined by system identification as follows:

Table 5.2. Summary of Graphical and Identification (Matlab) transfer functions for 8 tests

Test #	pH response Transfer Function from graphical method	Matlab first order Transfer Function with delay		Matlab second order Transfer Function	
		Transfer Function	%	Transfer Function	%
1	$G(S) = \dfrac{-80.0\,e^{-8.0\,S}}{15.0\,S+1}$	$G(S) = \dfrac{-77.75\,e^{-8.23\,S}}{8.2\,S+1}$	88.8	$G(S) = \dfrac{-63.5}{(68.2\,S+1)(0.0657\,S+1)}$	20.84
2	$G(S) = \dfrac{-320.83\,e^{-8.0\,S}}{22.0\,S+1}$	$G(S) = \dfrac{-294.2\,e^{-15.56\,S}}{11.04\,S+1}$	80.7	$G(S) = \dfrac{-293.7\,e^{-8.35\,S}}{(14.5\,S+1)(6.68\,S+1)}$	83.6
3	$G(S) = \dfrac{-25.4\,e^{-8.0\,S}}{12.0\,S+1}$	$G(S) = \dfrac{-24.92\,e^{-10.74\,S}}{7.71\,S+1}$	95.14	$G(S) = \dfrac{-24.88}{(9.06\,S+1)(7.6\,S+1)}$	86.7
4	$G(S) = \dfrac{-36.0\,e^{-8.0\,S}}{49.0\,S+1}$	$G(S) = \dfrac{-30.22\,e^{-14.63\,S}}{35.3\,S+1}$	81.5	$G(S) = \dfrac{-28.94}{(29.36\,S+1)(8.67\,S+1)}$	88.64
5	$G(S) = \dfrac{-137.65\,e^{-20.0\,S}}{20.0\,S+1}$	$G(S) = \dfrac{-124.55\,e^{-32.0\,S}}{6.45\,S+1}$	83.9	$G(S) = \dfrac{-110.0\,e^{-25.4\,S}}{(5.39\,S+1)(5.39\,S+1)}$	79.2
6	$G(S) = \dfrac{-16.3\,e^{-8.0\,S}}{12.0\,S+1}$	$G(S) = \dfrac{-16.3\,e^{-12.17\,S}}{6.83\,S+1}$	94.3	$G(S) = \dfrac{-16.15\,e^{-10.16\,S}}{(12.6\,S+1)(0.678\,S+1)}$	84.2
7	$G(S) = \dfrac{-14.5\,e^{-11.0\,S}}{10.0\,S+1}$	$G(S) = \dfrac{-12.75\,e^{-7.0\,S}}{10.24\,S+1}$	87.66	$G(S) = \dfrac{-12.9\,e^{-7.007\,S}}{(14.98\,S+1)(0.707\,S+1)}$	79.2
8	$G(S) = \dfrac{37.5\,e^{-8.0\,S}}{22.0\,S+1}$	$G(S) = \dfrac{48.87\,e^{-6.8\,S}}{4.8\,S+1}$	68.8	$G(S) = \dfrac{49.1\,e^{-7.49\,S}}{(4.24\,S+1)(3.83\,S+1)}$	59.7

5.2.2. Parametric model based on optimization ARX representation

A difference method technique was used to determine a polynomial representation of the output response to that of the input step change. An ARX model based on a difference equation presented that was presented in chapter 4. The difference equation is a straight forward method to determine a model for a response of a process when excited with a pre-determined input change. Matlab determines an ARX model on the basis of a least square method of error sum. ARX polynomial models would be used in a future process control scheme as they are a better process control transfer functions than PID controllers.

5.2.2.1 Experiment 280.0 mg PVA/L, Step change from 1.0 to 5.0 [H$_2$O$_2$]/[PVA]

As was stated in chapter 4, a process may be identified by a step testing technique. In this section, the deviation of the pH response of the change in the concentration of hydrogen peroxide would be transferred to Matlab work station. The deviation of the input variable, the concentration of hydrogen peroxide, would be also entered into Matlab work space. The time domain would also be transferred with the exact time of the step change as the zero. When ident is typed into the work space, a data import window appears to transfer the deviation of both the pH response as well as the deviation of the concentration of the hydrogen peroxide. Ident window asks for the start of time and the sampling period in seconds. The steps to find transfer functions for a certain step change and known experimental conditions are stated in detail in the Appendix.

Then import data icon would be selected from the main ident window, to load the pH response and input data into the work space. The pH response data and the hydrogen peroxide input data are imported to the time domain. The Import data screen comes up, and the deviation of the input data of the hydrogen peroxide mass flowrate into the reactor is loaded in the input box. The deviation of the pH output response data is loaded to the output box. In the sample time box, the sample period of the data collected is written as 420 sec. The deviation data of both the pH response and the input hydrogen peroxide mass flow rate are now imported to ident box.

After the data are imported to ident, the Estimate list icon appears, and the method of modeling would be selected. In this case the polynomial modeling is selected with the z-transform was chosen for the sampling period discrete time. The ARX method was chosen for a polynomial model in the z-transform, as the experimental data acquired in this study are discrete. The ARX model is

72

a polynomial model that is based on the least square error method. In the Ident Matlab, after stating the output and the input deviation, choosing the ARX polynomial model and stating the output, the input as well as the delay parameter, mat lab would calculate the ARX model with the best fit.

 The ARX polynomial model window opens, with the default order of [4 4 1] and zero input delay. The input delay should be corrected to 1 sampling period of delay, and the order selection button is chosen so that the best order for the polynomial model of our input-output data is selected by ident.

After entering an input delay of 1, referring to one sample period approximation of delay time, and selecting Order Selection Icon, a choice of the range of ARX model is chosen.   The polynomial Models window appears with a default order range of [1:10 1:10 1:10]. To ensure extra accuracy, the order is modified to [1:6 1:6 1:6]. When correcting the order range and pressing the estimate button, a best polynomial order would be selected as a combination MDL and AIC criteria for the best fit. The best fit for an order range of [1:6 1:6 1:6], is [6 6 6] with a data misfit score of 0.0000016%. To get the best fit polynomial into the ident window, the Insert button is selected.

Figure 5.28, presents the system identification window after the input and input deviation data have been imported from Matlab command window to the identification window. The data were imported to the time domain in the system identification. A model method was chosen to represent the response data related to the change in input and the model would be presented on the right of the system identification window.
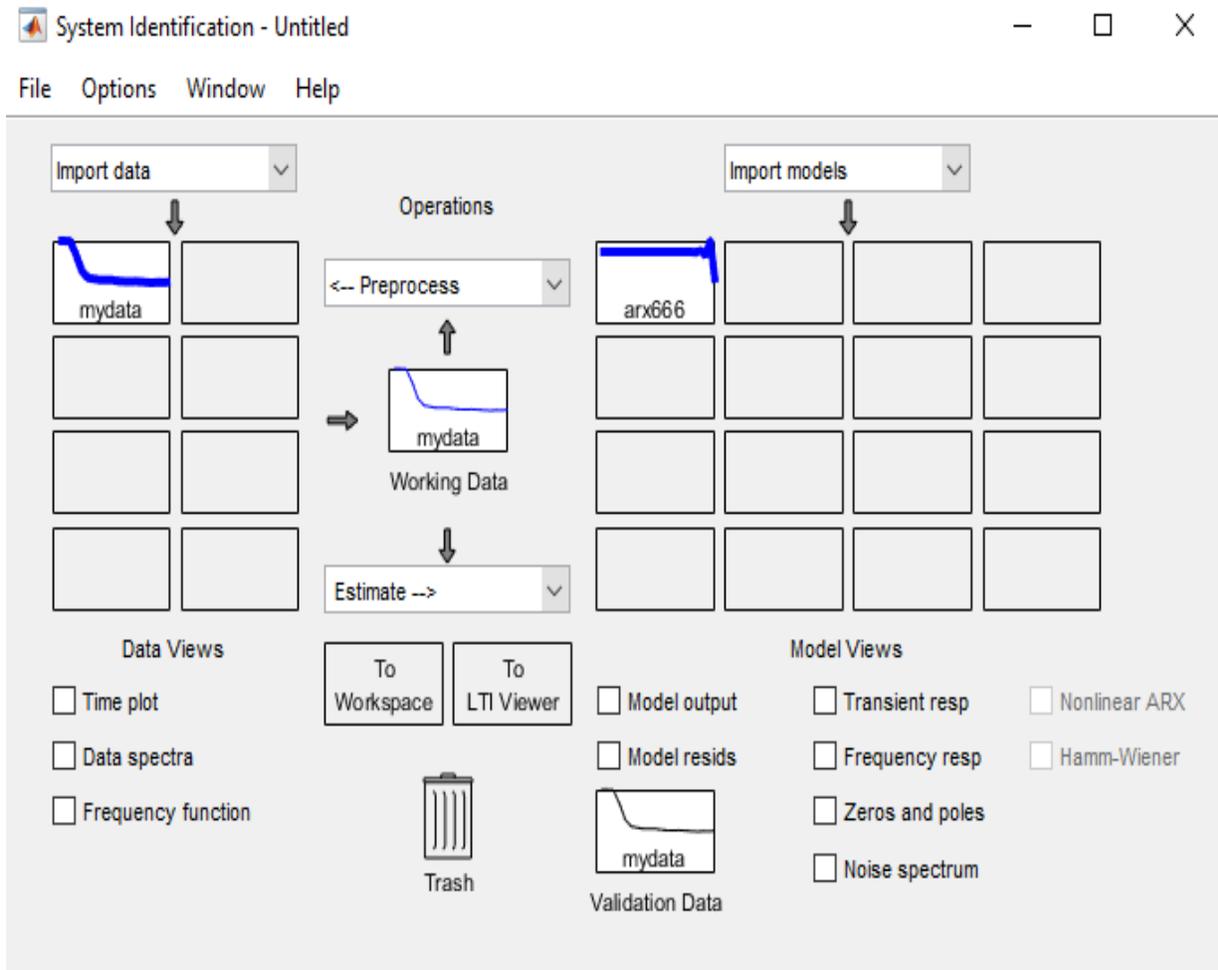
Figure 5.28. Matlab Ident window, after importing pH, and H_2O_2 concentration deviation data.

 As it can be seen in the Appendix G, the System Identification window, the best polynomial fit of the order [6 6 6] is transferred from the best fit window selection to the window of the system Identification. To transfer the polynomial parameters, a double click on the polynomial model box icon opens the following polynomial model information window for the specific model that fits the pH response data with the input variable. By selecting the present button on the polynomial model information window, the model is transferred to the command window of Matlab. The information of the best fit polynomial of the input output data is extracted.

An ARX polynomial model of an order [6 6 6], is presented in Figure 5.29, for the experimental conditions 280.0 mg PVA/L, step change 1.0-5.0 [H_2O_2]/[PVA]. An order choice of [1:6 1:6 1:6],

resulted in an ARX best fit order of [6 6 6]. The ARX model presenting the pH response of 280.0 mg PVA/L, and a step change from 1.0 to 5.0 mass ratio [H₂O₂]/[PVA], had 6 parameters for the A(z) and 6 parameters for the B(z) and a representation of 99.56% of the pH response data.

The equations shown in the figure:

$$A(z) = 1 + 1.154z^{-1} - 3.661z^{-2} + 2.285z^{-3} - 1.22z^{-4} - 1.377\ z^{-5} + 1.958\ z^{-6}$$

$$B(z) = 15.84\ z^{-6} + 3.547\ z^{-7} - 15.27\ z^{-8} - 7.555\ z^{-9} + 1.562z^{-10} - 1.316z^{-11}$$

$$A(z)y(t) = B(z)u(t) + e(t)$$

ARX model
pH response data

ARX polynomial model: Best fit Order of: [6 6 6], from [1:6 1:6 1:6] order choice. 99.56% Representation e(t): white Noise parameter.
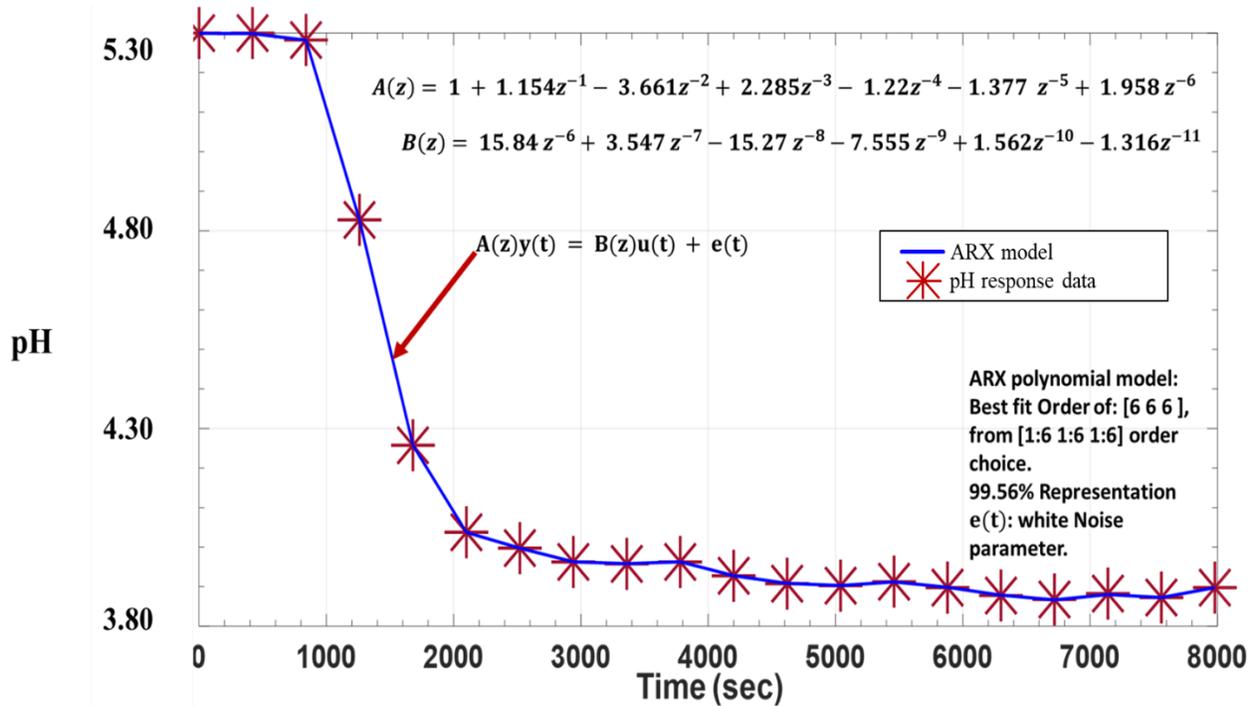
Figure 5.29. ARX polynomial model with the order of [6 6 6], 280.0 mg PVA/L, step change from 1.0 to 5.0 [H₂O₂]/[PVA]. Order choice of [1:6 1:6 1:6].

When decreasing the order choice range to [1:5 1:5 1:5], a best fit order for this specific range was selected by system identification of [5 5 4]. For the A(z) polynomial, 5 parameters were calculated and 5 parameters were calculated for the B(z). The percent representation corresponding to an ARX model with an order of [5 5 4], was estimated to be 98.56 %. Figure 5.30 illustrates the ARX polynomial model over the pH data with an order of [5 5 4].

$$A(z) = 1 - 0.996z^{-1} - 0.500z^{-2} + 0.690z^{-3} - 1.04z^{-4} + 0.949\ z^{-5}$$

$$B(z) = 3.00\ z^{-4} + 3.21\ z^{-5} + 1.10\ z^{-6} - 5.55\ z^{-7} - 4.00z^{-8}$$

$$A(z)y(t) = B(z)u(t) + e(t)$$

ARX polynomial model:
Best fit Order of: [5 5 4],
from [1:5 1:5 1:5] order choice
98.56 % Representation
$e(t)$: white Noise parameter.
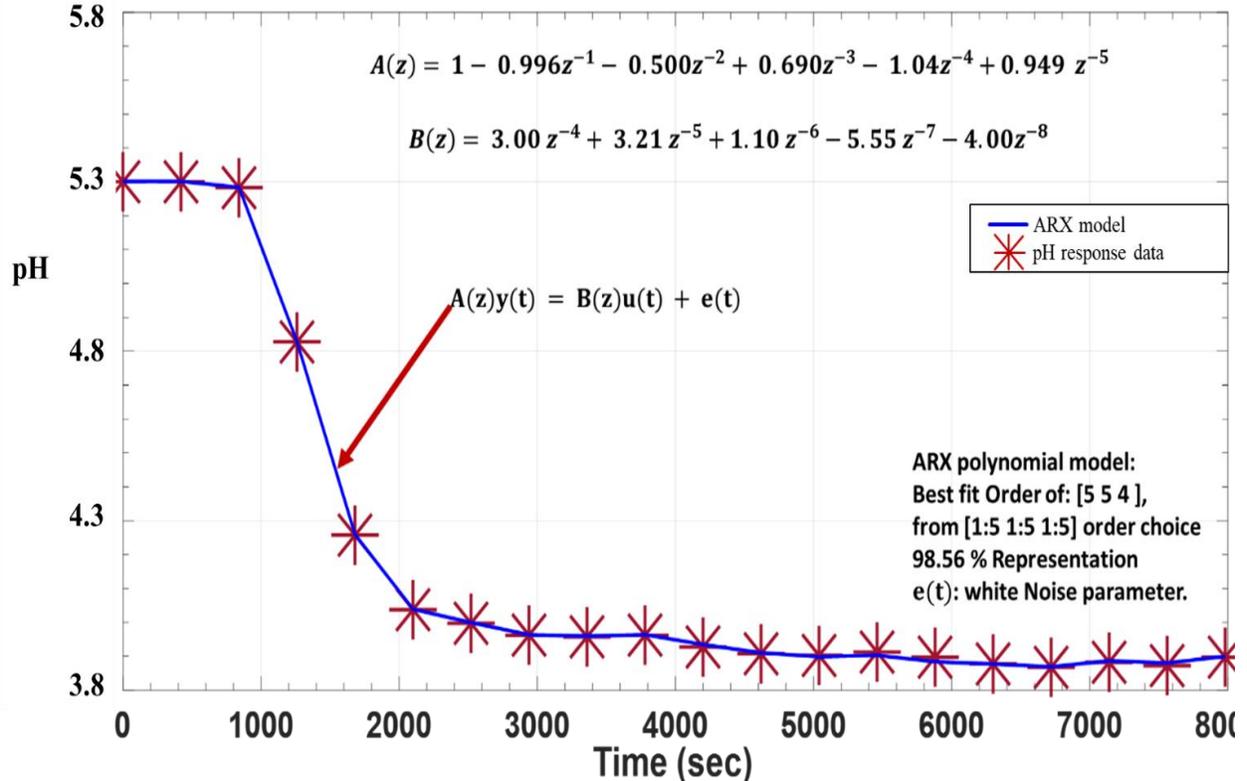
Figure 5.30. ARX polynomial model [5 5 4], best fit of the pH deviation data of 280.0 mg PVA/L, step change from 1.0 to 5.0 $[H_2O_2]/[PVA]$.

An order range [1:7 1:7 1:7] was selected with one sample delay time period and resulted in an ARX model of [7 5 6]. Best fit of order choice for the 280.0mg PVA/L, step change from 1.0-5.0 $[H_2O_2]/[PVA]$, was a polynomial model with the order, [7 5 6]. The ARX model with an order of [7 5 6], has an estimated representation of 98.91 % with 7 parameters for the output variable $y(t)$, and 5 parameters for the input variable $u(t)$ and a delay of 6. Figure 5.31 presents the ARX [7 5 6] model.
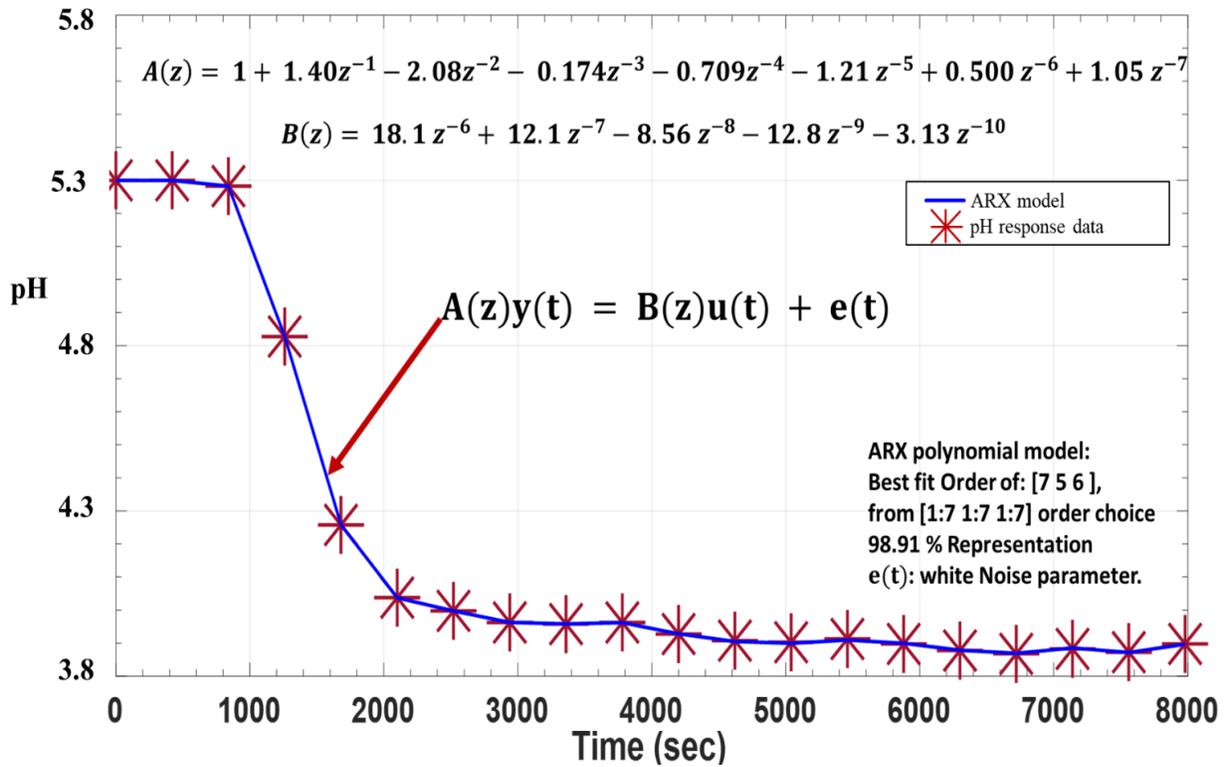
Figure 5.31. ARX polynomial model with the order of [7 5 6], 280.0 mg PVA/L, Step change from 1.0 to 5.0 [H$_2$O$_2$]/[PVA]. Order choice of [1:7 1:7 1:7].

Table 5.3 summarizes transfer function representations of the pH response data for 280.0 mg PVA/L, step change from 1.0 to 5.0 [H$_2$O$_2$]/[PVA], without including the delay period response data.

Table 5.3. Transfer functions representations without delay of 280.0 mg PVA/L, step change from 1.0 to 5.0[H_2O_2]/[PVA], Test #3

Step Change	# of poles and zeros	S-domain (continuous t)	%	Z-domain (Discrete t) $t_k = kT$	%
14.0 to 70.0 mg H_2O_2/min	1pole, no zeros	$G(S) = \dfrac{-24.53}{359.84\,S + 1}$	70.81	$G(z) = \dfrac{-11.0}{1 - 0.558\,z^{-1}}$	86.37
	2 poles, no zeros	$G(S) = \dfrac{-24.2}{1.95*10^6\,s^2 + 2.75*10^3\,s + 1}$	83.53	$G(z) = \dfrac{-15.5}{1 - 0.316\,z^{-1} - 0.0556\,z^{-2}}$	93.35
	2 poles, 1 zero	$G(S) = \dfrac{-1.52*10^4\,s - 25.0}{3.09*10^5\,s^2 + 1.54*10^3\,s + 1.00}$	95.47	$G(z) = \dfrac{-8.42 - 7.35\,z^{-1}}{1 - 0.291\,z^{-1} - 0.0687\,z^{-2}}$	93.34
	3 poles, no zeros	$G(s)$ $= \dfrac{-24.7}{4.63*10^7\,s^3 + 2.24*10^5\,s^2 + 8.53*10^2\,s + 1.00}$	94.35	$G(z)$ $= \dfrac{-4.32}{1 - 1.16\,z^{-1} + 0.434\,z^{-2} - 0.0976z^{-3}}$	97.21
	3 poles, 1 zero	$G(S)$ $= \dfrac{-5.06*10^4\,s - 25.3}{4.86*10^7\,s^3 + 6.59*10^5\,s^2 + 2.56*10^3\,s + 1.00}$	97.25	$G(z)$ $= \dfrac{-2.52 - 2.05\,z^{-1}}{1 - 1.15\,z^{-1} + 0.426\,z^{-2} - 0.0982\,z^{-3}}$	97.14
	3 poles, 2 zeros	$G(S)$ $= \dfrac{-8.00*10^7\,s^2 + 6.59*10^4\,s - 25.6}{1.25*10^9\,s^3 + 4.19*10^6\,s^2 + 2.97*10^2\,s + 1.00}$	78.53	$G(z)$ $= \dfrac{-0.322 - 1.11\,z^{-1} - 2.20\,z^{-2}}{1 - 1.25\,z^{-1} + 0.503\,z^{-2} - 0.110\,z^{-3}}$	97.25

5.2.2.2 Experiment 280.0 mg PVA/L, Step change from 1.0 to 0.20 [H₂O₂]/[PVA]

A process model selection with 2 poles and 1 zero all real roots, underdamped model was chosen for the average concentration of 280.0 mg PVA/L, and a step change from 1.0 to 0.20 mass ratio [H₂O₂]/[PVA]. The model presents a smooth transfer function with a percent representation of 88.91 %. Although the representation of this particular model over the pH response is less than 90%, the smoothness of the solid line may be a better representation of the process when designing a proper controller. Figure 5.32 presents an underdamped transfer function in the s transform, with 1 zero and 2 poles.

$$G(s) = \frac{k_p\,(1-\tau_z\,s)e^{-\theta s}}{1+2\zeta\tau_w\,s+(\tau_w\,s)^2} = \frac{-33.4\,(1-492.46\,s)}{1+2\zeta 951.5\,s+(951.5\,s)^2}$$

$$G(s) = \frac{-33.4\,(1-492.46\,s)}{1+2187\,s+(951.5\,s)^2}$$

88.91% Representation
$\tau_z = -492.5$
$\tau_w = 951.5\ Sec$
$\zeta = 1.15$
$\theta = 0\ sec$
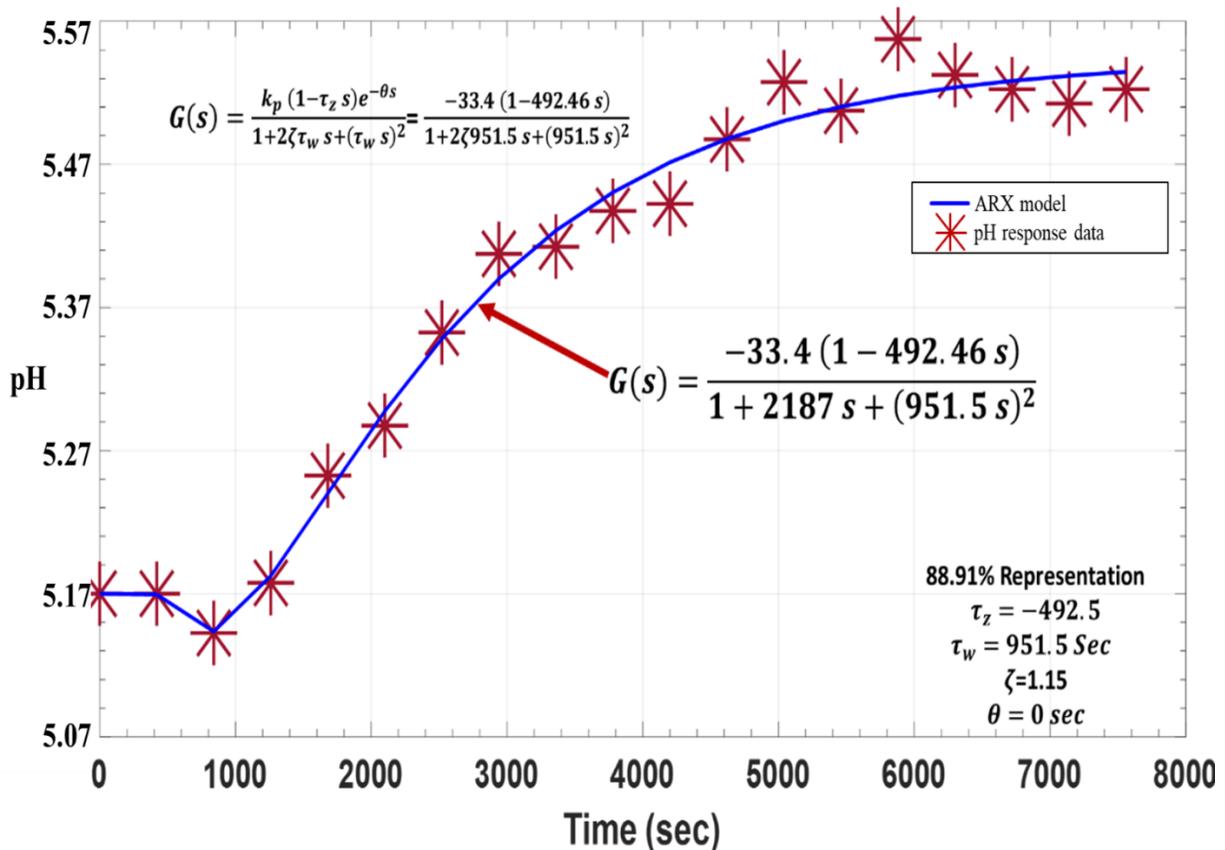
Figure 5.32. Transfer function with two poles, with one zero underdamped and no delay term, 280.0 mg PVA/L, step change from 1.0 to 0.20 [H₂O₂]/[PVA].

Figure 5.33 illustrates a transform transfer function that represents the pH of 280 mg PVA/L, and a step change from 1.0 to 0.20 [H₂O₂]/[PVA]. The model has 2 real poles and 1 real zero and the time delay in this model was considered to be zero. The model has an estimated representation of 88.91 % and runs smooth over the pH response data.

The figure contains the equations:

$$G(s) = \frac{k_p\,(1-\tau_z\,s)e^{-\theta s}}{1+2\zeta\tau_w\,s+(\tau_w\,s)^2} = \frac{-33.4\,(1-492.46\,s)}{1+2\zeta 951.5\,s+(951.5\,s)^2}$$

$$G(s) = \frac{-33.4\,(1-492.46\,s)}{1+2187\,s+(951.5\,s)^2}$$

ARX model

pH response data

88.91% Representation
$\tau_z = -492.5$
$\tau_w = 951.5\ Sec$
$\zeta = 1.15$
$\theta = 0\ sec$
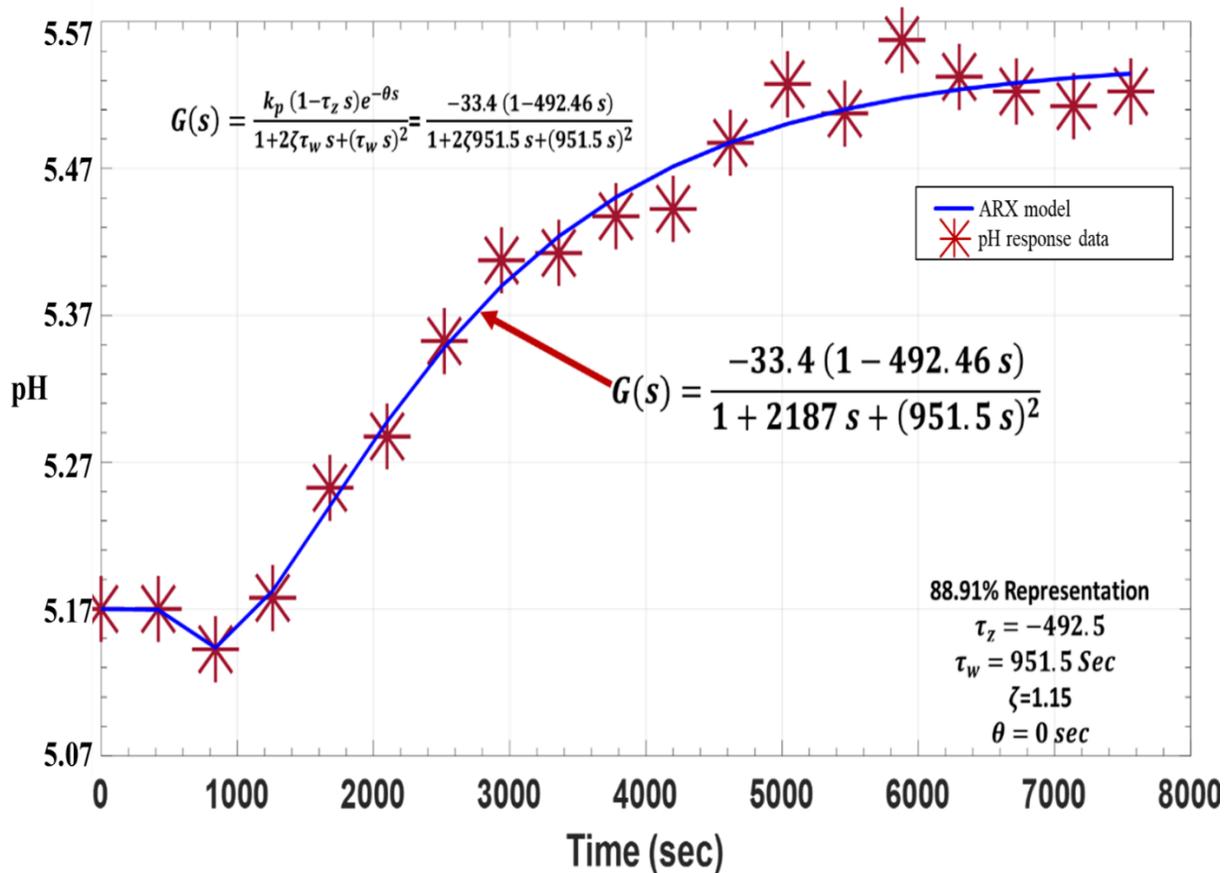
Figure 5.33. Transfer function with two poles, one zero and no delay term, 280.0 mg PVA/L, Step change from 1.0 to 0.20 [H₂O₂]/[PVA].

2 real poles with no zero model for the same experimental test has an estimated representation of 88.55 %. A time delay of 5 minutes and 45 seconds was estimated for the process model transfer function. A first time constant of 25 minutes and 30 seconds was estimated for this particular

transfer function. Figure 5.34 presents the transfer function on blue solid line over the pH response data in red for 280.0 mg step change from 1.0 to 0.20 [H₂O₂]/[PVA].
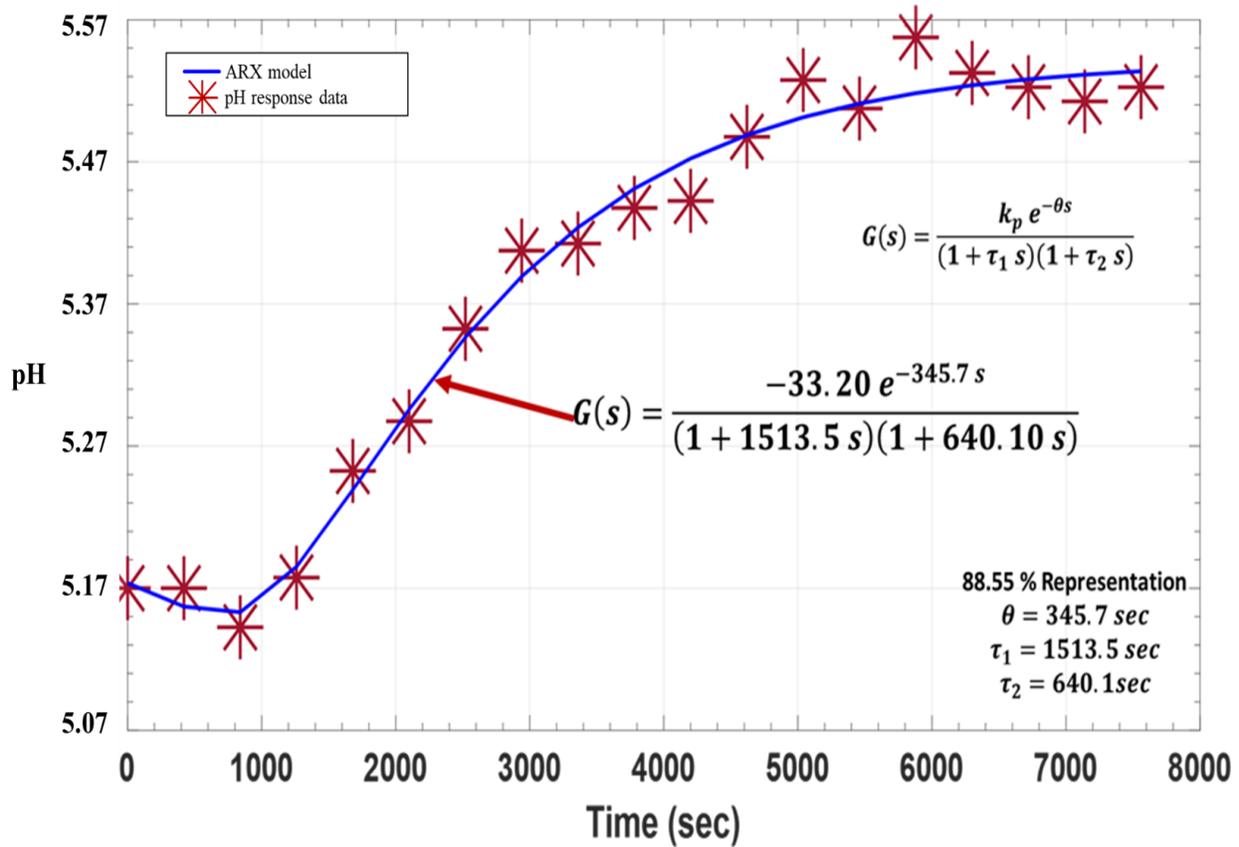
Figure 5.34. Transfer function with two poles, a delay term and no zeros, process modeling Matlab 280.0 mg PVA/L, step change from 1.0 to 0.20 [H₂O₂]/[PVA].

Figure 5.35 represents a process model transfer functions with 3 real poles and roots. An Underdamped TOPTD transfer function with a zero. The transfer function model has a representation of 88.18% with a smooth solid line over the pH response data of 280 mg PVA/L with a step change from 1.0 to 0.20 [H₂O₂]/[PVA]. A total of 7 parameters for the TOPTD transfer function was determined. The process gain was determined to be

$$K = -34.5 \frac{pH.Min}{g \ H_2O_2}$$

The time constants from the highest to the lowest were found to be 34 minutes, 3 minutes 30 seconds and 49 seconds respectively corresponding to the three poles. The underdamped factor ζ

81

was determined to be 0.118, and a delay value of 13 minutes and 29 seconds was measured. Finally, a zero of 1.32 was found for this particular TOPTD model. Figure 5.35 illustrates TOPTD underdamped Transfer Function in blue solid line and the red starts represents the pH response data.
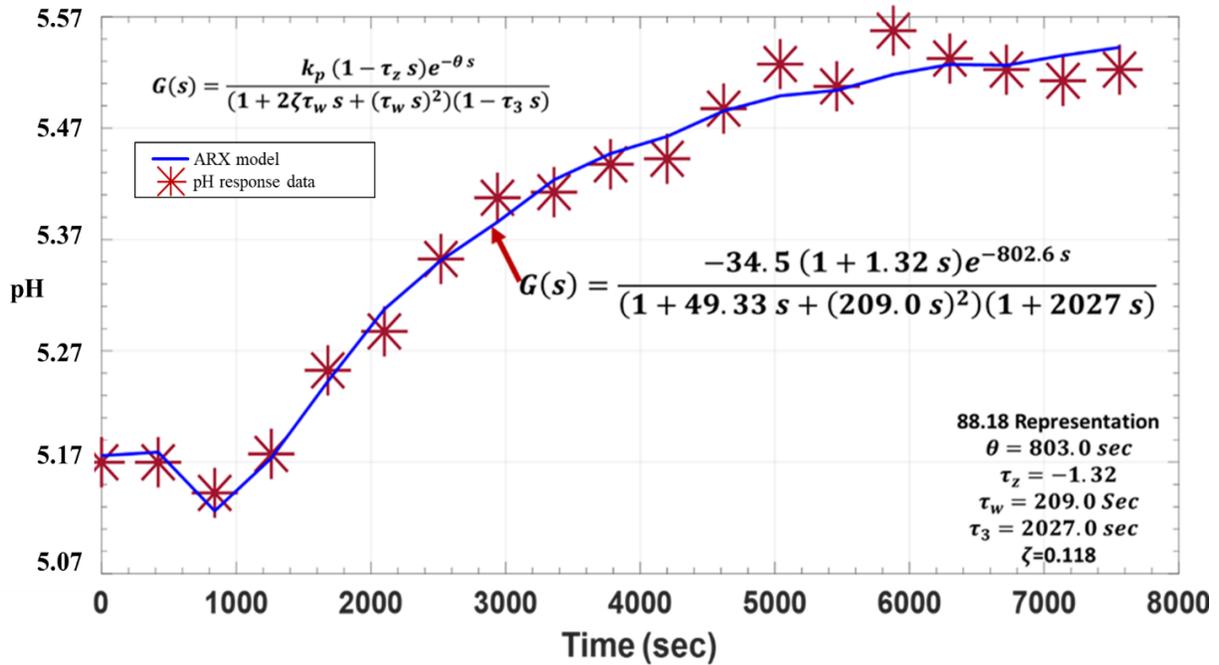
Figure 5.35. 3 poles, with delay and one zeros, underdamped model Matlab 280.0 mg PVA/L, step change from 1.0 to 0.20 [H₂O₂]/[PVA].

A transfer function with 1 pole, a time delay and a zero was estimated for the average concentration of 280 mg PVA/L, and a step change from 1.0 to 0.20 [H$_2$O$_2$]/[PVA]. The model has an estimated representation of 88.03%. A time delay of 13 minutes and 36 seconds was estimated for this model. 33 minutes were estimated for the time constant of this transfer function. The transfer function is illustrated in Figure 5.36.

82
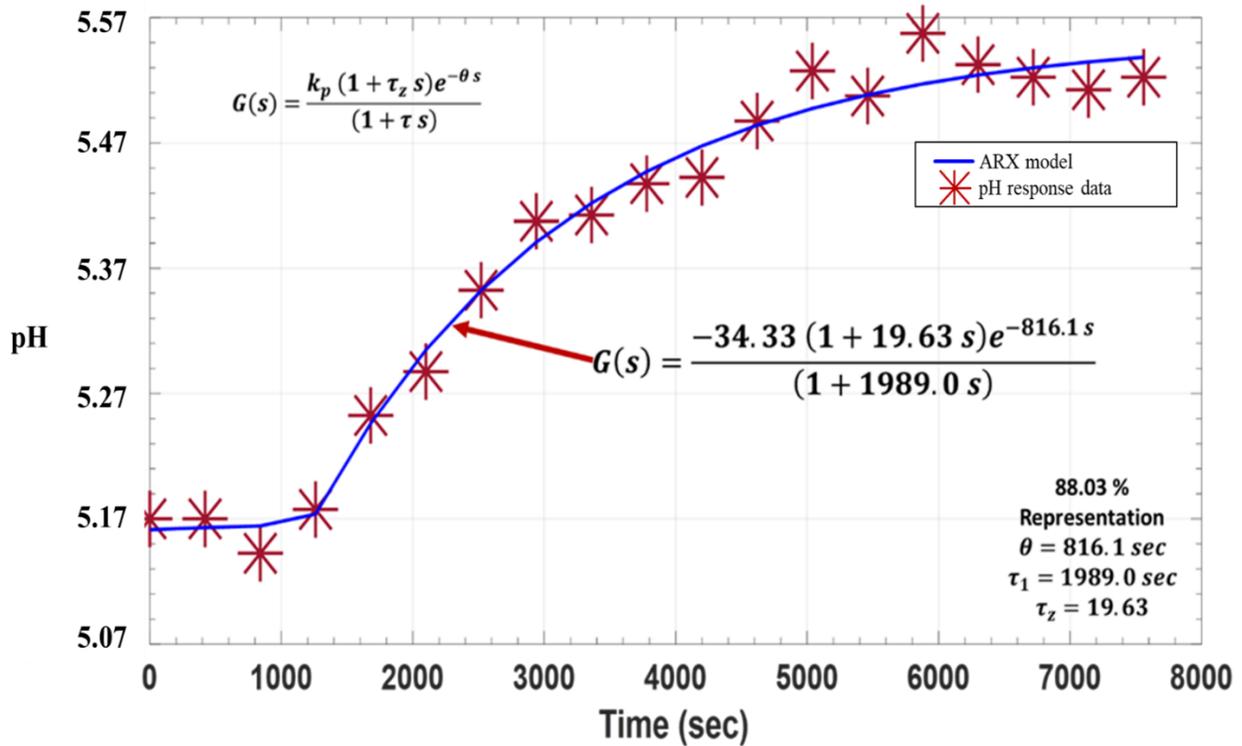
Figure 5.36. FOPTD with 1 poles, a delay term and a zeros 280.0 mg PVA/L, step change from 1.0 to 0.20 [H$_2$O$_2$]/[PVA].

A first order transfer function with time delay was estimated for the average concentration of 280.0 mg PVA/L, and a step change from 1.0 to 0.20 [H$_2$O$_2$]/[PVA]. The solid line remains parallel to the pH deviation points until it departs from the initial steady state. The model has an estimated representation of 88.03%. The transfer function is illustrated in Figure 5.37.
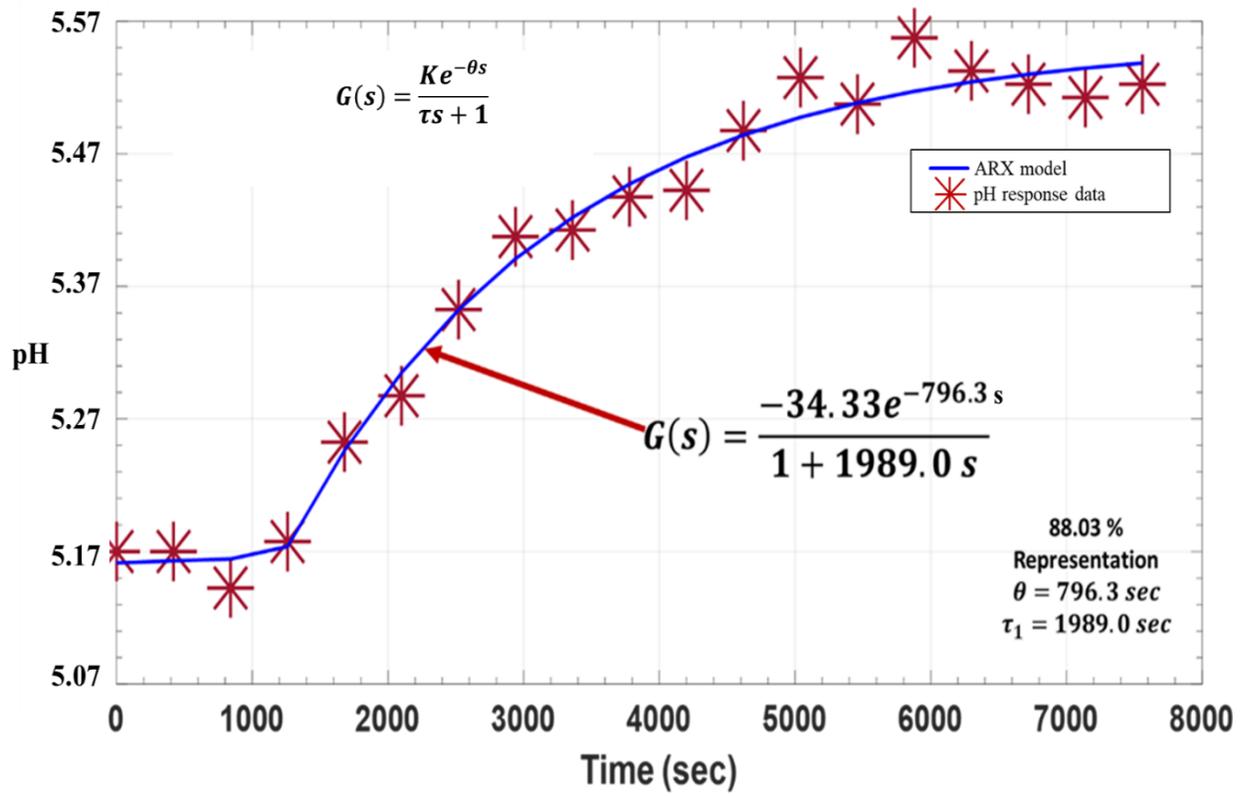
Figure 5.37. FOPTD with no zeros, process modeling Matlab 280.0 mg PVA/L, step change from 1.0 to 0.20 [H₂O₂]/[PVA].

An ARX model with an order of [6 6 5], was estimated for the 280.0 mg PVA/l, step change from 1.0 to 0.20 [H₂O₂]/[PVA]. 88.93 % representation was estimated for the pH response data. The model resulted in 6 parameters for the A(z), and 6 parameters for the B(z) and a delay of 5. The ARX model with an order of [6 6 5], presents a smooth solid line when approaching the second steady state. Figure 5.38 illustrates the ARX polynomial model in blue and the pH response data in red stars.
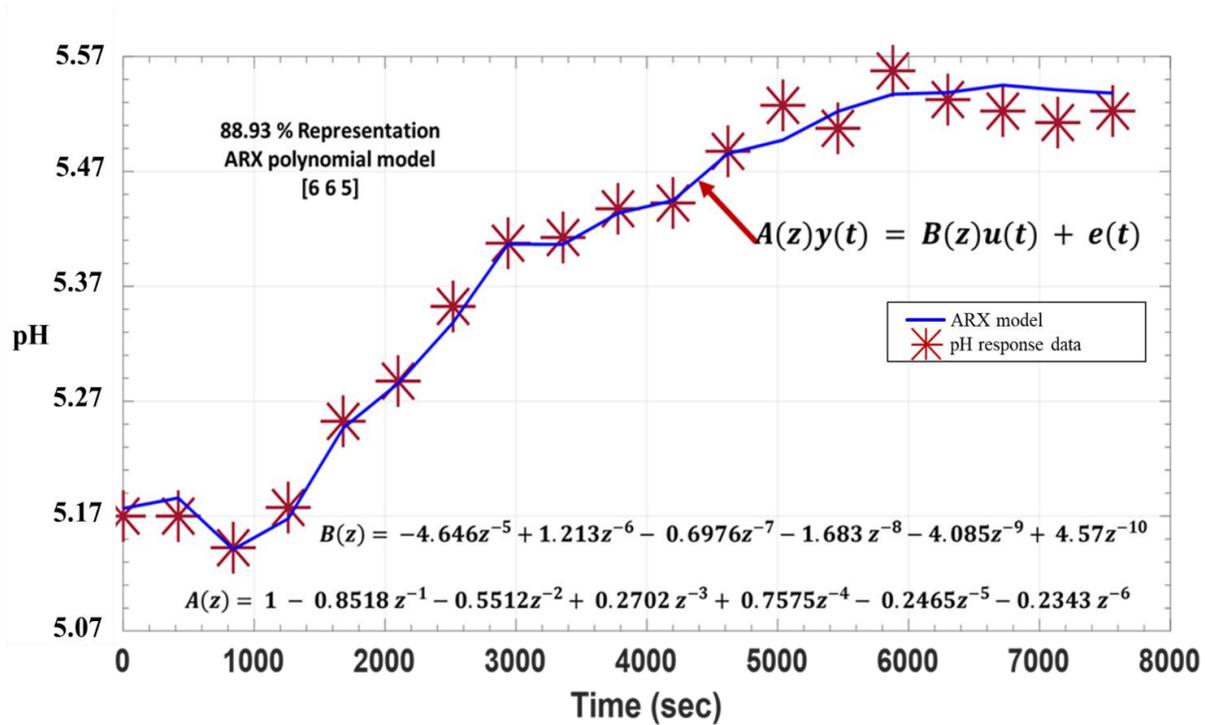
Figure 5.38. ARX polynomial model of order [6 6 5] of pH data response of 280.0 mg PVA/L, step change from 1.0 to 0.20 [H_2O_2]/[PVA]. Order choice of [1:6 1:6 1:6].

An order range of [1:7 1:7 1:7] was chosen for the system identification to choose a best fit. An ARX model with an order of [7 4 6] was chosen as a best fit. An estimated representation percent was calculated to be 91.02 %. The model is observed to have sharp turning points before reaching the plateau. Although the model has a high representation of 91.02%, the sharp turns in the ARX model may not be suitable for controller design. Figure 5.39 represents the ARX model with the order [7 4 6] for the response pH data for the average PVA concentration of 280.0 mg/L, and a step change from 1.0 to 0.20 [H_2O_2]/[PVA].
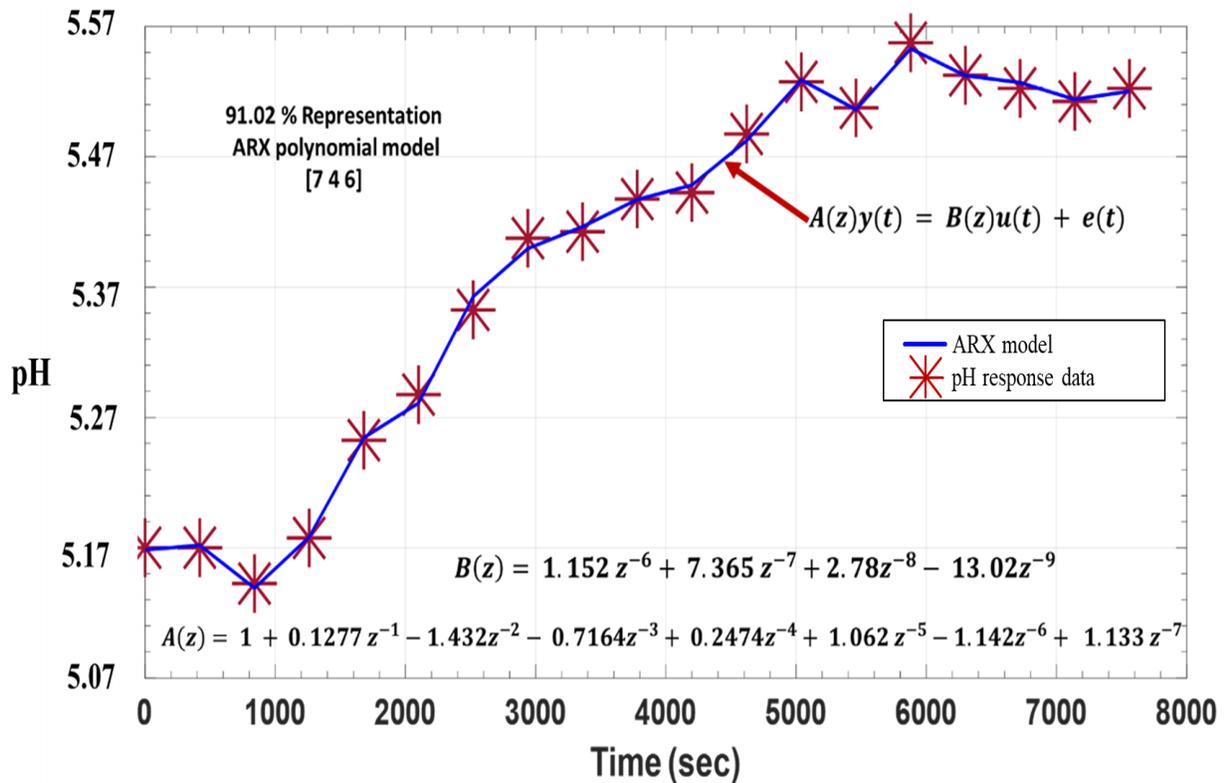
Figure 5.39. ARX polynomial model of order [7 4 6] of pH data response of 280.0 mg PVA/L, Step change from 1.0 to 0.20 [H₂O₂]/[PVA]; Order choice of [1:7 1:7 1:7].

Although the ARX model with the order [5 5 4], has an estimated representation of 88.45 % in comparison to the ARX of [7 4 6] of the same test of a representation of 91.02, the ARX model with the order [5 5 4] runs smoother over the pH response data points. As the model gets a higher fitting representation, it may run in an overfitting problem that results in a non-realistic representation of the process. Figure 5.40 represents the ARX model of the order [5 5 4] with a smoother blue solid ARX model.
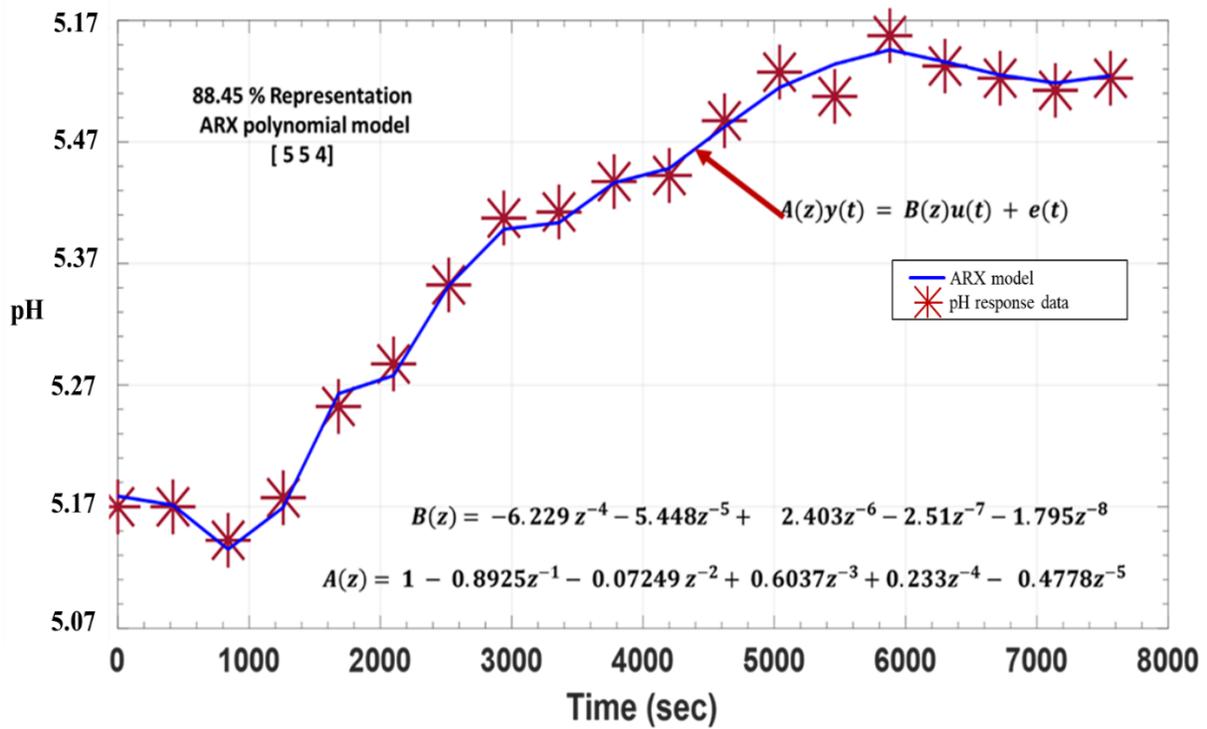
Figure 5.40. ARX polynomial model of order [5 5 4] of pH data response of 280.0 mg PVA/L, Step change from 1.0 to 0.2 [H_2O_2]/[PVA]. Order choice of [1:5 1:5 1:5].

Table 5.4 summarizes transfer function representations of the pH response data for 280.0 mg PVA/L, step change from 1.0 to 0.20 [H_2O_2], without including the delay period response data.

**Table 5.4.** Transfer functions representations without delay of, 280.0 mg PVA/L, step change from 1.0 to 0.20 [H$_2$O$_2$]/[PVA]. Test #4.

Step Change	# of poles and zeros	S-domain, (continuous t)	%	Z-domain (Discrete t) $t_k = kT$	%
14.0 to 2.80 mg H$_2$O$_2$/min	1 pole, no zeros	$G(s) = \dfrac{-33.9}{1 + 1867.4\,s}$	85.95	$G(z) = \dfrac{-6.57}{1 - 0.809\,z^{-1}}$	83.7
	2 poles, no zeros	$G(s) = \dfrac{-34.1}{1.07 * 10^5 s^2 + 1.97 * 10^3\,s + 1}$	86.7	$G(z) = \dfrac{-9.12}{1 - 0.404\,z^{-1} - 0.331 z^{-2}}$	86.3
	2 poles, 1 zero	Low Representation		$G(z) = \dfrac{-2.84 - 5.64\,z^{-1}}{1 - 0.507\,z^{-1} - 0.246\,z^{-2}}$	86.4
	3 poles, no zeros	Low Representation		$G(z) = \dfrac{-2.49}{1 - 0.713\,z^{-1} - 0.956\,z^{-2} + 0.757\,z^{-3}}$	88.0
	3 poles, 1 zero	$G(s) = \dfrac{4.80 * 10^3 s - 17.7}{5.98 * 10^7 s^3 + 9.11 * 10^6 s^2 + 2.84 * 10^3\,s + 1}$	88.1	$G(z) = \dfrac{4.76 - 6.03\,z^{-1}}{1 - 0.813\,z^{-1} - 0.974\,z^{-2} + 0.840\,z^{-3}}$	88.2
	3 poles, 2 zeros	$G(S) = \dfrac{-2.65 * 10^6 s^2 + 5.30 * 10^2 s - 33.7}{1.17 * 10^8 s^3 + 1.10 * 10^5 s^2 + 1.81 * 10^3\,s + 1}$	87.56	$G(z) = \dfrac{8.89 + 1.65\,z^{-1} - 11.4\,z^{-2}}{1 - 1.25\,z^{-1} - 0.176\,z^{-2} + 0.465\,z^{-3}}$	88.3

5.2.2.3. Experiment 280.0 mg PVA/L, Step change from 0.12 to 0.024 [H₂O₂]/[PVA]

A FOPTD transfer function was determined for the average concentration of 280.0 mg PVA/L, and a step change from 0.12 to 0.024 [H₂O₂]/[PVA]. Three parameters of the FOPTD was estimated by system identification, the process gain, the time constant and the time delay. The process gain was determined to be:

$k = -133.9 \frac{pH.min}{g\, H_2O_2}$, a time constant of 387 seconds an equivalent of 6 minutes and 27 seconds, and a time delay of 31 minutes and 30 seconds. The data fitting representation was estimated by system identification to be 83.43 %. Figure 5.41 presents the SOPTD transfer function in the blue solid line, and the pH response data points in red stars.
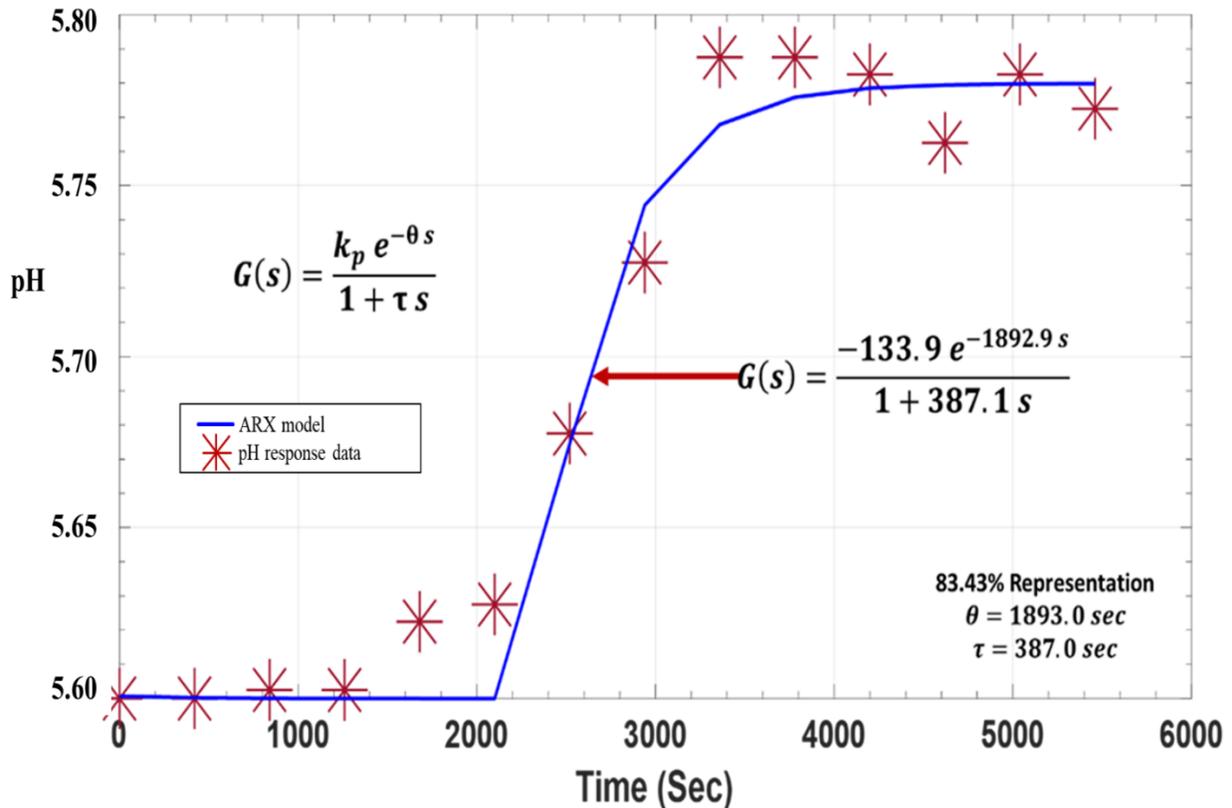
Figure 5.41. FOPTD transfer function model, 1 pole, no zero and a delay term, 280.0 mg PVA/L, Step Change from 0.12 to 0.024 [H₂O₂]/[PVA].

A SOPTD transfer function was selected to represent the pH response data and a fitting estimation of 75.53 % was estimated. A process gain of

$k = -119.5 \frac{pH.min}{g\,H_2O_2}$, a delay time of 1255 second and an initial time constant of 517 seconds and a second time constant of 329 seconds an equivalence of 21, 8.6 and 5.5 minutes respectively. Figure 5.42 represents the SOPTD model as the blue solid line and the pH response in red stars.
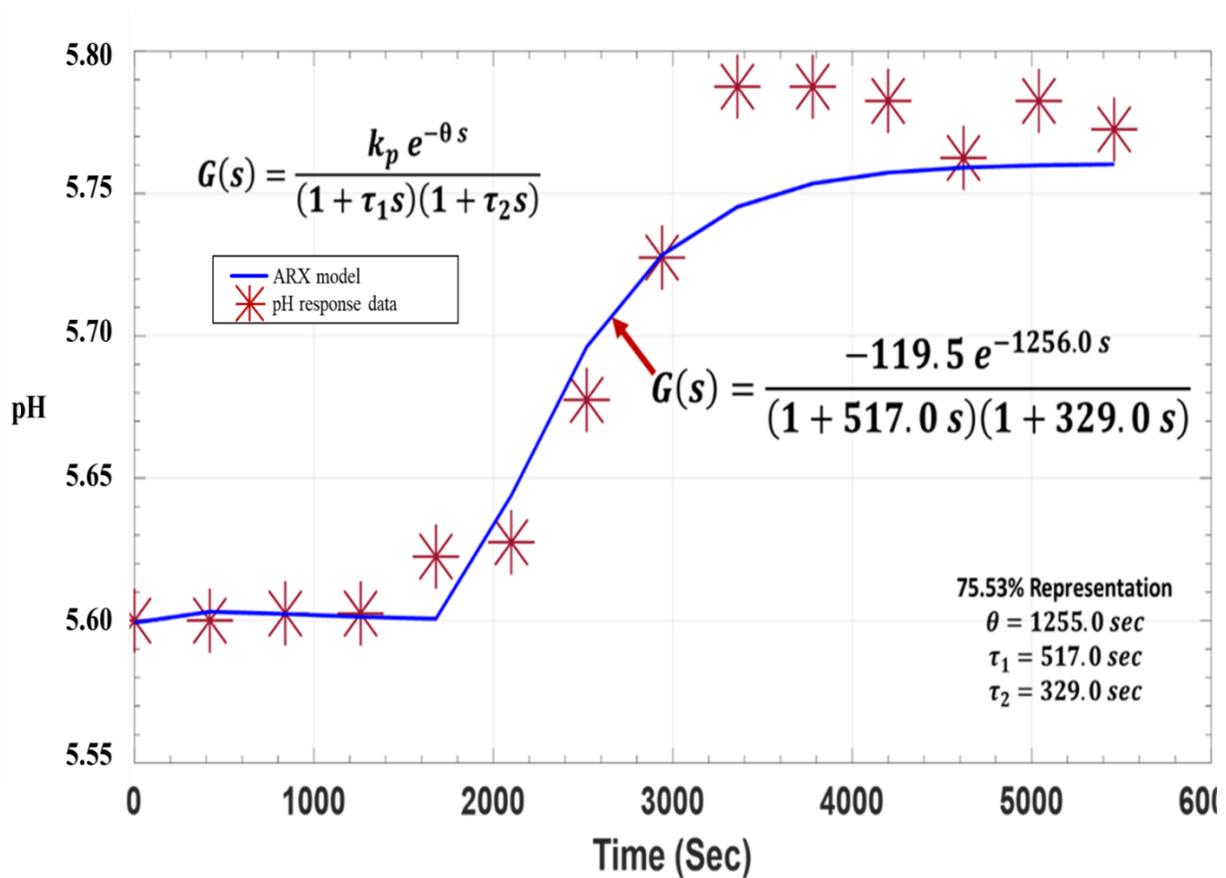
Figure 5.42. Second order transfer function model, 2 poles, no zero, and a time delay term, 280.0 mg PVA/L, Step change from 0.12 to 0.024 [H₂O₂]/[PVA].

A FOPTD model with a zero in the nominator resulted in an estimated representation of 83.43%.
A process gain of

$$K = -133.9 \frac{pH.min}{g \ H_2O_2}$$

A process time constant of 387 seconds a time delay of 1893 seconds and zero of 0.392. Figure 5.43 illustrates the FOPTD model in solid blue line and the pH response data in red stars.
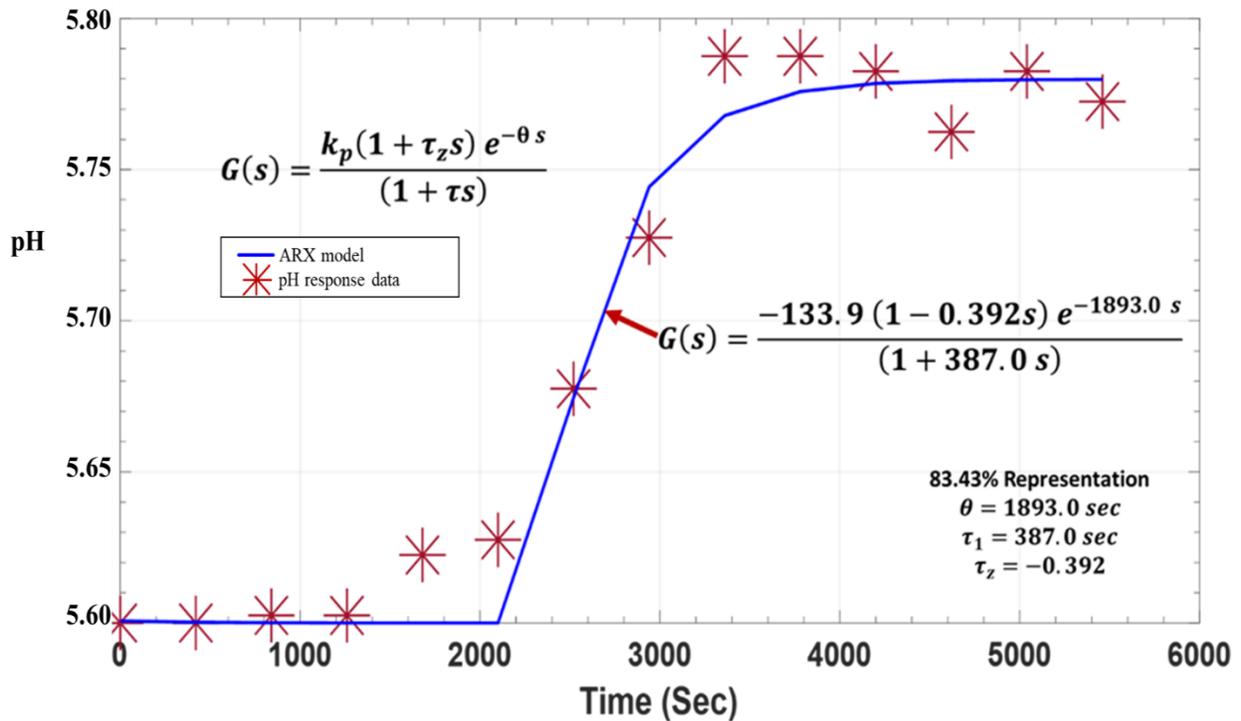
Figure 5.43. First order with one zero, Transfer function model, 1 poles 1, zero and a time delay term, 280.0 mg PVA/L, step change from 0.12 to 0.024 [H_2O_2]/[PVA].

Figure 5.44 illustrates an underdamped SOPTD model with a zero term (process head). A fitting representation of 84.28% was estimated for the transfer function. An underdamped coefficient ζ was estimated to be 0.649. The time delay was estimated to be 1708 seconds, a time constant of 380 seconds, and a zero of 4.04.
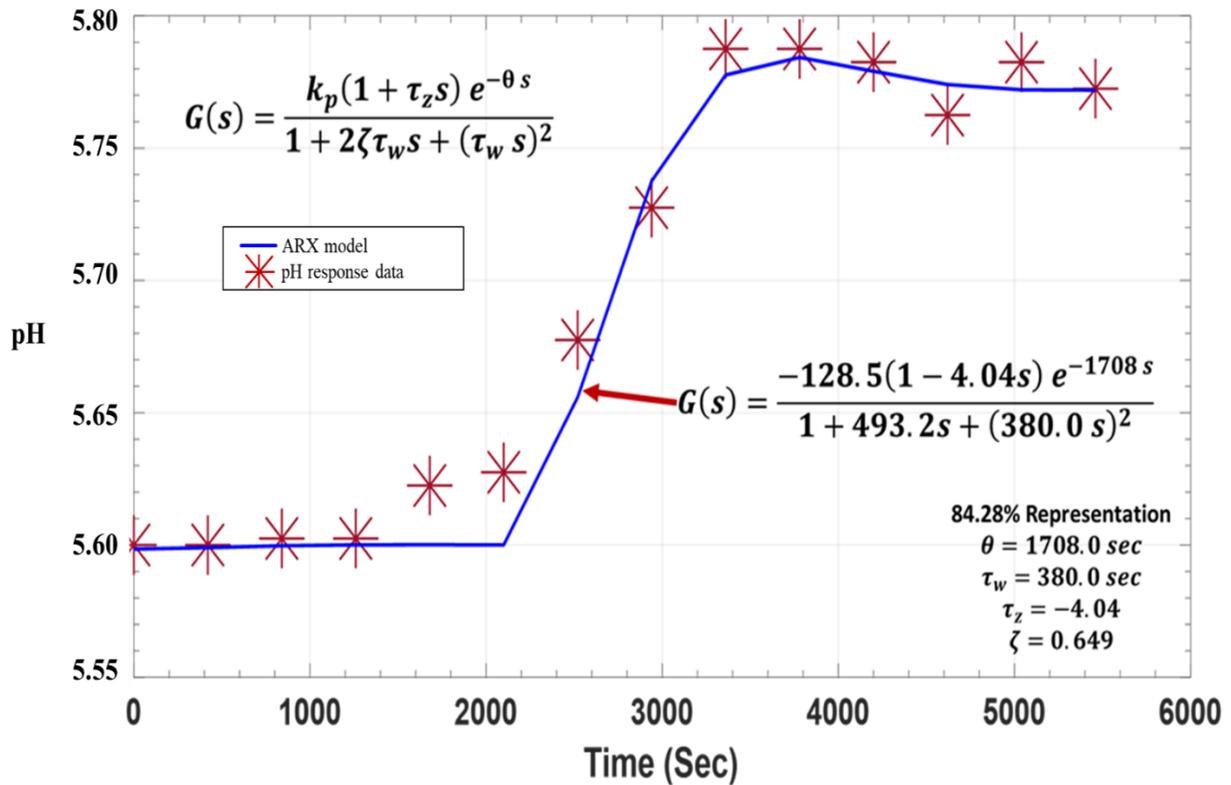
Figure 5.44. Second order, underdamped with one zero, Transfer function model, 2 poles,1 zero, and a time delay term, 280.0 mg PVA/L, step change from 0.12 to 0.024 [H_2O_2]/[PVA].

In figure 5.45 the underdamped TOPDT was estimated with a fitting representation of 87.07%. An underdamped coefficient ζ of 0.569 was estimated. A time delay of 1708 seconds, a time constant of 1042 seconds and a zero at 939.5 seconds was determined. A third time constant was estimated to be 375 seconds an equivalence of 6 minutes.
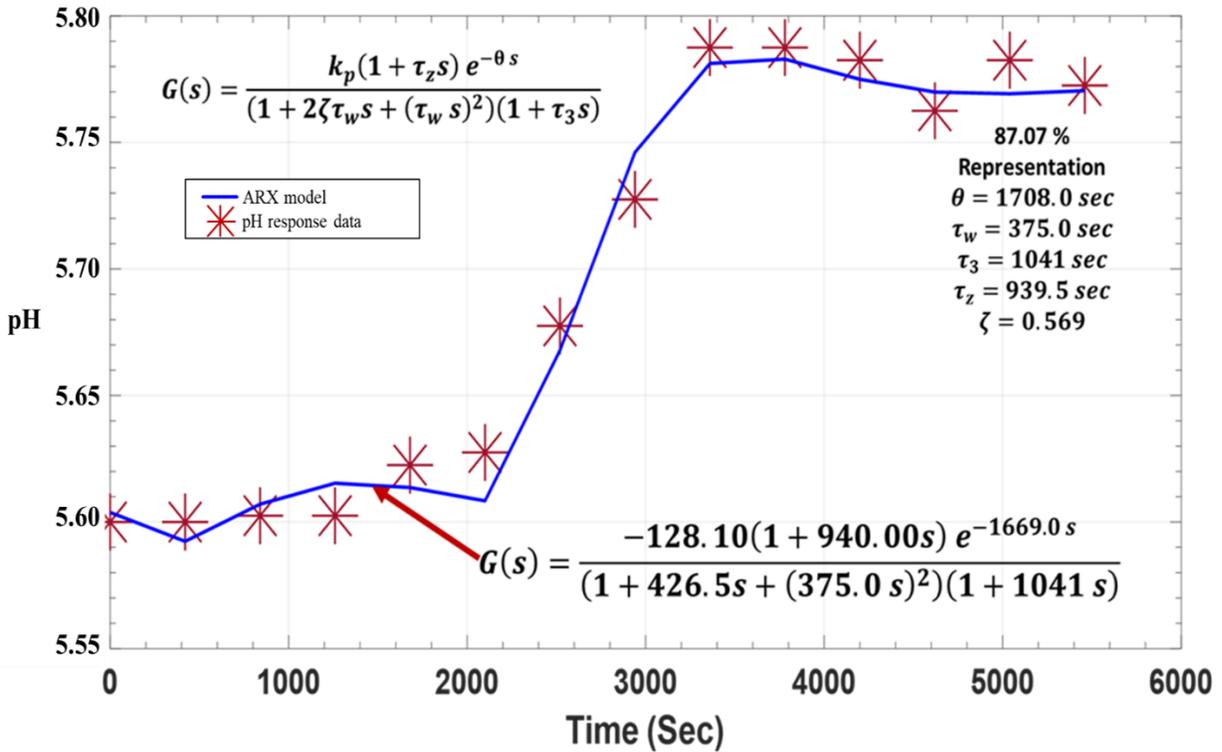
Figure 5.45. Third order, underdamped with one zero, 3 poles, and a delay term transfer function model, 280.0 mg PVA/L, step change from 0.12 to 0.024 [H₂O₂]/[PVA].

An ARX model with an order of [6 1 1] was determined using the optimization method of least square error by process identification. Although, an ARX with high representation data fitting of 99.77% was estimated, the model performs sharp points. Four parameters were determined for the output parameters y(t), and one parameter was determined for the input u(t). Figure 5.46 represents the ARX model for the response pH data for the average concentration of 280.0 mg PVA/L, and a step change of 0.12 to 0.024 [H₂O₂]/[PVA].
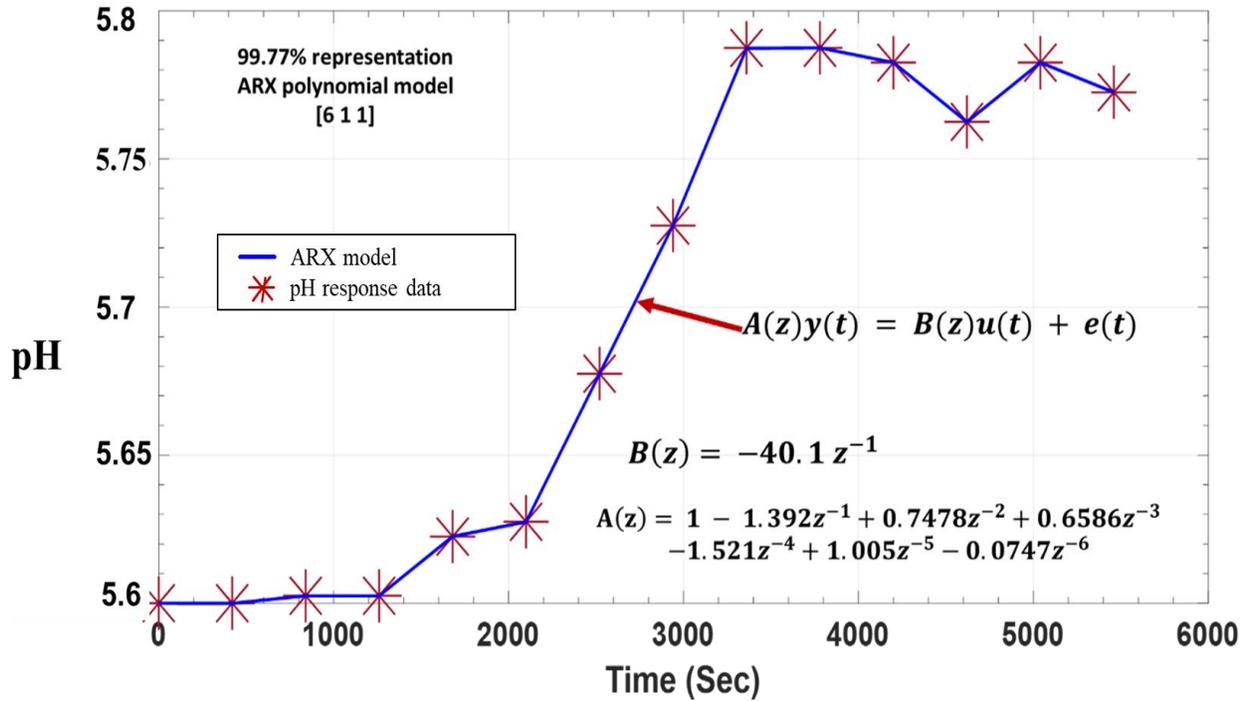
Figure 5.46. ARX [6 1 1], polynomial model in the z-transform of effluent pH response, of 280.0 mg PVA/L, step change from 0.12 to 0.024 [H₂O₂]/[PVA]; Model Order choice by Ident Matlab, from [1:6 1:6 1:6]. 99.77% representation.

Figure 5.47 represents an ARX with an order of [5 3 4] model with a 99.66 % data fitting. The model still has sharp turns that wouldn't properly present the process response.
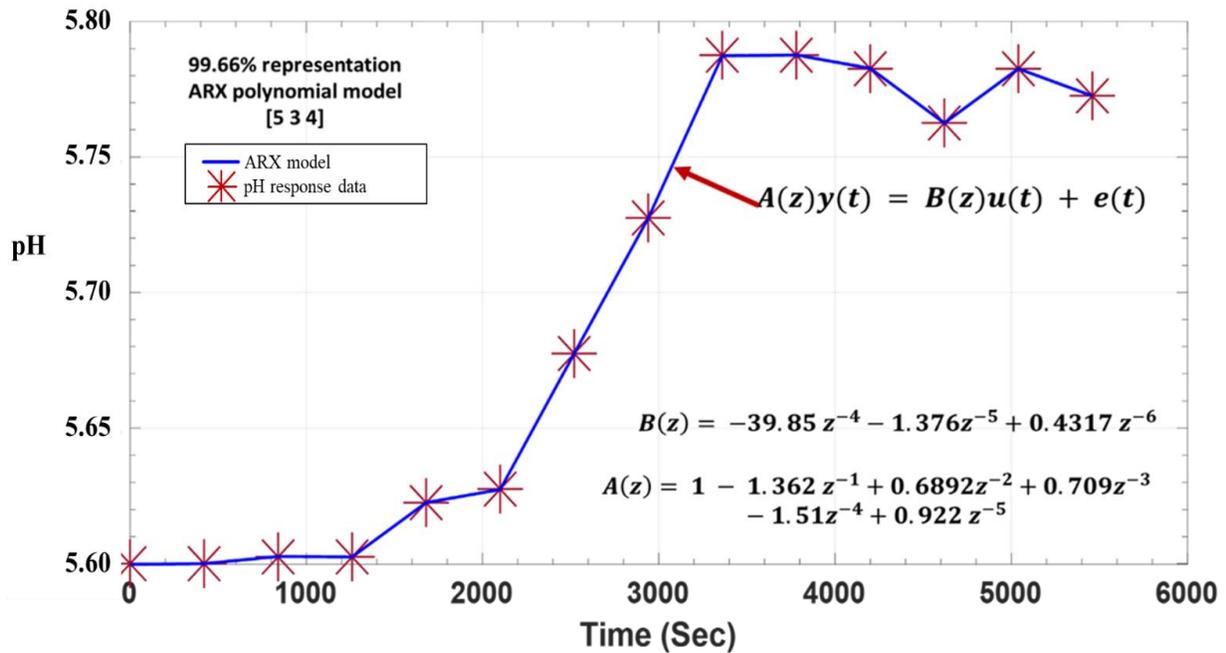
Figure 5.47. ARX [5 3 4], polynomial model in the z-transform of effluent pH response, of 280.0 mg PVA/L, step change from 0.12 to 0.024 [H_2O_2]/[PVA]; Model Order choice by Ident Matlab, from, [1:5 1:5 1:5]. 99.66 % representation.

Figure 5.48 represents an ARX model with an order of [5 1 1] for the pH data response of 280.0 mg PVA/L, a step change from 0.12 to 0.024 [H_2O_2]/[PVA] with a fitting estimation of 86.43 %. Although this particular ARX model has a lower data fitting score, it runs smoother over the pH response data and is a be better representation of the process response for a controller design. Figure 5.49 illustrates an ARX model with an order of [2 1 1], and a 76 % data fitting representation. Although the ARX model in Figure 5.49 runs smooth throw the pH response data, it does miss the character of the pH response data for the average PVA concentration of 280.0 mg PVA/L, a step change from 0.12 to 0.024 [H_2O_2]/[PVA].
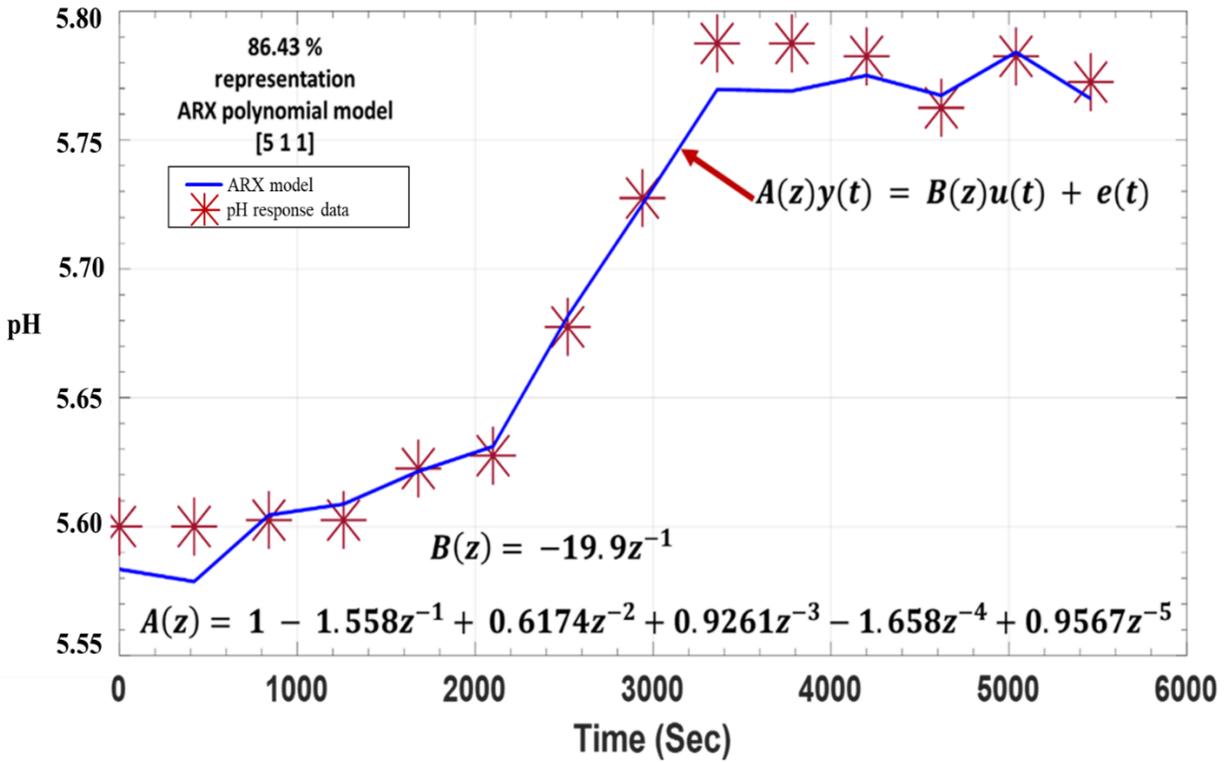
Figure 5.48. ARX [5 1 1] polynomial model in the z-transform of effluent pH response, of 280.0 mg PVA/L, step change from 0.12 to 0.024 [H$_2$O$_2$]/[PVA]; Model Order choice by Ident Matlab, from, [1:7 1:7 1:7], and an 86.43 % representation.
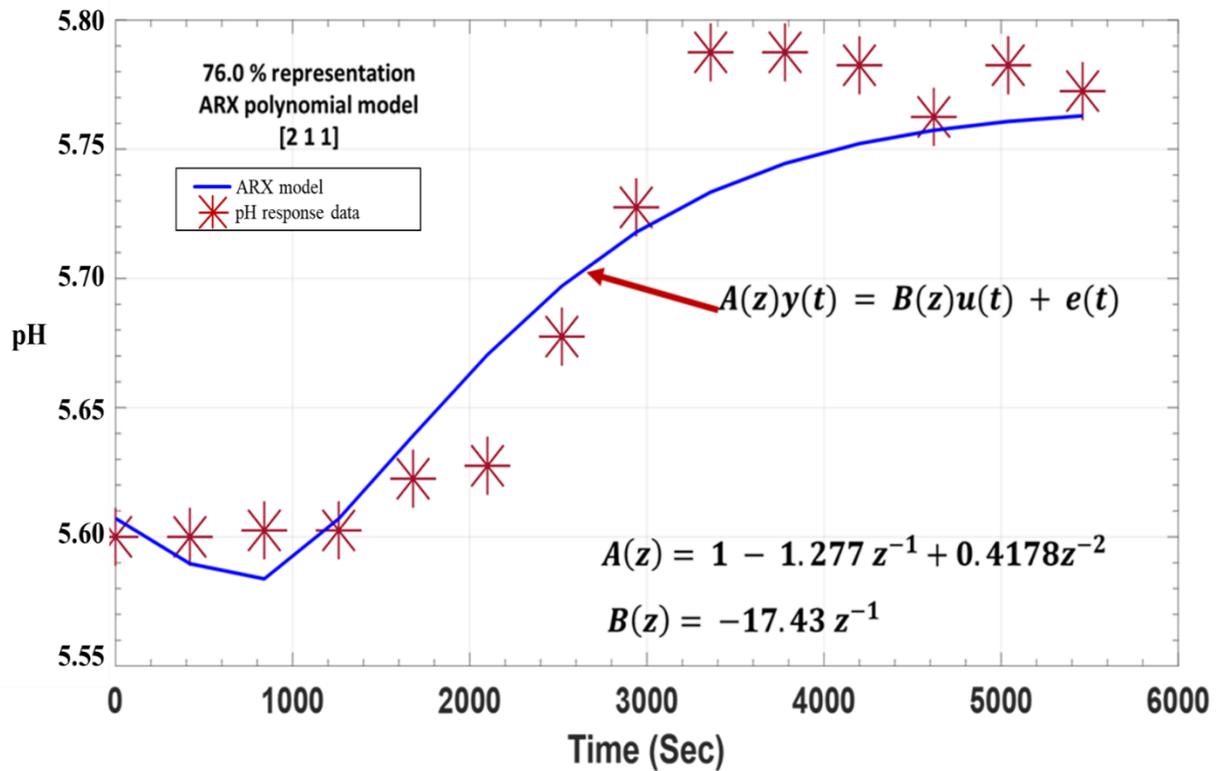
**Figure 5.49.** ARX [2 1 1], polynomial model in the z-transform of effluent pH response, of 280.0 mg PVA/L, step change from 0.12 to 0.024 [H$_2$O$_2$]/[PVA]; model order choice by Ident Matlab, from, [1:10 1:10 1:10], and data fitting score of 76.0 %.

5.2.3 Character of best fitting model

For a model to properly represent a response data it should possess a low square error sum throughout the data and should represent the data smoothly with no sharp edges. As was observed in the previous section, some ARX models have high fitting representation but lacks the smoothness over the response data. On the other hand, as was observed in Figure 5.49, the model runs smoothly over the data but consequently misses the character of the response. The ARX model that was determined with an order of [2 1 1], had a fitting representation of 76%.

5.2.3.1 Over fitting model

When a model represents a response data in relation to a change in an input variable, an over fitting may occur. Over fitting is clearly observed when a model accurately represents the response data but moves through the response data with sharp edges. The model may have high representation score but would not be suitable for a controller design. An example in Figure 5.46 of over fitting is the ARX model representation of 280.0 mg PVA/L, with a step change from 0.12 to 0.024 [H_2O_2]/[PVA] and an order of [6 1 1].

5.2.3.2 Under fitting model

An example of under fitting is apparent in Figure 5.49 where the ARX model with an order of [2 1 1], flows smoothly over the pH response data but misses the characters of the output. Table 5.5 summarizes transfer function representations of the pH response data for 280.0 mg PVA/L, step change from 0.12 to 0.024 [H_2O_2]/[PVA], without including the delay period response data.

5.2.4 Transfer function utilization in a controller block diagram

The transfer functions and ARX models that were determined in this study may be used in future work to design a controller to regulate the flow of hydrogen peroxide into the reactor. As the transfer function would be programmed into the controller computer, the controller would compare between the on-line measured pH values of the effluent and a pH set point. The controller would

measure the error and would order a peristaltic pump to either increase or decrease the flow of hydrogen peroxide into the reactor. The correction of the flow of hydrogen peroxide would correct the pH value back to its set point for maximum conversion. The following block diagram illustrates the mechanism for a possible hydrogen peroxide controller:
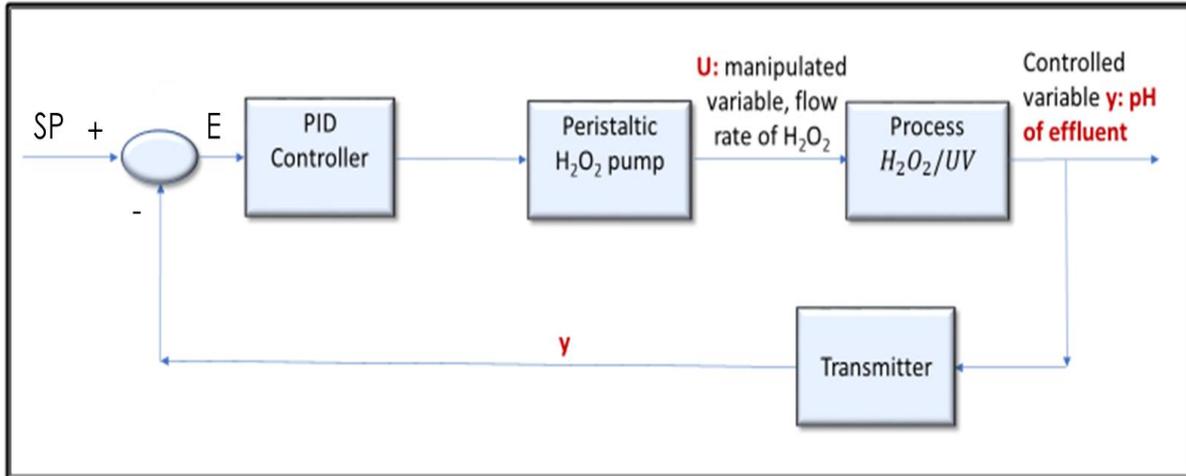
➤ **Set point**: pH optimum value-specified or reference value
➤ **Process variable**: pH actual measured variables (y)
➤ **Manipulated variable:** mass flow rate of the H_2O_2 into the controller.

Figure 5.50. Block diagram for an AOP controller design using ARX polynomial models of PVA degradation process UV/H_2O_2.

Table 5.5. Transfer functions representations without delay of, 280.0 mg PVA/L, step change from 0.12 to 0.024 [H_2O_2]/[PVA], Test # 5.

Step Change	# of poles and zeros	S–domain, (continuous t)	%	Z-domain (Discrete t) $t_k = kT$	%
1.68 to 0.336 mg H_2O_2/min	1 pole, no zeros	Low Representation		Low Representation	
	2 poles, no zeros	$G(s) = \dfrac{-110.0}{7.04 * 10^5 s^2 + 6.78 * 10^2 s + 1}$	83.25	Low Representation	
	2 poles, one zero	$G(s) = \dfrac{3.71 * 10^4 s - 115.6.0}{5.57 * 10^5 s^2 + 6.93 * 10^2 s + 1}$	84.36	$G(z) = \dfrac{-27.88 + 6.17 z^{-1}}{1 - 1.47 z^{-1} + 0.672 z^{-2}}$	81.75
	3 poles no zeros	$G(s) = \dfrac{-168.8}{5.23 * 10^8 s^3 + 4.59 * 10^5 s^2 + 2.23 * 10^3 s + 1}$	89.3	Low Representation	
	3 poles, one zero	$G(s) = \dfrac{5.13 * 10^4 s - 142.9}{2.45 * 10^8 s^3 + 4.08 * 10^5 s^2 + 1.40 * 10^3 s + 1}$	90.69	$G(z) = \dfrac{-43.88 + 15.4\ z^{-1}}{1 - 1.67\ z^{-1} + 1.33\ z^{-2} - 0.455\ z^{-3}}$	87.85
	3 poles 2 zeros	$G(s) = \dfrac{-1.6 * 10^7 s^2 + 4.24 * 10^4 s - 134.2}{1.30 * 10^8 s^3 + 3.37 * 10^5 s^2 + 1.04 * 10^3 s + 1}$	92.36	$G(z) = \dfrac{-66.67 + 113.3\ z^{-1} - 55.94\ z^{-2}}{1.00 - 2.15\ z^{-1} + 1.77\ z^{-2} - 0.544\ z^{-3}}$	84.1

CHAPTER 6
CONCLUSIONS AND RECOMMENDATIONS

6.1. Conclusions

In conclusion a step testing method was employed to dynamically identify the degradation of the polyvinyl alcohol solution in a photochemical continuous reactor with the presence of hydrogen peroxide (H_2O_2). The step testing was applied on three different PVA concentrations to cover the nonlinearity of the UV/H_2O_2 process. First order plus time delay model (FOPTD) for pH responses and TOC responses were determined using graphical technique. 8 FOPTD and 5 FOPTD models were determined for pH and TOC responses respectively. FOPTD and SOPTD were then determined for pH responses for all tests using system identification algorithms. Each FOPTD and SOPTD had a data fitting score percent that was provided by Matlab to assess the validity and accuracy of the model. Finally, ARX polynomial models were extracted for 280.0 mg PVA/L tests using system identification toolbox. A response data fitting score was calculated for each ARX model to reflect the model accuracy.

For the scope of this study, two responses were measured for a single input alteration. The pH and the TOC of the effluent of the treated PVA polymeric solution samples were measured as the output variables. A series of experimental tests were performed. The experimental design consists of three different initial PVA concentrations: 60.0, 280.0, and 500.0 mg PVA/L. Eight experimental tests were completed for different hydrogen peroxide mass flowrates ranging from 0.336 to 125 mg H_2O_2/min. For every test, a transfer function was experimentally determined to describe the dynamics of the UV/H_2O_2 photochemical reactor for the degradation of PVA polymer. With the future intent of developing a controller to regulate the hydrogen peroxide flow into the reactor, several transfer functions in s-space and z-space were developed from the input-output experimental data set.

The experimental design consists of degrading three different PVA solutions under UV light for different concentrations of hydrogen peroxide. In each case, the content of H_2O_2 in the inlet solution was subjected to a positive step change and also to a negative step change. By keeping the PVA solution volumetric flow rate invariant, guarantees a constant residence time, which

translates to a constant process dead-time. Alternatively, the tests demonstrated that different steady state gains were obtained, which reflect the nonlinear nature of the process.

Consequently, several different transfer functions of different order and different steady state gains were constructed from the data collected in the scheduled experimental design. In most cases, the transfer functions that were obtained using graphical method was not able to adequately predict the experimental data. Alternatively, a more reliable identification technique was attempted to produce first and second order transfer function with delay and also an Auto-regression exogenous input (ARX), polynomial models. The computations of the ARX model was performed using the Matlab identification toolbox.

Matlab software helps to calculate polynomial models for the set of the pH response data, and the input of the concentration of the hydrogen peroxide. The transfer functions for different initial concentrations of PVA, demonstrate the response of the system for specific hydrogen peroxide input changes.

6.2. Future Work and Recommendations

In future work, one or two inputs such as a sudden increase in the PVA concentration and the concentration of hydrogen peroxide, should be tested with two photochemical reactors in series or in parallel, to investigate the output variables. The intensity and the type of the UV light may be investigated as inputs for the PVA degradation in a UV/H_2O_2 process. The flow rate of hydrogen peroxide may be investigated as an input variable to measure the corresponding pH and TOC response data. The final concentrations of both the hydrogen peroxide as well as the PVA in solution effluent should be investigated in future work as an output variable for a predetermined step change. An AOP's Matlab Identification toolbox may be developed especially for pH responses to estimate best fits for response data. The best fits would be used to design controllers to stabilize the effluent pH by regulating the hydrogen peroxide feed into the photoreactor. The pH of the effluent must be controlled in order to minimize H_2O_2 residuals in the effluent streams and to maximize TOC removal and polymer degradation as well as to minimize H_2O_2 scavenging effect.

Another example of two inputs step testing is the flow rate of hydrogen peroxide coupled with the flow rate of PVA to measure the pH and TOC output responses. The Intensity of The UV light coupled with the hydrogen peroxide influent concentration may also be another possible input variables investigation for future work.

LIST OF APPENDICES

APPENDIX A.

A.1. Preparation of 60.0 mg/L of polyvinyl alcohol.
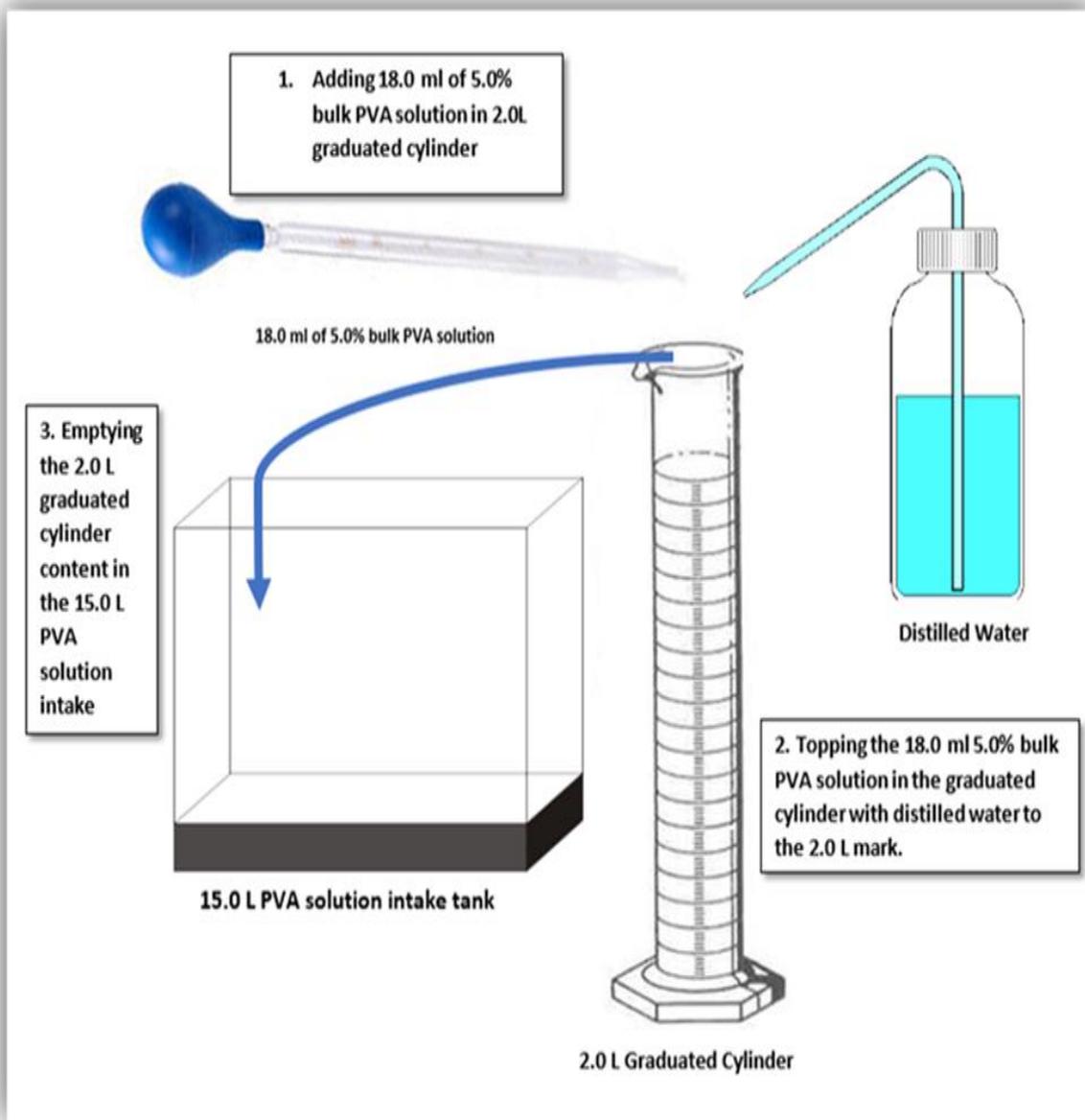
Figure A.1 Preparation of 60.0 mg PVA/L. In the preparation of 60.0 mg PVA/L, PAV solution, 18.0 ml of PVA bulk solution was pipetted into the 2.0 L graduated cylinder, then the graduated cylinder was topped with distilled water until it reached the 2.0 L mark on the graduated

cylinder. After the 2.0 L was poured into the intake tank, an additional 13.0 L was added to the intake tank of distilled water only. The following figure illustrates the addition of the 13.0 L of distilled water to the initial 2.0 L of PVA solution, to finally result in the 0.06 g PVA/L solution.
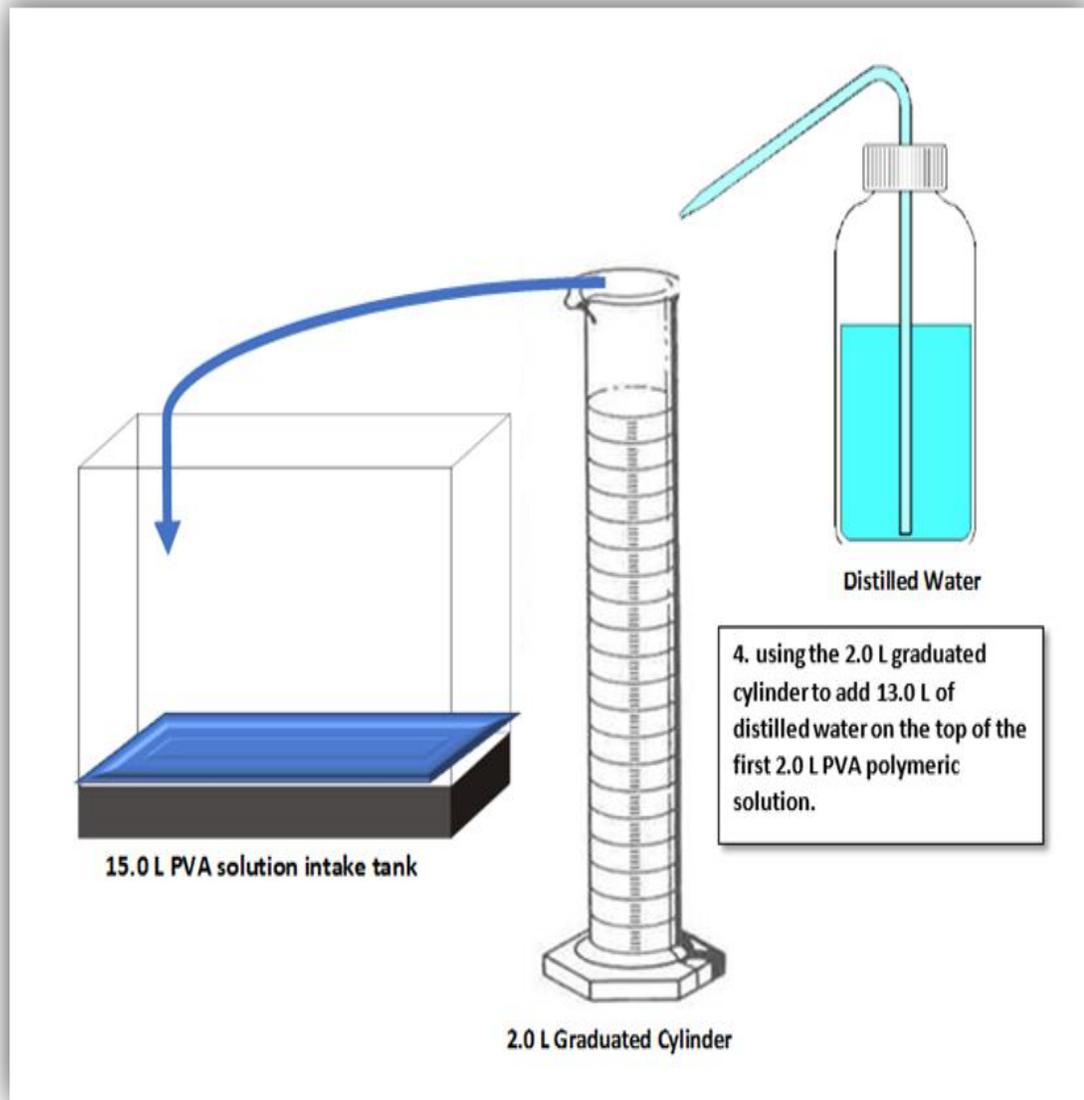
Figure A.2. Initial steps of preparing 15.0 L of 0.06 g PVA/L solution. Addition of 13.0 L of distilled water using the 2 .0 L graduated cylinder to the initial 2.0 L PVA solution prepared with the 18.0 ml of bulk PVA.

When adding the amount of 0.9 PVA into 15.0 L of distilled water, the resulting PVA solution would have a concentration of 0.06 g PVA /l, 60 mg PVA/L.

A.2. Preparation of 6.0 g H₂O₂/L, as the initial concentration for the degradation of 60.0 mg PVA/L, PVA polymeric solution.

2.0 ml of bulk 30.0 % bulk

Topping the 100.0 ml volumetric flask with distilled water.

A100ml

100.0 ml volumetric flask for the preparation of H₂O₂ solutions
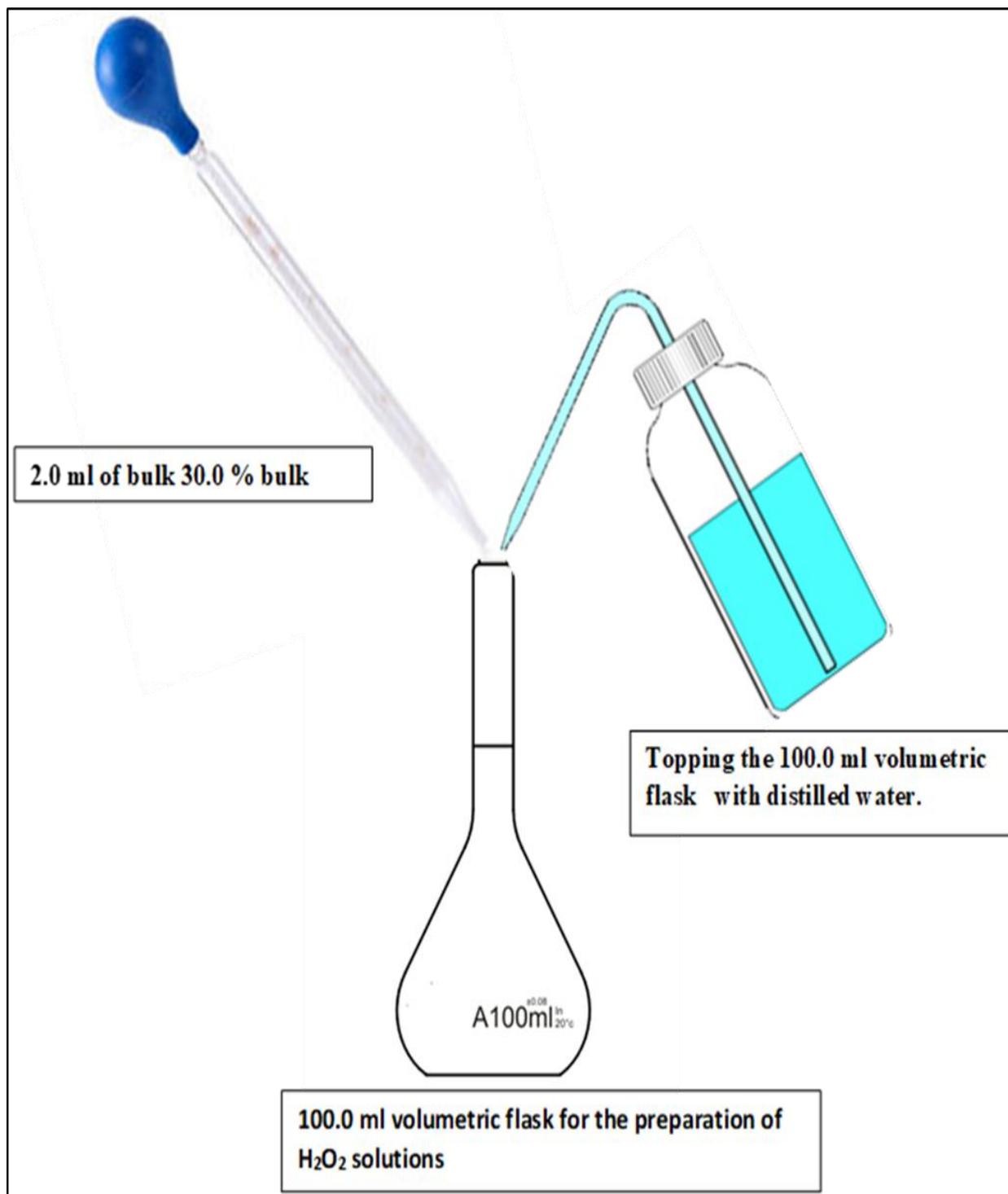
Figure A.3. Illustration of preparing 6.0 g H_2O_2/L, hydrogen peroxide solution as the initial input concentration into the photochemical reactor at a constant flow rate of 0.5 ml/min.

A.3. Preparation of 30.0 g H₂O₂/L, as the step change concentration for the 60.0 mg PVA/L, PVA polymeric solution

10.0 ml of bulk 30.0 % bulk

Topping the 100.0 ml volumetric flask with distilled water.

A100ml

100.0 ml volumetric flask for the preparation of H₂O₂ solutions
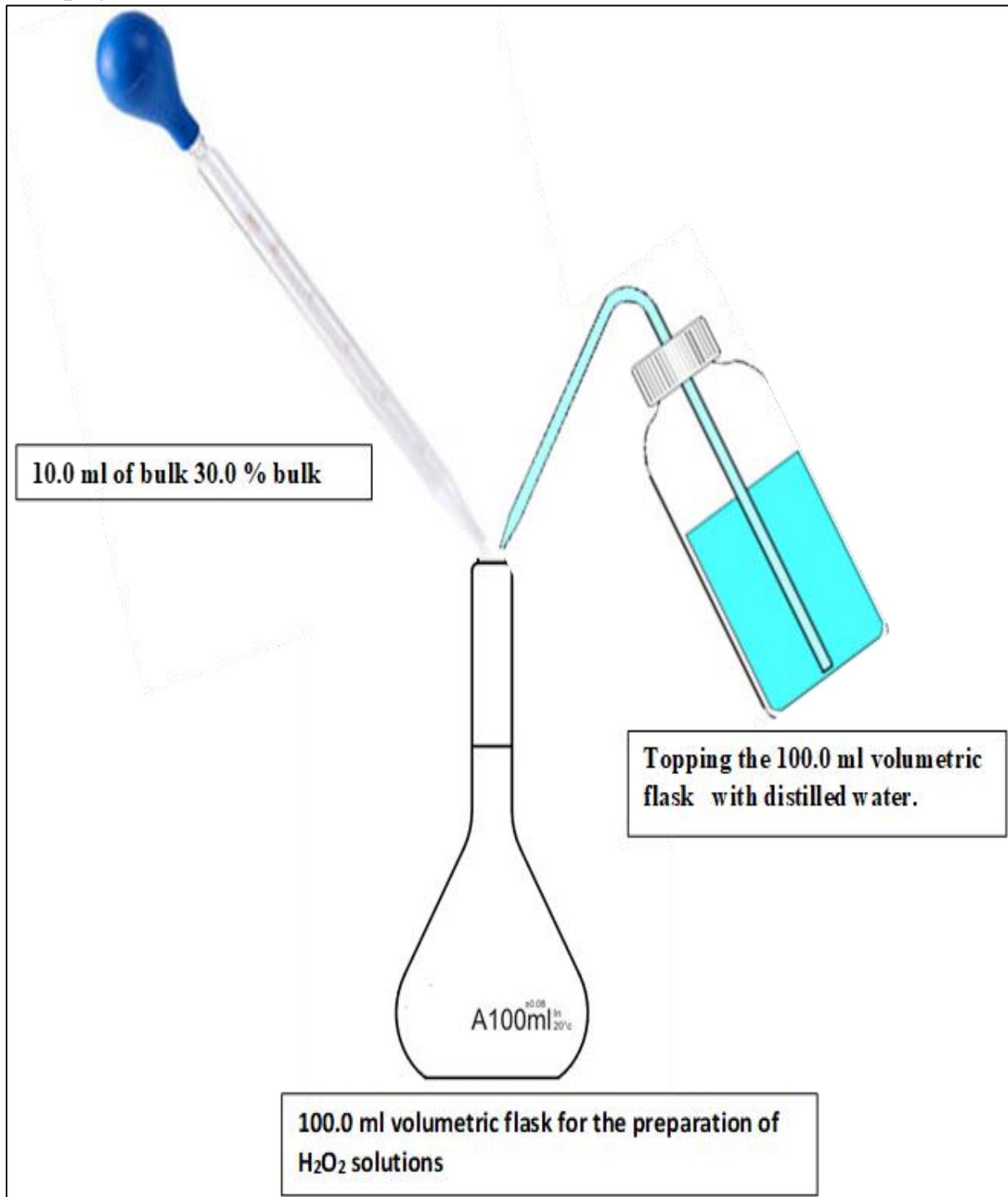
Figure A.4. Illustration of preparing 30.0 g H₂O₂/L, hydrogen peroxide solution as the step change input concentration for the 60.0mgPVA/L, step change 1.0-5.0 [H₂O₂]/[PVA].
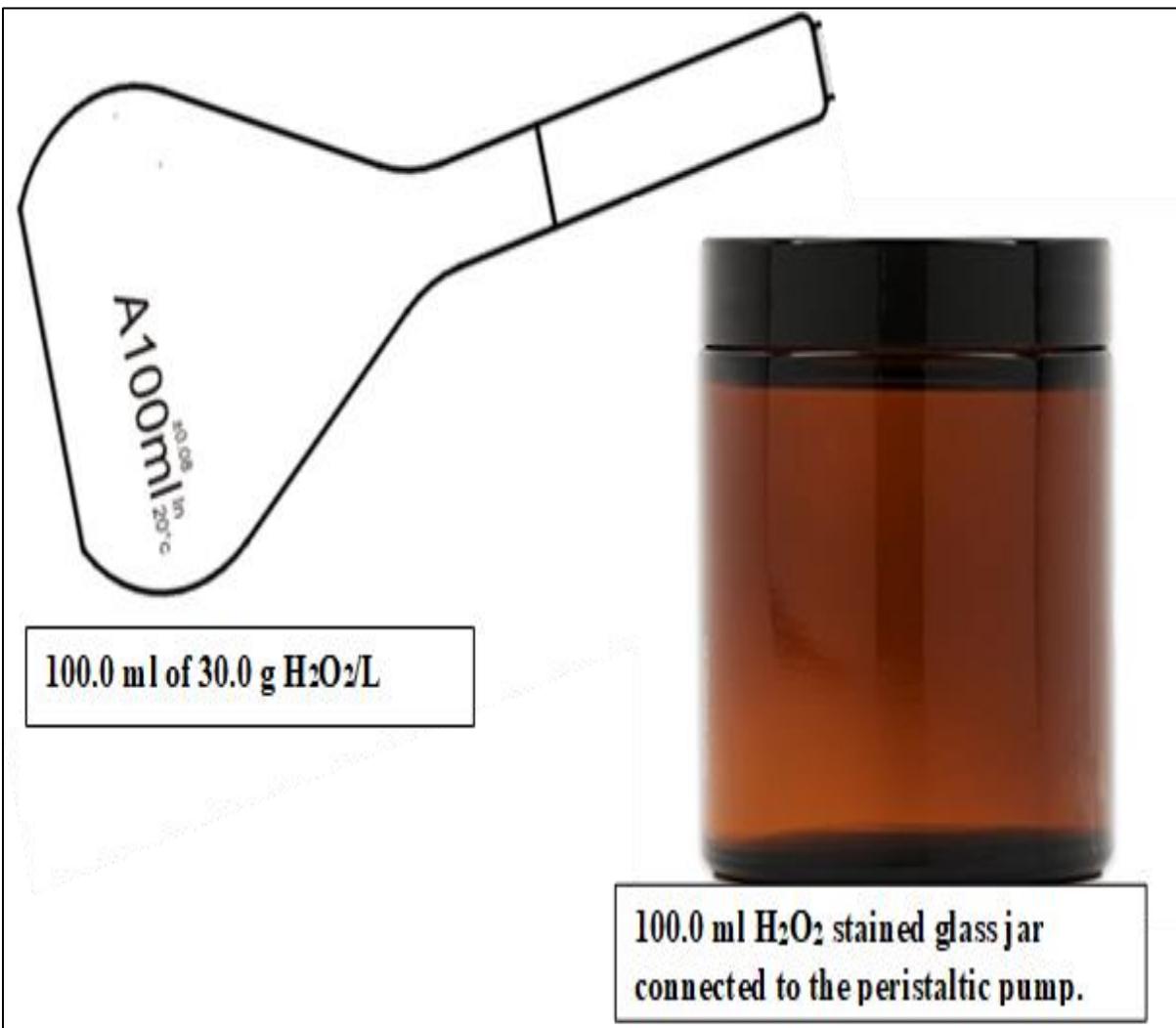
Figure A.5. Illustration of the transferring of the 100.0 ml of 30.0 g H_2O_2/L, hydrogen peroxide solution into the tanned jar that is connected to the Hydrogen peroxide peristaltic pump to start a step change from 1.0-5.0 $[H_2O_2]/[PVA]$.

APPENDIX B.

Additional Experimental Data

B.1. Calculations of Experiment 60.0 mg PVA/L, Step Change from 1.0 to 0.20 [H$_2$O$_2$]/[PVA]

$$\frac{0.06\ g\ PVA}{L} \times \frac{50\ ml}{min} \times \frac{1\ L}{1000\ ml} = \frac{0.003\ g\ PVA}{min}$$

$$\frac{6.0\ g\ H_2O_2}{L} \times \frac{0.5\ ml}{min} \times \frac{1\ L}{1000\ ml} = \frac{0.003\ g\ H_2O_2}{min}$$

$$\frac{1.2\ g\ H_2O_2}{L} \times \frac{0.5\ ml}{min} \times \frac{1\ L}{1000\ ml} = \frac{0.0006\ g\ H_2O_2}{min}$$

$$0.20 = \frac{[H_2O_2]}{[PVA]}$$

$$[H_2O_2] = 0.2[PVA]$$

$$[H_2O_2] = 0.2 \times \frac{0.003\ g}{min}$$

$$[H_2O_2] = 0.003\ \frac{g\ H_2O_2}{min}$$

$$step-change\ To$$

$$[H_2O_2] = 0.0006 \frac{g\ H_2O_2}{min}$$

B.2. Calculations of Experiment 60.0 mg PVA/L, Step change from 0.12 to 0.024 [H$_2$O$_2$]/[PVA].

$$\frac{0.06\ g\ PVA}{L} \times \frac{50\ ml}{min} \times \frac{1\ L}{1000\ ml} = \frac{0.003\ g\ PVA}{min}$$

$$\frac{0.72\ g\ H_2O_2}{L} \times \frac{0.5\ ml}{min} \times \frac{1\ L}{1000\ ml} = 0.00036 \frac{g\ H_2O_2}{min}$$

$$\frac{0.144\ g\ H_2O_2}{L} \times \frac{0.5\ ml}{min} \times \frac{1\ L}{1000\ ml} = 0.000072 \frac{g\ H_2O_2}{min}$$

$$0.12 = \frac{[H_2O_2]}{[PVA]}$$

$$[H_2O_2] = 0.12 \times [PVA]$$

$$[H_2O_2] = 0.12 \times \frac{0.003\ g}{min}$$

$$[H_2O_2] = 0.00036\ \frac{g\ H_2O_2}{min}$$

$$step - change\ To$$

$$[H_2O_2] = 0.000072\ \frac{g\ H_2O_2}{min}$$

B.3. Calculations of Experiment 280.0 mg PVA/L, Step change of 1.0 to 0.20 [H₂O₂]/[PVA].

$$\frac{0.28\ g\ PVA}{L} \times \frac{50\ ml}{min} \times \frac{1\ L}{1000\ ml} = \frac{0.014\ g\ PVA}{min}$$

$$\frac{28.0\ g\ H_2O_2}{L} \times \frac{0.5\ ml}{min} \times \frac{1\ L}{1000\ ml} = \frac{0.014\ g\ H_2O_2}{min}$$

$$To$$

$$\frac{5.6\ g\ H_2O_2}{L} \times \frac{0.5\ ml}{min} \times \frac{1\ L}{1000\ ml} = \frac{0.0028\ g\ H_2O_2}{min}$$

$$0.20 = \frac{[H_2O_2]}{[PVA]}$$

$$[H_2O_2] = 0.2[PVA]$$

$$[H_2O_2] = 0.2 \times \frac{0.014\ g}{min}$$

$$[H_2O_2] = 0.014\ \frac{g\ H_2O_2}{min}$$

$$step - change\ To$$

$$[H_2O_2] = 0.0028\ \frac{g\ H_2O_2}{min}$$

B.4. Calculations of Experiment 280.0 mg PVA/L, Step change of 1.0 to 5.0 [H₂O₂]/[PVA]

$$\frac{0.28 \ g \ PVA}{L} \times \frac{50 \ ml}{min} \times \frac{1 \ L}{1000 \ ml} = \frac{0.014 \ g \ PVA}{min}$$

$$\frac{28.0 \ g \ H_2O_2}{L} \times \frac{0.5 \ ml}{min} \times \frac{1 \ L}{1000 \ ml} = \frac{0.014 \ g \ H_2O_2}{min}$$

TO

$$\frac{140.0 \ g \ H_2O_2}{L} \times \frac{0.5 \ ml}{min} \times \frac{1 \ L}{1000 \ ml} = \frac{0.07 \ g \ H_2O_2}{min}$$

$$5.0 = \frac{[H_2O_2]}{[PVA]}$$

$$[H_2O_2] = 5.0 \times [PVA]$$

$$[H_2O_2] = 5.0 \times \frac{0.014 \ g}{min}$$

$$[H_2O_2] = 0.014 \ \frac{g \ H_2O_2}{min}$$

$$step - change \ To$$

$$[H_2O_2] = 0.07 \ \frac{g \ H_2O_2}{min}$$

B.5. 280.0 mg PVA/L, Step change, 0.12 to 0.024 [H₂O₂]/[PVA]

$$\frac{0.28 \ g \ PVA}{L} \times \frac{50 \ ml}{min} \times \frac{1 \ L}{1000 \ ml} = \frac{0.014 \ g \ PVA}{min}$$

$$\frac{3.36 \ g \ H_2O_2}{L} \times \frac{0.5 \ ml}{min} \times \frac{1 \ L}{1000 \ ml} = \frac{0.00168 \ g \ H_2O_2}{min}$$

TO

$$\frac{0.672 \ g \ H_2O_2}{L} \times \frac{0.5 \ ml}{min} \times \frac{1 \ L}{1000 \ ml} = \frac{0.000336 \ g \ H_2O_2}{min}$$

$$0.12 = \frac{[H_2O_2]}{[PVA]}$$

$$[H_2O_2] = 0.12 \times [PVA]$$

$$[H_2O_2] = 0.12 \times \frac{0.014 \, g}{min}$$

$$[H_2O_2] = 0.00168 \, \frac{g \, H_2O_2}{min}$$

$$step - change \, To$$

$$[H_2O_2] = 0.000336 \, \frac{g \, H_2O_2}{min}$$

B.6. Calculations of Experiment 500.0 mg PVA/L, Step change of 1.0 to 0.20 [H₂O₂]/[PVA]

$$\frac{0.5 \, g \, PVA}{L} \times \frac{50 \, ml}{min} \times \frac{1 \, L}{1000 \, ml} = \frac{0.025 \, g \, PVA}{min}$$

$$\frac{50.0 \, g \, H_2O_2}{L} \times \frac{0.5 \, ml}{min} \times \frac{1 \, L}{1000 \, ml} = \frac{0.025 \, g \, H_2O_2}{min}$$

$$TO$$

$$\frac{10.0 \, g \, H_2O_2}{L} \times \frac{0.5 \, ml}{min} \times \frac{1 \, L}{1000 \, ml} = \frac{0.0028 \, g \, H_2O_2}{min}$$

$$0.20 = \frac{[H_2O_2]}{[PVA]}$$

$$[H_2O_2] = 0.2[PVA]$$

$$[H_2O_2] = 0.2 \times \frac{0.025 \, g}{min}$$

$$[H_2O_2] = 0.025 \, \frac{g \, H_2O_2}{min}$$

$$step - change \, To$$

$$[H_2O_2] = 0.005 \, \frac{g \, H_2O_2}{min}$$

B.7. Calculations of Experiment 500.0 mg PVA/L, Step change of 1.0 to 5.0 [H₂O₂]/[PVA]

$$\frac{0.5 \, g \, PVA}{L} \times \frac{50 \, ml}{min} \times \frac{1 \, L}{1000 \, ml} = \frac{0.025 \, g \, PVA}{min}$$

$$\frac{50.0 \, g \, H_2O_2}{L} \times \frac{0.5 \, ml}{min} \times \frac{1 \, L}{1000 \, ml} = \frac{0.025 \, g \, H_2O_2}{min}$$

$$TO$$

$$\frac{250.0 \; mg \; H_2O_2}{L} \times \frac{0.5 \; ml}{min} \times \frac{1 \; L}{1000 \; ml} = \frac{0.125 \; g \; H_2O_2}{min}$$

$$5.0 = \frac{[H_2O_2]}{[PVA]}$$

$$[H_2O_2] = 5.0 \times [PVA]$$

$$[H_2O_2] = 5.0 \times \frac{0.025 \; g}{min}$$

$$[H_2O_2] = 0.025 \; \frac{g \; H_2O_2}{min}$$

$$step - change \; To$$

$$[H_2O_2] = 0.125 \; \frac{g \; H_2O_2}{min}$$

B.8. Calculations of Experiment 500.0 mg PVA/L, Step change from 0.12 to 0.024 [H₂O₂]/[PVA].

$$\frac{0.50 \; g \; PVA}{L} \times \frac{50 \; ml}{min} \times \frac{1 \; L}{1000 \; ml} = \frac{0.025 \; g \; PVA}{min}$$

$$\frac{6.0 \; g \; H_2O_2}{L} \times \frac{0.5 \; ml}{min} \times \frac{1 \; L}{1000 \; ml} = \frac{0.003 \; g \; H_2O_2}{min}$$

$$TO$$

$$\frac{1.2 \; g \; H_2O_2}{L} \times \frac{0.5 \; ml}{min} \times \frac{1 \; L}{1000 \; ml} = \frac{0.0006 \; g \; H_2O_2}{min}$$

$$0.12 = \frac{[H_2O_2]}{[PVA]}$$

$$[H_2O_2] = 0.12 \times [PVA]$$

$$[H_2O_2] = 0.12 \times \frac{0.025 \; g}{min}$$

$$[H_2O_2] = 0.003 \; \frac{g \; H_2O_2}{min}$$

$$step - change \; To \qquad\qquad [H_2O_2] = 0.0006 \; \frac{g \; H_2O_2}{min}$$

APPENDIX C.

C.1. UV Light Theory

$$c = \lambda \times v$$

$v:$ is the Radiation Frequency s^{-1}

$\lambda:$ is the UV radiation wavelength in units of m

$c:$ Is the speed of light in $\dfrac{m}{s}$

$$\frac{m}{s} = m \times \frac{1}{s}$$

A quantum E is the minimum amount of energy that can be stored in an electromagnetic wave at that wavelength. That is clear in Planck's equation:

$$E = h \times v$$

$E:$ is the quantum of maximum energy strored as an electromagnatic wave in a specific wavelength.

$h:$ Planck's constant that relates the photon particle of energy to the frequency of the UV light.

$$Planck's\ Constant: 6.63 \times 10^{-34} \frac{m^2}{s} \times kg$$

$$c = \lambda \times v$$

Planck's constant also relates the energy of the photon emitted by the UV light to the speed of light and the wave length of the UV light as follows:

$$E = h.v$$

$$E = h \times \frac{c}{\lambda}$$

where $E:$ is the quantum energy stored in an electromagnatic wave related to the UV wavelength.

$h:$ the Planck's constant that relates the amount of energy stored in an electromagnatic wave to frequency.

c: The speed of light in $\frac{m}{s}$.   ($300{,}000{,}000.0\frac{m}{s}$)

$J = N.m$

$J = kg \times \frac{m}{s^2} \times m$

plancks constant units: $kg \times \frac{m}{s^2} \times m \times s$

plancks constant units: $\frac{m^2}{s} \times kg$

Planck's constant in units of $(J.s)$ or $(N.m.s)$ or $\left(Kg \times \frac{m}{s^2} \times m \times s \right)$

Planck's constant in units of $\left(Kg \times \frac{m^2}{s} \right)$

The value of Planck's constant is: $6.63 \times 10^{-34} J.s$

The radiation transfer equation can be attained from, the photon balance as follows:

$$\frac{dI_\lambda}{dS} + K_\lambda I_\lambda = 0$$

I_λ: specific monochromic intensity of the UV light in $\frac{W}{m^2}$.

S: is the distance from the UV surce to the molecule absorbing the UV energy in the treated solution.

K_λ: UV Absorption coefficent constant of the UV light being absorbed by the chemical species.

The boundary condition of the radiation transfer equation as follows: -

at $S = 0$, meaning the UV light wave didnt travel from the UV source yet, the S would be zero.

At $S = 0$, the SMI of the UV source would equal to the initial intensity emitted from the UV lamp.

at $S = 0$, the SMI of the UV source would equal to the initial intensity emitted

116

from the UV lamp.

$$at\ S = 0,\ \ I_\lambda = I_o$$

The UV absorption coefficient K_λ, is proportional to the radiation absorbed.

The UV absorption coefficient is also proportional, to the concentration of the chemical species.

The following proportionality may be written as:

$K_\lambda\ \alpha\ \ \varepsilon \times C_i$

ε: *Molar absorptivity of the chemical species.*

C_i: *Concentration of the Checmial species that absorbed the UV light.*

K_λ: *UV Absorptian coefficent.*

The absorptivity coefficient may be written as the product of the molar absorptivity constant and the concentration of the chemical solution that have absorbed the UV radiation as follows:

$$K_\lambda = \varepsilon \times C_i$$

$I_\lambda = I_o e^{\left(-\int_0^b \varepsilon \times C_i . dS\right)}$

I_o: *The incedient UV light intensity in* $\frac{W}{m^2}$ *at the boundary condition* $S = 0$.

I_λ: *Reflected UV light intensity of the Chemcial species in* $\frac{W}{m^2}$ *at the boundary* $S = b$.

S: *The distance travelled by the UV light from the UV light source to the*
 chemical species.

b: *The actual distance travelled by the UV light from the UV light source to the*
 chemical species.

ε: *The molar absorpitivity of the chemial species of the UV light.*

C_i: *The concentartion of the chemical species that is absorbing the UV light.*

Beer Lambert relates the absorptivity to the medium that the UV light is travelling through in terms of number of species, the concentration of each species, and the molar absorptivity of each spices to the UV light. Beer Lambert equation is written as follows:

$$10^{-A} = \frac{I_\lambda}{I_o}$$

Where A is written as follows:

$$A = b \sum_{i=1}^{N} (\varepsilon_i . C_i)$$

A: Is a dimensionless parameter that quantifies the absorbed UV light by the chemical species.

The absorbed light intensity absorbed by the chemical species I_a, is the difference between the incident light intensity at the boundary condition S=0, and the reflected light intensity absorbed by the chemical species at S=b. The equation relating the absorbed light intensity with both the incident and the reflected is written as follows:

$$I_a = I_0 - I_\lambda$$

The fraction of absorbed Intensity by an exact chemical species is written as follows:

$$f_i = \frac{\varepsilon_i \times C_i}{\sum_{i=1}^{N}(\varepsilon_i \times C_i)}$$

The amount of UV light that is absorbed by a certain chemical species is written as follows:

$$I_{ai} = f_i \times I_o \left[1 - e^{\left(-2.303b \sum_{i=1}^{N}(\varepsilon_i \times C_i)\right)}\right]$$

Only quantum light absorbed by the molecule can be effective in alternating the molecule, and can be translated as the quantum yield.

The quantum yield can be expressed as follows:

$$\emptyset_i = \frac{Number\ of\ moles\ of\ Chemical\ species\ transformed\ by\ UV\ light.}{Number\ of\ photons\ of\ whave\ length\ \lambda, absorbed\ by\ the\ transformed\ chemical\ species.}$$

Local volumetric rate of absorption may be expressed as follows:

$$R_{UV,i} = -\phi_i f_i I_o \left[1 - e^{\left(-2.303b \sum_{i=1}^{N}(\varepsilon_i \times C_i)\right)}\right]$$

$$I_{ai} = f_i I_o$$

$$-\phi_i = \frac{R_{UV.i}}{I_{ai}}$$

$$R_{UV,i} = -\frac{dC_i}{dt}$$

$$\phi_i = \frac{-\frac{dC_i}{dt}}{I_{a,i}}$$

APPENDIX D.

D.1. Calculation of time needed for the PVA solution to reach the reactor

From the influent tank to the mixing point
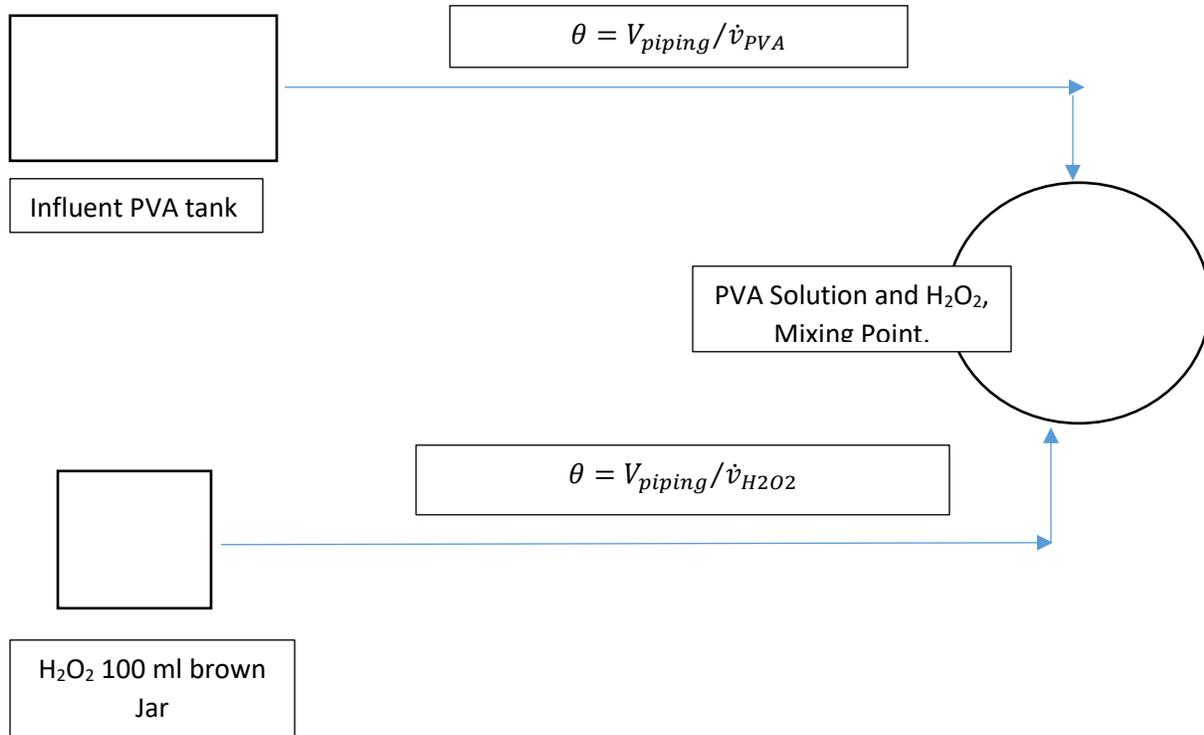
Figure D.1. Flow chart of the residence time of PVA as well as the hydrogen peroxide prior to entering the photochemical reactor.

$Total\ piping\ volum\ from\ influent\ tank\ to\ the\ mixing\ point$

$$= \left(\pi(\frac{2.5}{8})^2 \times 13.75\ inch\right) + (\pi\left(\frac{2.5}{8}\right)^2 \times 4.0\ inch) + \left(\pi\left(\frac{2.5}{8}\right)^2 \times 5.0\ inch\right)$$

$$+ \left(\pi\left(\frac{2.5}{8}\right)^2 \times 1.5\ inch\right) + (\pi\left(\frac{1.5}{8}\right)^2 \times 14.75\ inch) + (\pi\left(\frac{2.5}{8}\right)^2 \times 5.125\ inch)$$

$$+ (\pi\left(\frac{2.5}{8}\right)^2 \times 15.75\ inch) + (\pi\left(\frac{1.5}{8}\right)^2 \times 19.75\ inch) + (\pi\left(\frac{1}{8}\right)^2 \times 25.75\ inch)$$

Total piping volum from influent tank to the mixing point
$$= 4.22inch^3 + 1.227inch^3 + 1.534inch^3 + 0.46inch^3 + 1.63inch^3$$
$$+ 1.5723inch^3 + 4.83inch^3 + 2.18inch^3 + 1.264inch^3$$

Total piping volum from influent tank to the mixing point $= 18.92\ inch^3$

$$18.92\ inch^3 \times \frac{16.387\ cm^3}{(1\ inch)^3}$$

Total piping volum from influent tank to the mixing point $= \mathbf{310.042\ cm^3}$

$$\theta_{0\ PVA} = \frac{Total\ piping\ volum\ from\ influent\ tank\ to\ the\ mixing\ point}{\dot{v}_{PVA}}$$

$$\theta_{0\ PVA} = \frac{310.043\ cm^3}{50\ cm^3/min}$$

$$\boldsymbol{\theta_{0\ PVA} = 6.2\ min}$$

Now we calculate
$$\boldsymbol{\theta_{0\ H_2O_2}}$$

D.2. For a 60 mg PVA/L density calculation

$$\rho_{PVA}: 1.19\ \frac{g}{cm^3}$$

$$\rho_{H_2O}: 1.00\ \frac{g}{cm^3}$$

For a mixture with known mass fractions, the density of a solution would be an additive property as follows:

$$\rho_{PVA\ solution} = (X_{PVA} \times \rho_{PVA}) + (X_{H_2O} \times \rho_{H_2O})$$

PVA solution we have is a 5%

Now it is desired to prepare 60 mg PVA/L

$$1000 \; ml \; of \; PVA \; solution \; - \rightarrow 50 \; g \; PVA$$

$$X \; PVA \; solution \; - \rightarrow 0.06 \; g \; PVA$$

Therefore, the volume of PVA solution needed to prepare 1 L of PVA solution is 1.2 ml PVA bulk.

Of the 1.2 ml of bulk PVA, 5% is PVA.

$$1000 \; ml \; of \; PVA \; Bulk \; - \rightarrow 50 \; g \; PVA$$

$$1.2 \; ml \; of \; PVA \; Bulk \; - \rightarrow X \; g \; PVA$$

$$1000 \; ml \; of \; PVA \; solution \; - - - - - \rightarrow 1.2 \; ml \; of \; Bulk \; PVA + 998.8 \; ml \; of \; distilled \; water$$

$$1000 \; ml \; of \; PVA \; solution-$$
$$\rightarrow 1.14 \; ml \; distilled \; water + 0.06g \; PVA + 998.8 \; ml \; of \; distilled \; water$$

$$1000 \; ml \; of \; PVA \; solution- \rightarrow 0.06g \; PVA + 999.94 \; ml \; of \; distilled \; water$$

$$1000 \; ml \; of \; PVA \; solution- \rightarrow 0.06g \; PVA + 999.94 \; g \; of \; distilled \; water$$

$$\rho_{PVA \; solution} = (X_{PVA} \times \rho_{PVA}) + (X_{H_2O} \times \rho_{H_2O})$$

$$\rho_{PVA \; solution} = \left(6.0 \times 10^{-5} \times 1.19 \frac{g}{cm^3}\right) + \left(0.99994 \times 1.0 \frac{g}{cm^3}\right)$$

$$\rho_{PVA\ solution} = \left(7.14 \times 10^{-5}\, \frac{g}{cm^3}\right) + \left(0.99994\, \frac{g}{cm^3}\right)$$

$$\boldsymbol{\rho_{PVA\ solution} = 1.00001\, \frac{g}{cm^3}}$$

D.3. H_2O_2 solution calculation

$$0.060\ PVA\ \frac{g}{L} \times 50\, \frac{cm^3}{min} \times \frac{L}{1000\ cm^3} = 3.0 \times 10^{-3}\, \frac{g\ PVA}{min}$$

$$H_2O_2\, \frac{g}{L} \times 0.50\, \frac{cm^3}{min} \times \frac{L}{1000\ cm^3} = 3.0 \times 10^{-3}\, \frac{g\ H_2O_2}{min}$$

For this specific run, H$_2$O$_2$ concentration is:

$$6.0\ H_2O_2\, \frac{g}{L}$$

$1000\ ml\ of\ bulk\ H_2O_2\ \text{--------------------------}\rightarrow 300\ g\ H_2O_2$

$X\ ml\ of\ bulk\ H_2O_2\ \text{-----------------------------}\rightarrow 6.0\ g\ H_2O_2$

$X\ ml\ of\ bulk\ H_2O_2 = 20\ ml\ per\ 1\ L\ total$

$X\ ml\ of\ bulk\ H_2O_2 = 2.0\ ml\ per\ 100\ ml\ total$

Assuming additive volumes for this part of the problem.

$100\ ml\ flask\ \text{--------}\rightarrow 98.0\ ml\ distilled\ water + 2.0\ ml\ of\ bulk\ H_2O_2$

$100\ ml\ flask\ \text{---}\rightarrow 98.0\ ml\ distilled\ water + 0.6\ g\ H_2O_2 + 1.4\ ml\ of\ distilled\ water$

$$100 \ ml \ flask \ - --\rightarrow 99.4 \ g \ distilled \ water + 0.6 \ g \ H_2O_2$$

$$\rho_{H_2O_2 \ solution} = \left(X_{H_2O_2} \times \rho_{H_2O_2}\right) + \left(X_{H_2O} \times \rho_{H_2O}\right)$$

$$\rho_{H_2O_2 \ solution} = \left(6.0 \times 10^{-3} \times 1.45 \frac{g}{cm^3}\right) + \left(0.994 \times 1.0 \ \frac{g}{cm^3}\right)$$

$$\rho_{H_2O_2 \ solution} = \left(8.7 \times 10^{-3} \frac{g}{cm^3}\right) + \left(0.994 \ \frac{g}{cm^3}\right)$$

$$\boldsymbol{\rho_{H_2O_2 \ solution} = 1.003 \frac{g}{cm^3}}$$

The density of the solution of the mixing point of the hydrogen peroxide solution as well as the PVA solution:

$$\rho_{PVA \ and \ H_2O_2} = \left(X_{PVA} \times \rho_{PVA}\right) + \left(X_{H_2O} \times \rho_{H_2O}\right) + \left(X_{H_2O_2} \times \rho_{H_2O_2}\right)$$

D.4. Per minute calculation basis in the mixing point

$$m_{H_2O_2 solution} = 0.5000 \ \frac{cm^3}{min} \times 1.0027 \frac{g}{cm^3}$$

$$\dot{m}_{H_2O_2 solution} = 0.5014 \frac{g}{min}$$

$$m_{PVA \ solution} = 50.0000 \frac{cm^3}{min} \times 1.0000114 \frac{g}{cm^3}$$

$$\dot{m}_{PVA \ solution} = 50.0006 \frac{g}{min}$$

$$\dot{m}_{Total \ mixture} = \dot{m}_{H_2O_2 solution} + \dot{m}_{PVA \ solution}$$

$$\dot{m}_{Total \ mixture} = 50.0006 \frac{g}{min} + 0.5014 \frac{g}{min}$$

$$\boldsymbol{\dot{m}_{Total \ mixture} = 50.5020 \frac{g}{min}}$$

D.5. Total mixture density from the thermotical values of density for pure PVA, H₂O₂, and Water as follows:

$$\rho_{PVA}: 1.19 \ \frac{g}{cm^3}$$

$$\rho_{H_2O}: 1.00 \ \frac{g}{cm^3}$$

$$\rho_{H_2O_2} = 1.45 \ \frac{g}{cm^3}$$

$$\dot{m}_{\text{Total mixture}} = 50.50192 \ \frac{g}{min}$$

$$X_{H_2O} = \frac{50.49592}{50.50192 \ g}$$

$$X_{PVA} = \frac{0.003g}{50.50192 \ g}$$

$$X_{H_2O_2} = \frac{0.003}{50.50192 \ g}$$

$$\dot{m}_{\text{Total mixture}} = 50.502 \ \frac{g}{min}$$

$$\rho_{total} = \frac{\dot{m}_{\text{Total mixture}}}{\dot{Q}_{Total \ mixture}}$$

$$\rho_{total} = \frac{50.502 \ g/min}{50.500 \ ml/min}$$

$$\boldsymbol{\rho_{total} = 1.0000 \ g/ml}$$

D.6. Estimated time delay in the photochemical reactor

$$\theta = \frac{V_{eff}}{Q_{PVA+H_2O_2}}$$

Where the V_{eff} is the effective volume of the photochemical reactor

$Q_{PVA+H_2O_2}$ is the volumetric flow rate of the PVA and the hydrogen peroxide solution mixture entering the photochemical reactor.

$$\theta = \frac{430.0 \ cm^3}{50.5 \ cm^3/min}$$

$$\theta = 8.5 \ minutes$$

APPENDIX E.

E.1. Matlab ARX, Polynomial fit steps, for 280.0 mg PVA/L, step change from 1.0-5.0 [H₂O₂]/[PVA]

After defining the input and output data in deviation form in the command window, system identification window will appear when typing the word (Ident) in the command box as follows:
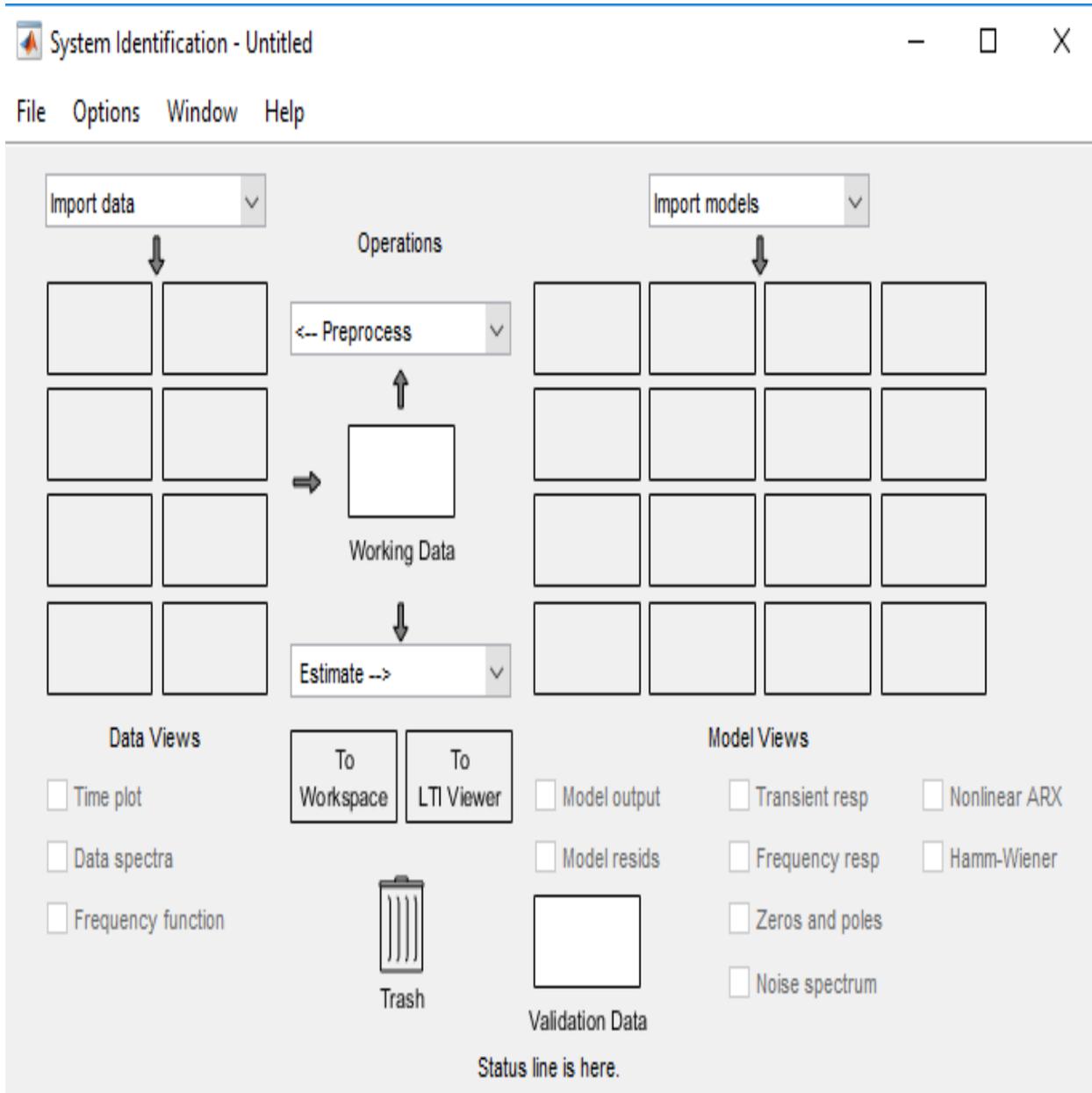
Figure E.1. Ident Matlab window, for importing data, and selecting an appropriate model.

The time domain data would be selected to import the input and output data in deviation form.
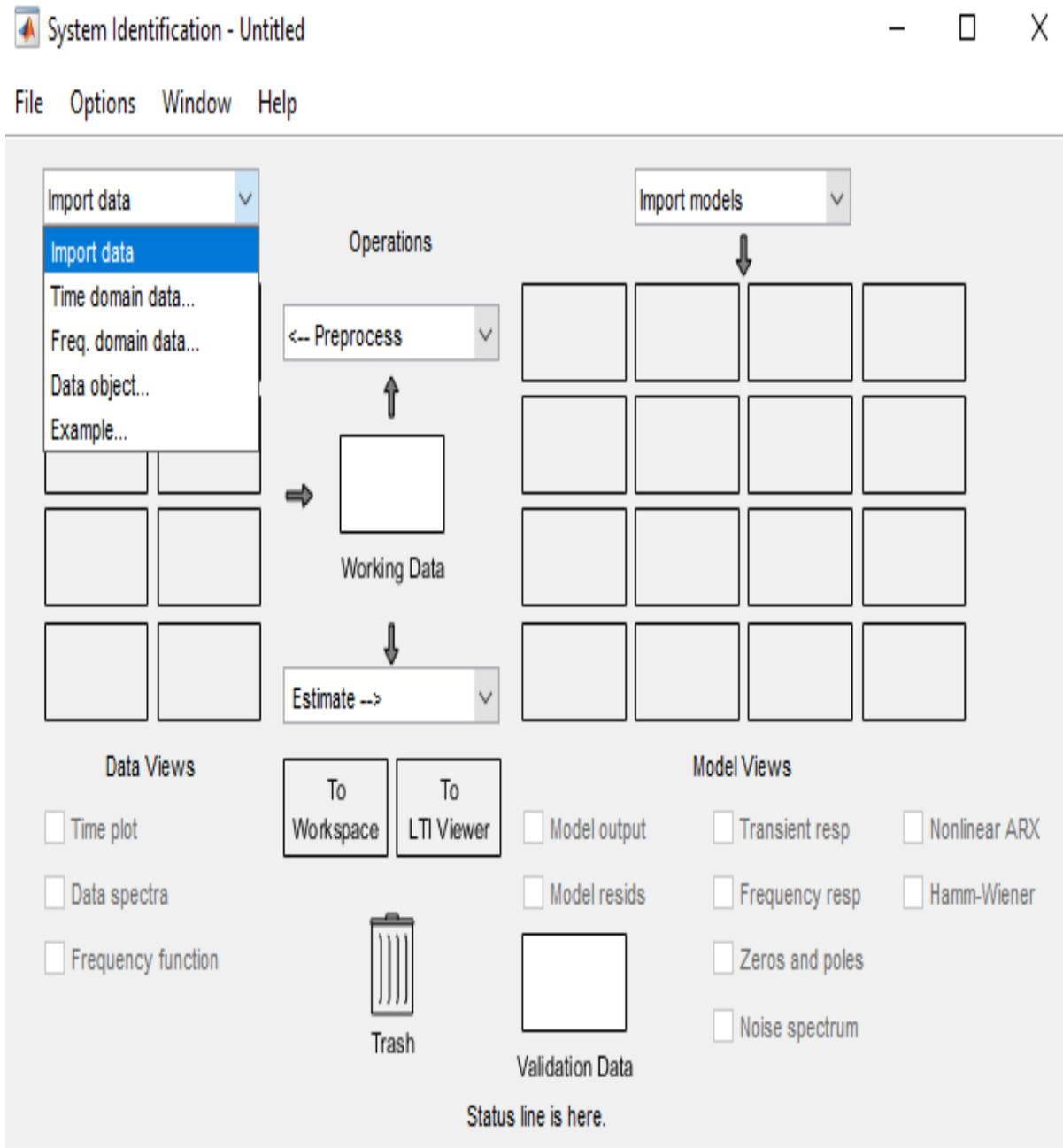
Figure E.2. Selecting the time domain data import.
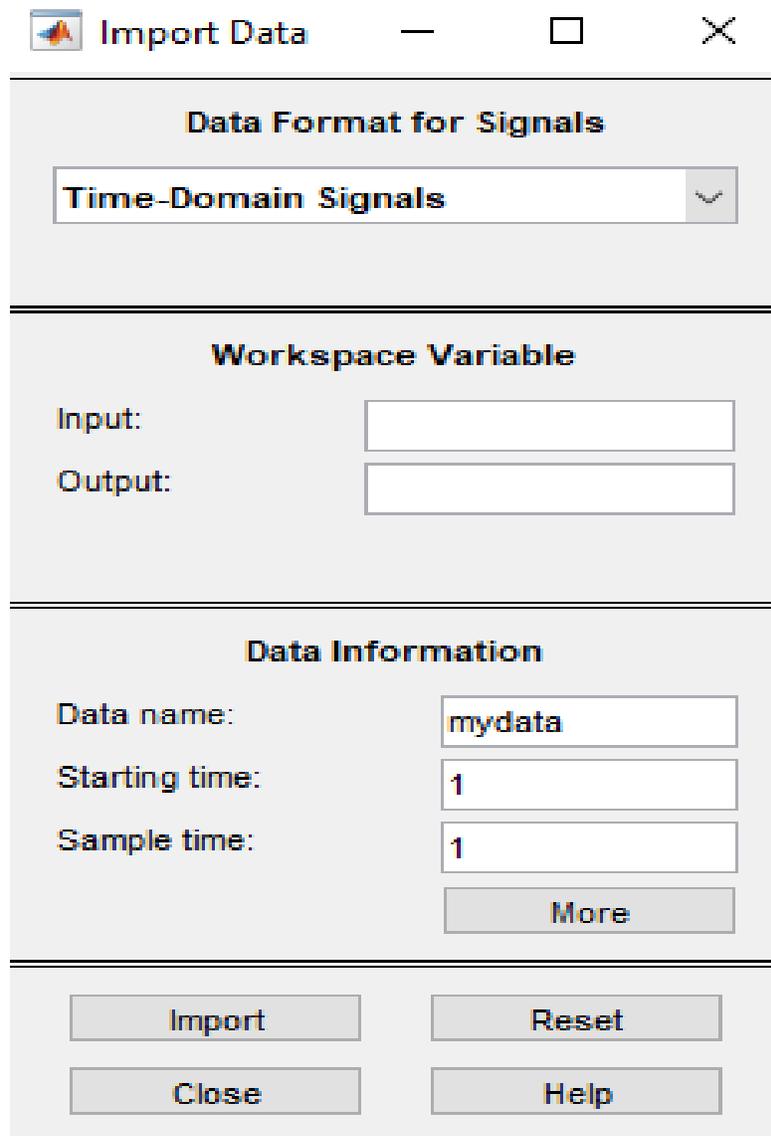
Figure E.3. Matlab-Ident input-output import data window.

The Import data screen comes up, and the deviation of the input data of the hydrogen peroxide mass flowrate into the reactor is loaded in the input box. The deviation of the pH output response data is loaded to the output box.
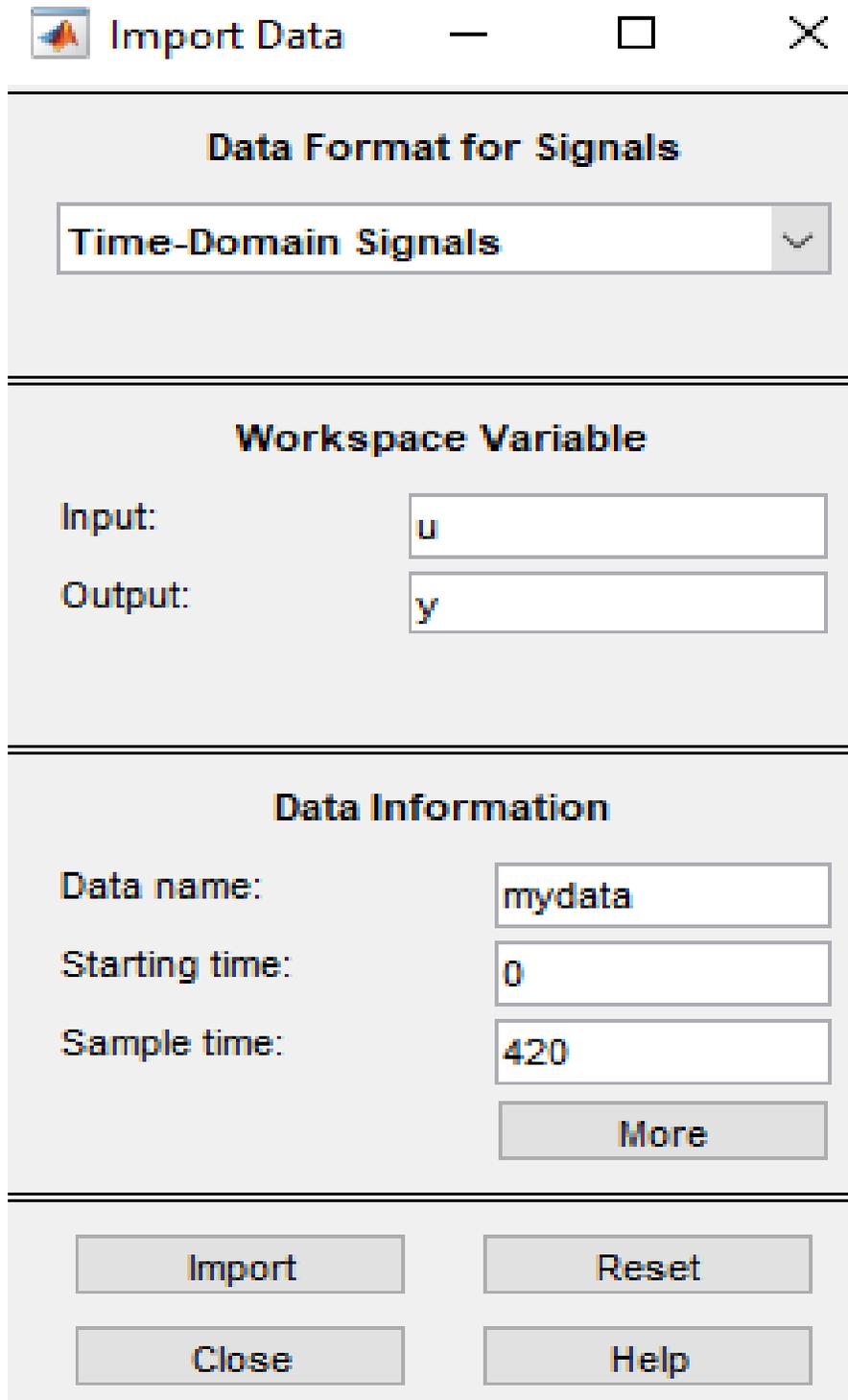
Figure E.4. Importing input and output data from the command window to the system identification toolbox. Selecting the starting time, and the sample period in seconds.

In the sample time box, the sample period of the data collected is written as 420 seconds. The input and output data in deviation form would be imported to the system identification toolbox as can be seen in Figure E.5.
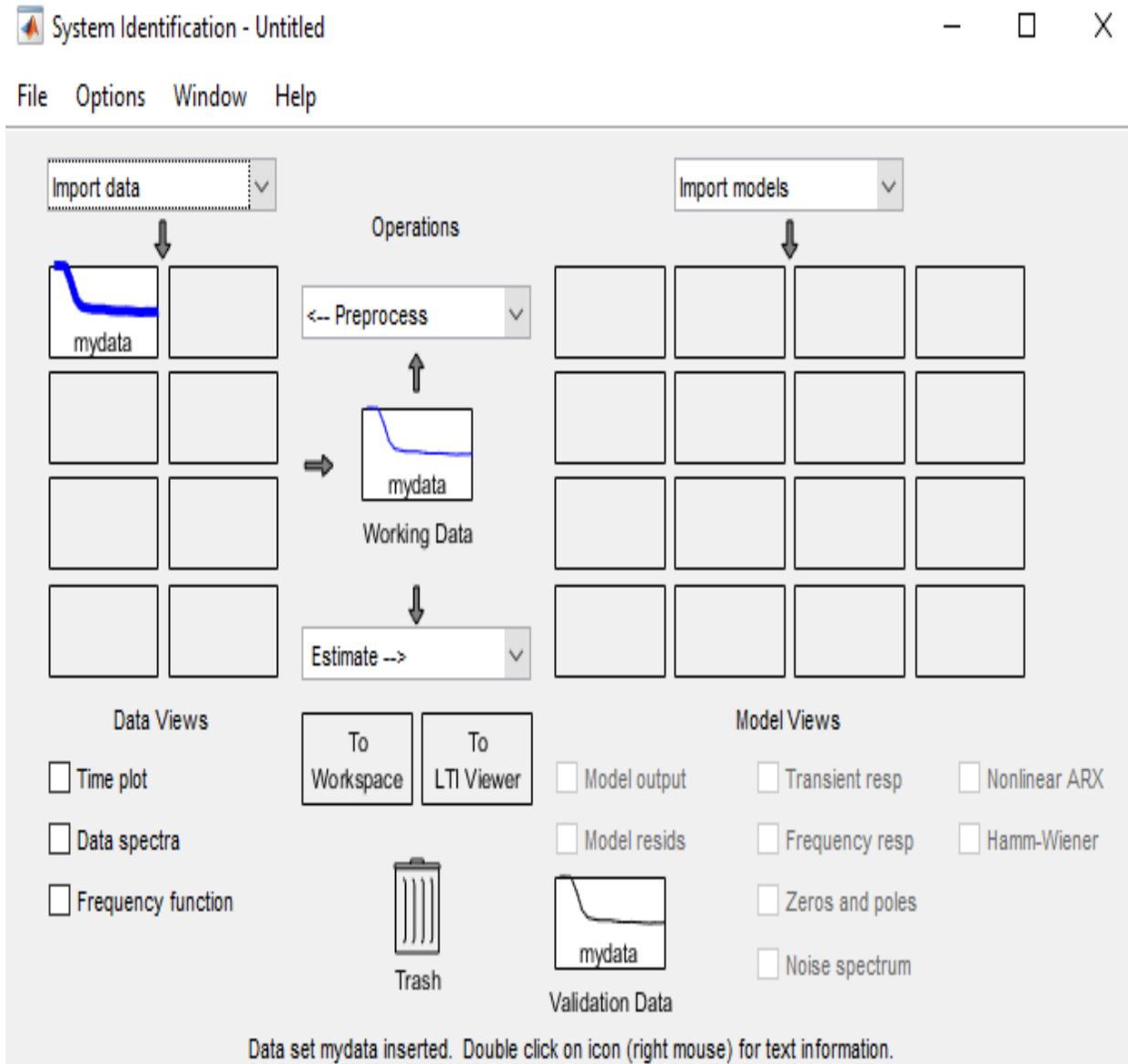

Figure E.5. Ident-Matlab window after importing input and output data.

The model corresponding to the response of a certain step change would be chosen from the estimate list as can be seen in Figure E.6.
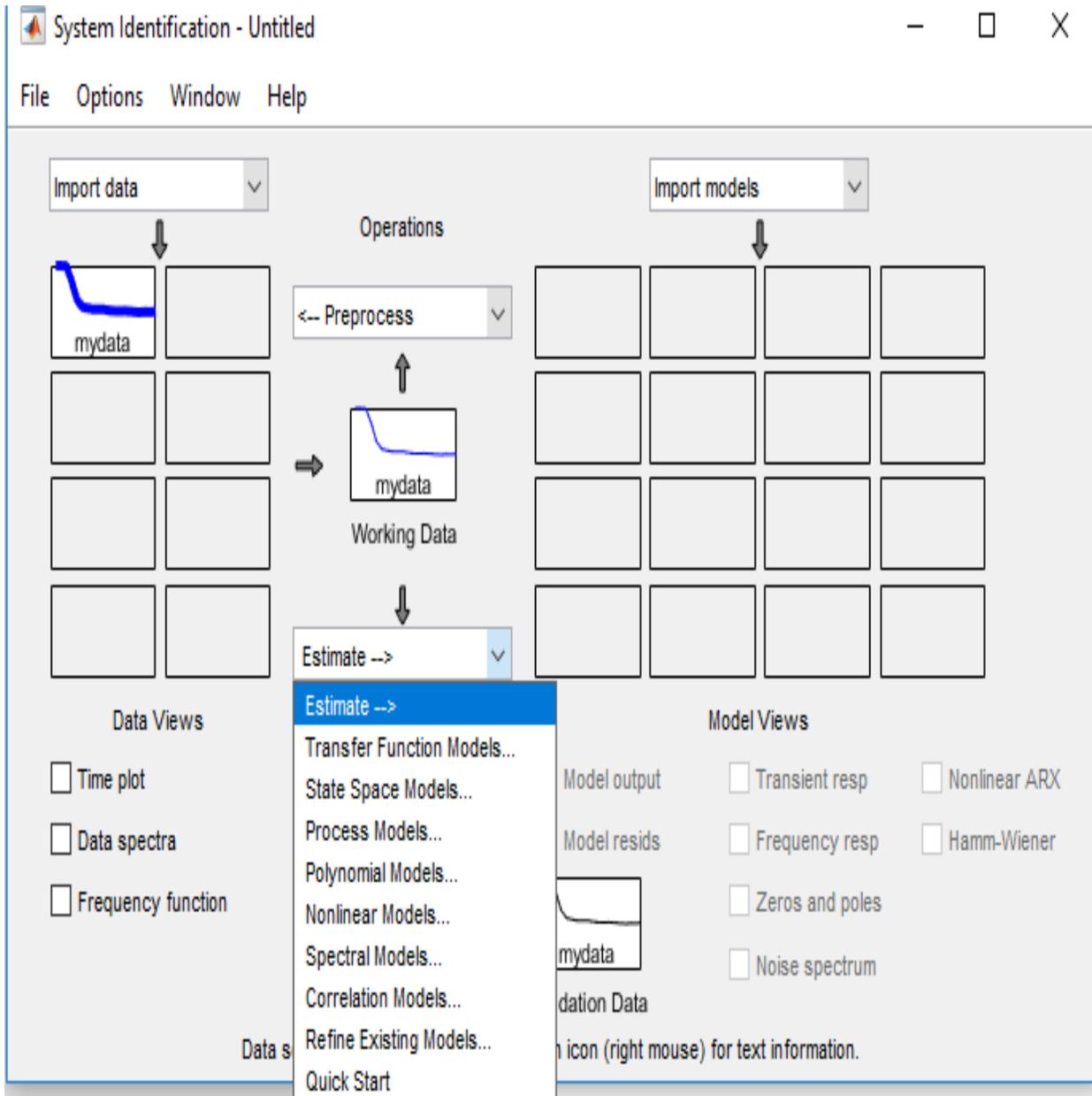

Figure E.6. Ident Matlab window, choosing the model that wants to be applied on the input-output data of the step change.

From the Estimate list the method of response data identification would be chosen. In this case the ARX polynomial model is chosen for this specific response data.

Figure E.7. Matlab-ident-ARX Polynomial model identification window.

The polynomial model window opens, with the default order of [4 4 1], and zero input delay. The input delay should be corrected to 1, and the order selection button is pressed for Matlab to choose the best order for the polynomial model of our input-output data.
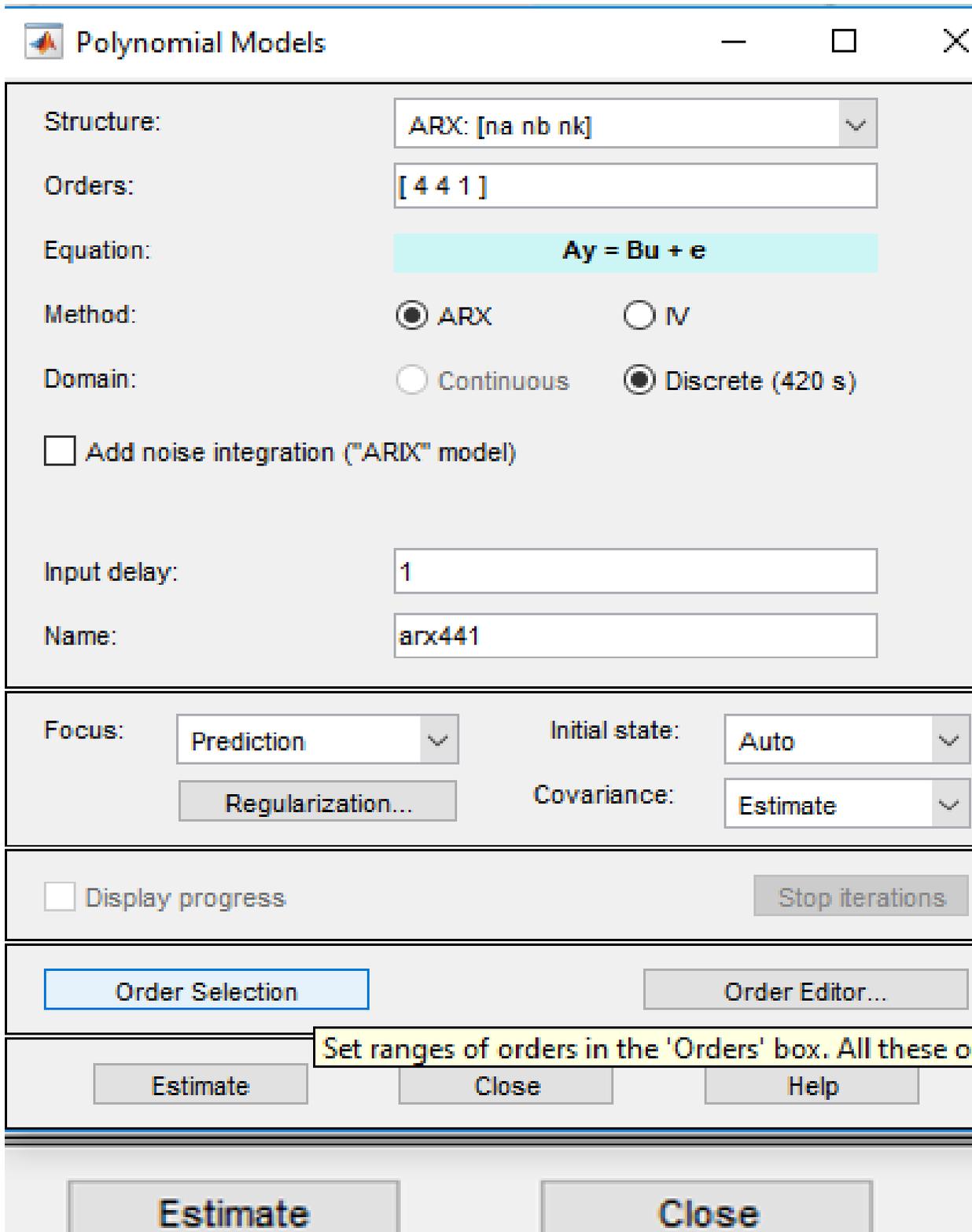
Figure E.8. Input delay of one sample period was chosen. Order selection of [4 4 1] was also chosen.

After choosing an input delay of 1 corresponding to one sample period of delay time, and pressing Order Selection Icon, the following window appears:
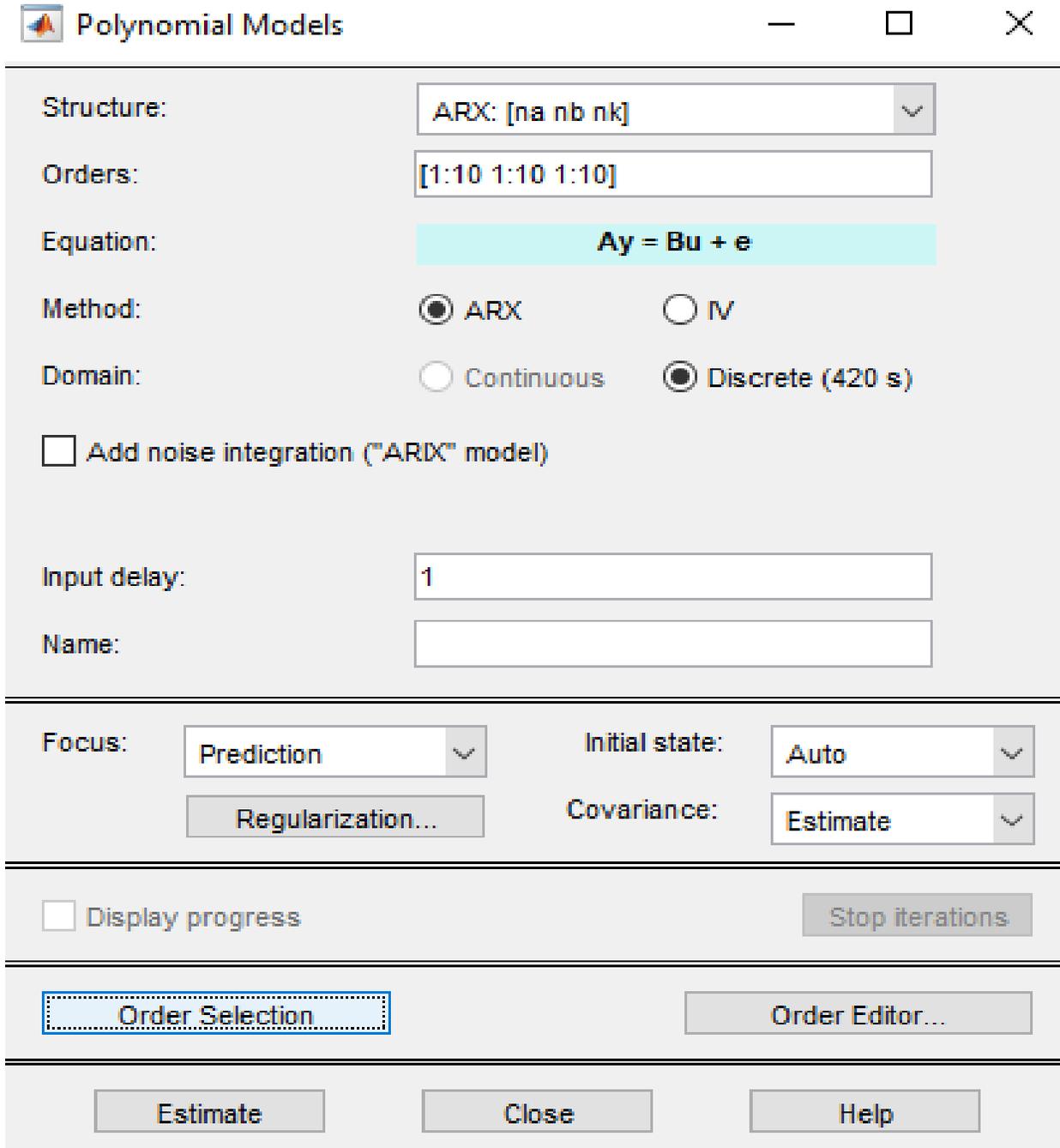
Figure E.9. Default order selection of [1:10 1:10 1:10]. The Order then selected for maximum accuracy, [1:6 1:6 1:6], [1:7 1:7 1:7], and [1:5 1:5 1:5].

The ARX polynomial Models window appears with a default order range of [1:10 1:10 1:10]. To insure extra accuracy, the order range is modified, to [1:6 1:6 1:6]. When correcting the order range and pressing the estimate button, a best polynomial order would be selected as a combination of MDL and AIC criteria for best fit.
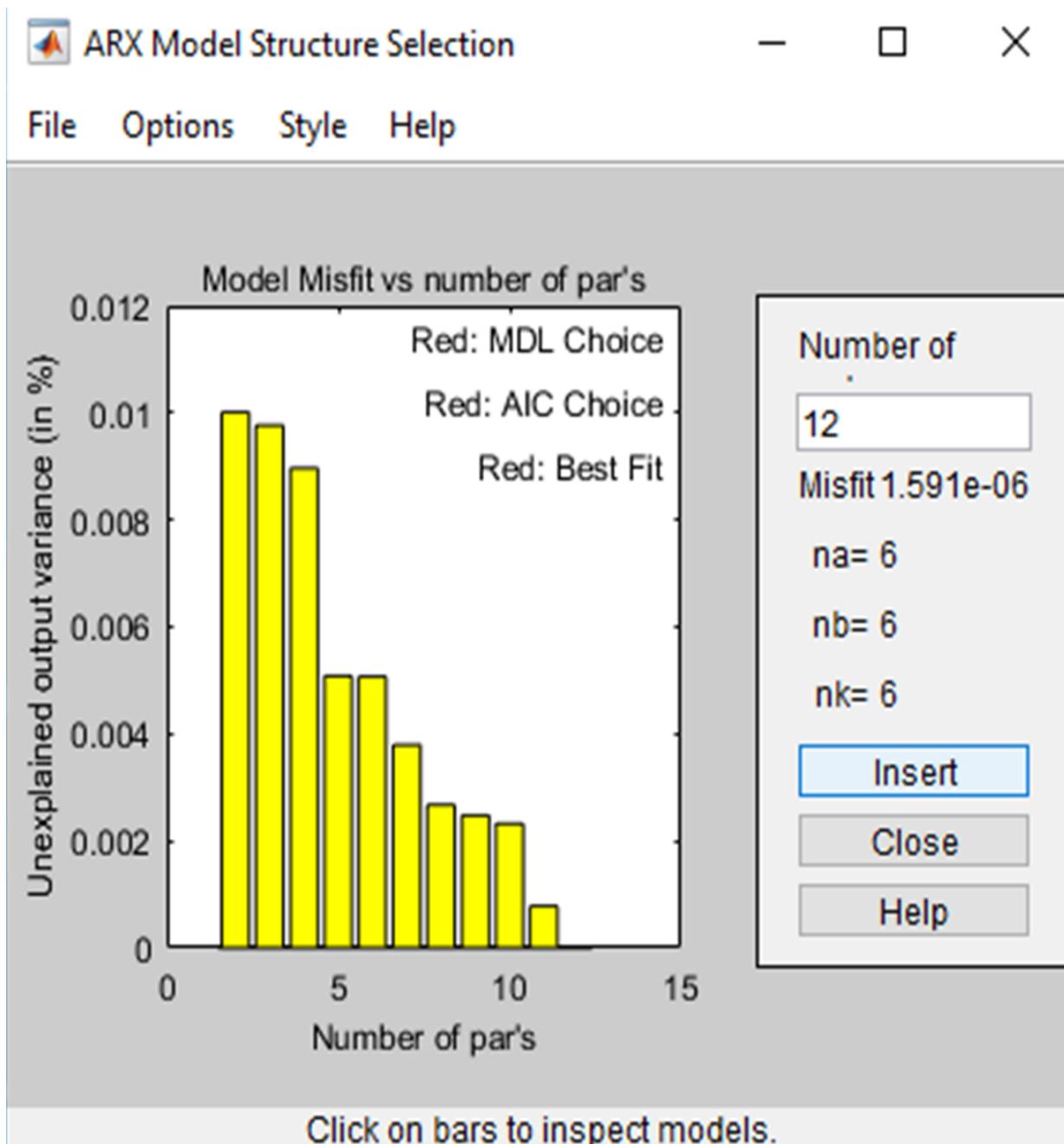
Figure E.10. Order selection best fit, of an order section of [1:6 1:6 1:6], 280.0mgPVA/L, and Step change of 1.0 to 5.0 [H$_2$O$_2$]/[PVA].

The best fit for an order range of [1:6 1:6 1:6], is [6 6 6], with a misfit % of 0.000001591%. To get the best fit polynomial into the ident window, the Insert button is pressed as follows:
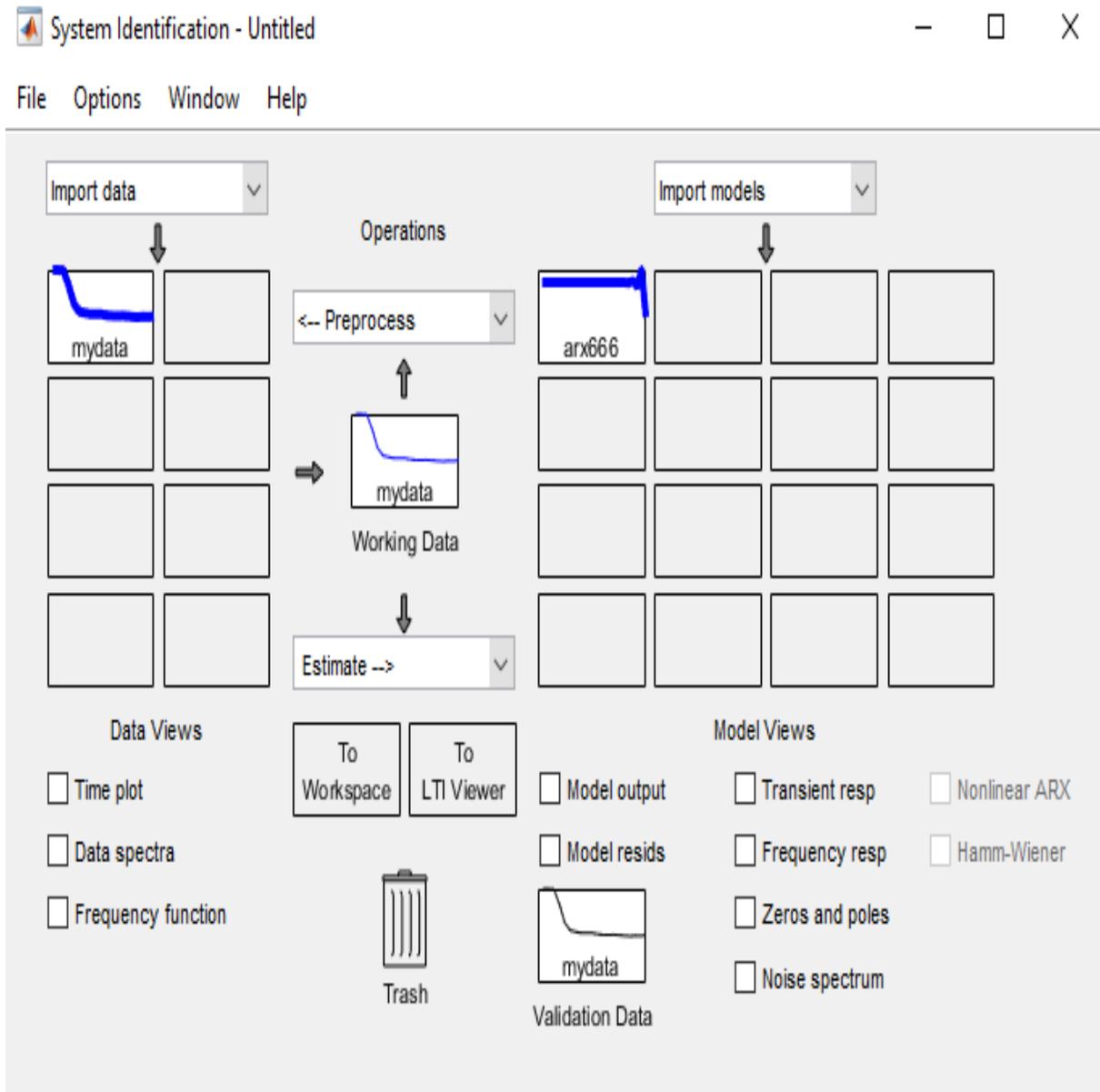
Figure E.11. Order selection best fit, of an ARX model order range of [1:6 1:6 1:6], was [6 6 6], of the pH response of 280.0 mg PVA/L, step change from 1.0 to 5.0 $[H_2O_2]/[PVA]$. Best fit ARX model of [6 6 6] was calculated by system identification.

As can be seen in the System Identification window, the best polynomial fit of the order [6 6 6], is transferred from the best fit window selection to system Identification window. To transfer the polynomial parameters, a double click on the polynomial model box icon opens the following ARX polynomial model parameters window:
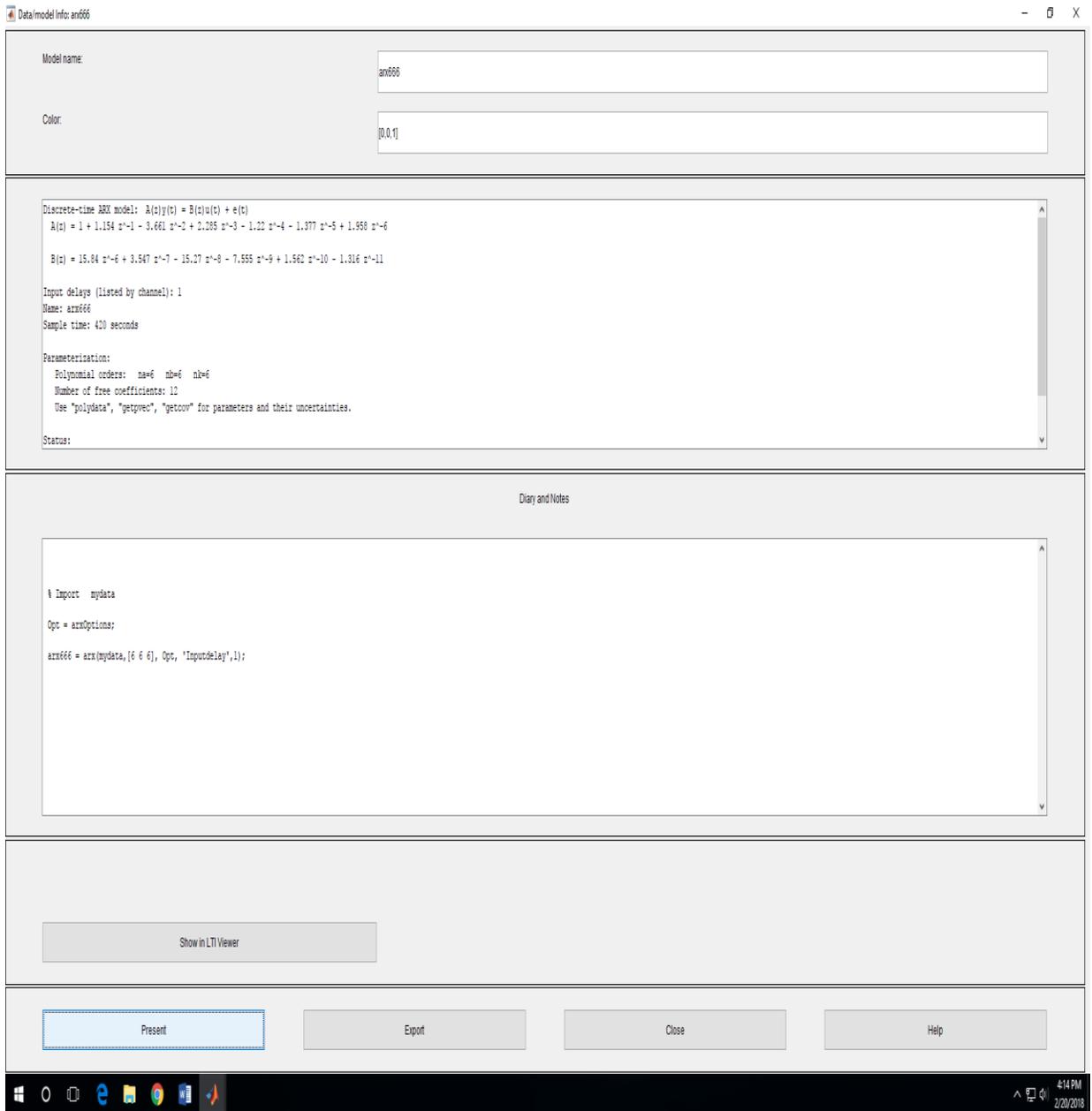
Figure E.12. ARX polynomial model of the order [6 6 6] parameters window.

When pressing the present button on the polynomial model information window, the model is transferred to the command window of Matlab. The parameters of the best fit ARX polynomial model of the pH output data is extracted.

arx666 =

Discrete-time ARX model: A(z)y(t) = B(z)u(t) + e(t)

A(z) = 1 + 1.154 (+/- 0.6425) z^-1 - 3.661 (+/- 0.9209) z^-2 + 2.285 (+/- 0.4338) z^-3 - 1.22 (+/- 0.3458) z^-4
                                                        - 1.377 (+/- 0.7185) z^-5 + 1.958 (+/- 0.5741) z^-6

B(z) = 15.84 (+/- 4.201) z^-6 + 3.547 (+/- 2.773) z^-7 - 15.27 (+/- 3.316) z^-8 - 7.555 (+/- 2.292) z^-9 + 1.562 (
                                                        +/- 0.4355) z^-10 - 1.316 (+/- 0.2896) z^-11

Input delays (listed by channel): 1

Name: arx666

Sample time: 420 seconds

Parameterization:
   Polynomial orders: na=6   nb=6   nk=6
   Number of free coefficients: 12
   Use "polydata", "getpvec", "getcov" for parameters and their uncertainties.

Status:
Estimated using ARX on time domain data "mydata".
Fit to estimation data: 99.56% (prediction focus)
FPE: 9.386e-05, MSE: 4.94e-06
More information in model's "Report" property.
>>

Figure E.13. ARX polynomial model of [6 6 6], parameters were displayed on the command window, as the present button was clicked.

141

E.2. ARX, Matlab, polynomial 280.0 mg PVA/L, step change from 1.0-5.0 [H₂O₂]/[PVA], order choice of [1:5 1:5 1:5]

Figure E.14. Order selection of [1:5 1:5 1:5], was applied to pH response of 280.0 mg PVA/L, for a step change from 1.0 to 5.0 [H₂O₂]/[PVA].

The best order of this specific pH response of 280 mg PVA/L, with a step change from 1.0 to 5.0 [H$_2$O$_2$]/[PVA] with an order range of [1:5 1:5 1:5] was calculated to be [5 5 4] as can be seen in the following window:
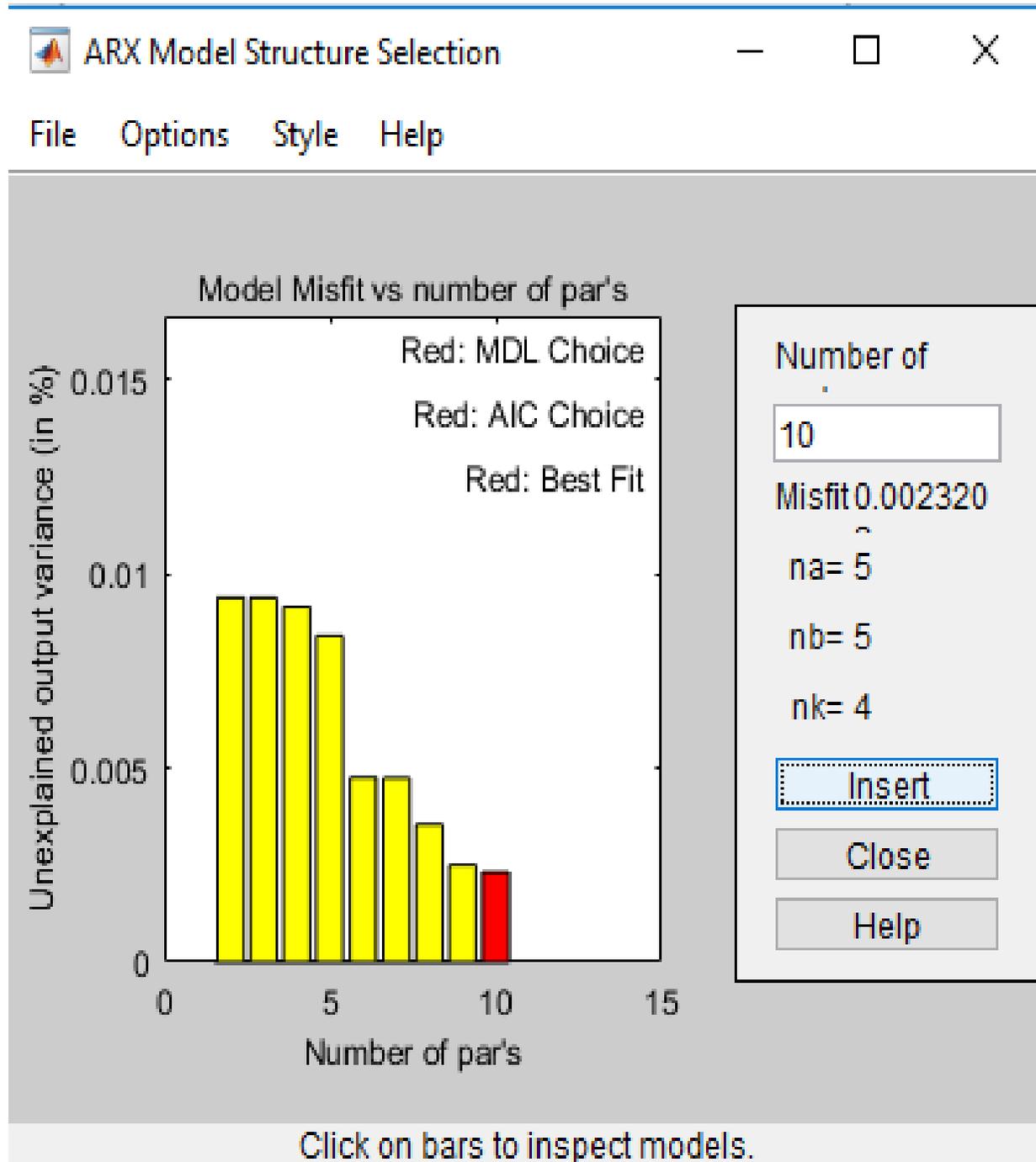
Figure E.15. The best fit plot produced by the Matlab, suggested the red column best fit of

[5 5 4]. Order range of [1:5 1:5 1:5]. 280.0 mg PVA/l, step change of 1.0 to 5.0 [H$_2$O$_2$]/[PVA].

As we insert the best fit into the System Identification window, the following window appears:
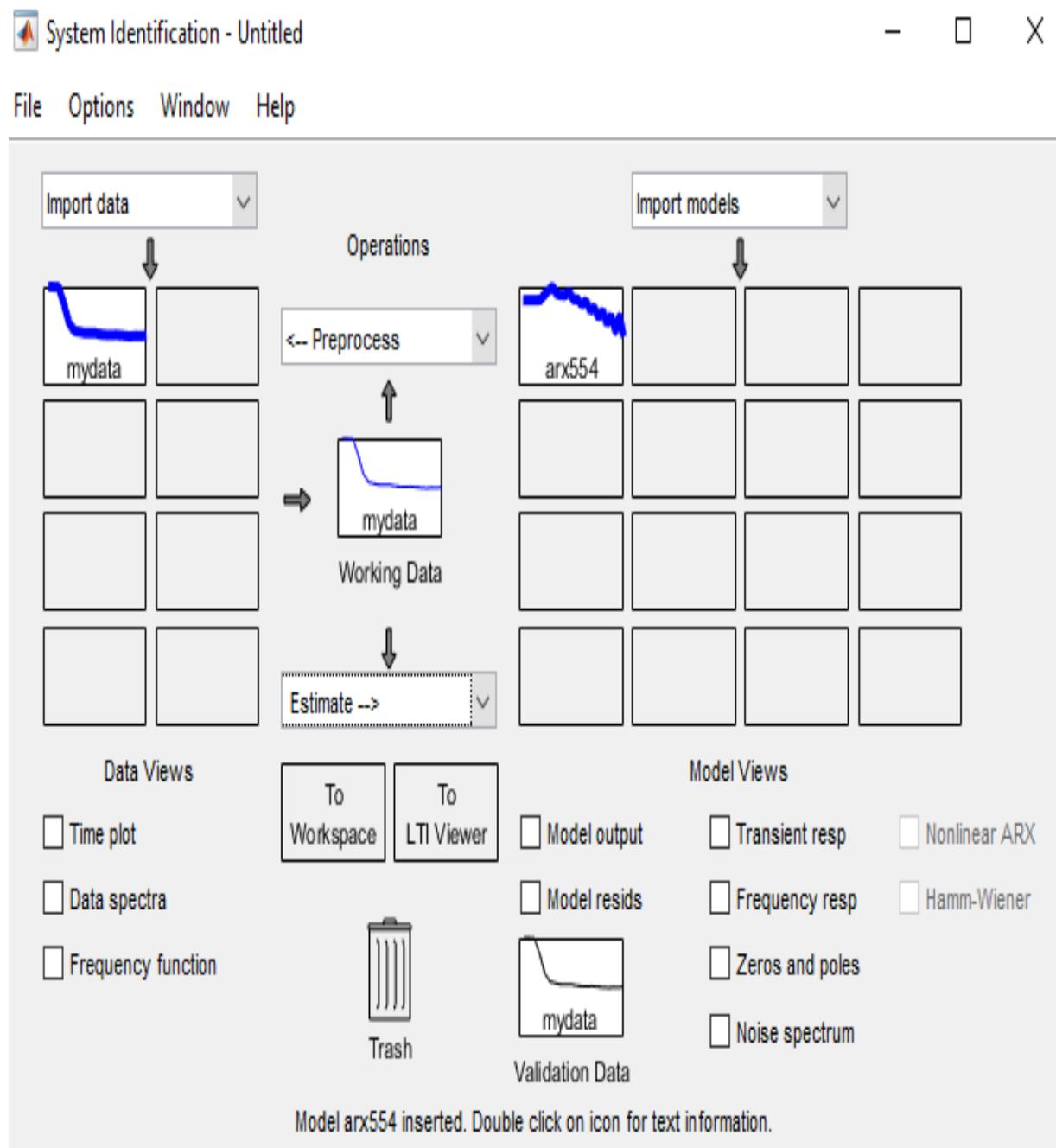
Figure E.16. An ARX best fit of an order of [5 5 4], for the pH response data corresponding to a step change of hydrogen peroxide concentration from 1.0 to 5.0 [H$_2$O$_2$]/[PVA] for the 280 mg PVA/L test.

A double click is applied to the window of the model arx554 to attain the polynomial model information for the set of input output deviation data. After the model box appears, the present button is pressed to display the polynomial model parameters in the command window.


```
Data/model Info: arx554                                         —    □    ✕

Model name:              arx554

Color:                   [0,0,1]


Discrete-time ARX model:  A(z)y(t) = B(z)u(t) + e(t)                    ^
  A(z) = 1 - 0.9959 z^-1 - 0.4997 z^-2 + 0.6901 z^-3 - 1.044 z^-4 + 0.9485 z^-5

  B(z) = 3 z^-4 + 3.212 z^-5 + 1.1 z^-6 - 5.555 z^-7 - 3.995 z^-8

Input delays (listed by channel): 1
Name: arx554                                                           ∨


                           Diary and Notes                             ^


  % Import    mydata

  Opt = arxOptions;

  arx554 = arx(mydata, [5 5 4], Opt, 'Inputdelay',1);                  ∨



      Show in LTI Viewer


     Present              Export              Close              Help
```
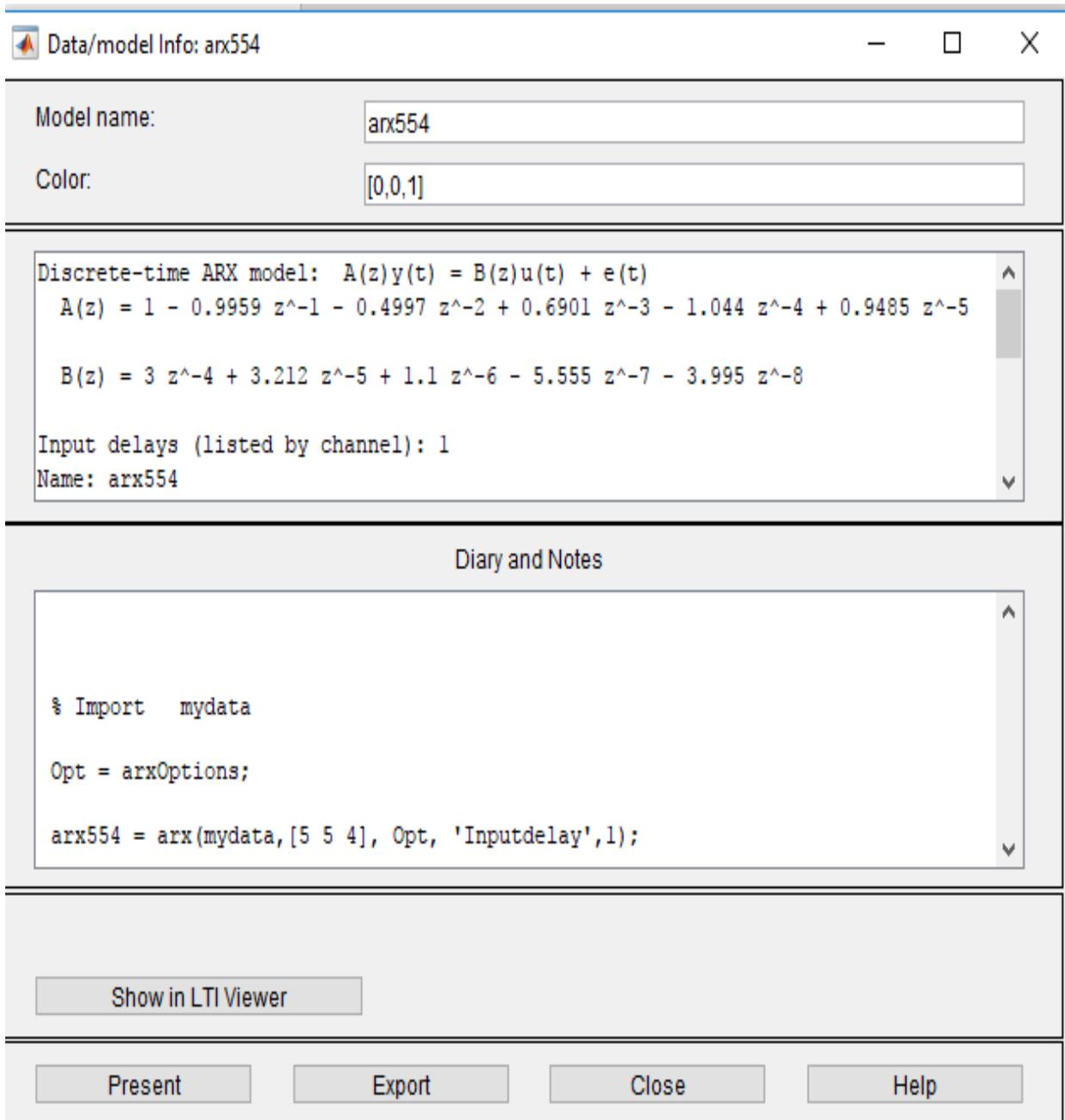
Figure E.17. ARX polynomial model of [5 5 4], information window.

When over imposing the ARX polynomial model over the pH response data corresponding to the step change the following Figure results:


$$A(z) = 1 - 0.996z^{-1} - 0.500z^{-2} + 0.690z^{-3} - 1.04z^{-4} + 0.949\ z^{-5}$$

$$B(z) = 3.00\ z^{-4} + 3.21\ z^{-5} + 1.10\ z^{-6} - 5.55\ z^{-7} - 4.00z^{-8}$$

$$A(z)y(t) = B(z)u(t) + e(t)$$

ARX polynomial model:
Best fit Order of: [5 5 4],
from [1:5 1:5 1:5] order choice
98.56 % Representation
e(t): white Noise parameter.
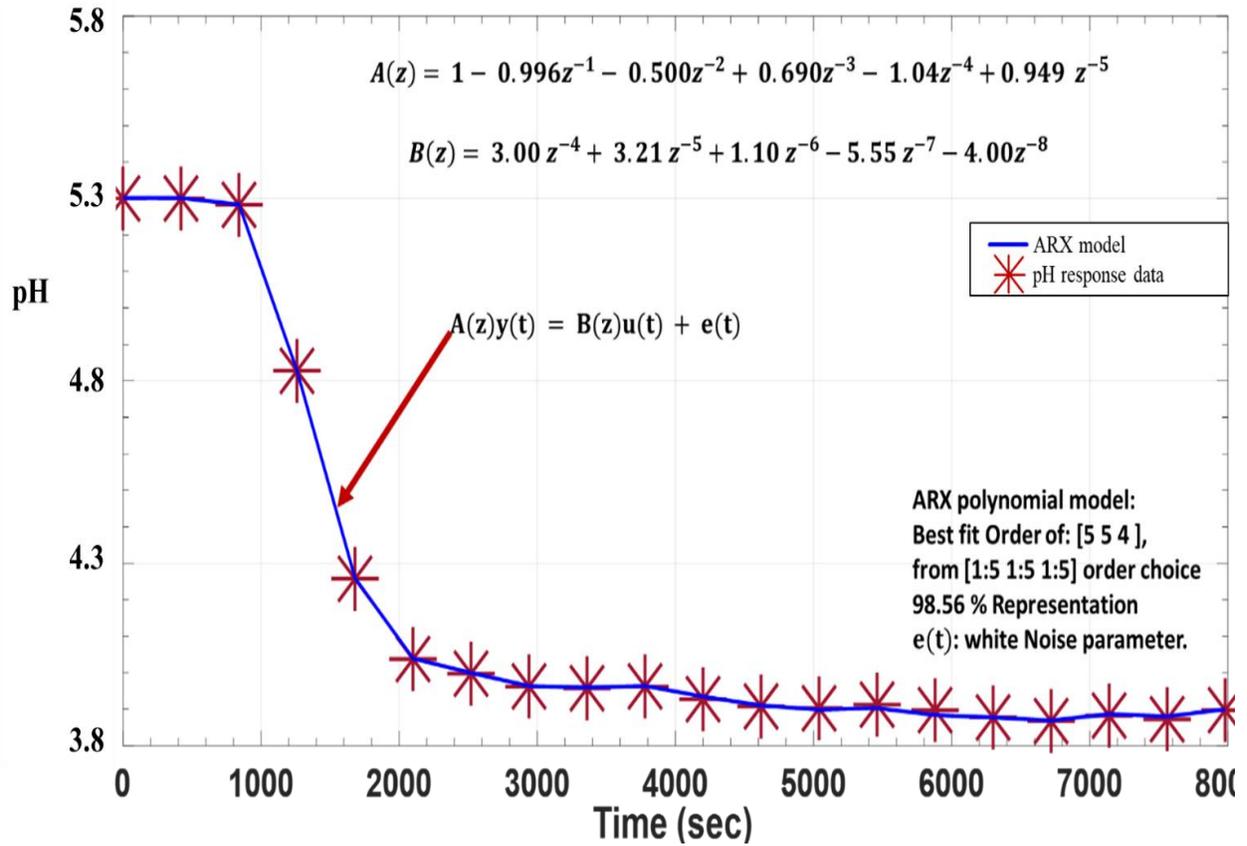
Figure E.18. ARX polynomial model [5 5 4], best fit of the pH response data of 280.0 mg PVA/L, step change from 1.0 to 5.0 [H_2O_2]/[PVA].

E.3. ARX, Matlab, polynomial 280.0 mg PVA/L, step change from 1.0 to 5.0 [H$_2$O$_2$]/[PVA], order range choice of [1:7 1:7 1:7]
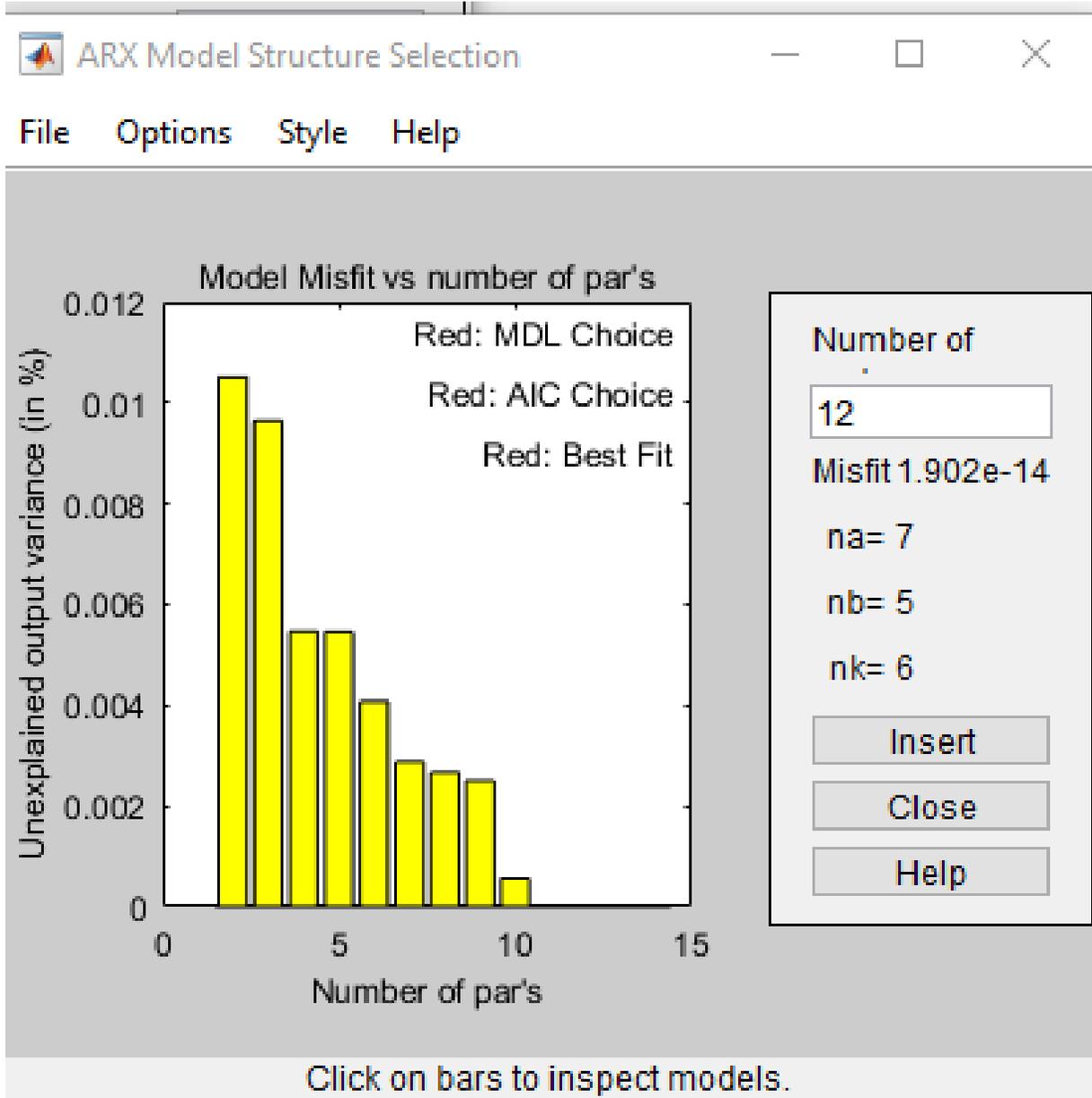
**Figure E.19.** Best fit plot produced by system identification with a best fit order of [7 5 6]. 280.0 mg PVA/L, step change from 1.0 to 5.0 [H$_2$O$_2$]/[PVA]. Order range of [1:7 1:7 1:7].

E.4. System identification ARX, Polynomial model for 280.0 mg PVA/L, step change from 1.0 to 0.20 [H₂O₂]/[PVA]

Figure E.20. Order selection of [1:6 1:6 1:6], was applied, 280.0 mg PVA/L, step change from 1.0 to 0.20 [H₂O₂]/[PVA].
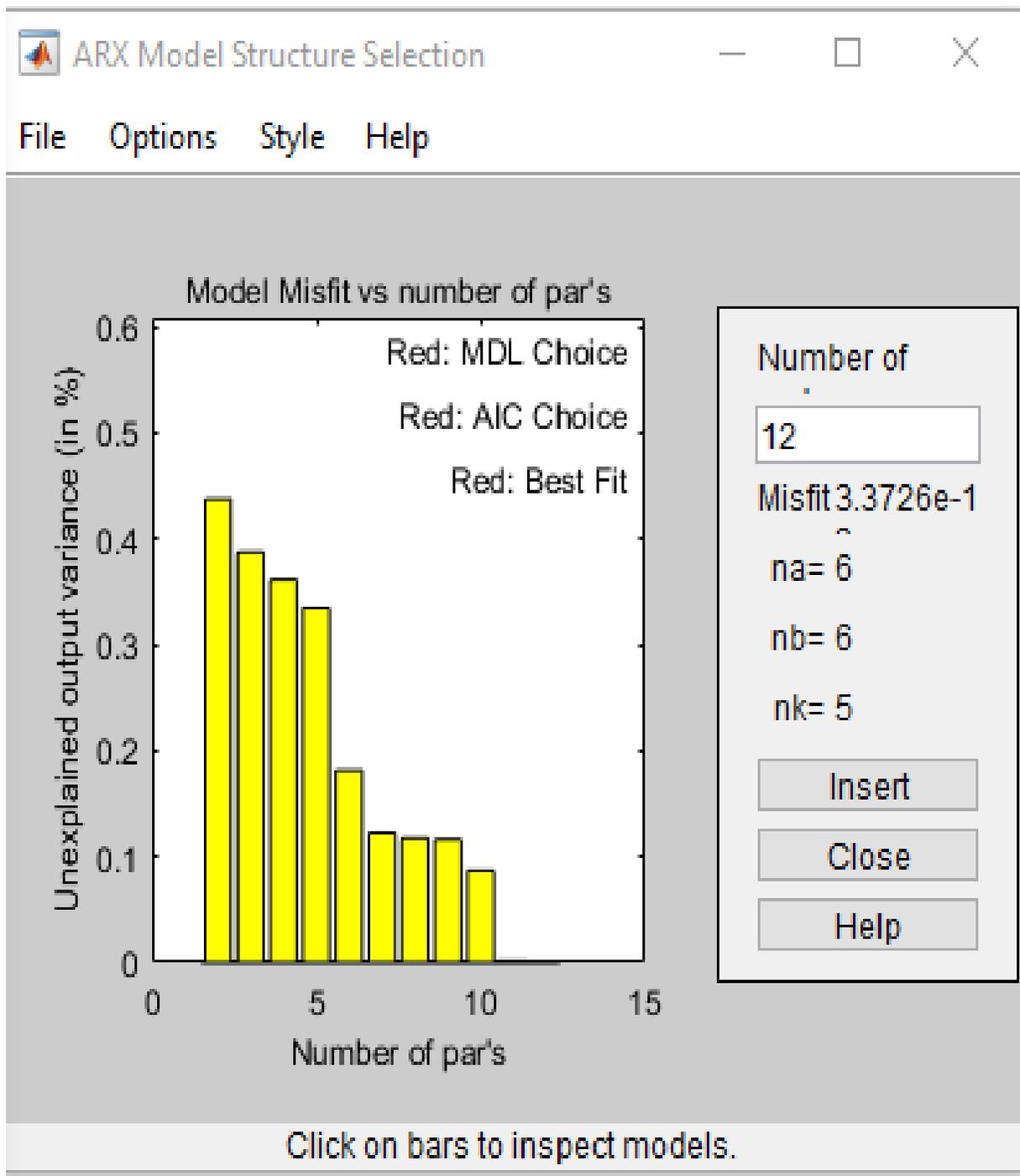
Figure E.21. A best fit plot produced by the system identification, calculated a best fit of [6 6 5]. 280.0 mg PVA/L, step change from 1.0 to 0.20 [H₂O₂]/[PVA]. Order range of [1:6 1:6 1:6].
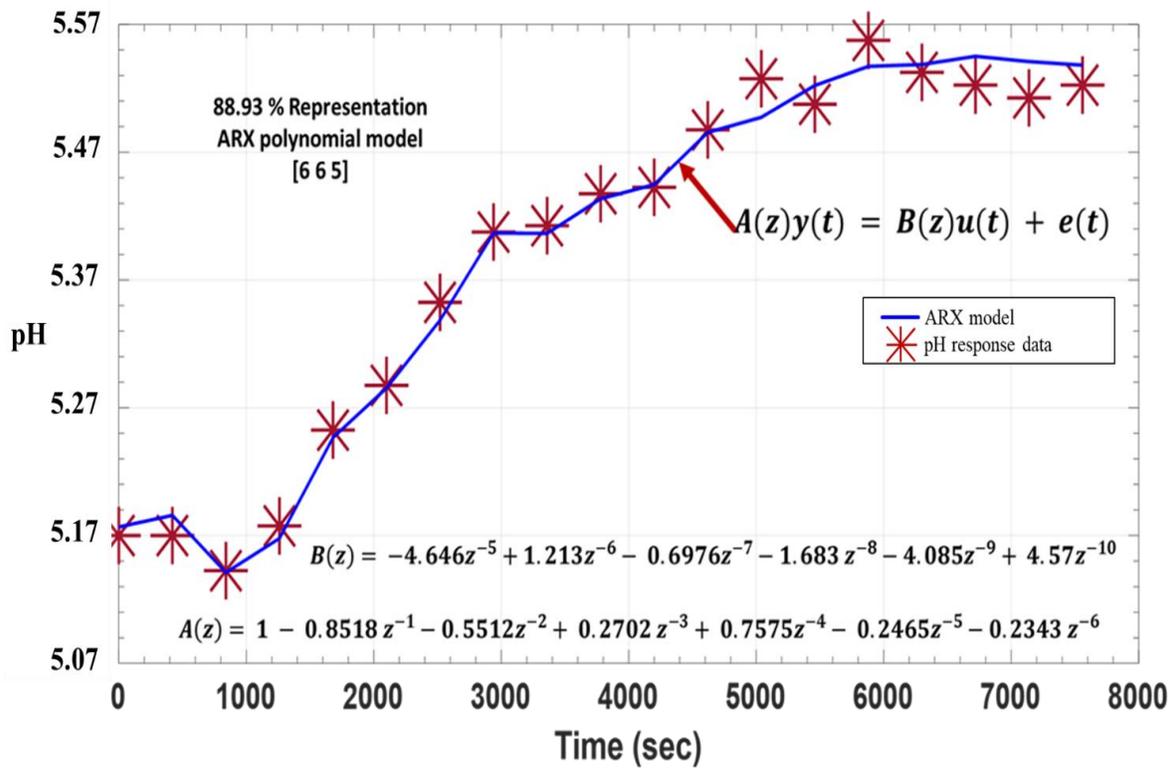
Figure E.22. ARX polynomial model of order [6 6 5] of pH data response of 280.0 mg PVA/L, step change of 1.0 to 0.20 [H_2O_2]/[PVA]. Order choice of [1:6 1:6 1:6].

Figure E.23. Order selection of [1:7 1:7 1:7] was applied to the 280.0 mg PVA/L, step change of 1.0-0.20 [H_2O_2]/[PVA] pH response data.
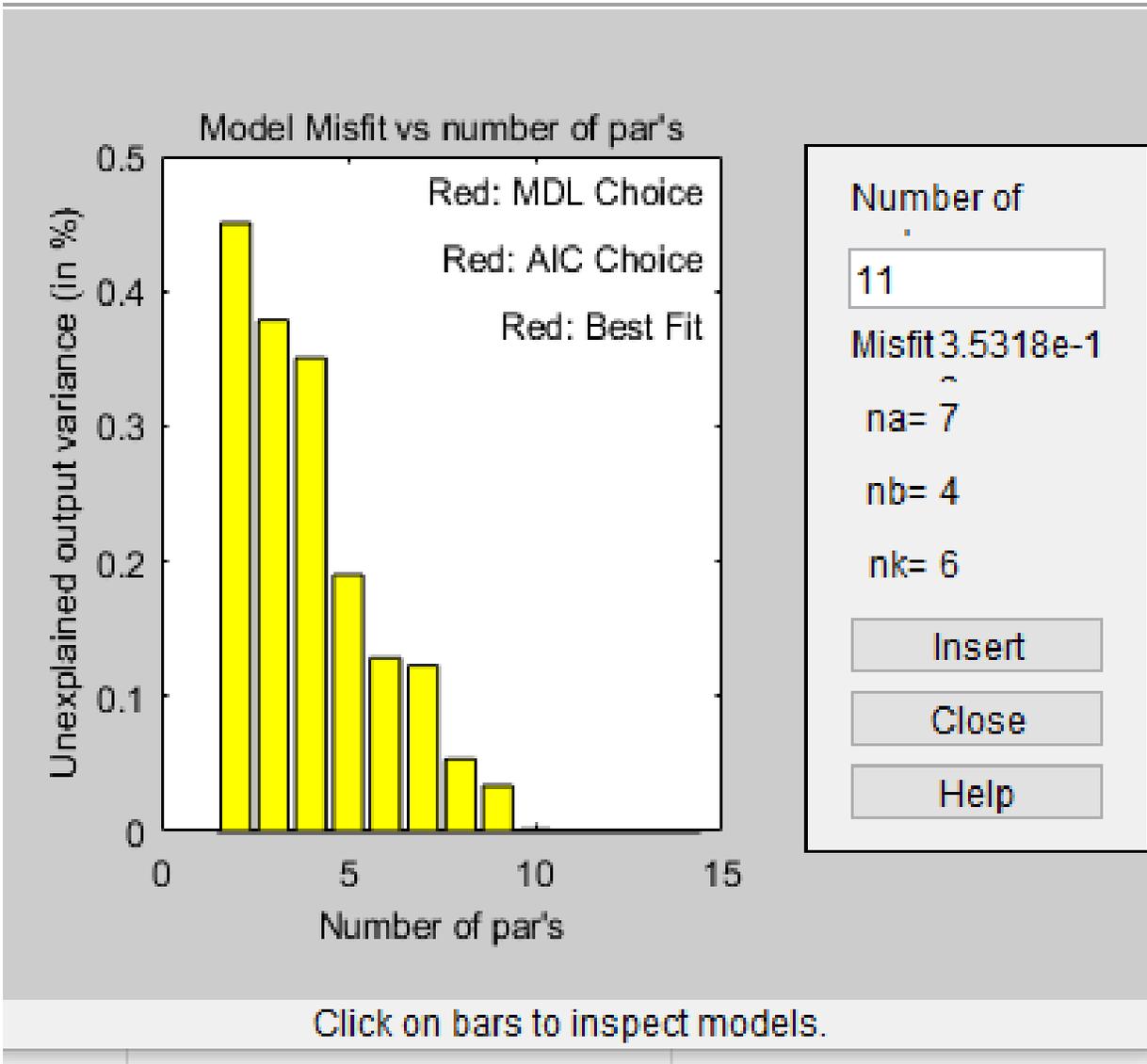
Figure E.24. A best fit plot produced by the system identification toolbox, calculated a best fit ARX order of [7 4 6]. 280.0 mg PVA/L, step change of 1.0 to 0.20 [H₂O₂]/[PVA]. Order range of [1:7 1:7 1:7].

Over imposing the ARX model with an order of [7 4 6] over the pH response data of 280 mg PVA/L, step change from 1.0 to 0.2 resulted in Figure E.25 as follows:

The figure contains the following text and equations:

91.02 % Representation
ARX polynomial model
[7 4 6]

$A(z)y(t) = B(z)u(t) + e(t)$

Legend: ARX model; pH response data

$B(z) = 1.152\,z^{-6} + 7.365\,z^{-7} + 2.78z^{-8} - 13.02z^{-9}$

$A(z) = 1 + 0.1277\,z^{-1} - 1.432z^{-2} - 0.7164z^{-3} + 0.2474z^{-4} + 1.062\,z^{-5} - 1.142z^{-6} + 1.133\,z^{-7}$

Axis labels: pH (vertical); Time (sec) (horizontal)
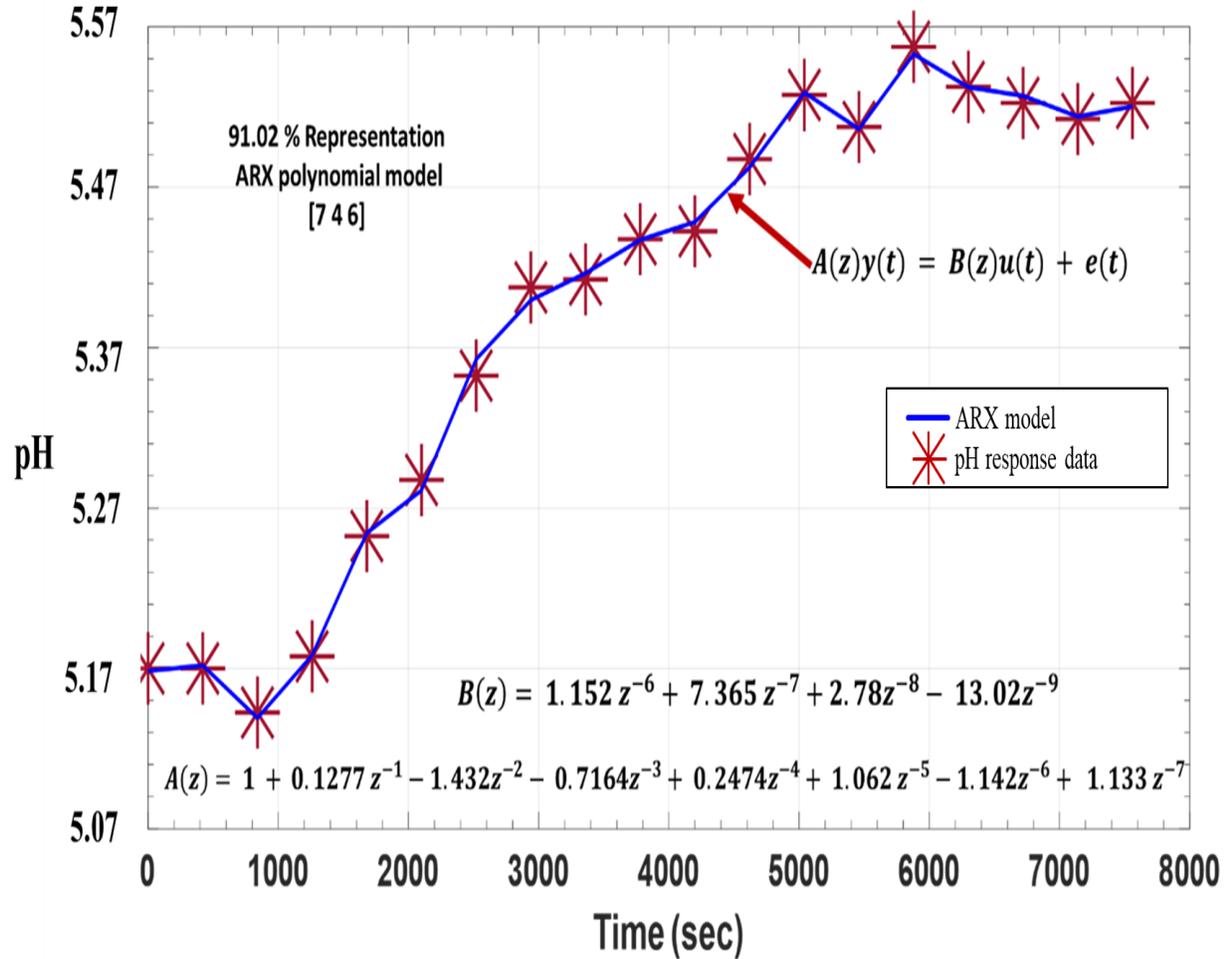
**Figure E.25.** ARX polynomial model of order [7 4 6] of pH response data of 280.0 mg PVA/L, step change from 1.0 to 0.20 [H$_2$O$_2$]/[PVA]. Order choice of [1:7 1:7 1:7].

Selecting an order range of [1:5 1:5 1:5] for the pH response data of 280 mg PVA/L, step change from 1.0 to 0.20 with an input delay of one sampling period as the following Figure:

Figure E.26. Order range selection of [1:5 1:5 1:5], was applied to the pH response data of a 280.0 mg PVA/L, step change from 1.0-0.20 [H_2O_2]/[PVA].
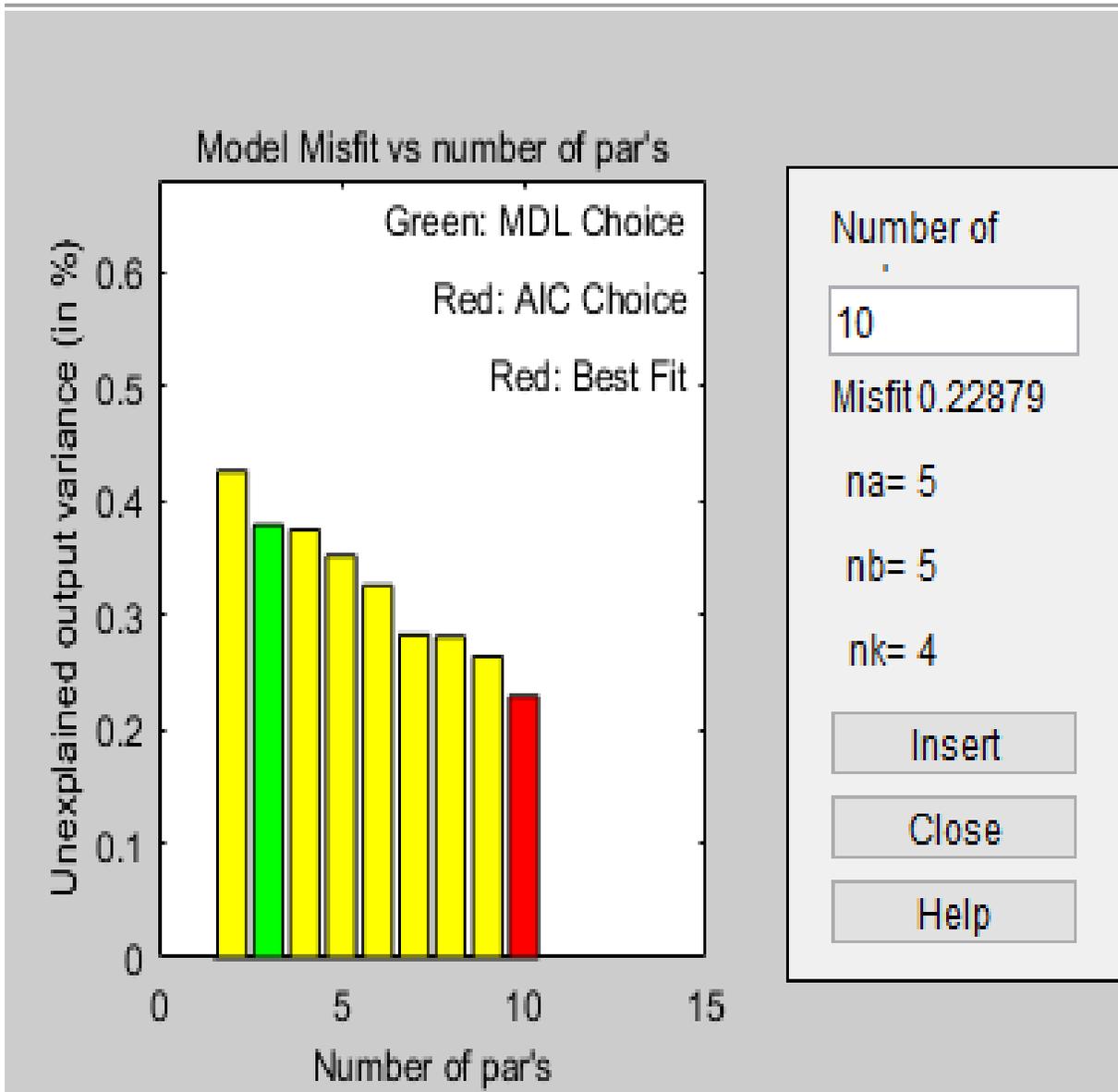
Figure E.27. A best fit plot produced by system identification suggested the red column best fit of an ARX order of [5 5 4]. 280.0 mg PVA/L, step change from 1.0 to 0.2 $[H_2O_2]/[PVA]$. Order range of [1:5 1:5 1:5].

E.5. ARX Polynomial models, for 280.0 mg PVA/L, step change from 0.12 to 0.024 [H₂O₂]/[PVA]

An order range of [1:6 1:6 1:6] was chosen for an ARX model corresponding to pH response data as follows:
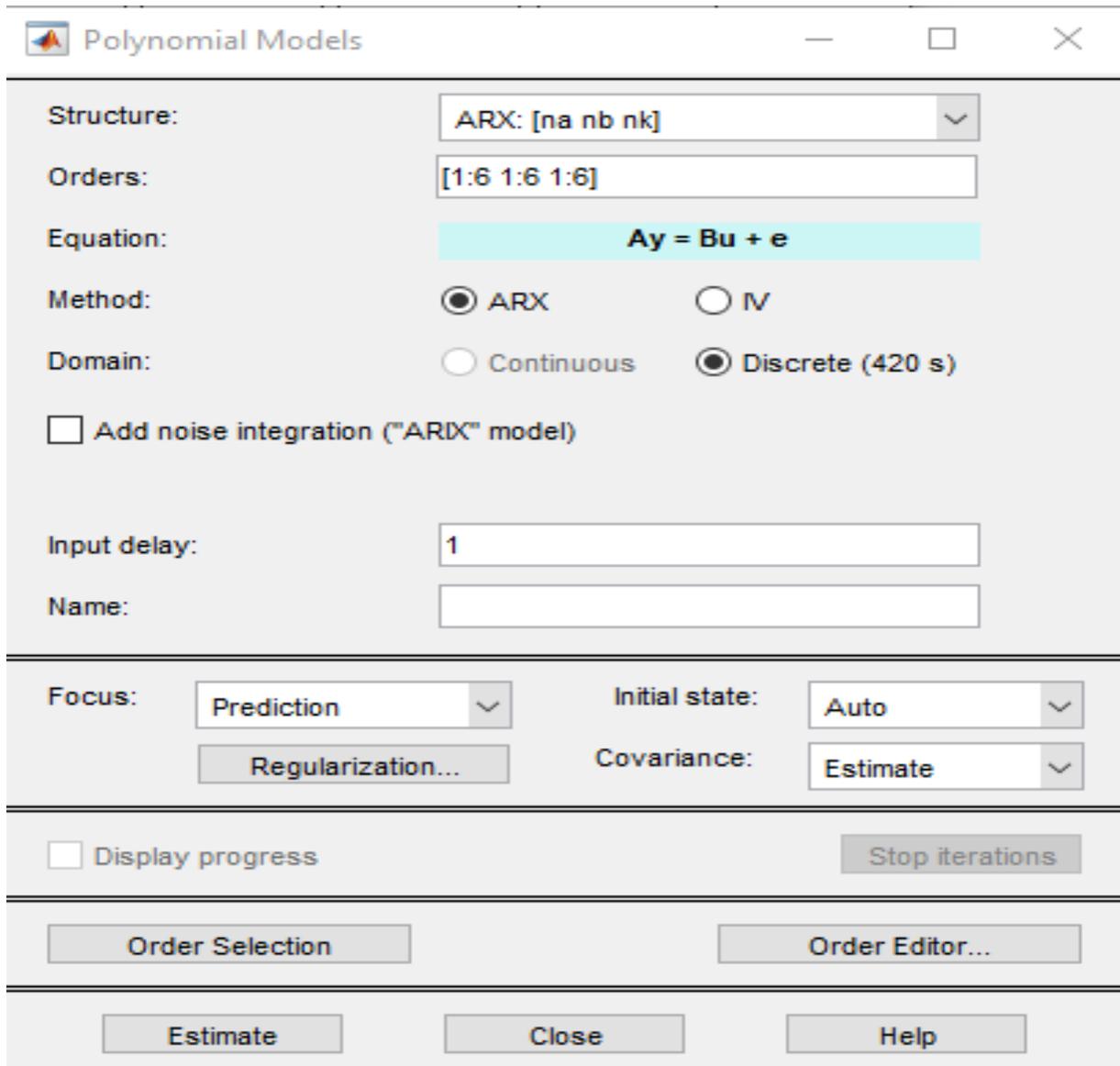
Figure E.28. Order selection of [1:6 1:6 1:6], was applied to pH response data of the 280.0 mg PVA/L test, step change of 0.12 to 0.024 [H₂O₂]/[PVA].

A best fit ARX order of [6 1 1] was calculated for the pH response data of 280 mg PVA/L, step change from 0.12 to 0.024 [H$_2$O$_2$]/[PVA].
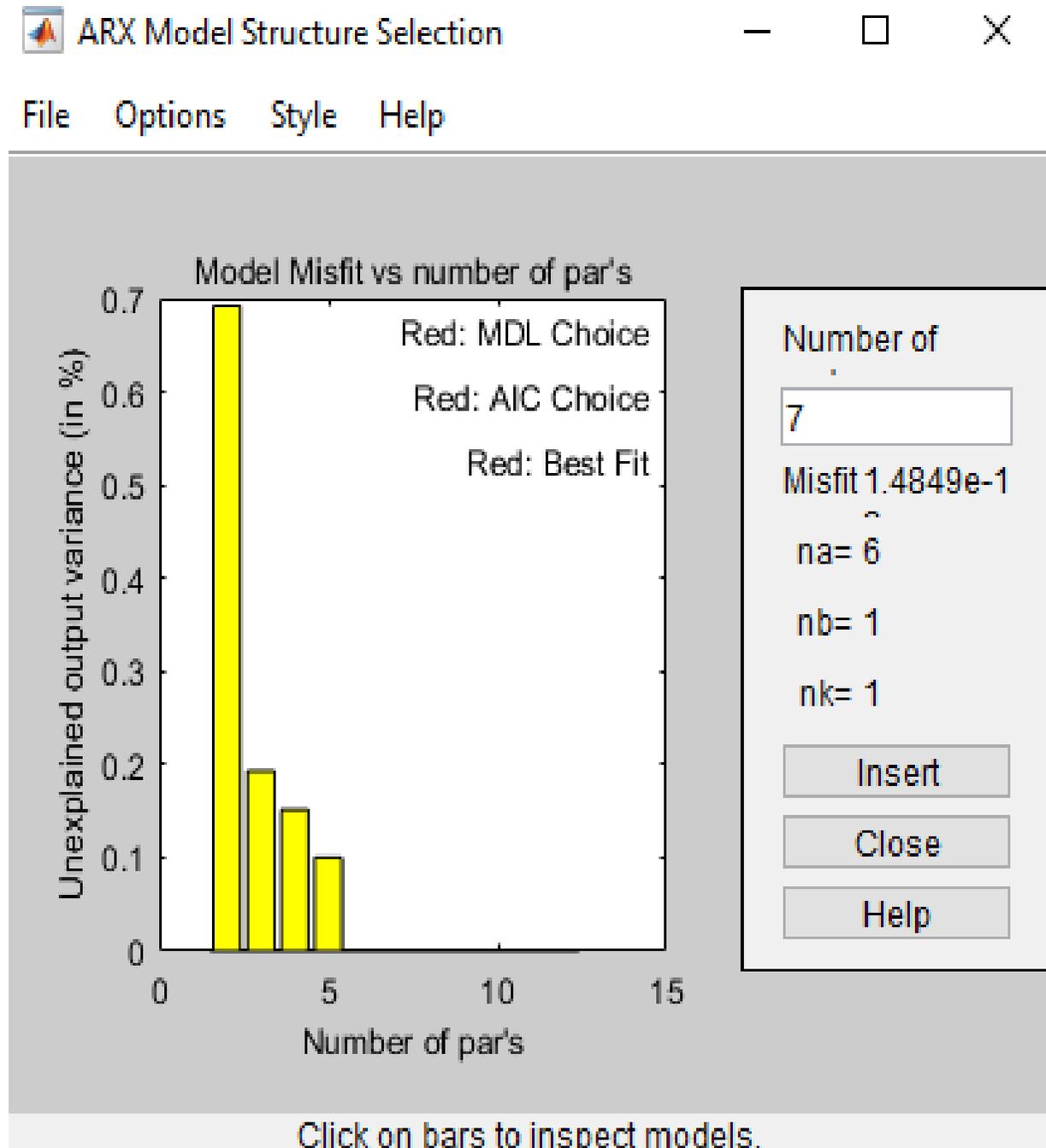
Figure E.29. The best fit plot produced by the System identification toolbox, calculated a best fit of [6 1 1]. 280.0 mg PVA/L, step change of 0.12 to 0.024 [H$_2$O$_2$]/[PVA]. Order range of [1:6 1:6 1:6].
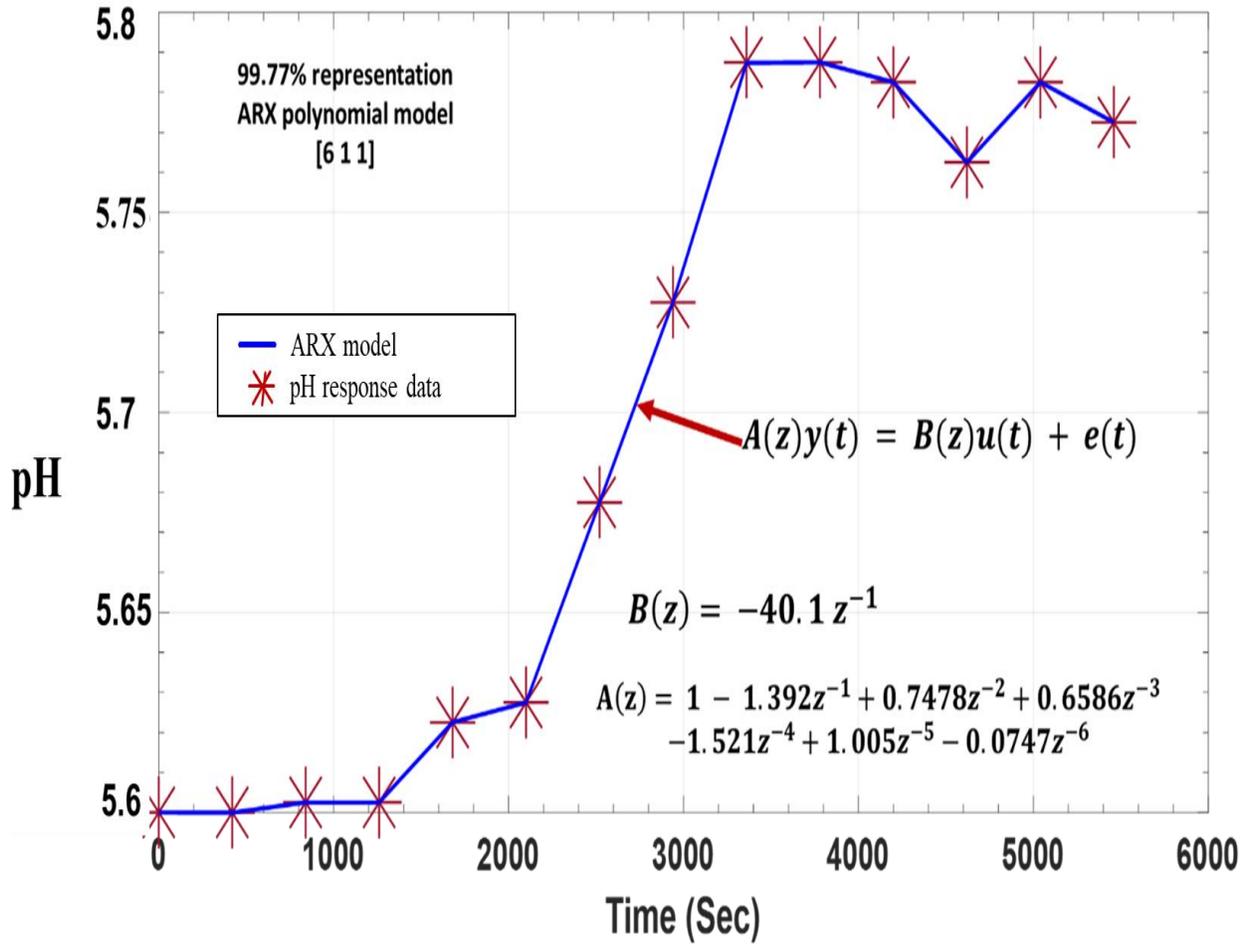
Figure E.30. ARX [6 1 1], polynomial model in the z-transform of effluent pH response, of 280.0 mg PVA/L, step change from 0.12 to 0.024 [H$_2$O$_2$]/[PVA]. Model Order range of [1:6 1:6 1:6] and a 99.77% data fitting.

Figure E.31. Order range of [1:5 1:5 1:5], was chosen for the pH response data of 280.0 mg PVA/L, step change from 0.12 to 0.024 [H₂O₂]/[PVA].

An ARX order of [5 3 4] was calculated by system identification for best fit as can be seen in Figure 32.
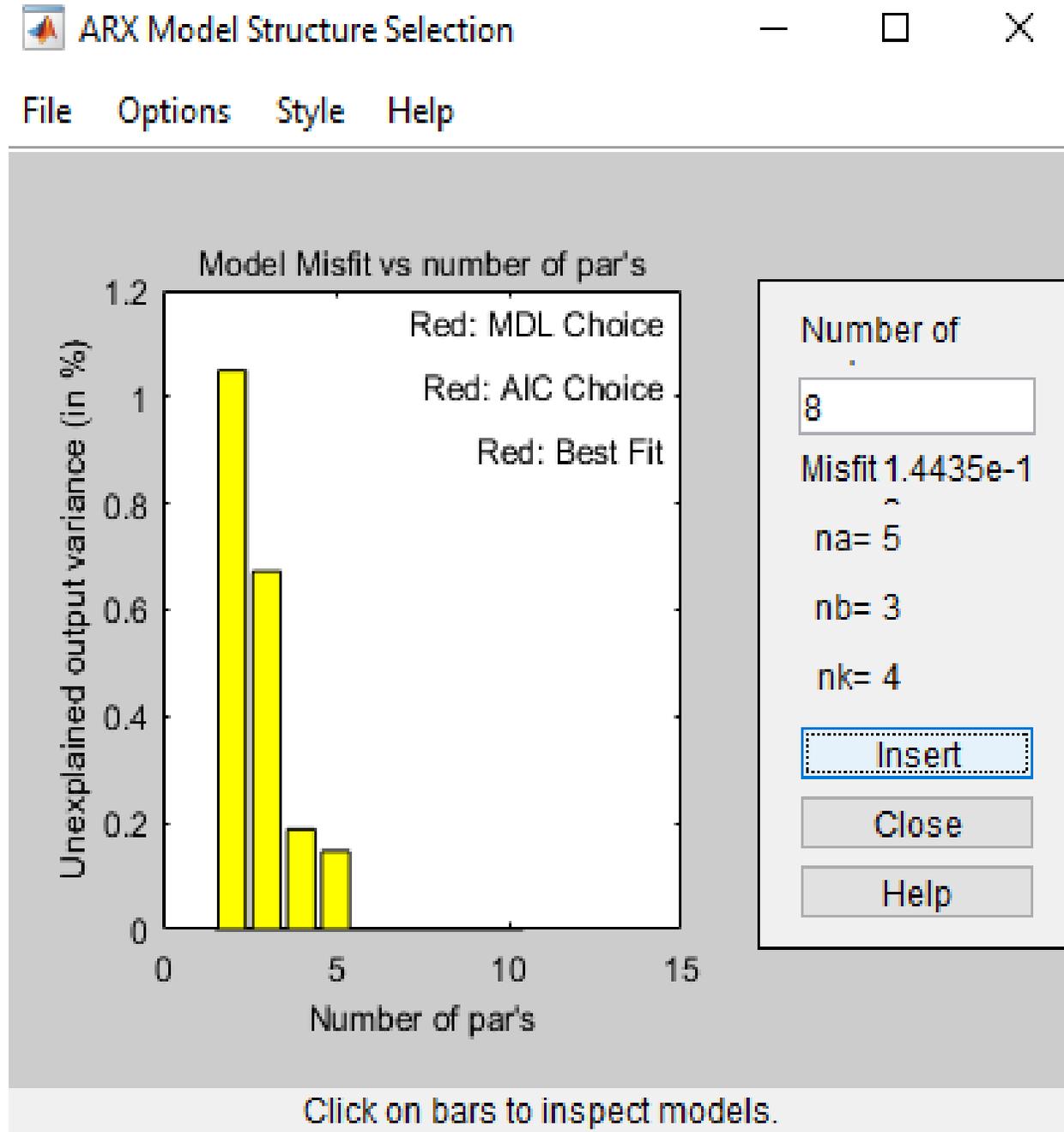
Figure E.32. A best fit plot produced by the System identification, calculated a best fit order of [5 3 4], corresponding to the pH response data of the 280.0 mg PVA/L, step change of 0.12 to 0.024 [H$_2$O$_2$]/[PVA]. Order range of [1:5 1:5 1:5].
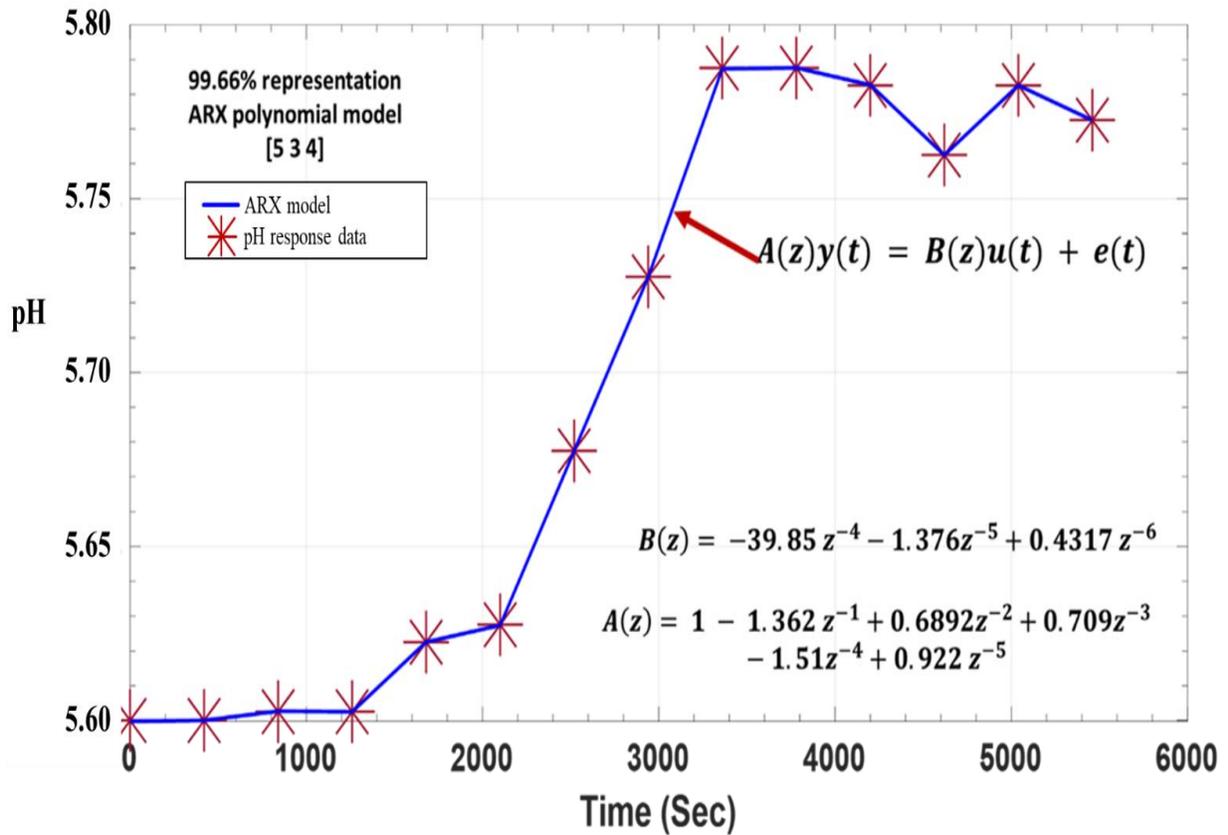
Figure E.33. ARX [5 3 4], polynomial model in the z-transform of effluent pH response, of 280.0 mg PVA/L, step change from 0.12 to 0.024 [H_2O_2]/[PVA]. Model Order range of [1:5 1:5 1:5] and a 99.66% pH response data fitting.

An ARX model order range of [1:7 1:7 1:7] was selected for the 280 mg PVA/L, step change from 0.12 to 0.024 [H_2O_2/[PVA] as can be seen in Figure E.34.

Figure E.34. ARX order range of [1:7 1:7 1:7], was selected for the pH response of the 280.0 mg PVA/L, step change from 0.12 to 0.024 [H_2O_2]/[PVA].
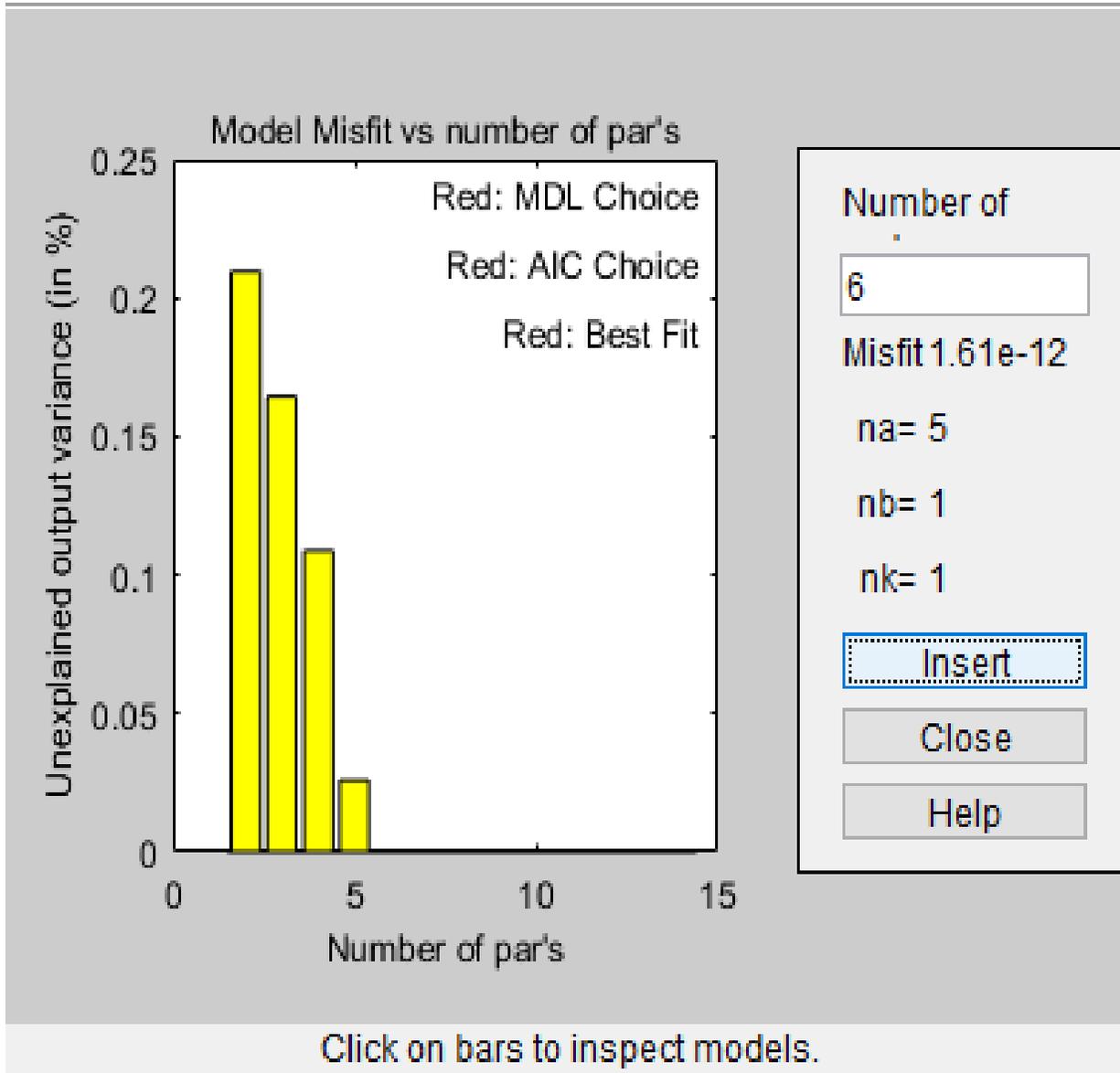
**Figure E.35.** A best fit plot produced by System identification, suggested a best fit of [5 1 1]. 280.0 mg PVA/L, step change of 0.12 to 0.024 [H_2O_2]/[PVA]. Order range of [1:7 1:7 1:7].

When over imposing the ARX model with an order of [5 1 1] over the pH response data of the 280 mg PVA/L with a step change from 0.12 to 0.024 [H_2O_2]/[PVA] the following figure results:

86.43 %
representation
ARX polynomial model
[5 1 1]

— ARX model
✳ pH response data

$A(z)y(t) = B(z)u(t) + e(t)$

$B(z) = -19.9z^{-1}$

$A(z) = 1 - 1.558z^{-1} + 0.6174z^{-2} + 0.9261z^{-3} - 1.658z^{-4} + 0.9567z^{-5}$
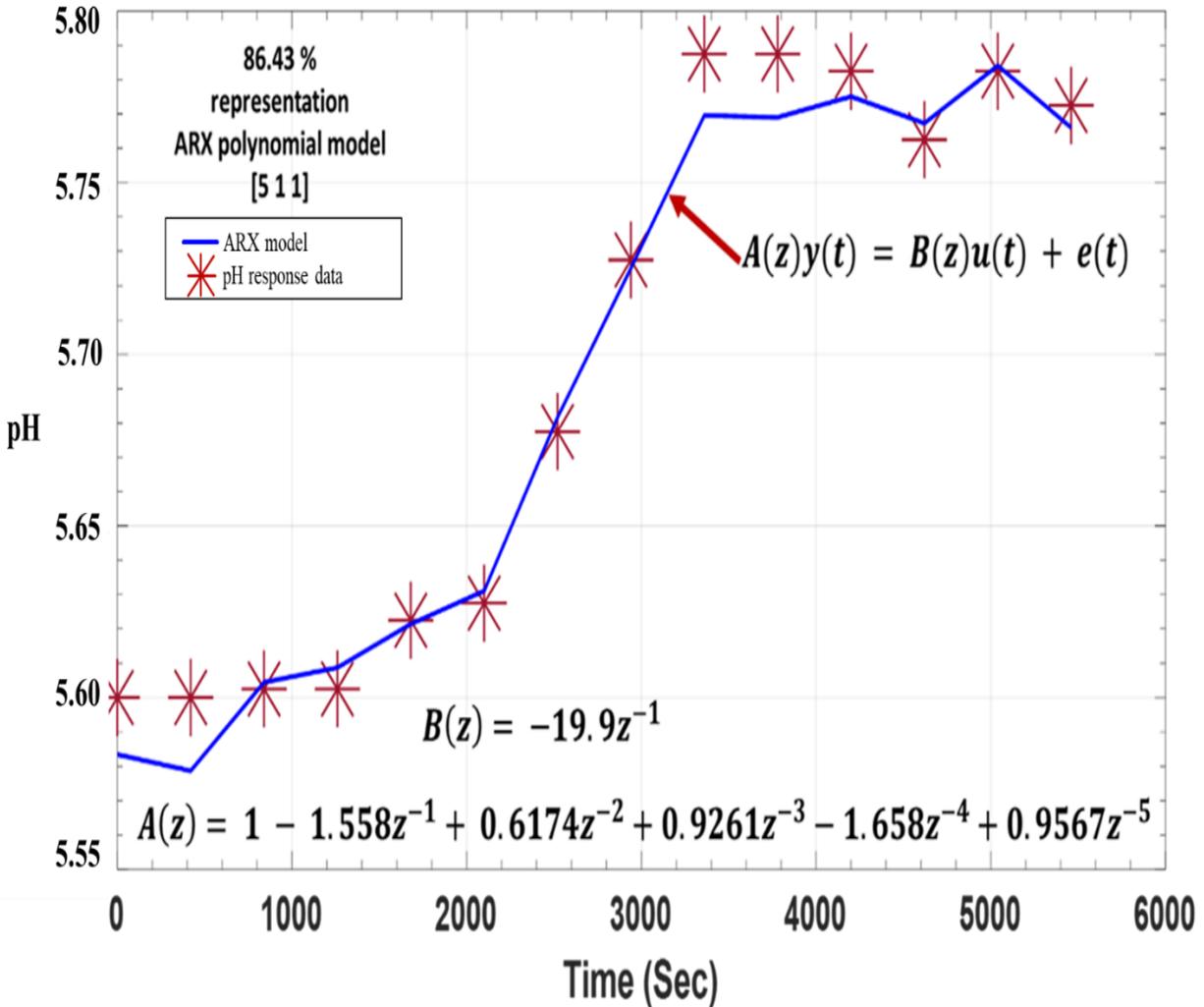
Figure E.36. ARX model with an order of [5 1 1] of effluent pH response, of 280.0 mg PVA/L, step change of 0.12 to 0.024 [H_2O_2]/[PVA]. Model Order range of [1:7 1:7 1:7]. Data fitting score of 86.43%.

Increasing the order range from [1:7 1:7 1:7] to [1:10 1:10 1:10] the accuracy of the ARX model decreases. An ARX order for best fit is chosen by system identification to be [2 1 1] as can be seen in Figure E.38.

Figure E.37. Order selection of [1:10 1:10 1:10], was applied, 280.0 mg PVA/L, Step change of 0.12 to 0.024 [H_2O_2]/[PVA].
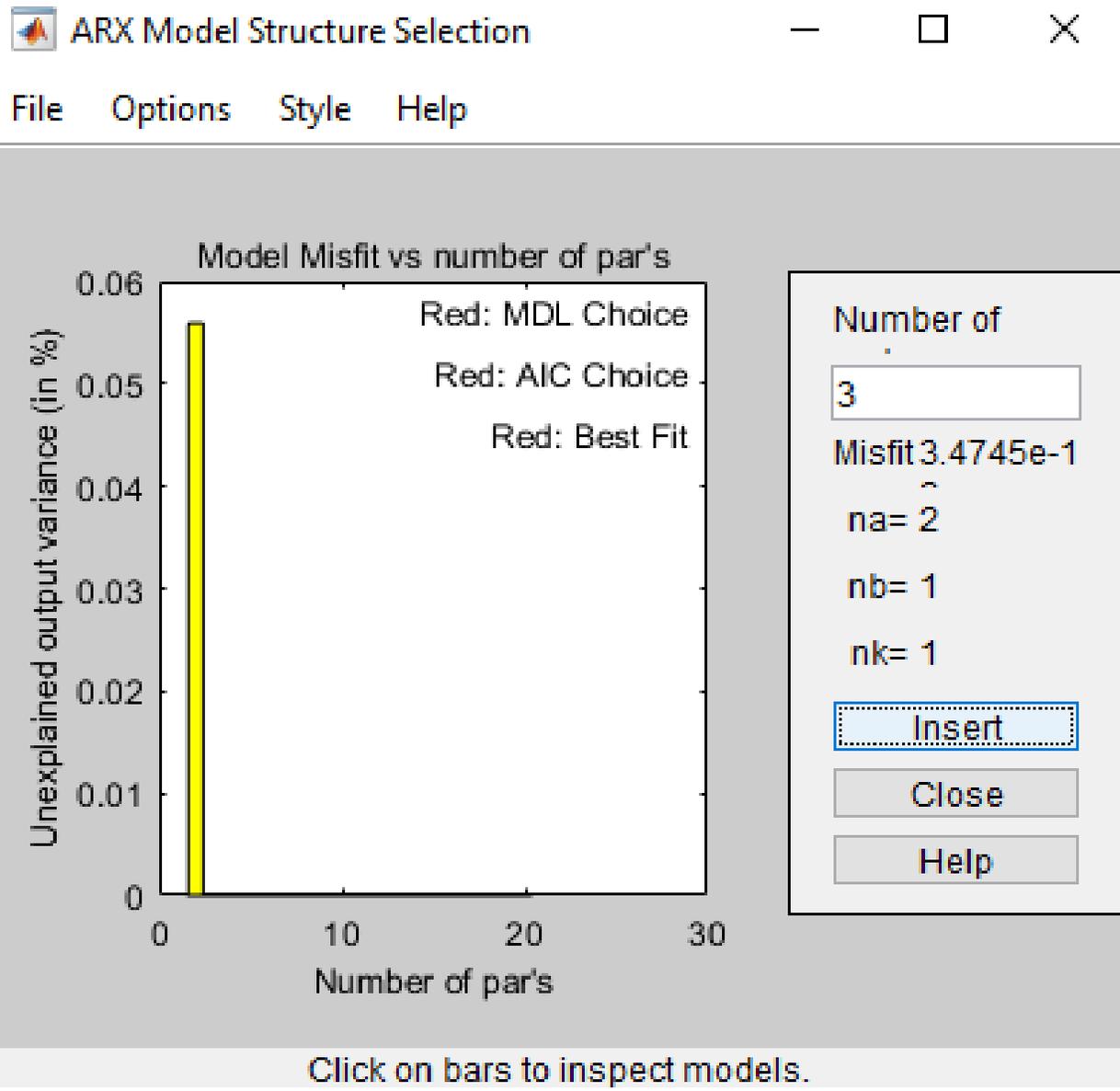
Figure E.38. The best fit plot produced by the Matlab, suggested the best fit of [2 1 1]. 280.0 mg PVA/L, Step change of 0.12 to 0.024 [H$_2$O$_2$]/[PVA]. Order choice between [1:10 1:10 1:10].

When over imposing the ARX model with the order [2 1 1] over the pH response data of the 280 mg PVA/L, step change from 0.12 to 0.024 [H₂O₂]/[PVA], Figure E.39 is produced as follows:
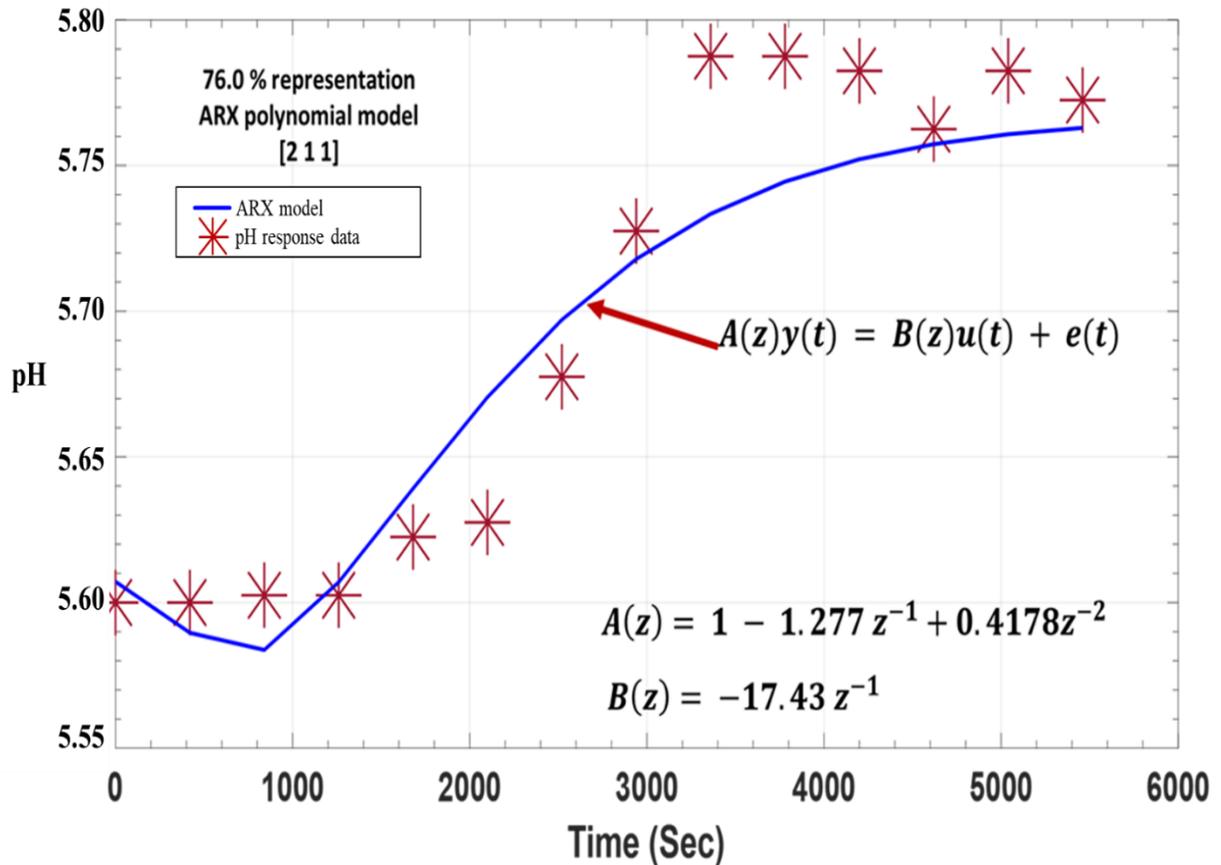
**Figure E.39.** ARX [2 1 1], polynomial model of the effluent pH response, of 280.0 mg PVA/L, step change from 0.12 to 0.024 [H₂O₂]/[PVA]. Model Order range of [1:10 1:10 1:10]. pH response data fitting of 76.0 %.

APPENDIX F.

Example standard deviation calculation of FOPTD parameters of pH response of test # 1:

$$s = \sqrt{\frac{1}{N-1}\sum_{i=1}^{N}(x_i - \bar{x})^2}$$

For the FOPTD for test 1 and its replicate:

$$G(S) = \frac{-80.0e^{-8.0S}}{15.0s + 1}$$

and

$$G(S) = \frac{-81.67e^{-8.0S}}{13.2s + 1}$$

The process gain standard deviation:

$$s_{gain} = \sqrt{\frac{1}{2-1}\sum_{i=1}^{N}(-80.0 - (-80.835))^2 + (-81.67 - (-80.835))^2}$$

$$s_{gain} = 1.18$$

Time constant standard deviation:

$$s_{gain} = \sqrt{\frac{1}{2-1}\sum_{i=1}^{N}(15 - 14.1)^2 + (13.2 - 14.1)^2}$$

$$s_{gain} = 1.27$$

APPENDIX G.

Matlab code for drawing transfer function 60.0 mg PVA/L, step change from 1.0 to 0.20 [H$_2$O$_2$]/[PVA].

x= [114

119

126

133

140

147

154

161

168

175

182

189

196

203

210

];

xx=x-114; time in minutes.

% pH response data vector.

>> y1= [4.76

4.76

4.86

4.91

5.02

5.27

5.34

5.38

5.38

5.48

5.44

5.50

5.45

5.46

5.48

];

yy1=y1-4.76   % deviation form of the pH output response

% Input values vector of hydrogen peroxide mass flow rates in units of mg H_2O_2/min.

u1= [0.003

0.0006

0.0006

0.0006

0.0006

0.0006

0.0006

0.0006

0.0006

0.0006

0.0006

0.0006

0.0006

0.0006

0.0006

0.0006

];

uu1=u1-0.003; % deviation form of the input variable (The mass flow rate of hydrogen peroxide H_2O_2 in units of mg H_2O_2/min)

>> xx1=x1-114; time in minutes.

Type the word Ident into the command window to access System identification tool box.

Insert uu1 as the input vector in the system identification tool box, and yy1 as the output response vector of the same window.

>> x2= [121

126

133

140

147

154

161

168

175

182

189

196

203

210

217

224

231

238

245

]; time in minutes.

xx2=x2-121   % time t=0 at the time of step change

>> y2= [4.90

4.91

5.02

5.09

5.20

5.29

5.48

5.48

5.49

5.44

5.48

5.50

5.48

5.49

5.52

5.55

5.49

5.50

5.51

];

yy2=y2-4.90   % deviation form of pH output response of the replicate.

u2= [0.003

0.0006

0.0006

0.0006

0.0006

0.0006

0.0006

0.0006

0.0006

0.0006

0.0006

0.0006

0.0006

0.0006

0.0006

0.0006

0.0006

0.0006

0.0006

0.0006

];

uu2=u2-0.003; % The input change in unit of mg H_2O_2/min in deviation form.

Type the (Ident) word in the command window to access the system identification tool box to import the input uu2 and the output yy2.

Insert uu2 as the input vector in the system identification tool box, and yy2 as the output response vector of the same window.

>> k1=5.48-4.7567;

>> k2=5.5067-4.8967 ;

>> tau1=22 ;

>> tau2=20 ;

>> sys1=tf (k1, [tau1 1]) ;

>> sys1.inputd=1;

>> ss1.outputd=7;

>> sys1.outputd=7;

>> sys2=tf (k2, [tau2 1]);

>> sys2.inputd=1;

>> sys2.outputd=7;

>> [n, m, X] =step(sys1);

>> [n, m, X] =step(sys1);

>> [N, M, P] =step(sys2);

>> nn=n+4.7567;

\>\> NN=N+4.8967;

\>\> plot (xx, y,'*');

\>\> hold on

\>\> plot (m, nn);

\>\> plot (XX, Y,'^');

\>\> plot (M, NN);

LIST OF REFERENCES

Aarthi, T., Shaama, M. S., and Madras, G. (2007). Degradation of Water Soluble Polymers under Combined Ultrasonic and Ultraviolet Radiation. *Industrial Engineering Chemical Resource, 46*, 6204-6210. doi:10.102/ie070287

Allison, B. J., and Ogawa, S. (2003). Design and tuning of valve position controllers with industrial applications. *The Institute of Measurement and Control, 25*(1), 3-16. doi:10.1191/0142331203tm072oa

Almquist, C., Fyda, S., Godby, N., and Miller, M. E. (2017). An Investigation on the Use of Ultraviolet Light Emitting Diodes (UV LEDs) in a Plug-Flow Reactor for Water Treatment. *Enviromental Progress and Sustainable Energy, 36*(3), 857-863. doi:10.1002/ep

Alpert, S. M., Knappe, D. R., and Ducoste, J. J. (2010). Modeling the UV/hydrogen peroxide advanced oxidation process using computational fluid dynamics. *Water Research, 44*, 1797-1808. doi:10.1016/j.watres.2009.12.003

Anandanatarajan, R., Chidambaram, M., and Jayasingh, T. (2006). Limitations of a PI controller for a first-order nonlinear process. *ISA Transactions, 45*(2), 185-199.

Ardekani, M. (2015). Sequencing treatment of industrial wastewater with ultraviolet/H_2O_2 advanced oxidation and moving bed bioreactor. *Int J Env Health Eng, 4*(5), 1-7.

Bajarangbali, R., Majhi, S., and Pandey, S. (2014). Identification of FOPDT and SOPDT process dynamics using closed loop test. *ISA Transactions, 53*, 1223-1231. doi:10.1016/j.isatra.2014.05.014

Behnajady, M. A., and Modirshahla, N. (2006). Evaluation of Electrical Energy Per Order (EEO) with Kinetic Modeling on Photooxidative Degradation of C. I. Acid Orange 7 in a Tubular Continuous-Flow Photoreactor. *Industrial Engineering Chemical resources, 45*, 553-557. doi:10.1021/ie050111c

Behnajady, M. A., Modirshahla, N., and Fathi, H. (2006). Kinetics of decolorization of an azo dye in UV alone and UV/H_2O_2 processes. *Journal of Hazardouse Materials*, 816-821. doi:10.1016/j.jhazmat.2006.01.017

Behnajady, M. A., Vahid, B., Modirshahla, N., and Shokri, M. (2009). Evaluation of electrical energy per order (Eeo) with kinetic modeling on the removal of Malachite Green by US/UV/H_2O_2 process. *Desalination, 249*, 99-103. doi:10.1016/j.desal.2008.07.025

Bielski B., Cabelli D. (1991). Highlights of current research involving superoxide and perhydroxyl radicals in aqueous solutions. *Int. J. Radiat. Biol*. 59(2): 291-319.

Boyjoo, Y., Ang, M., and Pareek , V. (2013). Some aspects of photocatalytic reactor modeling using computational fluid dynamics. *Chemical Engineering science, 101*, 764-784. doi:10.1016/j.ces.2013.06.035

Buxton G., Greenstock C., Helman W., Ross A. (1988). Critical review of rate constants for reactions of hydrated electrons, hydrogen atoms and hydroxyl radicals (•OH/•O) in aqueous solution. *Phys. Chem. Ref. Data*.17: 513-886.

Chen, J., Deng, B., and Kim, C. N. (2011). Computational fluid dynamics (CFD) modeling of UV disinfection in a closed-conduit reactor. *Chemical Engineering Science, 66*, 4983-4990. doi:10.1016/j.ces.2011.06.043

Cogan, B., and de Paor, A. M. (2011). Analytic root Locus and Lambert w function in control of a process with time delay. *Journal of Electrical Engineering, 62*(6), 327-334. doi:10.2478/v1087-011-0052-9

Corripio, A., and Smith, C. (1997). *Principles and Practice of Automatic Process Control* (Seconed ed.). John Wily and Sons Inc.

Daneshvar, N., Behnajady, M. A., and Asghar, Y. Z. (2007). Photooxidative degradation of 4-nitrophenol (4-NP) in UV/H_2O_2 process: Influence of operational parameters and reaction mechanism. *Journal of Hazardous Materials, B139*, 275-279. doi:10.1016/j.jhazmat.2006.06.045

Ducoste, J. J., and Alpert, S. M. (2015). Computational fluid dynamics modeling alternatives for UV-initiated advanced oxidation processes. *Water Quality Research Journal Of Canada, 50*(1), 4-20. doi:10.2166/wqrjc.2014.035

Duran, J. E., Mohseni, M., and Taghipour, F. (2015). Computational modeling of UV photocatalytic reactors: model development, evaluation, and application. *Water Quality Research Journal of Canada, 50*(1), 21-33. doi:10.2166/wqrjc.2014.031

Felis, E., Ledakowicz, S., and Miller, J. (2011). Degradation of bisphenol A using UV and UV/H$_2$O$_2$ processes. *Water Environment Research, 83*(12), 2154-2158.

Ghafoori, S. (2013). Modeling, simulation and optimization of advanced oxidation processes for treatmrnt of polymeric wastewater. *PhD dissertation*, 258 p. Toronto, Canada: Ryerson University.

Ghafoori, S., Mehrvar, M., and Chan, P. (2014). Photoreactor scale-up for degradation of aqueous poly (vinyl alcohol) using UV/H2O2 process. *Chemical Engineering Journal*, 133-142.

Ghafoori, S., Mowla, A., Jahani, R., Mehrvar, M., and Chan, P. (2015). Sonophotolytic degradation of synthetic pharmaceutical wastewater: Statistical experimental design and modeling. *Journal of environmental management, 150*, 128-137.

Ghassoul, M. (2012). PH Control Using MATLAB. In MATLAB - A Fundemental Tool for Scientific Computing and Engineering Applications. *1*, 243-268. INTECH.

Ghorai, P., Majhi, S., and Pandey, S. (2017). Modeling and Identification of Real-Time Processes Based on Nonzero Setpoint Autotuning Test. *Journal of Dynamic Systems, measurement, and control, 139*(2), 021010.

Guo, H.-G., Gao, N.-Y., Chu, W.-H., Li, L., Zhang, Y.-J., Gu, J.-S., and Gu, Y.-L. (2012). Photochemical degradation of ciprofloxacin in UV and UV/H$_2$O$_2$ process: kinetics, parameters, and products. *Environ Sci Pollut Res*, 3202-3213.

Hamad, D. (2015). Experimental Investigation of Polyvinyl Alcohol Degradation in UV/H$_2$O$_2$ Photochemical Reactors Using Different Hydrogen Peroxide Feeding Strategies. *PhD dissertation*, 189 p. Toronto, Canada: Ryerson University.

Hamad, D., Dhib, R., and Mehrvar, M. (2016). Photochemical Degradation of Aqueous Polyvinyl Alcohol in a Continuous UV/H$_2$O$_2$ Process : Experimental and Statistical Analysis. *J Polym Environ, 24*, 72-83.

Hamad D., Mehrvar M., and Dhib R. (2018). Photochemical Kinetic Modeling of Degradation of Aqueous Polyvinyl Alcohol in a UV/H$_2$O$_2$ Photoreactor. *Journal of Polymers and the Environment.* . https://doi.org/10.1007/s10924-018-1190-y

Hankett, J. M., Welle, A., Lahann, J., and Chen, Z. (2014). Evaluating UV/H$_2$O$_2$ Exposure as DEHP Degradation Treatment for Plasticized PVC. *J. Appl. POLYM. SCI.*, 40649. doi:10.1002/APP.40649

Harimurti, S., Rahmah, A., Omar, A., and Murugesan, T. (2014). UV/H$_2$O$_2$ process for removal of Total Organic Carbon from refinery effluent: Screening of influence factors using response surface methodology. *Advanced Materials Research, 917*, 168-177.

Horiuchi, J.-I., Shimizu, T., Tada, K., and Kobayashi, M. (2002). Selective production of organic acids in anaerobic acid reactor by pH control. *Bioresour Technol, 82*(3), 209-213.

Jenny, R. M., Simmons III, O. D., Shatalov, M., and Ducoste, J. J. (2014). Modeling a continuous flow ultraviolet light emitting diode reactor using computational fluid dynamics. *Chemical Engineering Science, 116*, 524-535. doi:10.1016/j.ces.2014.05.020

Liu , Y., Ren, J., Wang, X., and Fan, Z. (2016). Mechanismand reaction pathways for microcystin-LR degradation through UV/H$_2$O$_2$ treatment. *PLoS ONE, 11*(6), 0156236. doi:10.1371/journal.pone.0156236

Liu, T., and Furong, G. (2008). Alternative Identification Algorithms for obtaining a First-Order Stable/Unstable Process Model from a Single Relay Feedback Test. *Ind. Eng. Chem. Res., 47*, 1140-1149. doi:10.1021/ie070856d

Lutterbeck, C. A., Wilde, M. L., Baginska, E., Leder, C., Machado, Ê. L., and Kümmerer, K. (2015). Degradation of 5-FU by means of advanced (photo)oxidation processes: UV/H$_2$O$_2$, UV/Fe^{2+}/H$_2$O$_2$ and UV/TiO$_2$ — Comparison of transformation products, ready biodegradability and toxicity. *Science of the Total Environment, 527*, 232-245. doi:10.1016/j.scitotenv.2015.04.111

Mahvi, A. H., Akbari, H., Hozhabri, K., Mostafapour, F. K., Khamarinia, M., and Khorshid, A. R. (2012). Application of UV/H$_2$O$_2$ process for enhancement of industrial wastewater biodegradability. *Fresenius Environmental Bulletin, 21*(4a), 1015-1021.

Majhi, S. (2007). Relay based identification of processes with time delay. *Journal of process control, 17*, 93-101. doi:10.1016/j.procont.2006.09.005

Martz, M. (2012). Effective wastewater treatment in the pharmaceutical industry. *Pharmaceutical Engineering, 32*, 48-62.

Mehrvar, M., and Tabrizi , B. (2006). Combined photochemical and biological processes for the treatment of linear alkylbenzene sulfonate in water. *Environ. Sci. Health, 41*(4), 581-597.

Mehrvar, M., Tabrizi, B., and Abdel-Jabbar, N. (2005). Effects of pilot-plant photochemical pretreatment (UV/H$_2$O$_2$) on the biodegradability of aqueous linear alkylbenzene sulfonate (LAS). *Int. J. Photoenergy, 7*(4), 169-174.

Modirshahla , N., and Behnajady, M. A. (2005). Photooxidative degradation of Malachite Green (MG) by UV/H$_2$O$_2$: Influence of operational parameters and kinitic modeling. *Dyes and Pigments 70*, 45-59. doi:10.1016/j.dyepig.2005.04.012

Mowla, A. (2013). Combination of sonophotolysis and aerobic activated sludge processes for treatment of synthetic pharmaceutical wastewater. *MASc Thesis*, 155 P. Toronto, Canada: Ryerson University.

Mowla, A., Mehrvar, M., and Dhib, R. (2014). Combination of sonophotolysis and aerobic activated sludge processes for treatment of synthetic pharmaceutical wastewater. *Chemical Engineering Journal, 255*(1), 411-423. doi:10.1016/j.cej.2014.06.064

Passino, K. M., and Yurkovich, S. (1998). Fuzzy Control (Vol. 20). Addison-Weley Longman, Inc.

Pelckmans, K. (2012). Lecture Notes for a course on System Identification. Lecture Notes, 153 p. Uppsala, Sweden: Uppsala University.

Peng Z., Kong L. X. (2007). A thermal degradation mechanism of polyvinyl alcohol/silica nanocomposites. *Polymer Degradation and Stability*, 92, 1061-1071. doi:10.1016/j.polymdegradstab.2007.02.012

Peres, J. G., Silvio, U. d., Teixeira, A. S., Guardani, R., and Vianna Jr., A. S. (2014). Study of an Annular Photoreactor with Tangential Inlet and Outlet: I. Fluid Dynamics. *Chemical Engineering Technology, 38*(No.2), 311-318. doi:10.1002/ceat.201400186

Pramod, S., and Chidambaram, M. (2000). Closed loop identification of transfer function model for unstable bioreactors for tuning PID controllers. *Bioprocess Engineering, 22*, 185-188.

Raghavan, H., Tangirala, A. K., Gopaluni, R. B., and Shah, S. L. (2006). Identification of chemical processes with irregular output sampling. *Control Engineering Practice*(14), 467-480. doi:10.1016/j.conengprac.2005.01.015

Ramachandran, R., Lakshminarayanan, S., and Rangaiah, G. (2005). Process identification using open-loop and closed-loop step response. *Journal of the Institution of Engineers, Singapore, 45*(6), 1-13.

Ramakrishnan, V., and Chidambaram, M. (2003). Estimation of a SOPTD transfer function model using a single asymmetrical relay feedback test. *Computers and Chemical Engineering, 27*, 1779-1784. doi:10.1016/S0098-1354(03)00138-8

Ramarathnam, J., and Tangirala, A. K. (2008). On the use of Poisson wavelet transform for system identification. *Jpurnal of Process Control, 19*, 48-57. doi:10.1016/j.jprocont.2008.02.001

Rani, D. K. (2013). pH Control Approaches- An Overview. *Chemical Industry Digest, 72-76*.

Rizvi, H., Ahmad, N., Yasar, A. B., n, and Khan, H. (2013). Disinfection of UASB-Treated Municipal Wastewater by H_2O_2, UV, Ozone, PAA, H_2O_2/Sunlight, and Advanced Oxidation Process: Regrowth Potential of Pathogens. *Pol. J. Environ. Stud., 22*(4), 1153-1161.

Rosario-Ortiz, F., Wert, E. C., and Snyder, S. A. (2010). Evaluation of UV/H_2O_2 treatment for the oxidation of pharmaceuticals in wastewater. *Elsvier Water Research, 44*, 1440-1448.

Royaee, S. J., Sohrabi, M., and Shafeghat, A. (2014). Wastewater treatment using photo-impinging streams cyclone reactor: Computational fluid dynamics and kinetics modeling. *Korean J. Chem. Eng. , 31*(2), 240-247. doi:10.1007/s11814-013-0191-8

Rubén, L., Alberto, L., and Guillermo, H. (2016). Open Loop Step test used for Process Identification and PID tuning controller by Genetic Algorithms. *Research Journal of Recent Sciences, 5*(1), 16-26.

Santoro, D., Raisee, M., Moghaddami, M., Ducoste, J., Sasges, M., Liberti, L., and Notarnicola, M. (2010). Modeling Hydroxyl Radical Distribution and Trialkyl Phosphates Oxidation in UV-H_2O_2 Photoreactors Using Computational Fluid Dynamics. *Environmental Science Technology, 44*(16), 6233-6241. doi:10.1021/es1000962

Santos, L., Poli, A. L., Cavalheiro, C. C., and Neumann, M. G. (2009). The UV/H2O2-photodegradation of Poly(ethylene glycol) and Model Compounds. *J Braz. Chem. Soc., 20*(8), 1467-1472.

Scali, C., Marchetti, G., and Semino, D. (1999). Relay with Additional Delay for Identification and Autotuning of. *Ind. Eng. Chem. Res., 38*, 1987-1997. doi:10.1021/ie9806161

Segneanu, A. E., Orbeci, C., Lazau, C., Sfirloaga, P., Vlazan, P., Bandas, C., and Grozescu, I. (2013). Waste Water Treatment Method. *Water Treatment Walid Elshorbagy, IntechOpen*, 53-80. doi:10.5772/53755

Shahrestani, M. M., Rahimi, A., and Momeni, M. (2017). Experimental Study and Mathematical Modeling of NO Removal Using the UV/H_2O_2 Advanced Oxidation Process. *Chemical Engineering Technology, 40*(6), 1149-1157. doi:10.1002/ceat.201600643

Siamak , E., and Taghipour, F. (2010). Simulation of UV Photoreactor for Degradation of Chemical Contaminants: Model Development and Evaluation. *Environmental science and technology, 44*(6), 2056-2063. doi:10.1021/es902391t

Song, C., Wang, L., Ren, J., Lv, B., Sun, Z., Yan, J., . . . Liu, j. (2016). Comparative study of diethyl phthalate degradation by UV/H_2O_2 and UV/TiO2: kinetics, mechanism, and effects of operational parameters. *Environmental Science and Pollution Research, 23*(3), 2640-2650. doi:10.1007/s11356-015-5481-8

Sree, P. R., Srinivas, M. N., and Chidambaram, M. (2004). A simple method of tuning PID controllers for stable and unstable FOPTD systems. *Computers and Chemical Engineering, 28*, 2201-2218. doi:10.1016/j.compchemeng.2004.04.004

Stephanopoulos, G. (1984). *Chemical process control : An introduction to theory and practice* (illustrated, reprint ed.). the University of Michigan, N.J, USA: PTR Prentice Hall International.

Sung, S. W., and Lee, I.-B. (1999). On-Line process identification and PID controller autotuning. *Korean J. Chem. Eng., 16*, 45-55.

Suzuki, T. (1976). Purification and Some Properties of Polyvinyl Alcoholdegrading Enzyme Produced by Pseudomonas 0_3. *Agr. Biol. Chem, 40*(3), 497-504. doi:10.1080/00021369.1976.10862089

Tabrizi, G., and Mehrvar, M. (2004). Integration of advanced oxidation technologies and biological processes: Recent developments, trends, and advances. *Environ. Sci. Heal., 39*(11-12), 3029-3081.

Taghizadeh M. T., Yeganeh N., Rezaei M. (2015). The investigation of thermal decomposition pathway and products of poly(vinyl alcohol) by TG-FTIR. *Journal of Applied Polymer Science*, 42117, 1-12. doi: 10.1002/app.42117

Tan, C., Gao, N., Deng, Y., Zhang, Y., Sui, M., Deng, J., and Zhou, S. (2013). Degradation of antipyrine by UV, UV/H_2O_2 and UV/PS. *Journal of Hazardous Materials, 260*, 1008-1016. doi:10.1016/j.jhazmat.2013.06.060

TOMA, L. (2016). Comparative Analysis of pH Control Methods. *ACTA Technica Napocensis Electronics and Telecommunications, 57*(4), 21-26.

Vaferi, B., Bahmani, M., Keshavarz, P., and Mowla, D. (2014). Experimental and theoretical analysis of the UV/H_2O_2 advanced oxidation processes treating aromatic hydrocarbons and MTBE from contaminated synthetic wastewaters. *Journal of Environmental Chemical Engineering, 2*, 1252-1260.

Vivek, S., and Chidambaram, M. (2005). Identification using single symmetrical relay feedback test. *Computers and Chemical Engineering, 29*, 1625-1630. doi:10.1016/j.compchemeng.2005.01.002

Wang, D., Duan, X., He, X., and Dionysiou, D. D. (2016). Degradation of dibutyl phthalate (DBP) by UV-254 nm/H_2O_2 photochemical oxidation: kinetics and influence of various process parameters. *Environmental Science and Pollution Research , 23*(23), 23772-23780. doi:10.1007/s11356-016-7569-1

Wang, L., Ji, Y., Lu, J., Kong, D., Yin, X., and Zhou, Q. (2017). Comparative study of the formation of brominated disinfection byproducts in UV/H_2O_2 oxidation processes in the presence of bromide. *Environmental Science Pollution Resource, 24*(29), 23219-23225. doi:10.1007/s11356-017-9935-z

Ye, Z., Wang, Q.-G., Lin, C., Hang, C. C., and Barabanov, A. E. (2007). Relay feedback analysis for a class of servo plants. *Journal of Mathematical Analysis and Applicarions, 334*(1), 28-42. doi:10.1016/j.jmaa.2006.12.037

Zhang, W., Xiao, X., An, T., Song, Z., Fu, J., Sheng, G., and Cui, M. (2003). Kinetics, degradation pathway and reaction mechanism of advanced oxidation of 4-nitrophenol in water by a UV/H_2O_2 process. *J Chem Technol Biotechnol, 78*, 788-794.

Zhou, H., and Smith, D. (2002). Advanced technologies in water and wastewater treatment. *J. Environ. Sci., 1*, 247-264.

Zotesso, J., Cossich, E. S., Janeiro, V., and Tavares, C. (2016). Treatment of hospital laundry wastewater by UV/H_2O_2 process. *Environmental Science and Pollution Research, 24*(7), 6278-6287. doi:10.1007/s11356-016-6860-5